Dissecting the epigenetic signaling underlying early myogenic differentiation

Saadia Khilji

Thesis submitted to the University of Ottawa in partial fulfillment of the requirements for the Doctorate in Philosophy degree in Cellular and Molecular Medicine

Department of Cellular and Molecular Medicine
Faculty of Medicine
University of Ottawa

Authorizations

1. Permission to include the full article: Khilji, S., Hamed, M., Chen, J., and Li, Q. (2018). Loci-specific histone acetylation profiles associated with transcriptional coactivator p300 during early myoblast differentiation. Epigenetics *13*, 642–654 as part of a dissertation/thesis was obtained from Taylor & Francis as an open access article distributed under the CC-BY-NC-ND license.

2. Permission to include the full article: Hamed, M., Khilji, S., Dixon, K., Blais, A., Ioshikhes, I., Chen, J., and Li, Q. (2017). Insights into interplay between rexinoid signaling and myogenic regulatory factor-associated chromatin state in myogenic differentiation. Nucleic Acids Research *45*, 11236–11248 as part of a dissertation/thesis was obtained from Oxford University Press. License Number: 4936640728164.

3. Permission to include the full article: Khilji, S., Hamed, M., Chen, J., and Li, Q. (2020). Dissecting myogenin-mediated retinoid X receptor signaling in myogenic differentiation. Communications Biology *3*, 1–12 as part of a dissertation/thesis was obtained from Springer Nature as an open access article distributed under the terms of the Creative Commons CC BY license.

Abstract

While skeletal myogenesis is tightly coordinated by myogenic regulatory factors, epigenetic determinants have emerged as vital mechanisms of myogenic regulation as well. The epigenetic network provides the blueprint by which extra-cellular signals, such as bexarotene, a clinically approved agonist of retinoid X receptor (RXR), impact lineage-specific gene expression. We have previously established that bexarotene promotes the specification and differentiation of the skeletal muscle lineage however, the role of RXR signaling and how it effects global gene expression to promote myogenic differentiation is unclear. Here, we utilized integral RNA-seq and ChIP-seq analyses to understand the mechanistic activation of myogenic regulatory elements and the functional mode of myogenic transcriptional regulators. Our results describe an enrichment of loci-specific histone acetylation at enhancers associated to the histone acetyltransferase, p300, particularly when it is recruited by muscle master regulator, MyoD and define a role for p300 in the establishment and regulation of myogenic loci. Similarly, dissection of rexinoid-responsive gene expression revealed that rexinoid-enhanced myoblast differentiation is reconciled largely via a direct regulation of MyoD and residue-specific histone acetylation to promote a coordination of exit from the cell cycle to an activation of muscle-related genes including the differentiation marker, myogenin. Accordingly, we also uncovered a significant association of myogenin with rexinoid-responsive gene expression and its distribution to poised enhancers where RXR signaling augments residue-specific histone acetylation, particularly H4K8ac and H3K9ac, at enhancers co-occupied by p300 and myogenin. Importantly, we also utilized global transcriptional profiling of rexinoid-enhanced differentiation to identify the novel myogenic target, Tmem182. We show for the first time that Tmem182 expression is MyoD dependent and that the transmembrane protein is important for myoblast differentiation. In

addition, we report increased enrichment of p300 as well as rexinoid-responsive histone acetylation at the Tmem182 promoter such that it may represent global trends in which myogenin cooperates with p300, in the installation of an epigenetic signature associated to rexinoid responsive gene expression. Thus, we provide novel molecular insights into the mechanisms of transcriptional activation underlying myogenic programs in the context of RXR signaling. Our study presents a valuable foundation for pharmacological correction of epigenetic regulators to treat muscle-related diseases and for the identification of additional myogenic targets and molecular interactions for therapeutic development.

Dedication

This thesis is dedicated to my mother and father, Shamim Akhtar and Pervez Ahmad, whom have been a constant source of strength throughout my career. They have always pushed me towards the pursuit of knowledge, education, and have believed in me at times when I did not. As parents, they have suffered through unimaginable hardships to give their children better lives, for which I will always be grateful. Their unwavering support and encouragement have been invaluable to the completion of this thesis and I am extremely blessed to have such generous souls in my life.

I also dedicate this thesis to my adoring husband, Haris Ghauri, for his endless love, patience and support. He has helped me through the most difficult times by listening to me, making me laugh and always having faith in my success. I have not made it easy for him, but he is and always will be a constant source of comfort and happiness.

I would also like to thank both of my amazing brothers, Shahzad and Waqas Khilji, who exemplify the nature of brothers so well. They are supportive, loving and always a pillar of strength. I would also like to thank my family in Canada and beyond inclusively, for their unending encouragement and support.

Acknowledgements

I would like to express my sincere gratitude to my supervisor and mentor, Dr. Qiao Li, for the opportunity to work in her laboratory. Her encouragement, guidance and motivation throughout my Ph.D. studies have made this research possible. Thank you for pushing me to become a logical thinker, an attentive writer and a better scientist overall.

I would also like to thank the members of my thesis advisory committee, Dr. Jeffrey Dilworth Dr. Michael Downey, and Dr. David Lohnes for their insightful discussions and their valued guidance throughout my project.

Thanks to all my lab mates, past and present: Dr. Munerah Hamed, Matthew Pona, Dr. Hongsheng Liang, Dr. Aili Gao, Dr. Yuan Li, Yan Mach, and Katie Dixon. Thank you for your support, dynamic banter, thoughtful discussions and for making the duration of my studies so enjoyable. I am especially grateful to my friend, Dr. Garima Kulshreshtha, with whom discussions about life and science helped me immensely.

I would also like to thank the funding resources. This research was supported by Operating Grants from the Natural Sciences and Engineering Research Council of Canada (NSERC) and the Cancer Research Society to Dr. Qiao Li [#250174 and #21126, respectively]. My education was supported by a Canada Graduate Scholarship – Master's (Canadian Institutes of Health Research), Ontario Graduate Scholarship, a Postgraduate Scholarship from the NSERC, and an Excellence Scholarship from the University of Ottawa.

Table of Contents

List of Figures

Chapter One: Introduction

Chapter Two: Loci-specific histone acetylation profiles associated with transcriptional coactivator p300 during early myoblast differentiation

Chapter Three: Insights into interplay between rexinoid signaling and myogenic regulatory factor-associated chromatin state in myogenic differentiation

Chapter Four: Dissecting myogenin-mediated retinoid X receptor signaling in myogenic differentiation

Chapter Five: Functional and regulatory characterization of novel myogenic target, Tmem182 in the context of RXR signaling

List of Tables

Chapter Two: Loci-specific histone acetylation profiles associated with transcriptional coactivator p300 during early myoblast differentiation

Chapter Three: Insights into interplay between rexinoid signaling and myogenic regulatory factor-associated chromatin state in myogenic differentiation

List of Abbreviations

9CRA	9-cis Retinoic Acid
AF	Activating Function
Angptl4	Angiopoietin-like 4
AP-1	Activating Protein-1
AR	Androgen Receptor
ATRA	All-Trans Retinoic Acid
Bex	Bexarotene
bHLH	basic Helix-Loop-Helix
BMP4	Bone Morphogenetic Protein 4
CBP	CREB-Binding Protein
CDK	Cyclin-Dependent Kinase
CER	Core Enhancer Region
ChIP-seq	Chromatin Immunoprecipitation-sequencing
CpG	Cytosine-Phospho-Guanine
CT	Cycle Threshold
Ctl	Control
CTPB	N-(4-Chloro-3-trifluoromethyl-phenyl)-2-ethoxy-6-pentadecyl-benzamide
CTX	Cardiotoxin
CypB	Cyclophilin B
DM	Differentiation Medium
DMD	Duchenne Muscular Dystrophy
DMEM	Dulbecco ’s Modified Eagle Medium
Dnmt	DNA Methyltransferase
DR	Direct Repeats
ER	Estrogen Receptor
ESC	Embryonic Stem Cell

Ezh2	Enhancer of Zeste Homolog 2
FBS	Fetal Bovine Serum
FC	Fold Change
FDA	United States Food and Drug Administration
FDR	False Discovery Rate
FPKM	Fragments Per Kilobase of transcript per Million mapped reads
FXR	Farnesoid X Receptor
GCN5	General Control Nonderepressible 5
GEO	Gene Expression Omnibus
GM	Growth Medium
GO	Gene Ontology
GR	Glucocorticoid Receptor
HAT	Histone Acetyltransferase
HCNCE	Highly Conserved Non-Coding Elements
HDAC	Histone Deacetylase
HOMER	Hypergeometric Optimization of Motif EnRichment
HP1	Histone Protein 1
HRE	Hormone Response Element
HS	Horse Serum
Id	Inhibitor of Differentiation
IGV	Integrated Genome Viewer
IR	Inverted Repeats
KAT	Lysine Acetyltransferase
LBD	Ligand Binding Domain
LXR	Liver X Receptor
MACS	Model-based Analysis for ChIP-seq
Mef2	Myocyte Enhancer Factor 2
MPC	Myogenic Progenitor Cell

MRF	Myogenic Regulatory Factor
MyoD1	Myogenic Differentiation 1
NCoR	Nuclear receptor Co-Repressor
ncRNA	non-coding RNA
NP-40	Nonidet P-40
NR	Nuclear Receptor
OSCC	Oral Squamous Cell Carcinoma
Pax	Paired box
PBM	Protein-Binding Microarrays
PBS	Phosphate-Buffered Saline
PCAF	p300/CBP-Associated Factor
PhastCons	Phylogenetic Conservation
PIC	Pre-Initiation Complex
PPAR	Peroxisome Proliferator-Activated Receptor
PR	Progesterone Receptor
PRC2	Polycomb Repressive Complex 2
PXR	Pregnane X Receptor
RAR	Retinoic Acid Receptor
RNA Pol II	RNA Polymerase II
RNA-seq	RNA-sequencing
RPS26	Ribosomal Protein S26
RXR	Retinoid X Receptor
SC	Satellite Cell
SE	Super-Enhancer
Shh	Sonic Hedgehog
Six	Sine oculus homeobox
SMRT	Silencing Mediator of Retinoid and Thyroid hormone receptors
SRF	Serum Response Factor

SWI/SNF	SWItch-Sucrose Non-Fermentable
TBP	TATA-Binding Protein
TF	Transcription Factor
THR	Thyroid Hormone Receptor
TrxG	Trithorax Group
TSS	Transcription Start Site
VDR	Vitamin D Receptor
WCE	Whole-Cell Extraction

Chapter One: General Introduction

Human development entails the formation of highly complex tissues, comprised of specialized cells with distinct gene expression profiles. The role of tissue-specific transcription factors (TFs) in this process has been well established, but epigenetic determinants have recently emerged as vital mechanisms in governing cell fate decisions and their subsequent transformations. In the current study, we present the latest understanding for the role of epigenetic modifications in stem cell differentiation. In particular, we focus towards epigenetic networks regulating muscle-specific gene expression and utilize the approach of ligand-enhanced myogenic differentiation to reveal the mechanisms underlying cell type-specific gene expression. As such, understanding the epigenetic mechanisms controlling transcriptional programs will improve our mechanistic understanding of tissue development which may facilitate therapeutic development to target epigenetic modulators for the selective control of gene expression in diseased states.

1. Epigenetic regulation of gene expression

Genomic DNA, which contains all the information required for an organism to live, is generally identical in each cell of that organism. In contrast, the epigenome, defined as chemical modifications to the genome that do not affect the DNA sequence, is highly cell-type specific and plays an important role in both repression and activation of gene transcription. Importantly, epigenetic changes are mitotically and/or meiotically heritable and thus may result in heritable deviations in phenotype (Wu Ct and Morris, 2001).

A key characteristic of eukaryotic genomes is the packaging of long DNA molecules into a compact, dense structure known as chromatin. Chromatin is generally in a state of transcriptional repression (heterochromatin) where structural changes are required to transition into a state of

transcriptional competence (euchromatin). The epigenome plays an essential role in governing this transition by modifying chromatin or nuclear architecture largely via three systems including DNA methylation, non-coding RNA (ncRNA) and the focus of this study, histone modifications (Bannister and Kouzarides, 2011; Kouzarides, 2007). The interactions between these factors maintain the delicate balance in the changing forms of chromatin that repress, preserve or induce tissue-specific transcriptional programs in a dynamic and reversible process.

1.1 Non-coding functional DNA elements

Stem cell differentiation is driven by the transcriptional activation of lineage-specific genes. These highly organized molecular mechanisms are in part guided by non-coding regulatory DNA sequences, which include promoters, enhancers and insulators. Promoters span a small region directly upstream of the transcription start site (TSS) and contain a binding site for RNA polymerase II (RNA Pol II), as well as specific primary regulatory elements which play a direct role in recruiting members of the transcription initiation complex. Enhancers are positive regulators of transcription that directly influence the recruitment of the transcriptional machinery to the TSS. They can do this in part by interacting with promoters from tens to hundreds of kilobases away as the elements physically engage in three-dimensional space (Vernimmen and Bickmore, 2015). Interestingly, enhancers function independent of their orientation and their position relative to the TSS. As such, regulatory elements ensure that genes are turned on or off in response to appropriate signals in order to maintain a precise level of expression (Schoenfelder and Fraser, 2019). In this way, non-coding regulatory elements warrant firm spatio-temporal regulation of gene expression (Perenthaler et al., 2019). The role of non-coding sequences and

how they regulate development of tissues with physiologically and functionally distinct characteristics is thus an intriguing area of research.

1.2 Chromatin modifications in transcriptional regulation

Chromatin is a highly organized complex of negatively charged DNA and positively charged histones which are small, globular proteins with long N-terminal tails. DNA is packaged around histone proteins to form the basic unit of chromatin, the nucleosome. Each nucleosome consists of approximately 146 base-pairs of DNA wrapped around 8 core histone proteins including two copies of H2A, H2B, H3, and H4 (Kornberg, 1974). This association of DNA to histones facilitates packaging of DNA into a densely compact structure which limits access of transcriptional regulators. Thus, chromatin constitutes a repressive state of gene expression where posttranslational modifications of both histone proteins and DNA are important regulators of gene expression (Radman-Livaja and Rando, 2010). Modifications to histone tails were first revealed by the pioneering studies of Vincent Allfrey in the early 1960s (Allfrey et al., 1964), and functionally serve two main purposes: the creation of recruitment signals for non-histone proteins and/or the alteration of chromatin structure. As chromatin modifications alter the physical interaction between histones and DNA, chromatin transitions into open or compact states, directly affecting TF access to DNA for the control of gene activation or repression (Radman-Livaja and Rando, 2010).

The N-terminal tails of histones are subject to numerous post-translational modifications facilitated by a large number of histone-modifying enzymes (Moran-Salvador and Mann, 2017).

The most commonly studied range of histone modifications include acetylation, methylation, ubiquitination, phosphorylation, SUMOylation and ADP-ribosylation. The distinct combination of histone modifications, known as the histone code, determines the transcriptional competence of chromatin, and thus guides the pendulum of gene transcription towards specific biological functions (Jenuwein and Allis, 2001).

The list of histone modifications affecting transcription continues to grow as studies attempt to define their complex mechanisms of action. Many types of covalent modifications have been associated with active gene transcription, but histone acetylation is one of the best characterized (Barnes et al., 2019). The process of acetylation involves transfer of acetyl groups to the lysine residues of histone N-terminal tails, resulting in neutralization of the positive charge of highly basic histone tails, thereby decreasing their affinity to the negatively charged DNA (Kouzarides, 2007). This alters the conformational structure of the chromatin and essentially increases accessibility for transcriptional regulatory proteins to bind to DNA (Hong et al., 1993; Lee et al., 1993). In this way, post-translational modification of histone tails can regulate DNA transcription as well as DNA replication and repair (Podobinska et al., 2017). Histone acetylation is generally associated with gene activation and most commonly attributed to lysines of H3 at positions 9, 14, 18, and 27 and at positions 5, 8, 12, and 16 for the N-tail of H4 (Barnes et al., 2019). Moreover, lysine residues can be mono-, di-, or trimethylated to provide additional levels of control (Santos-Rosa et al., 2002). As part of the histone code hypothesis, the functional outcome of individual histone modifications can be best assessed when examined as a component of the surrounding modifications. Accordingly, Wang *et al.* assessed the genomic localization of 39 histone modifications in human $CD4^+$ T cells (Wang et al., 2008b). They found

that H4K8ac and H3K9ac in particular comprised the "backbone" of 17 modifications that define active promoters, while H4K8ac was also associated with actively transcribed regions (Wang et al., 2008b). As a crucial mark of active promoters, H3K9ac also has a high co-occurrence with other promoter marks including H3K14ac and H3K4me3, suggesting a coordinated regulation of active histone marks (Karmodiya et al., 2012). Although, histone acetylation is largely regarded as an activation mark, H4K20ac is an exception to this rule as it has been associated with transcriptional repression in HeLa-S3 cells (Kaimori et al., 2016).

In contrast to histone acetylation, histone methylation can result in the activation or repression of gene transcription depending on the number of methyl groups added and their location (Bannister and Kouzarides, 2011; Suganuma and Workman, 2011). For instance, methylation of lysines 4, 36, and 79 on histone H3 are associated with active transcription, whereas methylation of lysines 27 and 9 on H3 and lysine 20 on H4 are strongly associated with silent heterochromatin (Gerber and Shilatifard, 2003). Moreover, H3K4me3, deposited by the Trithorax group (TrxG) of proteins, is an important signature of transcriptional activation and is largely detected at promoters and 3'end of actively transcribed genes (Berger, 2007). In contrast, mono- or di-methylation of H3K4 can distinguish promoter and enhancer elements, as H3K4me1 enrichment is used to mark tissue-specific enhancers (Creyghton et al., 2010; Heintzman et al., 2009; Lee et al., 2013). Furthermore, certain residues such as H3K9 have a dual role, as they can activate transcription when acetylated and just as easily silence genes upon methylation (Kouzarides, 2007). Given this, H3K9ac is a hallmark of active promoters, but H3K9 methylation is largely associated with heterochromatin (Barski et al., 2007; Wang et al., 2008b). Interestingly, methylation of H3K9 is required for subsequent binding of histone protein 1

(HP1), a family of adapter molecules which are thought to initiate heterochromatin formation via multimerization of HP1 molecules on nearby nucleosomes, suggesting that H3K9 also plays a distinct role in large-scale transcriptional repression (Bannister et al., 2001; Lachner et al., 2001). Similarly, H3K27me3 is mainly attributed with gene silencing and is largely deposited at inactive promoters and intergenic regions by components of the Polycomb repressive complex 2 (PRC2), including enhancer of zeste homolog 2 (Ezh2) (Barski et al., 2007). Accordingly, embryonic stem cell (ESC) differentiation is inhibited as key developmental genes required for cell lineage specification are repressed by H3K27me3 deposition (Boyer et al., 2006; Juan et al., 2016). Additionally, H3K27me3 is inversely-correlated with regions containing high amounts of DNA methylation suggesting a potential antagonism between H3K27me and DNA methylation (Brinkman et al., 2012).

ESCs in particular, present an interesting example of chromatin state complexity, where certain regulatory regions are marked by both active and repressive histone modifications. The presence of H3K4me3 in combination with the repressive H3K27me3 signifies a bivalent or poised state (Bernstein et al., 2006). First observed in mouse ESCs, bivalency is hypothesized to prevent either complete gene silencing or heightened levels of gene expression, in essence preventing unsystematic perturbations in gene expression (Bernstein et al., 2006). Genes associated with linear progression specifically, are characterized by bivalency as they are poised for stem cell differentiation (Spivakov and Fisher, 2007; Voigt et al., 2013). Notably, nearly half the genes denoted by bivalency in ESCs remained so following lineage commitment to myogenic progenitor cells (MPCs) and only a small portion of those genes resolved to a monovalent state after differentiation to mature myotubes (Asp et al., 2011; Liu et al., 2013). The presence of

bivalency in stem cells and somatic cells thereby represents an efficient mechanism for a rapid transcriptional response to environmental cues.

Enhancer regions have garnered much attention in epigenetic research since their emergence as key cis-regulatory elements that govern lineage specific gene expression. Enhancers can also be further categorized as "poised" or "active" where the poised state is marked by both activating H3K4me1 and repressive H3K27me3. As such, poised enhancers represent a state between repression and activation and are generally characterized by increased accessibility compared to inactive enhancers (Bernstein et al., 2006; Creyghton et al., 2010; Rada-Iglesias et al., 2011). Poised enhancers primed by H3K4me1 are activated by the deposition of H3K27ac and removal of H3K27me3 (Bernstein et al., 2006; Creyghton et al., 2010; Rada-Iglesias et al., 2011). Interestingly, Zentner *et al.* proposed that the enrichment of H3K36me3, phosphorylated RNA Pol II and RNA transcript detection at enhancer regions can further distinguish highly active enhancers from less active enhancers, while the presence of H3K4me1 in the absence of H3K27ac represents an "intermediate" class of enhancers (Zentner et al., 2011). Moreover, loss of either H3K4me1 or H3K27ac can result in enhancer decommissioning (Creyghton et al., 2010; Rada-Iglesias et al., 2011; Whyte et al., 2012). Additionally, analogous to bivalent promoters, poised enhancers regulate genes governing lineage development as a tool to ensure rapid activation of gene expression (Rada-Iglesias et al., 2011). In this way, poised enhancers and bivalent promoters may act as "switches" for each step of lineage progression that are primed to drive a molecular sequence of events and represent an important mechanism for driving lineage-specific gene expression (Nguyen et al., 2015).

1.3 Histone-modifying enzymes – Histone acetyltransferases

The core effectors of epigenetic regulation are histone-modifying enzymes. Generally associated with gene expression, histone acetylation is catalyzed by histone acetyltransferases (HATs) and removed by histone deacetylases (HDACs). Importantly, recent analysis of protein lysine acetylation through mass spectrometry data has revealed the acetylation of hundreds of non-histone proteins and the involvement of acetylation in many biological processes beyond gene transcription, from protein interaction, activity to localization (Choudhary et al., 2009). Thus, HAT enzymes are also generally referred to as lysine acetyltransferases (KATs). However, as our study is focused on the role of histone modifications in epigenetic regulation, we will continue to use the terminology of histone acetyltransferase/deacetylase.

Functionally, HATs catalyze the transfer of an acetyl group onto the ε-amino group of lysine side chains, converting its basic side chain into a neutral residue (Trisciuoglio et al., 2018). Notably, acetylation of histones can also create binding sites for chromatin remolding complexes to further promote transcriptional activation, a shared purpose amongst HAT members (Trisciuoglio et al., 2018). Interestingly, HATs do not bind DNA directly, but are recruited by TFs or other histone-modifying proteins and hence are not associated to any specific DNA sequence. While many of these epigenetic enzymes are ubiquitously expressed, tissue specificity is primarily determined by the identity of recruiting factors such as the TF MyoD for establishment of the skeletal muscle lineage (Puri et al., 1997a).

HATs are classified into two broad types based upon their cellular localization: Type A and B. Type B HATs are highly conserved, found predominately in the cytoplasm and acetylate newly

translated histones to facilitate their deposition into chromatin (Parthun, 2007). In contrast, the Type A HATs are found within the nucleus and acetylate histones contained within chromatin (Parthun, 2007). Type A nuclear HATs are more diverse than Type B and are categorized into 5 main families according to their homology and acetylation mechanisms. These include: the p300/CREB-binding protein (CBP) family, GNAT family (PCAF, Gnc5, ELP3), MYST family (Tip60, MOZ, MORF), transcriptional factor related HAT family (TAF1, TIFIIIC90), and the nuclear receptor co-activators (p600, SRC1, CLOCK) (Chen et al., 1997; Clements et al., 1999; Delvecchio et al., 2013; Hodawadekar and Marmorstein, 2007). Despite the structural homology amongst many HATs, their sequence homology is limited. However, these HATs all share a structurally conserved Acetyl Coenzyme A binding core, whereby the catalytic mechanism of acetylation is conserved (Delvecchio et al., 2013).

The GNAT family of HATs contains 12 enzymes that acetylate both histone and non-histone proteins. The two main members of this family are GCN5 (general control nonderepressible 5) and PCAF (p300/CBP-associated factor). Intriguingly, GCN5-null mice displayed embryonic lethality, whereas mice lacking GCN5 HAT activity ($GCN5^{hat/hat}$) were viable but exhibited cranial neural tube closure defects, suggesting that the functions of GCN5 extend beyond histone acetylation to include other GCN5 target proteins (Bu et al., 2007; Phan et al., 2005). In contrast, PCAF knockout mice showed no apparent physical phenotype, but presented with defects in learning and memory (Maurice et al., 2008; Yamauchi et al., 2000). Mice with combined loss of GCN5 and PCAF died earlier than GCN5 knockout mice, suggesting synergistic roles between GCN5 and PCAF *in vivo* (Xu et al., 2000). Notably, as both HATs also facilitate non-histone protein acetylation, the reported defects extend beyond a reduction of histone acetylation to

include their effect on non-histone targets as well. For instance, GCN5 knockout in neural stem and precursor cells revealed downregulation of ubiquitin pathway genes, implicating the enzyme as a positive regulator of the proteome (Martínez-Cerdeño et al., 2012). Interestingly, genetic and biomolecular analyses in *Drosophila* have shown a role for GCN5 in the deposition of histone H3 and H4 acetylation marks along entire chromosomes, in addition to its main role in targeted acetylation of histones at specific loci (Ciurciu et al., 2006; Wang et al., 2008a). Notably, since GNAT family members play vital roles in numerous cellular processes including transcription, DNA replication/repair and various cell signaling pathways, they have also been implicated in a range of diseases such as cancer, obesity, and metabolic disorders (Iyer et al., 2012; Sun et al., 2015; Wang and Dent, 2014).

The p300/CBP family of HATS are ubiquitously expressed in mammals and function as transcriptional co-activators for hundreds of transcription factors (Dancy and Cole, 2015; Goodman and Smolik, 2000). Accordingly, they have vital roles in embryogenesis, cellular proliferation and differentiation as they acetylate both histone and non-histone targets, such as the p53 transcription factor (Dancy and Cole, 2015; Goodman and Smolik, 2000; Gu and Roeder, 1997). Homozygous deletion of p300 or CBP in mice results in embryonic lethality with distinct phenotypes indicating that both HATs play diverse functions *in vivo* (Tanaka et al., 2000; Yao et al., 1998). In contrast, many *in vitro* studies with tissue culture cells have demonstrated a significant overlap in p300/CBP functionality, with limited number of differential roles (Kalkhoven, 2004). Consequently, p300/CBP are considered as functional homologs, often referred to as p300/CBP, as they share several conserved domains and overlap in their target genes (Arany et al., 1994). Importantly, p300 in particular, is required during cell cycle

progression and cellular differentiation including that of skeletal muscle. Moreover, various functional modes have been described for p300 as a transcriptional co-activator in which p300 regulates gene transcription via acetylation of histone and non-histone proteins (Fig. 1.1). In addition, p300 can serve as a scaffold to stabilize DNA-bound TFs or as a bridge between TFs and transcriptional pre-initiation complexes (Chen and Li, 2011; Rosenfeld et al., 2006) (Fig. 1.1). Interestingly, p300 has been shown to play an important role for maintaining higher-order chromosome structures by promoting cross-talks between enhancers and promoters, thereby utilizing a multifaceted approach to influence a cell's transcriptional network (Fang et al., 2014).

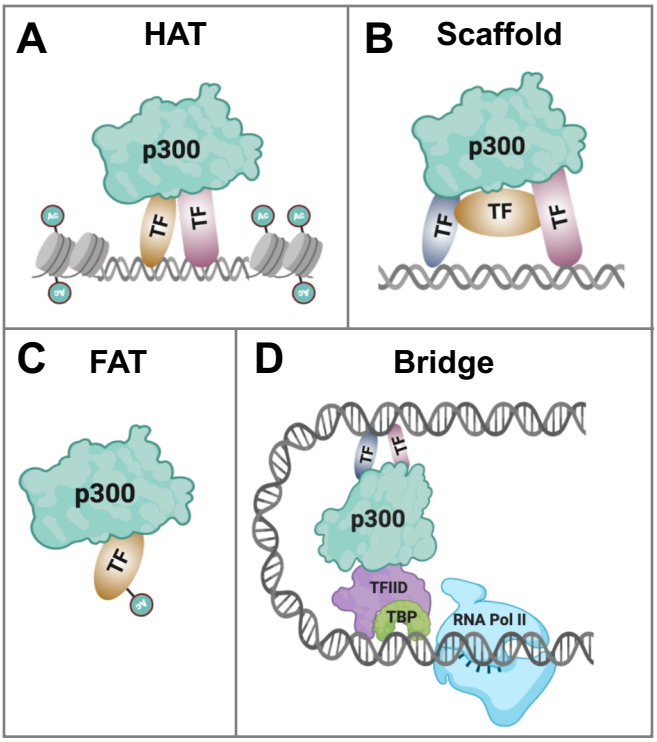

Figure 1.1 p300 is a transcriptional coactivator.

p300 regulates gene transcription by acting as: (A) a histone acetyltransferase (HAT); (B) a transcription factor acetyltransferase (FAT); (C) a scaffold for transcription factors; (D) a bridge to connect transcription factors and the basal transcriptional machinery to activate gene transcription. Adapted from Chen and Li, *Epigenetics*, 2011. Created with BioRender.com

Although p300/CBP are enriched at regions surrounding TSSs and correlate with gene activation (Wang et al., 2009), transgenic mouse reporter assays in combination with ChIP-seq experiments have shown that p300 binding in particular is a strong predictor of enhancers, as well as *in vivo* enhancer activity (Blow et al., 2010; Visel et al., 2009). Notably, inhibition of the p300/CBP bromodomain results in loss of H3K27ac specifically, from enhancers (Raisner et al., 2018). Relatedly, Raisner *et al.* revealed that H3K27ac is causative of, and not just correlative with enhancer activity as the p300/CBP bromodomain is critical for H3K27ac at enhancers where

repression of the modification dramatically diminished enhancer activity (Raisner et al., 2018). Furthermore, using p300/CBP and PCAF/GCN5 double knockout cells, Jin *et al*. demonstrated that PCAF/GCN5 are specifically required for H3K9ac whereas and p300/CBP target acetylation of H3K18/27 instead (Jin et al., 2011). Moreover, p300/CBP were required for the bulk of H3K18ac/H3K27ac and subsequent recruitment of RNA Pol II in double null mouse embryonic fibroblasts while acetylation of other histones residues was unaffected (Jin et al., 2011). Accordingly, genomic co-localization of p300 and H3K27ac is a widely used approach to identify cell-type-specific enhancers (Choi et al., 2016; Raisner et al., 2018). Interestingly, p300 is also greatly enriched at super-enhancers (SEs), defined as large clusters of enhancers that uniquely regulate lineage-specific gene transcription and consequently define cell identity (Whyte et al., 2013). Several recent studies have also implicated p300 as a reliable mark of SEs activated during cell transition states (Lee et al., 2019; Sen et al., 2019; Witte et al., 2015), further indicating an important role for p300 in lineage-specific gene expression. Furthermore, *Sen et al*. found that p300, but not CBP, induces a hyper-acetylated chromatin state in activation of enhancers for a senescence-specific gene expression program (Sen et al., 2019). However, since p300 has also been associated to acetylation of H3K56 in HeLa cells (Das et al., 2009) and to an increased H3K9 acetylation in primary hepatocytes (Bricambert et al., 2010), it is important to note that histone acetylation targets and cellular functions can be affected strongly by specific experimental approaches and cell type or system under study. Regardless, p300 is recognized as a strong predictor of enhancers and is associated with the function of tissue-specific TFs in lineage commitment (Puri et al., 1997b, 1997a).

1.4 Histone-modifying enzymes – Histone deacetylases

HDACs act as functional antagonists of HATs as they facilitate removal of acetyl groups. Loss of acetylation restores the positive charge of lysine residues which stabilizes the histone-DNA interaction and consequently, results in transcriptional repression. HDACs also deacetylate lysine residues on non-histone proteins including TFs that may be maintained in a deacetylated state in the absence of certain environmental cues (Shahbazian and Grunstein, 2007). Similar to HATs, HDAC proteins lack DNA-binding activity and are recruited to target genes via TFs or as part of large multiprotein complexes (Ruijter et al., 2003). As such, the association of HDACs to specific loci is dependent upon cell identity, distinct gene programmes, and the availability of partnering proteins.

Mammalian HDACs are classified into four broad classes based on their sequence similarity to their yeast counterparts (Class I, IIa, IIb, IV). Class I HDACs are ubiquitously expressed nuclear enzymes, whereas Class II HDACs shuttle between the nucleus and cytoplasm and have tissue-specific expression and functions. Class IV contains only HDAC11, which shares sequences similarity to both Class I and II proteins. Sirtuins represent Class III HDACs which require the NAD^+ cofactor for activity, contrasting to HDACs from the classical family which are dependent upon Zn^{2+} for deacetylase activity (Gregoretti et al., 2004; Ruijter et al., 2003). Sirtuins regulate many cellular processes including aging, stress response, and metabolism. HDACs are also upregulated in various types of cancers as they reverse chromatin acetylation to alter transcription of oncogenes and tumor suppressor genes (Witt et al., 2009). Their involvement in tumorigenesis has led to the development of many anticancer drugs that target HDACs specifically. Relatedly, the use of HDAC-inhibitors represents not only a promising treatment for

various cancers and non-oncologic diseases, but also provides a small molecule approach for further study of HDAC cellular functions (Marks, 2010; Witt et al., 2009). Hence, the balance between acetylation and deacetylation of histones is a delicate system in regulating gene expression. A disruption in this balance can lead to abnormal stability of chromatin structure, gene expression, and ultimately, epigenetic disease. Consequently, the control of HAT and HDAC activities is crucial for precise and timely expression of tissue-specific genes associated with development and function (Di Gennaro et al., 2004; Vahid et al., 2015).

2. Transcriptional regulation of skeletal myogenesis

As studies continue to highlight epigenetic control of gene expression as an important mechanism of numerous cellular processes, further research is warranted to uncover the role of epigenetics in tissue-specific processes and their diseased states (Berger, 2007). Since the regulatory networks underlying skeletal muscle development have been well characterized, myoblast differentiation provides a well-defined model system to study mechanisms of transcriptional regulation. In this section, we consider the genetic and epigenetic mechanisms involved in the establishment of the myogenic lineage and aim to summarize findings of how lineage-specific information encoded in chromatin can drive muscle stem cells through the different stages of myogenesis.

With approximately 640 muscles, skeletal muscle is the largest tissue by mass in the human body. Skeletal muscle is essential for functions including breathing, execution of voluntary movements, and its less appreciated but essential purpose, as a reserve for nutrients (Janssen et

al., 2000). Skeletal muscles are composed of bundles of striated myofibers each containing hundreds to thousands of individual myonuclei. These myofibers are arranged in parallel and are contained within a connective tissue network which fastens muscle to bones or to other muscles. Muscle function can be compromised due to a number of conditions including developmental muscular dystrophies, neuromuscular degenerative diseases, or cancers such as rhabdomyosarcomas (Morgan and Partridge, 2020). However, development of novel therapies to treat the various modalities of muscle disease are critically lacking. Therefore, our study explores the functional mode of myogenic regulatory elements and transcriptional regulators to promote muscle-specific gene expression in the goal that understanding the epigenetic signaling underlying skeletal muscle formation will provide value for future treatments targeting muscle disease and function.

2.1 The role of myogenic regulatory factors in skeletal myogenesis

The transition from myogenic progenitor cells to mature skeletal muscle is regulated by a complex network of signaling pathways. However, the process is principally coordinated by the sequential expression of basic helix-loop-helix (bHLH) proteins Myf5, MyoD, myogenin and MRF4, aptly termed myogenic regulatory factors (MRFs) (Braun et al., 1989; Davis et al., 1987; Rhodes and Konieczny, 1989; Wright et al., 1989) (Fig. 1.2). The first MRF was discovered over three decades ago by Davis, Weintraub and Lassar, whom described how transfection of a particular cDNA could transform fibroblasts and certain differentiated cell types into the skeletal muscle lineage (Davis et al., 1987). They termed this gene *Myogenic Differentiation 1* (*MyoD1*), setting the stage for the subsequent discovery of *myogenin* (Wright et al., 1989) and based upon

sequence homology, *Myf5* (Braun et al., 1989) and *MRF4* soon after (Rhodes and Konieczny, 1989). MRFs share the ability to activate skeletal muscle gene transcription when expressed ectopically in a variety of non-muscle cell types. However, MyoD was able to induce *de novo* myogenic gene expression most strongly, and is thus identified as the master regulator of skeletal muscle (Conerly et al., 2016; Davis et al., 1987; Edmondson and Olson, 1993).

Cooperating with additional lineage-specific factors, MRFs play an essential role in myogenesis with precise spatio-temporal expression in both the specification of "founder" cells to a skeletal muscle lineage and in governing their transition into myofibers (Fig. 1.2). As such, MRFs are divided into early factors including Myf5 and MyoD, which are expressed in proliferating myoblasts, while myogenin and MRF4 are considered late factors, that are increasingly expressed as myoblasts differentiate and proceed into fusion (Bergstrom and Tapscott, 2001; Rudnicki and Jaenisch, 1995) (Fig. 1.2). Subsequent studies revealed a role for MyoD during terminal differentiation and of MRF4 in the commitment of MPCs, highlighting the complex nature of the regulatory network of MRFs (Kassar-Duchossoy et al., 2004; Rawls et al., 1995). Moreover, MRF regulation is highly intertwined, with MyoD and myogenin able to participate in autoregulation and cross-regulation of one another (Edmondson et al., 1991; Naidu et al., 1995). MRF4 however, has no auto-activation role, yet can be activated by all other MRFs (Sirri et al., 2003).

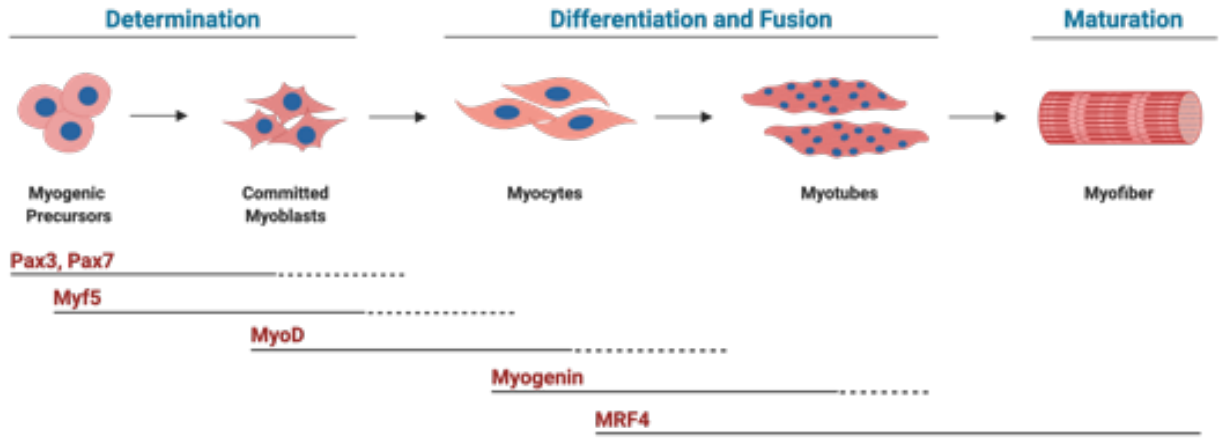

Figure 1.2 Sequential expression of MRFs regulates skeletal myogenesis.

Pax3 and Pax7 are initially expressed in embryonic myogenic progenitors. Over the course of myogenesis, expression of Pax3 and Pax7 is gradually lost, as Myf5 and MyoD expression is increased to promote proliferation and differentiation of myoblasts. Subsequently, myoblasts upregulate myogenin and differentiate into myocytes which upregulate MRF4 to form myotubes. The expression of Mrf4 also facilitates maturation of myotubes into myofibers. Created with BioRender.com.

Myf5 and MyoD are the first MRFs to be expressed during development and play overlapping roles in the commitment of MPCs to the skeletal muscle lineage (Bergstrom and Tapscott, 2001). Knockout studies in mice have revealed that *MyoD*$^{-/-}$ animals had physiologically and functionally normal skeletal muscle due to the compensatory effect of upregulated *Myf5* expression (Rudnicki et al., 1992). Comparatively, *Myf5*$^{-/-}$ animals died shortly after birth from respiratory failure due to a malformed ribcage, yet similar to MyoD-null animals, they had relatively normal skeletal muscle (Braun et al., 1992). *Myf5:MyoD* double-knockout mice however, displayed a complete loss of myoblasts and consequently, skeletal muscle, with MPCs that retained the ability to adopt non-muscle fates. These precursors also failed to activate

*myogeni*n expression, unlike *Myf5*$^{-/-}$ or *MyoD*$^{-/-}$ individual knockout mice, suggesting functional redundancy between Myf5 and MyoD in the activation of myogenin expression (Braun et al., 1992; Rudnicki et al., 1992, 1993). Importantly, the presence of MRF4 was not sufficient for normal tissue development in *Myf5:MyoD* double-knockout mice, suggesting that its function is intertwined with additional MRFs (Kassar-Duchossoy et al., 2004). These experiments also demonstrate that expression of at least Myf5 or MyoD is required for the development of muscle tissue. Notably, myogenin-null mice had normal *MyoD* expression but displayed a complete loss of skeletal muscle and death shortly after birth despite the presence of normal committed myoblasts, indicating that there is no compensation mechanism available for myogenin in the regulation of myoblast terminal differentiation (Hasty et al., 1993). Additionally, MPCs lacking MRF expression altogether are forced to adopt other non-myogenic fates (Gayraud-Morel et al., 2007). Taken together, decades of myogenic studies have highlighted the complexity of the transcriptional mechanisms underlying skeletal myogenesis and have shown that the proper commitment and development of skeletal muscle requires the coordinated expression of MRFs within multifaceted networks.

Structurally, MRFs share three common domains: (1) a cysteine/histidine rich transactivation domain near the N-terminus, which is followed by (2) a basic domain linked to a helix-loop-helix region and (3) a serine/threonine-rich domain, located near the carboxyl terminal (Puri and Sartorelli, 2000). The bHLH domain in particular is considered the main contributor to myogenesis as it facilitates heterodimerization with the ubiquitously expressed Class I bHLH E-proteins including E12, E47, and HEB/HTF4 (Lassar et al., 1991). As Class II HLH proteins, MRFs are characterized by tissue-specific expression and dimerization with other HLH proteins

facilitates a stable protein-DNA interaction (Massari and Murre, 2000; Shklover et al., 2007). Importantly, the conserved basic domain directs DNA binding to a consensus E-box (CANNTG), a specific DNA motif present in the promoter and enhancer regions of muscle and non-muscle specific genes. Due to the widespread presence of E-boxes, with approximately 14 million sites in the mouse genome, various studies have examined the determinants of E-box-associated TF specificity (Chang et al., 2015; Fong et al., 2012; Gordân et al., 2013; Heidt et al., 2007). Accordingly, Fong *et al*. surveyed the genomic distribution of two bHLH E-box-associated proteins, MyoD and NeuroD2 (Fong et al., 2012). The authors revealed that binding of both factors to shared E-box sites was associated with regional epigenetic modifications, specifically of H4 acetylation (Fong et al., 2012). In contrast, binding of either MyoD or NeuroD2 alone was predominantly associated with gene transcription. Furthermore, investigation of E-box-associated TFs including MyoD and Twist2 revealed that TF binding is cumulatively modulated by E-box accessibility, central dinucleotide pair and flanking sequences, which may vary between biological systems and conditions (Cao et al., 2010; Fong et al., 2012; Li et al., 2019). Thus, the myogenic program may be governed genetically by E-box components which determine factor binding specificity, but tissue lineage regulates the availability of specific E-boxes. As such, epigenetic control of E-box accessibility directly regulates the transcriptional response of E-box associated factors as required for gene expression (Fong et al., 2012). Interestingly, the biological reason underlying shared binding sites remains unclear, but some have hypothesized that histone modifications at many of these sites may contribute to yet unknown functions related to nuclear compartments or architecture (Fong et al., 2012). Collectively, since MRFs recognize and bind highly similar DNA sequences, how each factor is

specifically recruited to regulatory regions of target genes and how each factor differentially regulates transcription at a given locus remains unclear.

Although the MRFs Myf5 and MyoD, as well as class I E-proteins, are expressed in proliferating myoblasts, they may not activate transcription due to the presence of a group of proteins termed, inhibitor of differentiation (Id). Id proteins bind to MRFs/E-proteins and prevent their binding to DNA, ultimately halting the progression of differentiation. Given this, the downregulation of Id proteins is an important step required for differentiation to proceed (Sartorelli and Caretti, 2005; Tapscott, 2005). Similarly, other HLH TFs including Twist, MyoR, Myst-1, ZEB and I-mfa proteins influence the balance between differentiation and proliferation either by direct association with MRFs or by obstruction of their binding sites (Puri and Sartorelli, 2000). Additionally, members of the Mef2 and serum response factor (SRF) families of MADS-box transcription factors also act as transcriptional activators to co-regulate muscle gene transcription. Although Mef2 proteins have no myogenic potential on their own, they can augment myogenesis in cooperation with other MRFs by positively regulating MyoD, myogenin and MRF4 (Jin et al., 2016; Naidu et al., 1995). Similarly, MRFs have been shown to trans-activate Mef2 expression as well (Dodou et al., 2003; Ramachandran et al., 2008). Taken together, numerous transcriptional regulators cooperate to advance individual aspects of muscle development. Understanding the role each factor plays and how it is regulated is essential to fully comprehend the complex signaling pathways that govern developmental processes.

2.2 Embryonic skeletal myogenesis

Nearly all of the skeletal muscles in vertebrate animals originate from the mesoderm, one of the three primary germ layers (McGrew and Pourquié, 1998). The mesoderm is divided into axial, paraxial, intermediate, and lateral plates (McGrew and Pourquié, 1998). Limb and trunk skeletal muscles are derived from the paraxial mesoderm, whereas head and neck muscles originate from the axial, paraxial and lateral plates (Buckingham, 2001; Pu et al., 2015). As the first myogenic transcription factor expressed, paired box 3 (Pax3) guides unspecified mesodermal cells towards the myogenic lineage, forming the first MPCs. Ablation of Pax3 is embryonically lethal, as it is essential for ensuring myogenic potential and survival of progenitors in limb and trunk muscle (Buckingham and Relaix, 2007; Hutcheson et al., 2009). However, Pax3 does not exclusively regulate specification of the muscle lineage, as it is also expressed in the epithelial dermomyotome of the somite which gives rise to other progenitors including the dorsal dermis and endothelium of blood vessels (Ben-Yair and Kalcheim, 2008). Importantly, MPCs expressing Pax3 in the absence of the MRFs maintain their progenitor status and create a foundation for forelimbs, hindlimbs, as well as occipital and cervical mesenchyme (Birchmeier and Brohmann, 2000).

As embryonic development continues, MPCs delaminate from the dermomyotome and migrate to their final destinations including the limb buds (Kahane et al., 2002). The dermomyotome is an epithelial cell layer which gives rise to the skeletal muscles of the myotome, as well as the precursor cells of other skeletal muscles (Kahane et al., 2002). Following this migration, Pax3 induces *Myf5* expression which subsequently upregulates MyoD as Pax3 is downregulated (Endo, 2015). These cells are now determined as myoblasts and all large muscle groups are

established as primary myogenesis is completed by ~E14.5. As secondary myogenesis begins at ~E16.5, *Myf5/MyoD* expressing fetal myoblasts proliferate and subsequently upregulate myogenin and MRF4 as they enter the differentiation program (Endo, 2015). These myoblasts then fuse into pre-existing primary fibers or may even use primary fibers as a scaffold to build *de novo* secondary myofibers, which then form the majority of murine muscle (Endo, 2015).

As the central part of the dermomyotome loses its epithelial structure at approximately E10.5, $Pax3^{+}/Pax7^{+}$ proliferating progenitors migrate downward to the myotome as well (Buckingham and Relaix, 2007). The cells that lose *Pax7* expression are determined as myoblasts via the expression of Myf5 and Myod and subsequently contribute to myotome growth. A subset of the population retains $Pax3^{+}/Pax7^{+}$ expression and does not differentiate even as they are localized within the growing myocyte population in the myotome. These cells instead provide a reserve cell population for muscle growth during development and give rise to adult stem cells known as satellite cells (SCs). As the basement membrane is formed, SCs migrate to the space between the membrane and muscle fiber and provide a reserve population for muscle regeneration in adults (Buckingham and Relaix, 2007; Endo, 2015).

Signaling molecules secreted by tissues surrounding the dermomyotome are also crucial for MRF spatial distribution and myogenic specification. Sonic hedgehog (Shh) and Wnt (Wnt1/Wnt3) signals from the notochord, neural tube and dorsal ectoderm induce Myf5 expression and hence the myogenic fate in the epaxial dermomyotome (Gustafsson et al., 2002; Tajbakhsh et al., 1998). In contrast, Wnt7 directly activates MyoD in the hypaxial dermomyotome (Cossu et al., 2004), whereas bone morphogenetic protein 4 (BMP4) antagonizes

Wnt7 activity to prevent premature MyoD expression (Hirsinger et al., 1997). Similarly, Wnt family members including Wnt4, Wnt5a, and Wnt6 also activate Myf5 and MyoD expression. Other important upstream regulators include the sine oculus homeobox (Six) family members, Six1 and Six4, which activate both *Pax3* and *Myf5* expression (Grifone et al., 2007; Relaix et al., 2013). Six1/Six4 together with their cofactors Eya1/Eya2 induce myogenesis via a Pax3-mediated activation of MRFs (Grifone et al., 2007; Relaix et al., 2013). Hence, numerous upstream signaling pathways are required for downregulation of the somitic marker Pax3 and subsequent upregulation of MRFs, as myogenic progenitors transition into the muscle lineage.

2.3 Regulation of post-natal skeletal myogenesis

Derived from MPCs, SCs represent a reservoir of mitotically quiescent, adult myogenic stem cells that are positioned on the surface of the myofiber and beneath the basal lamina (Buckingham, 2006; Wang and Rudnicki, 2011). Essential for adult skeletal muscle regeneration (Lepper et al., 2011; Murphy et al., 2011; Relaix and Zammit, 2012), SCs share the embryonic origins of the muscle they are localized in and follow similar cell fate paths and transcriptional regulation as the muscle formed during embryonic development. Following birth, SCs continue to proliferate and provide new myonuclei for muscle growth via myofiber hyperplasia and hypertrophy up to approximately 3 weeks in mice, after which muscle growth occurs largely via hypertrophy (White et al., 2010). Upon returning to a state of quiescence or G_0, SCs downregulate all MRFs except Myf5, and are marked by high expression of Pax7 and lower levels of Pax3 (Beauchamp et al., 2000; Gayraud-Morel et al., 2012; Koishi et al., 1995).

Though normally quiescent, SCs quickly become activated in response to environmental cues such as exercise, injury or pharmaceuticals which all initially trigger cell proliferation. The degree of proliferation correlates with the extent of the signal from minimal proliferation with daily activities to much longer periods following traumatic muscle injuries (Yablonka-Reuveni, 2011). Notably, activated SCs proliferate for self-renewal (symmetrical) or proliferate followed by differentiation into committed myogenic cells (asymmetrical) to meet the current needs of the tissue. Now termed myoblasts, these committed cells are characterized by a decreased expression of *Pax7* and *Pax3* while *Myf5* and *MyoD* expression is upregulated. Approximately 90% of the $Pax7^{+}$ quiescent satellite cells express *Myf5*, suggesting that they are committed to the myogenic lineage and can only divide asymmetrically (Kuang et al., 2007; Relaix et al., 2006; Zammit et al., 2004). Meanwhile, a minority of SCs remain $Pax7^{+}/Myf5^{-}$ and can undergo asymmetrical or symmetrical division (Kuang et al., 2007). In contrast, the $Pax^{+}/Myf5^{+}$ cells localize near the plasma membrane of myofibers to enter the myogenic lineage as they begin to express *MyoD*, which is required for SCs to exit the cell cycle and begin differentiation (Zammit et al., 2004). This progression is enabled by a MyoD-mediated increase in the expression of cyclin-dependent kinase (CDK) inhibitors, including p21/CIP or p27, followed downstream by the repression of E2F-dependent genes, which are required for cell cycle progression (Blais and Dynlacht, 2004; Dhawan and Rando, 2005; Zhang et al., 1999). Interestingly, lower *MyoD* expression has been linked to a longer interval between proliferation and differentiation (Yablonka-Reuveni et al., 1999). Subsequent to *MyoD* upregulation, myogenin directs terminal differentiation of SCs into myonuclei (Said et al., 2017). Notably, proliferating myoblasts that are $Pax7^{+}/MyoD^{+}$ can revert to a $Pax7^{+}/MyoD^{-}$ status as *Pax7* directly suppresses the transcriptional activity and stability of *MyoD* (Olguin et al., 2007). These cells return to quiescence to maintain the stem cell pool

(Kuang et al., 2007). Although SCs can suppress *MyoD* expression to halt the differentiation pathway, myogenin expression inhibits *Pax7* expression to ensure terminal differentiation, demonstrating a reciprocal inhibitory mechanism between *Pax7* and the MRFs (Olguin et al., 2007).

As myoblasts transition through differentiation, they migrate and subsequently either fuse to pre-existing myofibers (hypertrophy) or less commonly, fuse together to form new myofibers (hyperplasia). The remaining SCs undergo self-renewal and maintain the muscle stem cell reservoir. The combination of proliferation and differentiation thus maintains the stem cell population and sustains postnatal muscle repair and growth (Dhawan and Rando, 2005; Wang and Rudnicki, 2011). Interestingly, although SCs are quite abundant in early postnatal life, accounting for approximately 30% of the nuclei underneath the basal lamina, their numbers gradually decrease to approximately 5% in adult skeletal muscles, irrespective of the health status of patients (Cheng et al., 2014; Shefer et al., 2006). This is attributed to the anti-apoptotic role of Pax7 where SCs die in the absence of Pax7, leading to muscle atrophy. The process cannot be prevented via Pax3 expression, indicating that Pax3 cannot compensate for the role of Pax7 in SCs (Kuang et al., 2007; Relaix et al., 2006).

2.4 Epigenetic regulation of skeletal myogenesis

The organization of postnatal muscle growth and regeneration has been widely used to study the cellular and molecular mechanisms underlying skeletal myogenesis. Numerous experimental models of muscle injury have provided *in vivo* simulations of the innate mechanisms of muscle

injury and repair. However, studying the epigenetic regulation of muscle regeneration in adults has proven to be a difficult task as SCs reside in a tightly controlled environmental niche required to maintain quiescence. Isolation and amplification of these cells in culture or the use of myogenic cell lines introduces a quiescence-proliferation artifact, which may not accurately represent true *in vivo* biology. Also, SCs are present in small numbers and it is often difficult to isolate enough cells for various experimental applications. Thus, the majority of molecular epigenetic studies, including ours have utilized immortalized C2C12 myoblasts, a non-transformed myogenic cell line obtained by continuous passaging of primary myoblasts (Yaffe and Saxel, 1977). C2C12 myoblasts are proliferating myoblasts that are more tolerant to genetic manipulation and represent a more homogenous population of muscle progenitor cells compared to primary myoblasts (Asp et al., 2011; Burattini et al., 2004). Gene expression studies in this widely used model have shown that C2C12 myoblasts closely represent the expression profile of primary myoblasts (Blais et al., 2005; Cao et al., 2010). Consequently, the epigenetic changes governing the transition from myogenic proliferation to terminal differentiation are better understood compared to the regulation of quiescent SCs and their activation. Nonetheless, various *in vitro* and innovative *ex vivo* studies have advanced our understanding of the epigenetic regulation of skeletal myogenesis, as discussed below (Akhtar-Zaidi et al., 2012; Dunham et al., 2012; Ji et al., 2015; Kundaje et al., 2015).

Epigenetic regulation plays an important role in governing gene expression programs of skeletal myogenesis including adult muscle regeneration. Notably, a significant feature of SCs in the quiescent state is the inhibition of myogenic genes which is mediated in part by deposition of H3K27me3 by the methyltransferase, Ezh2 (Asp et al., 2011; Caretti et al., 2004). In contrast, the

Pax7 promoter in quiescent SCs is enriched for H3K4me3 to ensure active expression of *Pax7*. Interestingly, Liu *et al*. demonstrated that a large number of genes in quiescent SCs are marked by the activating H3K4me3, in addition to repressive H3K27me3 (Liu et al., 2013). The authors identified ~1800 genes, many of which were lineage-specific genes (*Myf5/My*oD), that were marked by such bivalent domains, essentially priming those genes for rapid transcription upon SC activation (Liu et al., 2013). As such, activation of SCs is accompanied by downregulation of Ezh2 as the histone demethylase, UTX, is recruited to myogenic promoters instead to remove H3K27me3, resulting in H3K27 hypomethylation relative to quiescent SCs (Caretti et al., 2004; Faralli et al., 2016). Myogenic genes associated with UTX are subsequently targeted by the Ash2L/MLL2 methyltransferase complex to facilitate HK4me3 deposition. Hence, recruitment of the Ash2L/MLL2 complex to muscle-specific genes such as *Myf5* yields $Pax7^{+}/Myf5^{+}$ cells that transition further towards differentiation (McKinnell et al., 2008). Overall, the shift into differentiation is characterized by the erasure of repressive methylation marks and deposition of transcriptionally permissive modifications at muscle-specific loci. Notably, in coordination with the removal of repressive marks at muscle-specific genes, genes involved in cell-cycle progression or proliferation are inhibited as they become enriched in repressive modifications (Blais et al., 2007).

Skeletal myogenesis is governed by a number of chromatin-associated complexes and histone modifications which regulate the activation or repression of cell-type specific genes. Broadly, myoblast differentiation is accompanied by a global decrease in histone acetylation, specifically H3K9, H3K18, H3K27 and H4K12 acetylation (Asp et al., 2011). Accordingly, muscle-specific gene expression is driven instead by the localized action of HATs in combination with additional

myogenic regulators (Hamed et al., 2013; Khilji et al., 2018). For instance, despite a genome-wide decrease in total histone acetylation, H4 acetylation is augmented, particularly on MyoD target genes (Cao et al., 2010). Moreover, overexpression of myogenin in C2C12 myoblasts amplified hyperacetylation of H4 specifically at loci associated to late muscle genes, such that myogenin may induce chromatin remodeling of MyoD-initiated targets (Du et al., 2012). As such, the global decrease in histone acetylation is likely attributed to a downregulation of proliferation genes, while histone acetylation is increased at a subset of genes important for myogenic differentiation.

Relatedly, the regulatory regions of both *Myf5* and *MyoD* are associated with a differentiation-dependent increase in H3K18 and H3K27 acetylation. This is attributed to the actions of p300/CBP, a key set of HATs that drive myogenic gene expression via localized histone acetylation (Francetic et al., 2012; Hamed et al., 2013). Although p300 and CBP share many functions, genetic inactivation studies have revealed distinct roles for each HAT in skeletal myogenesis, where an increased incidence of haematological malignancies were reported in *CBP* heterozygous null mice compared to *p300* (Kung et al., 2000; Tanaka et al., 1997; Yao et al., 1998). Importantly, p300-null embryonic stem cells were unable to express Myf5 or MyoD coupled with impaired myogenesis, whereas CBP-null cells successfully formed multinucleated myotubes (Roth et al., 2003). Relatedly, p300 has been directly implicated in the regulation of myogenic master regulator, MyoD. As such, Hamed *et al.* utilized ChIP-qPCR to demonstrate significant enrichment of p300 at the MyoD core enhancer region accompanied by an increase in H3K27ac during myoblast differentiation (Hamed et al., 2013). Moreover, chemical inhibition of p300 HAT activity led to a decrease in acetylation of H3K9, H3K18 and H3K27 at *Myod1*

enhancers elements (Hamed et al., 2013). Taken together, these studies demonstrate that p300 is a key player in epigenetic regulation of myogenesis and that the HAT of activity of p300, but not CBP, is specifically required for skeletal myogenesis and MRF gene expression. Although, the importance of p300 for skeletal myogenesis is well established, the functional mode of p300 in transcriptional regulation during early myoblast differentiation remains less clear.

In addition to p300, loss of the HAT PCAF is sufficient to block skeletal myogenesis in mouse embryos (Polesskaya et al., 2001; Puri et al., 1997b; Roth et al., 2003). Both p300 and PCAF cooperate closely to regulate myoblast differentiation as they are recruited by MyoD, forming p300-PCAF-MyoD complexes at MyoD target promoters (Puri et al., 1997b). Interestingly, MyoD itself is a substrate for HAT enzymes, particularly PCAF, which also induces acetylation of myogenic facilitators such as Mef2. Utilizing *in vitro* cellular systems to study role of MyoD, a mechanism was delineated in which PCAF first acetylates MyoD resulting in an increase in its affinity to DNA and also creates an interaction surface that allows for recruitment of other transcriptional coactivators (Dilworth et al., 2004; Puri et al., 1997b). Subsequently, p300 is recruited by MyoD, where it may acetylate H3 and H4 at MyoD target loci to promote myogenic gene expression (Dilworth et al., 2004). Interestingly, while PCAF is required for transcriptional activation by MyoD during the early stages of differentiation, the HAT activity of p300 is required for terminal differentiation and cell fusion (Polesskaya et al., 2001). As such, the role of HATs in myogenesis extends beyond local modifications to chromatin acetylation and directly regulates the transcriptional activity of MRFs. Moreover, the targeting of p300 and PCAF to muscle-specific promoters creates a system for gene activation in which both HATs work cooperatively while playing distinct roles (Dilworth et al., 2004). HAT cooperation is also

evident from studies which have described increased transcription from p300/PCAF-associated loci, whereas PCAF alone was a moderate inducer (Dilworth et al., 2004).

Similar to HATs, HDACs play an important role in the activation and repression of muscle-specific loci during differentiation. The activity of class III HDACs, sirtuins, is dependent on the ratio of cellular [NAD^+]:[NADH]. Hence, SC activation is characterized by a switch from fatty acid oxidation to anaerobic glycolysis which reduces availability of free NAD^+. This results in an overall decrease in the activity of sirtuins such as Sirt1, and permits accumulation of acetylation at muscle-specific genes, which become primed for expression (Ryall et al., 2015). Relatedly, Sirt2 is found in complex with PCAF and MyoD in undifferentiated myoblasts where its ability to deacetylate H3K9 and H3K14 correlates with repression of muscle-specific gene expression (Fulco et al., 2003). Furthermore, since the activities of p300 and PCAF rely on autoacetylation, deacetylation of both HATS by Sirt2 represents an additional regulation by HDACs for fast and reversible fine-tuning of myogenic gene expression (Motta et al., 2004; Santos-Rosa et al., 2003; Thompson et al., 2004). In addition to sirtuins, HDACs 1-5 maintain muscle-specific TFs such as MyoD and myocyte enhancer factor 2 (Mef2) in a deacetylated state in the absence of differentiation-promoting signals (Di Padova et al., 2007; Perdiguero et al., 2009). As such, inactivation of HDAC activity is required for recruitment of myogenic TFs (MyoD, Mef2, myogenin) to their target loci as well as recruitment of HATs and chromatin remodelers to advance the differentiation program (Mal and Harter, 2003; Ohkawa et al., 2007). HDAC activity is diminished either via reduced expression or sequestration in the cytoplasm which permits histone acetylation accumulation and subsequent gene activation (McKinsey et al., 2000). Collectively, the activity of HDACs promotes a hypoacetylated chromatin environment at

muscle-specific loci prior to differentiation initiation. As differentiation begins, HDAC activity is reduced, while acetyltransferases promote hyperacetylation of histones and MRFs, creating a permissive chromatin environment at muscle-specific genes to advance the myogenic program.

2.5 Chromatin remodeling is required for myogenesis

Chromatin-remodeling enzymes are key players in the regulation of transcription, development, and cell cycle processes (Ho and Crabtree, 2010; Wilson and Roberts, 2011). The term remodeling refers to the dynamic and reversable modification of chromatin architecture, including disruption of histone–DNA contacts, movement of histone octamers in *cis* or in *trans* and increased accessibility of condensed genomic DNA to regulatory proteins and restriction endonucleases (Peterson and Workman, 2000). Chromatin remodeling is mediated by large multi-subunit, ATP-dependent chromatin remodeling complexes which use the free energy released during ATP hydrolysis to loosen DNA-histone association and enable the movement of nucleosomes from the DNA. The resulting alteration of chromatin structure promotes access for regulatory proteins and subsequent transcription. Both myogenic regulatory factors, Myf5 and MyoD, have the capacity to recruit chromatin-remodeling complexes to their target genes. Notably, both Myf5 and MyoD share two conserved regions (cysteine–histidine rich region and carboxy-terminal region) that differ from the corresponding regions of myogenin (Bergstrom and Tapscott, 2001; Gerber et al., 1997). This conservation between Myf5 and MyoD confers them the ability to promote open chromatin formation at previously silent muscle-specific loci via the recruitment of remodelers such as SWI/SNF (switch-sucrose non-fermentable), while myogenin promotes transcription of genes that have already been primed (de la Serna et al., 2005; Singh

and Dilworth, 2013). Moreover, SWI/SNF recruitment to myogenic loci is dependent upon the phosphorylation of its BAF60 subunit by the p38 kinase (Penn et al., 2004). Activation of the p38 pathway facilitates MyoD binding and recruitment of SWI-SNF and the RNA Pol II preinitiation complex to muscle-specific loci, setting the stage for gene activation (Penn et al., 2004; Simone et al., 2004). Inhibition of p38 was shown to prevent SWI–SNF recruitment and impeded muscle gene expression without modifying MyoD binding or recruitment of HATs (de la Serna et al., 2001). Given this, initiation of the myogenic program is nullified in the absence of a functional SWI/SNF chromatin-remodeling complex (de la Serna et al., 2001). Interestingly, the SWI/SNF complexes are characterized by the presence of a bromodomain which permits interaction with acetylated histones as well as HAT and HDAC enzymes, representing a coordinated response of chromatin-remodeling activities (Sif, 2004). Taken together, a model emerges in which MRF heterodimers are activated by phosphorylation or acetylation, in cooperation with the Mef2 family, recruiting SWI/SNF and RNA Pol II elongation complexes. DNA is subsequently demethylated and chromatin is hyperacetylated, promoting transcriptionally active myogenic loci.

The positive transcriptional effects of histone acetylation are also mirrored by demethylation of DNA. Studies utilizing the DNA methyltransferase inhibitor, 5-azacytidine, revealed an increased ability of fibroblasts to transdifferentiate into myoblasts. This effect was later attributed to demethylation of the MyoD promoter, a key target of DNA methylation in the control of myogenesis (Brunk et al., 1996; Jones et al., 1990). Since these pioneering experiments, DNA methylation has been recognized as one of the major repressive mechanisms regulating myogenic loci (Taylor and Jones, 1979). Mechanistically, DNA methylation refers to

the addition of a covalent methyl group to the 5′ position of a cytosine residue that in mammals, occurs almost exclusively in the context of CpG dinucleotides (Geiman and Robertson, 2002). It is estimated that as much as 80% of all CpG dinucleotides in the mammalian genome may be methylated (Jiang et al., 2004). In contrast, promoter regions of active genes are characterized by unmethylated CpG residues (Jang et al., 2017). DNA methylation at CpG sites is carried out by DNA methyltransferases (Dnmts) 1, 3a and 3b (Jones and Liang, 2009; Okano et al., 1999). Dnmt3a/Dnmt3b are responsible for initial installation of methylation patterns during embryogenesis, although all three Dnmt types are required for embryonic development (Li et al., 1992; Okano et al., 1999). There amount of data pertaining to the function of Dnmts during myogenesis is limited. However, studies have shown a maximal genome-wide demethylation following 48-hours of differentiating in mouse myoblasts, followed by a gradual remethylation (Jost et al., 2001). Moreover, demethylation of the MyoD distal enhancer and myogenin promoter are required for SC proliferation and differentiation (Lucarelli et al., 2001; Palacios and Puri, 2006). Muscle-specific Dnmt1 in particular, has been implicated in skeletal myogenesis as it is significantly upregulated in myotubes (Aguirre-Arteta et al., 2000). Liu *et al.* revealed that loss of Dnmt1 results in reduced expression of myogenic genes as well as impaired myogenic differentiation (Liu et al., 2016). This effect was attributed to the methylation and inhibition of *Id-1*, which is required for myogenesis to proceed (Liu et al., 2016). Therefore, DNA methylation plays an important role in skeletal myogenesis but the precise mechanisms governing methylation/demethylation remain unclear and the DNMTs and demethylases specific to each phase of myogenesis require further study.

In summary, although myogenesis is controlled largely by the temporal expression patterns of MRF family members, these factors do not act alone. Their association with Pax3, Pax7, and the ubiquitously expressed Six1/Six4 and Mef2 family of TFs adds additional layers of complexity and control to the myogenic program. In addition, the commitment of MPCs, their development into mature myofibers and adult muscle regeneration are all influenced by genetic and epigenetic regulators of chromatin. It has become clear that different epigenetic mechanisms function together to exert tight control over myogenic gene expression, however the precise spatio-temporal networks are not yet clearly defined. Notably, our understanding is thus far limited to only a few histone modifications. As genomic technologies continue to become more advanced and accessible, major strides in understanding these mechanisms will be revealed. Moreover, the vast majority of the mechanisms delineated thus far are based upon 2D cell culture systems which only measure population averages using immortalized myogenic cells, and thus will require future validation using *in vivo* models, as well as single-cell methods which may provide a more thorough understanding of epigenetic heterogeneity.

3. Nuclear Receptor Signaling

The nuclear receptor (NR) superfamily of TFs are a group of ligand-inducible factors that direct regulation of target genes involved in numerous processes from embryonic development, cell proliferation and differentiation, metabolism, and apoptosis. NRs respond to diverse signaling molecules including steroid hormones, lipids, and other small molecules or synthetic ligands (Dawson and Xia, 2012). Since NR activity can be modulated pharmacologically with relative simplicity, they have emerged as fundamental targets for therapeutic development. Relatedly,

NR ligands are currently used in the treatment of a number of diseases, such as retinoic acid in acute promyelocytic leukemia, tamoxifen in breast cancer and thiazolidinediones in type II diabetes (Germain et al., 2006). The success of these molecules in cancer treatment in particular is attributed to their anti-proliferative, pro-apoptotic, and differentiation-inducing effects (Bushue and Wan, 2010). Accordingly, we have found that bexarotene (LGD 1069 or Targretin), a clinically-approved RXR-specific agonist, enhances the specification and differentiation of the myoblast lineage (AlSudais et al., 2016; Le May et al., 2011). Since RXR is a dimerization partner for several nuclear receptors and regulates numerous cellular pathways, delineation of the NR signaling governing skeletal muscle development may allow targeted regulation of gene expression through the application of specific nuclear receptor ligands. Thus, in this section we explore the mechanistic action of NRs as TFs and how activation of RXR may mediate transcription in specific conditions. Our aim is to resolve the role of RXR-signaling in the regulation of myogenic expression during rexinoid-enhanced myoblast differentiation. These studies will create a foundation for the development of novel therapeutic strategies targeting NRs and their associated factors in the context of skeletal myogenesis.

3.1 Classification of Nuclear Receptors

The isolation of the first complete steroid receptor cDNA in 1985 introduced the role of hormone-receptor complexes in transcriptional regulation (Hollenberg et al., 1985). Today, there are 48 known NRs in humans, but several of those receptors remain as “orphans” with no known ligands (Burris et al., 2012; Mangelsdorf et al., 1995). It is unclear whether all of these receptors have distinct ligands, as some NRs are functional in the absence of ligands as well. All NRs in

general share a common structure including an amino-terminal ligand-independent transactivation domain (AF1), a conserved DNA-binding domain, the D domain responsible for nuclear localization, and a carboxy-terminal ligand-binding domain (LBD), which also facilitates dimer formation (Mangelsdorf et al., 1995). The most well-studied NRs include peroxisome proliferator-activated receptor (PPAR), liver X receptor (LXR), retinoic acid receptor (RAR), retinoid X receptor (RXR), farnesoid X receptor (FXR), pregnane X receptor (PXR), thyroid hormone receptor (THR), and vitamin D receptor (VDR). Depending upon the mode of action attributed to each NR, they can be grouped into four subtypes. Type I receptors are sequestered in the cytoplasm by chaperone proteins such as HSP90, and are released upon ligand binding allowing for receptor dimerization, nuclear localization sequence recognition and eventual entry into the nucleus (Echeverria and Picard, 2010). The ligand-receptor complex is then able to associate with transcriptional-coactivators that facilitate binding at the regulatory regions of NR target genes . Genome-wide studies have shown that NR binding sites are generally located distal to the TSS of target genes (Deblois and Giguère, 2008; Stender et al., 2010). Type I receptors include the androgen receptor (AR), the estrogen receptor (ER), and the progesterone receptor (PR). In contrast, type II receptors reside in the nucleus in the absence of their ligands and are constitutively bound to their target DNA response elements (Fig. 1.3). However, without the ligand bound, type II NRs associate with nuclear receptor co-repressors (NCoR) and/or silencing mediator of retinoid and thyroid hormone receptors (SMRT) corepressor complexes, which cooperate with HDAC enzymes to repress gene expression (Chen and Evans, 1995; Hörlein et al., 1995; Watson et al., 2012). Upon ligand binding, the NR conformation shifts to release the corepressor complexes and instead associates with coactivator complexes which include HATs such as p300 and PCAF (Glass and Rosenfeld, 2000). Ligands allosterically control chromatin

modifier association to type II NRs by changing the conformation of a short helix known as activating function 2 (AF2) (Glass and Rosenfeld, 2000). AF2 remains in an open conformation in the absence of ligand to allow for association to corepressors. However, in the presence of ligand, AF2 changes conformation, allowing it to directly interact with the ends of a short helix present in coactivator proteins (Nolte et al., 1998). This results in recruitment of coactivators and the release of corepressor proteins (Nolte et al., 1998). Interestingly, different ligands can alter the AF2 conformation in distinct ways to affect transcription (Glass and Rosenfeld, 2000). Type II receptors including VDR, PPAR, THR and RAR generally form heterodimers with the ubiquitously expressed retinoid X receptor (RXR), such that RXR can contribute to gene expression via multiple NRs and signaling pathways (Fig. 1.3). Type III receptors differ from Type I receptors simply in the organization of their hormone response elements (HRE), which are consensus DNA sequences that facilitate NR binding. The HREs for Type III NRs are arranged as direct repeats rather than inverted repeats for Type I receptors. Type IV receptors are unique as they bind as monomers to half-site HREs (Mangelsdorf et al., 1995).

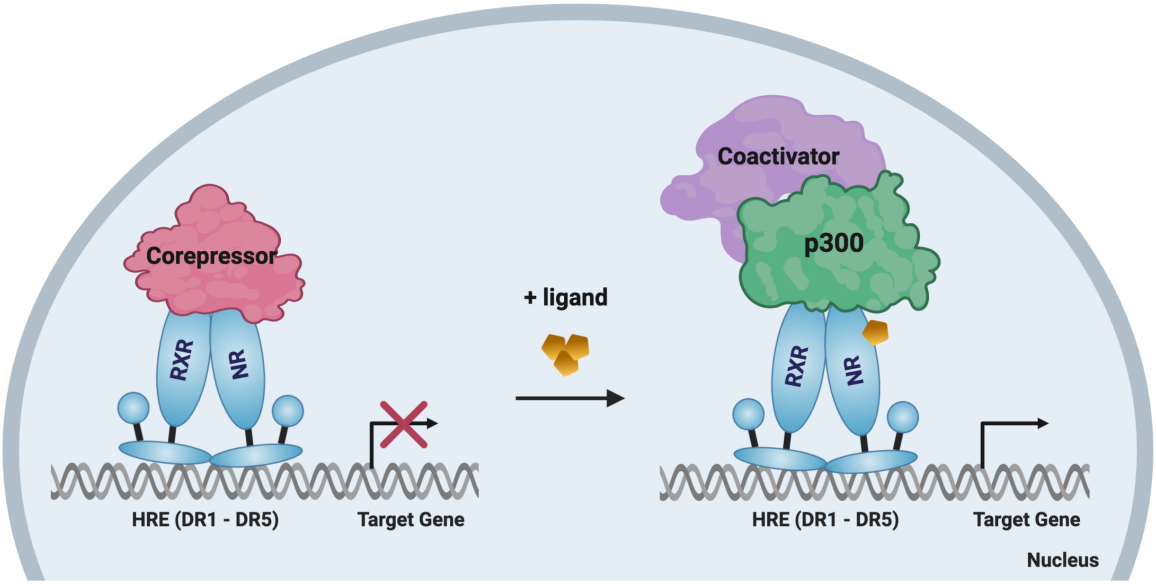

Figure 1.3 Mechanism of RXR signaling.

As a class II nuclear receptor, RXR is constitutively bound to consensus hormone response elements (HREs) as homo- or heterodimers. In the absence of ligand, RXR is bound to corepressor proteins. Ligand binding to RXR or its partner receptor causes a dissociation of corepressors and recruitment of coactivator proteins such as p300. The subsequent recruitment of additional proteins such as RNA polymerase facilitates target gene transcription. Created with BioRender.com.

3.2 Retinoid X Receptors

RXR is an essential member of the steroid hormone superfamily. It is integral to NR signaling as it partners with one third of the 48 other NRs, giving it the ability to modify and converge complex signaling pathways. RXR cooperates with partnering NRs in the form of permissive heterodimers or non-permissive heterodimers, which are ligand-dependent or -independent, respectively (Tanaka and De Luca, 2009). In the form of non-permissive heterodimers, RXR is not activated as the binding of the partner receptor allosterically inhibits RXR (RAR, VDR, TR)

(Bourguet et al., 2000; Gampe et al., 2000; Tanaka and De Luca, 2009). In contrast, permissive heterodimers can be activated by an RXR ligand on its own or by the ligand of the partnering receptor (PPAR, LXR, PXR). Permissive heterodimers also exhibit an additional regulatory feature of a synergistic response with simultaneous ligand activation of both partner receptors (Leblanc and Stunnenberg, 1995). Since RXR is a partner for a large array of NRs, varying levels of dietary lipids play an important role as ligands. In addition, small changes in the concentration of these molecules may lead to robust transcriptional and ensuing biological responses. Thus, the use of RXR ligands, known as "rexinoids", have wide-ranging pharmacological potential as they can be designed to activate single or several heterodimers (Desvergne, 2007; Mukherjee et al., 1997). In contrast, RXR partners in non-permissive heterodimers respond only to their own ligands and permit a transcriptional response that is directly proportional to the level of the activating hormone/ligand (Shulman and Mangelsdorf, 2005).

3.3 Role of RXR in skeletal muscle

RXR has three different isotypes α, β and γ, with at least one type being expressed in each tissue in the body. However, expression levels of these isotypes vary with cell type and differentiation status (Chiba et al., 1997). Tissue wide transcription profiles have revealed that RXRβ is ubiquitously expressed whereas RXRα is the predominant subtype expressed in skeletal muscle and RXRγ predominates in the brain and muscle (Barbosa-Morais et al., 2012). Knockout studies of the individual subtypes have shown that RXRα$^{-/-}$ mice died in utero with ocular and cardiac deformities (Kastner et al., 1994; Krezel et al., 1996; Sucov et al., 1994). Interestingly, RAR$^{-/-}$

fetuses presented with similar myocardium defects, suggesting that RXRα may be required for transduction of the RA signal in myocardial growth (Mendelsohn et al., 1994). In contrast, mice lacking either RXRβ or RXRγ did not display any obvious morphogenetic defects even in the absence of a RXRα allele ($RXR^{+/}$). These studies demonstrate the functional importance of RXRα during embryogenesis as it can compensate for loss of other RXR subtypes, allowing fundamental development processes to occur with a single RXRα allele (Krezel et al., 1996).

Utilizing *in vitro* studies, Zhu *et al*. revealed that all three RXR subtypes are abundantly expressed in committed C2C12 myoblasts (Zhu et al., 2009). Relatedly, treatment with RXR and RAR ligands, 9-cis-retinoic acid (9CRA) and all-trans retinoic acid (ATRA) respectively, induced myogenic differentiation which was synergistically enhanced in the presence of both ligands (Zhu et al., 2009). Moreover, adenoviral vector-mediated exogenous expression of RXRα induced differentiation of cultured myoblasts in a ligand-independent fashion (Zhu et al., 2009). Thus, RXR signaling may be required for skeletal myogenesis both in a ligand-independent and -dependent manner. Our studies have previously shown that bexarotene, an agonist specific for RXR, contributes to the specification of the skeletal muscle lineage and enhances myogenic differentiation through the function of RXRα as a TF (AlSudais et al., 2016; Le May et al., 2011). However, given the large selection of genes targeted by RXR, its genetic targets in myogenic progenitors are unclear. Additionally, how bexarotene influences myogenic gene expression to augment myoblast differentiation and fusion is yet to be determined.

3.4 Transcriptional regulation via nuclear receptors

As TFs, NRs bind to a consensus DNA sequence termed a HRE, commonly consisting of two half-sites that are specific to the NR. HREs are characterized by the DNA sequence of each half-site, the number of base-pairs between half-sites and the relative orientation of the half-sites. Genome-wide studies on NR binding have shown that approximately 70% of NR binding events contain a recognizable HRE, indicating a substantial portion of NR binding may involve interaction with other DNA-binding factors (Deblois and Giguère, 2008). An important feature of HREs is the length of the spacer defined by 0-5 bases (DR0-DR5) organized as direct repeats (DR), inverted repeats (IR), everted, palindromic, or even disordered. Hence, the binding NR dimer must recognize the sequence, spacing and orientation of the HRE for maximal affinity (Claessens and Gewirth, 2004; Cotnoir-White et al., 2011). Although DR spacer length was originally defined as the key determinant of DNA-binding specificity, there are limitations to this model as the number of NRs compared to spacer lengths suggests that either HREs can bind multiple types of NR dimers and/or that there are additional determinants of NR binding specificity beyond spacer length (Penvose et al., 2019). To understand the mechanisms underlying NR-HRE binding specificity, Penvose *et al*. recently utilized comprehensive protein-binding microarrays (PBMs) to compare the binding of 12 NR:RXRα dimers to 1600 unique sequences at each DR spacer length (Penvose et al., 2019). They found that NR-binding differences may result from variable mechanisms such as nucleotide preferences, DNA-binding-mode differences, as well as DR-spacing preferences. Interestingly, they observed that NRs can bind similarly on one DR spacing, while having distinct binding preferences for another DR spacing. Importantly, they integrated reporter gene experiments with PBMs to show that DR spacer preferences more closely reflect NR binding site activity rather than NR affinity (Penvose

et al., 2019). Moreover, since NR binding is also influenced by cofactor proteins, as well as tissue specific expression of other NRs and TFs, future studies aimed at studying the regulation of gene expression by NRs will need to consider the impact of cooperating TFs and cofactors for NR-binding mode, affinity, and activity in specific biological contexts.

As TFs, NRs regulate an array of biological processes. Underlying their function is the ability to interact with DNA, recruit chromatin modifiers and thus regulate gene transcription. A key to this mechanism is the relationship between NRs and lineage-determining tissue-specific transcription programmers that open the chromatin environment to provide access to additional signaling factors (Heinz et al., 2010). For instance, LXRs can interact with macrophage lineage determining factors including AP-1, whereas they also cooperate with hepatocyte lineage determining factors HNF4 and C/EBPα (Boergesen et al., 2012; Heinz et al., 2010). The binding of NRs to tissue specific sequences in each case is thus governed by the presence of lineage-controlled factors such that one NR is able to govern distinct transcriptional networks based upon the specific cell type (Heinz et al., 2010; Miranda et al., 2013). Since RXR-selective signaling promotes specification to the skeletal muscle lineage, the identity of myogenic factors that cooperate with RXR to enhance skeletal myogenesis remains to be determined (AlSudais et al., 2016; Le May et al., 2011).

3.5 RXR and transcriptional coactivators

Due to the constitutive association of type II NRs to DNA, a single bound NR dimer can behave as both a positive and negative regulator of transcription, where the fate of transcription is

dependent upon the presence of ligands which govern recruitment of particular coactivator/corepressor complexes (Bulynko and O'Malley, 2011). The list of coactivators involved in NR signaling includes SRC-1, TIF2, ACTR/RAC3/pCIP and p300 (Dilworth et al., 2000; Glass and Rosenfeld, 2000). Initially shown to function as transcription co-activators for glucocorticoid receptor (GR), RAR and TR, p300 is known to play a role in ERα- and RAR-signaling where transactivation of RAR is defective in p300-null mice (Chakravarti et al., 1996; Dilworth et al., 2000; Kamei et al., 1996; Kraus and Kadonaga, 1998; Yao et al., 1998). RXRs in particular, are also subjects for p300 acetylation, which promotes their binding to DNA, demonstrating the importance of p300 HAT activity for transcriptional initiation by RXR (Daniel et al., 2014; Dilworth et al., 2000; Zhao et al., 2007). Although co-activators play crucial roles in NR signaling, the specific co-activators recruited by each RXR dimer at distinct genetic loci, in response to specific ligands must be resolved.

4. Tmem182 - A novel regulator of myoblast differentiation

Skeletal myogenesis is a complex process requiring precise temporal expression of tissue-specific regulatory and structural proteins. Since a comprehensive understanding of muscle formation is imperative for therapeutic development targeting muscle-related diseases, we used condition-specific gene expression profiling to explore the activation of novel myogenic targets. By concentrating on genes of unknown function with expression profiles similar to myogenic regulators (MyoD and myogenin), we discovered a nearly 3-fold increase in the expression of a predicted transmembrane protein termed Tmem182, during the early stages of myogenic differentiation. Tmem182 was first described by Kuninger *et al*. in a study of novel genes that were induced during growth factor-mediated muscle cell survival and differentiation (Kuninger et al., 2004). Follow-up studies observed a 45-fold upregulation of Tmem182 transcript upon brown preadipocyte to adipocyte conversion, as well as a ~770-fold upregulation upon conversion of C2C12 myoblasts to myocytes (Wu and Smas, 2008). Since Tmem182 displays differentiation-dependent upregulation in myotube formation as well as adipogenesis, its function may be related to cellular pathways shared by both lineages. Notably, Tmem182 knockdown in C2C12 myoblasts resulted in a nearly 30% reduction of myogenin expression, further indicating a role for Tmem182 in a myogenic context (Wales et al., 2014). Interestingly, Tmem182 knockdown in oral squamous cell carcinomal (OSCC) cells reduced their cell adhesion ability towards to fibronectin and overexpression of Tmem182 led to a suppression of their invasion capability (Hsing et al., 2019). These experiments indicate that Tmem182 function may be related to cell motility specifically. Importantly, Hsing *et al*. revealed that these processes were regulated by TNF-α-induced miR-450a expression, which decreased cell adhesion as well as Tmem182 expression (Hsing et al., 2019). Taken together, the protein

sequence of Tmem182 lacks definitive homology with previously defined protein families and its function in any given system remains currently unknown. Therefore, characterization of the *in vitro* and *in vivo* regulation and function of Tmem182 and its potential roles in skeletal muscle development, regeneration, and disease must be determined and will provide further insights into the molecular underpinnings of muscle formation.

5. Rationale and Hypotheses

The importance of p300 in skeletal myogenesis and muscle-specific gene expression has been well established (Polesskaya et al., 2001; Puri et al., 1997b, 1997a). However, the functional mode of transcriptional regulation by p300, particularly at the early stage of myoblast differentiation, remains to be determined.

Given that RXR is a partner for several Type II NRs, it has the potential to regulate a wide variety of cellular processes. Interestingly, we have previously found that bexarotene, a synthetic agonist specific for RXR, promotes the specification and differentiation of the skeletal muscle lineage (AlSudais et al., 2016). Although the three RXR subtypes are highly conserved and functionally interchangeable as heterodimer partners, we have shown that bexarotene promotes myoblast differentiation, specifically via RXRα (AlSudais et al., 2016). However, the role of RXR signaling and how it effects global gene expression to promote myogenic differentiation remains unclear. Relatedly, we have used RXR signaling to identify increased expression of a putative myogenic target, Tmem182, during early myoblast differentiation. However, the cellular or molecular functions of Tmem182 in any given system remain to be determined.

Thus, I hypothesized that:

- p300-associated loci-specific histone acetylation is required for the regulation of myogenic enhancers and hence, myogenic gene expression.
- Rexinoid-enhanced myoblast differentiation is coupled with global changes in gene expression, including an upregulation of muscle-related genes.

- Tmem182 is an important player in skeletal myogenesis and may play a role in myoblast adhesion and migration processes.

The specific aims of this study were to:

(1) study the epigenetic landscape in committed muscle progenitor cells and classify observed patterns of chromatin modifications relevant to the myogenic lineage.

(2) Explore the association of p300 and loci-specific histone acetylation with distinct chromatin states at the onset of myoblast differentiation to further our understanding of the regulation of myogenic enhancers.

(3) Explore the molecular mechanisms underlying bexarotene-enhanced myogenic differentiation and identify genetic targets of RXR signaling in skeletal myoblasts.

(4) Characterize the role of Tmem182 in early myoblast differentiation, regeneration and muscle-related disease.

Chapter Two: Loci-specific histone acetylation profiles associated with transcriptional coactivator p300 during early myoblast differentiation

---

Khilji S., Hamed M., Chen J., Li Q. *Epigenetics*. 2018;13(6):642-654.

Loci-specific histone acetylation profiles associated with transcriptional coactivator p300 during early myoblast differentiation

Saadia Khilji[1, †], Munerah Hamed[1, †], Jihong Chen[2] and Qiao Li[1, 2,*]

[1] Department of Cellular and Molecular Medicine, [2] Department of Pathology and Laboratory Medicine, Faculty of Medicine, University of Ottawa, Ottawa, Ontario, Canada K1H 8M5

* To whom correspondence should be addressed: Tel: +1 613 562 5800 ext. 8488; Email: Qiao.Li@uOttawa.ca

† These authors contributed equally to this work.

Keywords: gene regulation; histone acetyltransferase; p300, histone acetylation; chromatin; stem cell differentiation

Abstract

Molecular regulation of stem cell differentiation is exerted through both genetic and epigenetic determinants over distal regulatory or enhancer regions. Understanding the mechanistic action of active or poised enhancers is therefore imperative for control of stem cell differentiation. Based on the genome-wide co-occurrence of different epigenetic marks in committed proliferating myoblasts, we have previously generated a 14-state chromatin state model to profile rexinoid-responsive histone acetylation in early myoblast differentiation. Here, we delineate the functional mode of transcription regulators during early myogenic differentiation using genome-wide chromatin state association. We define a role of transcriptional coactivator p300, when recruited by muscle master regulator MyoD, in the establishment and regulation of myogenic loci at the onset of myoblast differentiation. In addition, we reveal an enrichment of loci-specific histone acetylation at p300 associated active or poised enhancers, particularly when enlisted by MyoD. We provide novel molecular insights into the regulation of myogenic enhancers by p300 in concert with MyoD. Our studies present a valuable aptitude for driving condition-specific chromatin state or enhancers pharmacologically to treat muscle-related diseases and for the identification of additional myogenic targets and molecular interactions for therapeutic development.

Abbreviations: MRF, Muscle regulatory factor; HAT, Histone acetyltransferase; CBP, CREB-binding protein; ES, Embryonic stem; ATCC, American type culture collection; DM, Differentiation medium; DMEM, Dulbecco's Modified Eagle's Medium; GM, Growth medium; GO, Gene ontology; GREAT, Genomic regions enrichment of annotations tool; FPKM, Fragments per kilobase of transcript per million; GEO, Gene expression omnibus; MACS, Model-based analysis for ChIP-seq

Introduction

Gene expression programs associated with stem cell differentiation are largely regulated through distal regulatory elements characterized as enhancers which can be further defined as “active” or “poised” based on the combinations of condition-specific histone modification (Creyghton et al., 2010; Rada-Iglesias et al., 2011). Studies in hematopoietic stem cells have demonstrated that poised enhancers are established in lineage progenitors before their activation and are involved in gene expression during lineage differentiation . In addition, poised enhancers bivalently marked by H3K4me1 and H3K27me3, are dynamically modified during terminal differentiation and myotube formation where H3K27me3 is replaced by H3K27ac (Asp et al., 2011; Creyghton et al., 2010; Rada-Iglesias et al., 2011).

While histone acetylation events contribute to gene activation, the patterns of acetylation are diverse and distinct depending on the regulatory loci (Eberharter and Becker, 2002; Lee et al., 1993; Roh et al., 2005). A comprehensive mapping of 18 histone acetylation marks in $CD4^+$ T cells revealed that H3K9ac, H3K18ac, and H3K27ac are mainly located in regions surrounding the transcription start sites (TSS), whereas H4K8ac is elevated in promoter and transcribed regions of active genes (Halsall et al., 2012; Wang et al., 2008b). Nonetheless, the correlation of intergenic H3K9ac sites with multiple promoter and enhancer marks has been used to infer that H3K9ac can denote active enhancers as well as bivalent promoters in stem cells (Azuara et al., 2006; Karmodiya et al., 2012). Moreover, a combination of H3K4me1 and H3K27ac can serve as a readout of active enhancers (Creyghton et al., 2010; Heintzman et al., 2009; Rada-Iglesias et al., 2011; Zentner et al., 2011). The regulation of enhancer chromatin state thus interjects specific gene expression programs that govern the potential for cellular differentiation. As such,

we have previously generated a 14-state chromatin state model based on genome-wide co-occurrence of different epigenetic marks in committed proliferating myoblasts to uncover rexinoid-responsive histone acetylation associated with distinct myogenic loci (Hamed et al., 2017).

The differentiation of skeletal muscle precursors is sequentially regulated by muscle regulatory factors (MRFs). MyoD is involved in the initial step of myoblast differentiation, while myogenin is required for terminal differentiation and formation of multinucleated myotubes (Moncaut et al., 2013). The regulatory networks underlying skeletal muscle development have been studied in detail and thus myoblast differentiation provides a well-defined model system to study mechanisms of transcriptional regulation. Remarkably, studies of histone acetylation in the context of terminal differentiation have observed a near-complete loss of H3K9ac in contrast to a high level of H3K18ac on genes activated in myotubes as compared to proliferating myoblasts (Asp et al., 2011; Blum et al., 2012). Furthermore, the association of MyoD to distinct E-box motifs generally corresponds to enhancer assembly, marked by H3K27ac, and muscle-specific gene expression during myotube formation (Blum et al., 2012; Fong et al., 2012). As a result, MyoD binding becomes an index of myogenic enhancers (Creyghton et al., 2010), leading to the recruitment of histone acetyltransferases (HATs) which deposit the acetyl moiety required for enhancer activation (Blum et al., 2012).

One group of HATs, p300 and CREB-binding protein (CBP), are global coactivators of a variety of transcription factors involved in cell proliferation and differentiation (Arany et al., 1994; Chakravarti et al., 1996; Chen and Li, 2011; Goodman and Smolik, 2000). Nonetheless, genetic

studies in mice and embryonic stem cells (ESCs) have clearly shown that the intrinsic HAT activity of p300, but not CBP, is specifically required for skeletal myogenesis and MyoD gene expression (Polesskaya et al., 2001; Roth et al., 2003). Interestingly, depletion of MyoD in myotubes leads to a reduction of H3K27ac particularly, where the majority of myotube-specific enhancers bound by MyoD are co-occupied with p300 (Blum et al., 2012). While H2A and H2B can be acetylated by p300, H3K18 and H3K27 are the major in vivo acetylation targets of p300 (Jin et al., 2011). In addition, overexpression of p300 has been correlated to an increased H3K9 acetylation at distinct loci in primary hepatocytes (Bricambert et al., 2010). Therefore, p300 occupancy is known as the best chromatin signature of enhancers and has emerged as a valuable perception to identify novel regulatory elements for studies of transcriptional control, in addition to DNA sequence motifs (Blow et al., 2010; Heintzman et al., 2007; May et al., 2012; Nègre et al., 2011; Rada-Iglesias et al., 2011; Schwaiger et al., 2014; Shen et al., 2012; Visel et al., 2009).

The importance of p300 for an array of cellular processes including skeletal myogenesis and myotube formation, are well established (Blum et al., 2012; Chan and La Thangue, 2001; Polesskaya et al., 2001; Vo and Goodman, 2001). However, the functional mode of transcriptional regulation involving p300 particularly at the early stage of myoblast differentiation remains less clear, given that lineage-specific enhancers and loci-specific acetylation play a pivotal role in the control of genes pertinent to differentiation. In this study, we explore the association of p300 and loci-specific histone acetylation with distinct chromatin states at the onset of myoblast differentiation to discern the concerted action of MyoD and p300 in regulating myogenic expression.

Results

Residue-specific histone acetylation associated with p300 in early myoblast differentiation

While maintaining a high correlation with transcriptional programs of primary myoblasts, C2C12 myoblasts are less prone to spontaneous differentiation (Asp et al., 2011; Blais et al., 2005), thus become a system of choice for genome-wide studies of histone modification and associated transcriptional regulators, including p300 in myotubes and proliferating myoblasts (Blum et al., 2012). To study the role of p300 in the early steps of differentiation, we performed p300 ChIP-seq analysis in C2C12 myoblasts differentiated for 24 hours in comparison to proliferating myoblasts. As a result, 2,060 and 5,405 high confidence p300 peaks were identified in differentiating and proliferating myoblasts, respectively, through model-based analysis for ChIP-seq (MACS) (Fig. 2.1A, S2.1). Similar to a previous study with proliferating myoblasts (Blum et al., 2012), the majority of p300 read signals had an average peak coverage of about 500 bp (Fig. 2.1B). In addition, a greater number of p300 peaks were found in proliferating myoblasts and approximately 58% of p300 peaks in differentiating myoblasts were shared with that in proliferating myoblasts (Fig. 2.1A), suggesting a role for p300 in the establishment and regulation of muscle-specific loci prior to the commencement of differentiation.

Since p300 HAT activity is critical for myogenic differentiation (Polesskaya et al., 2001; Roth et al., 2003), we first used Western blot analysis to examine changes in the global levels of p300 and histone acetylation during early myoblast differentiation. As shown in figure 2.1C, the expression of myogenin, a specific marker of terminal differentiation, was induced (over 10-fold) by 24 hours of differentiation compared to proliferating myoblasts, but the level of p300 protein remained relatively steady (Fig. 2.1C, D). Interestingly, while there were no significant changes

in the global levels of H3K9ac, H3K18ac, and H3K27ac by 24 hours of differentiation, the levels of H4K8ac increased by about 2-fold (Fig. 2.1C, D). By and large, our analyses indicate that if there is a differentiation-dependent change in the levels of p300 and residue-specific histone acetylation, it may occur in a loci-specific manner rather than globally.

Utilizing our previously established chromatin state model based on the genome-wide co-occurrence of different epigenetic marks in proliferating myoblasts (Hamed et al., 2017), we next annotated different categories of p300 read signals through the progression of myoblast differentiation and found that p300 peaks are predominantly associated with active enhancers (Fig. 2.1E). Nevertheless, p300 signal density appeared increasingly enriched at poised enhancers during early differentiation, as the percentage of p300 peaks assigned to this state increased by about 3-fold, from approximately 5% in unique to proliferation to 15% in unique to differentiation (Fig. 2.1E), suggesting a role for p300 in the activation of muscle-specific loci during early differentiation.

We next used our previously generated residue-specific histone acetylation ChIP-seq data (Hamed et al., 2017), to profile loci-specific changes in histone acetylation during early myoblast differentiation. As shown in figure 2.1E and 2.1F, a differentiation-dependent enrichment was not only observed for H3K18ac and H3K27ac, known acetylation targets of p300 (Jin et al., 2011), but also for H3K9ac and H4K8ac, particularly at differentiation-unique p300 loci compared to that shared by proliferating and differentiating myoblasts. More importantly, the level of H3K9ac had the largest relative increase amongst the four acetylation marks examined, corresponding to a similar degree of increase in p300 signal enrichment (Fig. 2.1E, F).

Therefore, the level of p300 occupancy is intimately associated with loci-specific histone acetylation during early myoblast differentiation.

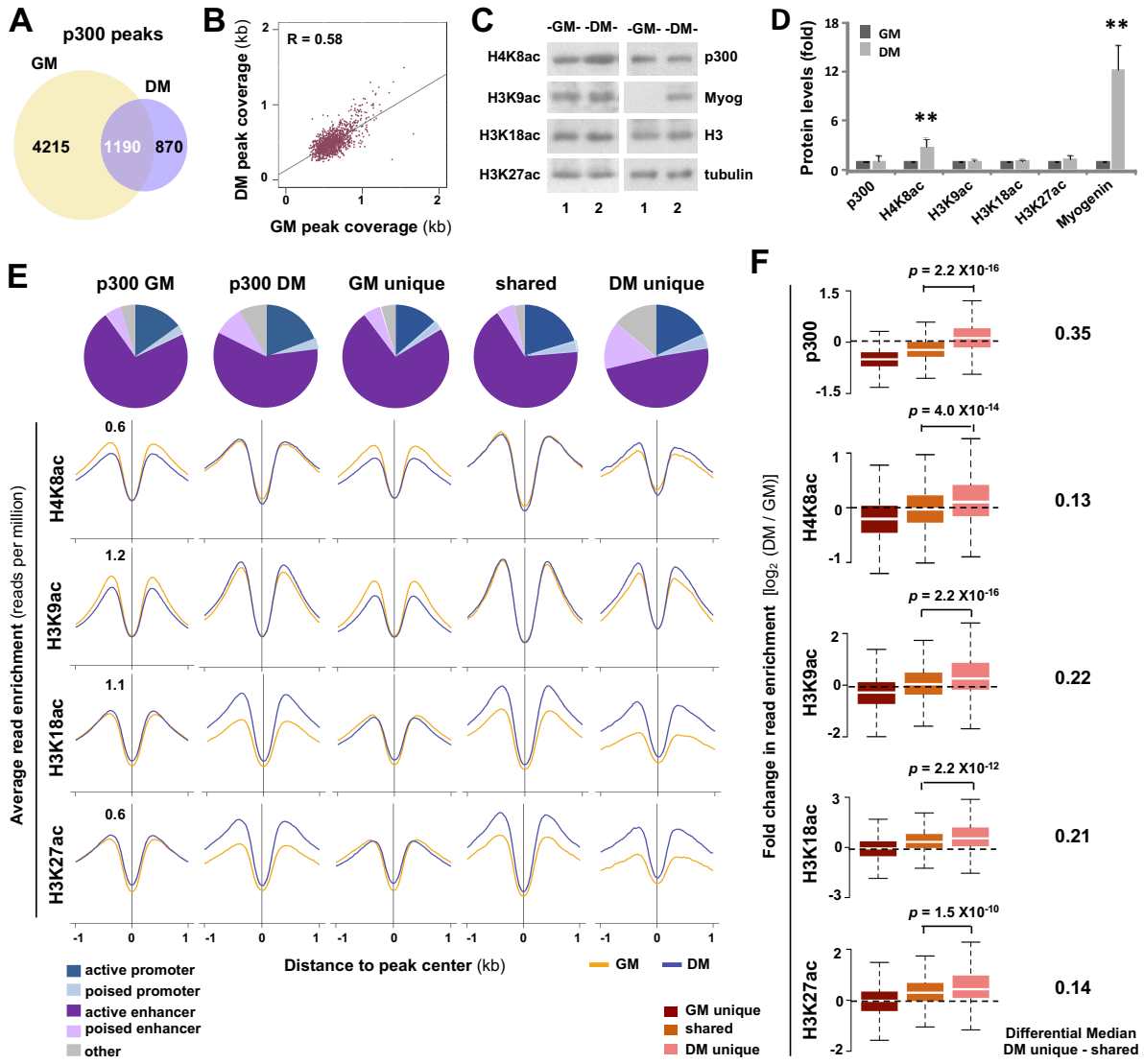

Figure 2.1 Histone acetylation at p300-associated loci in early myoblast differentiation.

A) Union analysis of p300 peaks in proliferating C2C12 myoblasts (GM) and myoblasts differentiated for 24 hours (DM). (B) Correlation plot of p300 peak coverage in proliferating and differentiating myoblasts, where each dot represents the absolute length of a p300 peak shared between GM and DM conditions (n = 1190; R = Spearman's correlation coefficient). (C) Western

analysis of p300, myogenin, and the indicated histone marks with β-tubulin as a loading control. (D) Quantification of the blots in panel C is presented as fold change in relation to proliferating myoblasts (error bars: SD; n = 3; **, $p < 0.01$). (E) Annotation of chromatin state association of the p300 peaks as categorized in Panel A. Shown are also the average read enrichment profiles of H4K8ac, H3K9ac, H3K18ac, and H3K27ac spanning 2 kb across the indicated p300 loci annotated above. (F) Boxplots present $\log_2$-fold change in signal enrichment at the p300 loci. The differential median between enrichment at p300 loci unique to differentiation or shared are displayed to the right (Wilcoxon signed-rank test, $p < 0.05$).

Connection of MRFs with p300 during early myoblast differentiation

To understand functionally the role of p300 in the regulation of early myogenic programs, we next performed GO analysis on shared or unique p300 peaks in relation to myoblast proliferation and differentiation. Interestingly, the GO terms most strongly connected to p300 peaks unique to proliferation were in a broad context of tissue and developmental processes, whereas differentiation-unique p300 peaks were more specifically associated with regulation of signal transduction, protein metabolism and modification (Fig. 2.2A), suggesting a distinct functional mode for p300 in the regulation of muscle development and maintenance processes.

To determine the requirement of p300 for target gene expression, we employed previously established p300 shRNA knockdown myoblasts (Chen et al., 2015). As shown in Fig. 2.2B, the mRNA levels of selected genetic targets identified through our p300 ChIP-seq analysis, increased markedly at the early stage of myoblast differentiation. In addition, the expression of these genes was impeded significantly following p300 shRNA knockdown, suggesting that p300 is required for the expression of these differentiation-dependent genes.

Moreover, *de novo* motif analysis of p300-associated loci revealed that Fra1 and RUNX binding sites were to some extent found amongst all categories examined (Fig. 2.2C). While Six1 motif (Laclef et al., 2003), was predicted for p300 loci shared or unique to proliferation (Fig. 2.2C), Tcf12 (Hu et al., 1992; Zhang et al., 1991) was assigned for p300 loci unique to proliferation. More importantly, MyoD or myogenin binding motifs were found predominantly at p300 loci shared or unique to differentiation (Fig. 2.2C). Taken together, our analyses suggest that p300 may be recruited mainly by MRFs to muscle-specific targets to mediate, at least in part, histone acetylation necessary for switching from proliferation to differentiation.

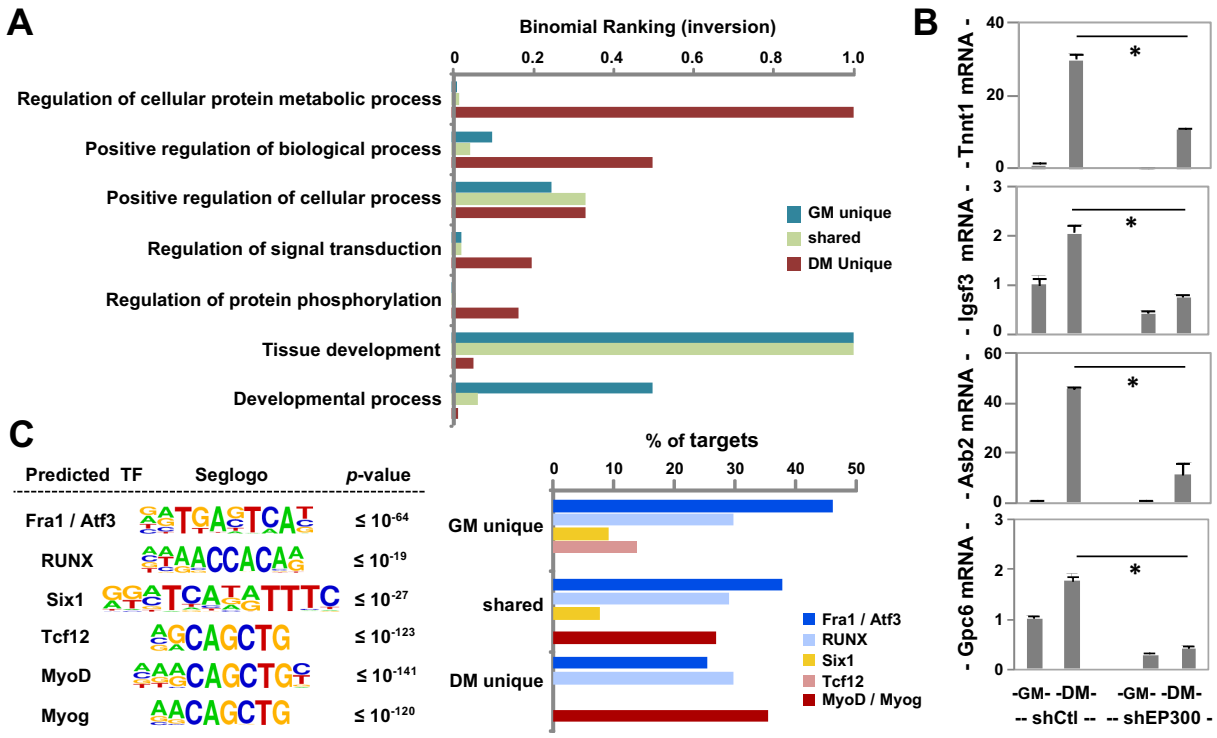

Figure 2.2 Functional annotation of p300-associated loci.

(A) GO enrichment analysis of p300-associated loci. Bar graph represents an inversion of binomial ranking for each term as output by GREAT. (B) RT-qPCR analysis of gene expression levels for p300-dependent differentiation responsive targets is presented as fold change relative to proliferating myoblasts, after normalization to internal control (error bars: SEM; n = 3; *, $p < 0.05$). (C) *De novo* motif analysis of p300 loci, where top-ranked motifs are displayed with *p*-values for the motifs being equal to or lower than the one stated in each category. Percentages of p300 loci bound by the predicted transcription factor motifs are presented as a bar graph to the right.

Condition-dependent chromatin state distribution of MyoD during early differentiation

Since MyoD is a master regulator of myogenesis, plays a pivotal role in enhancer assembly (Blum et al., 2012), and may cooperate with p300 to promote early myoblast differentiation (Fig.

2.2B), we thus also annotated publicly available genome-wide MyoD ChIP-seq data in proliferating C2C12 myoblasts and myoblasts differentiated for 24 hours (Yue et al., 2014). Union analysis of MyoD binding sites across the two conditions revealed twice as many MyoD peaks unique to differentiation compared to proliferation (Fig. 2.3A), highlighting the requirement of MyoD to control the transcriptional program pertinent to differentiation. Similar to p300, MyoD peak coverage had a relatively longer base pair length in proliferating myoblasts (Fig. 2.3B). Also similar to p300, the association of MyoD to poised enhancers increased substantially during the transition from proliferation to differentiation, from about 20% to 31%, which is more evident between MyoD peaks unique to proliferation and to differentiation, about 17% and 35% respectively (Fig. 2.3C). Our analysis thus suggests a specific role for MyoD in the activation of poised enhancers to mediate myoblast differentiation.

To delineate the mechanistic role of MyoD in early myoblast differentiation, we next quantified the change in residue-specific histone acetylation associated with MyoD peaks. As shown in figure 2.3C and D, a significant increase in the enrichment of H4K8ac and H3K9ac in particular was detected at the MyoD sites by 24 hours of differentiation, in addition to H3K27ac and H3K18ac. Furthermore, target gene expression increased a significantly correlating directly to the differentiation-dependent MyoD association, as determined by condition matching RNA-seq analysis (Fig. 2.3E) (Hamed et al., 2017). Interestingly, genes associated to MyoD peaks unique to proliferating myoblasts were the only group that did not exhibit an overall increase in expression during early differentiation. Taken together, our analyses revealed a residue-specific histone acetylation associated with MyoD which acts as a master regulator to establish myogenic transcription program pertinent to early differentiation (Bergstrom et al., 2002; Tapscott, 2005).

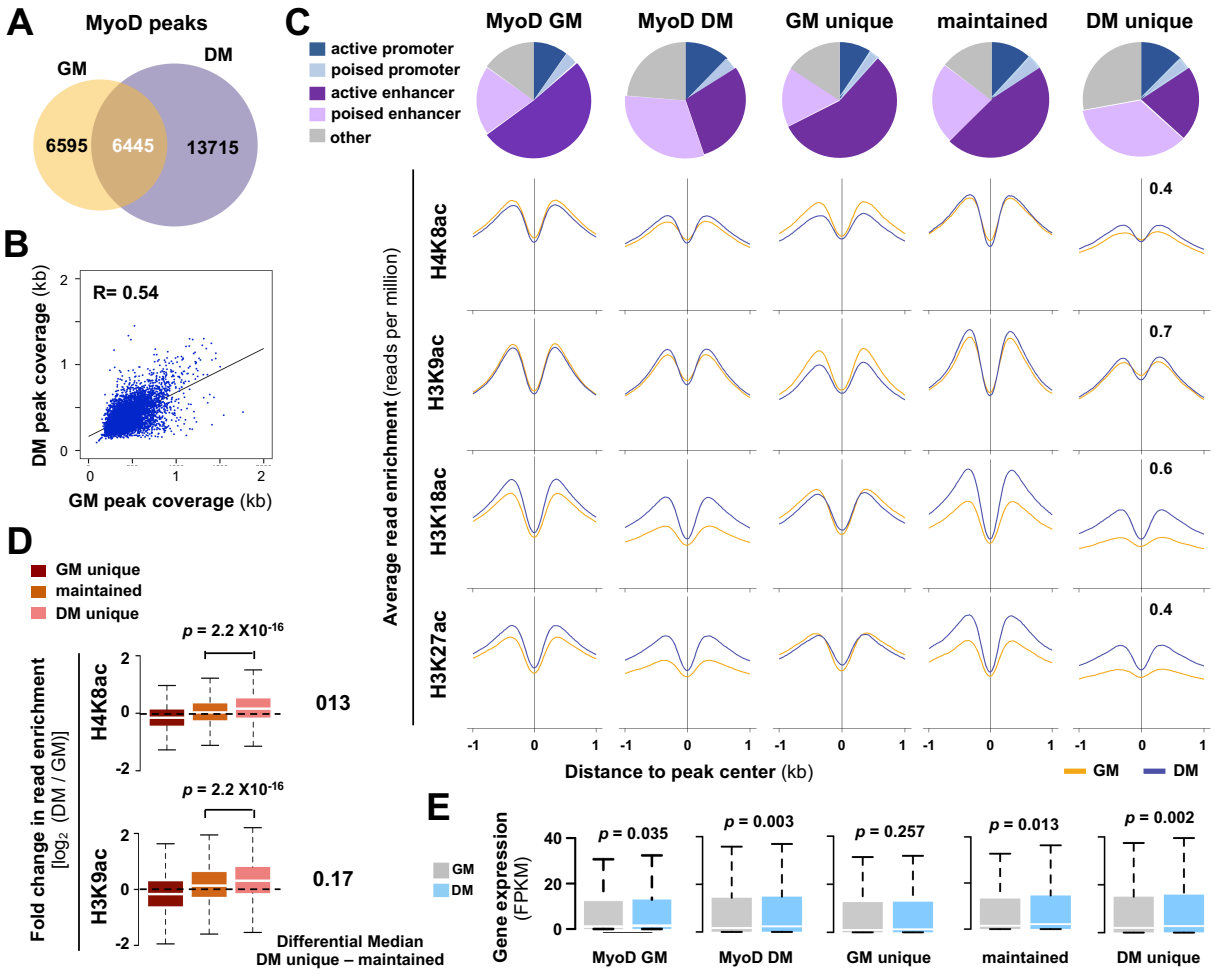

Figure 2.3 Characterization of MyoD sites in early differentiation.

(A) Venn diagram depicts unique or maintained MyoD peaks in C2C12 proliferating myoblasts (GM) and myoblasts differentiated for 24 hours (DM). (B) Correlation plot of MyoD peak coverage, in which each dot represents the absolute length of a MyoD peak, shared between GM and DM conditions (n = 6445; R = Spearman's correlation coefficient). (C) Chromatin state distribution of MyoD peaks as categorized in Panel A. The average read signal profiles for H4K8ac, H3K9ac, H3K18ac, and K3K27ac spanning 2 kb across MyoD binding sites are displayed below. (D) Boxplots present the quantification of $\log_2$-fold change in histone acetylation between differentiation and proliferation corresponding to the MyoD sites as categorized in Panel C. The difference in the median values of differentiation unique or maintained is displayed to the right. (E) The expression levels of ENSEMBL genes associated to

the MyoD peaks is presented as FPKM measured by RNA-seq analysis (Wilcoxon signed-rank test, $p < 0.05$).

Co-localization of MyoD with p300 during early myoblast differentiation

Since both p300 and MyoD were found to increasingly associate with poised enhancers during early myoblast differentiation, we next examined in detail the genome-wide co-localization of p300 and MyoD. As shown in figure 2.4A, p300 co-localized with MyoD in a comparable degree, about 32% and 38% respectively, in proliferating and differentiating myoblasts, reflecting a multi- functional link of MyoD with p300 during myogenesis. Interestingly, an apparent increase in the occupancy of poised enhancers by p300 was observed when p300 co-localized with MyoD, particularly in differentiating myoblasts, from about 8% to 12% (Fig. 2.4B). Nevertheless, no such increase was found in proliferating myoblasts, in which about 5% of p300 peaks associated to poised enhancers regardless of MyoD co-localization (Fig. 2.4B). Moreover, when the distance of p300 peaks to the nearest TSS was analysed, we found that the majority of p300 peaks located in the promoter regions (0 to -1 kb) lacked MyoD overlap (Fig. 2.4C). On the other hand, more p300 peaks co-localized with MyoD were found distal to the promoters (-1 to -50 kb), in regions where are more likely to be enhancers, active or poised (Fig. 2.4C). Thus, an increase in p300 recruitment to MyoD bound poised enhancers may be important for the initiation of myoblast differentiation.

The effect of p300 recruitment by MyoD during differentiation was also signified by an increase in the enrichment of H4K8ac and H3K9ac, principally in the presence of MyoD (Fig. 2.4B, D). In comparison, H3K18ac and H3K27ac are distinct in that their enrichments were correlated with

p300 occupancy during differentiation in the absence of MyoD as well (Fig. 2.4D). We next performed GO analysis to explore the functional differences of p300 occupancy with or without a MyoD overlap in differentiating myoblasts. As shown in figure 2.4E, loci occupied by p300 without MyoD was more connected to genes involved in overall fundamental processes such as tissue development, while loci co-occupied by p300 and MyoD were mostly linked to genes that participate in positive regulation of cellular and developmental processes. More interestingly, quantification of condition matching RNA-seq data (Hamed et al., 2017) revealed a significant increase in the expression of genes associated with p300 in differentiating myoblasts, but only when co-localized with MyoD (Fig. 2.4F). Therefore, our data shed new light into the functional mode of p300 when recruited by MyoD at the early stage of myoblast differentiation, in that the changes in loci-specific histone acetylation correlate with differentiation-specific myogenic expression.

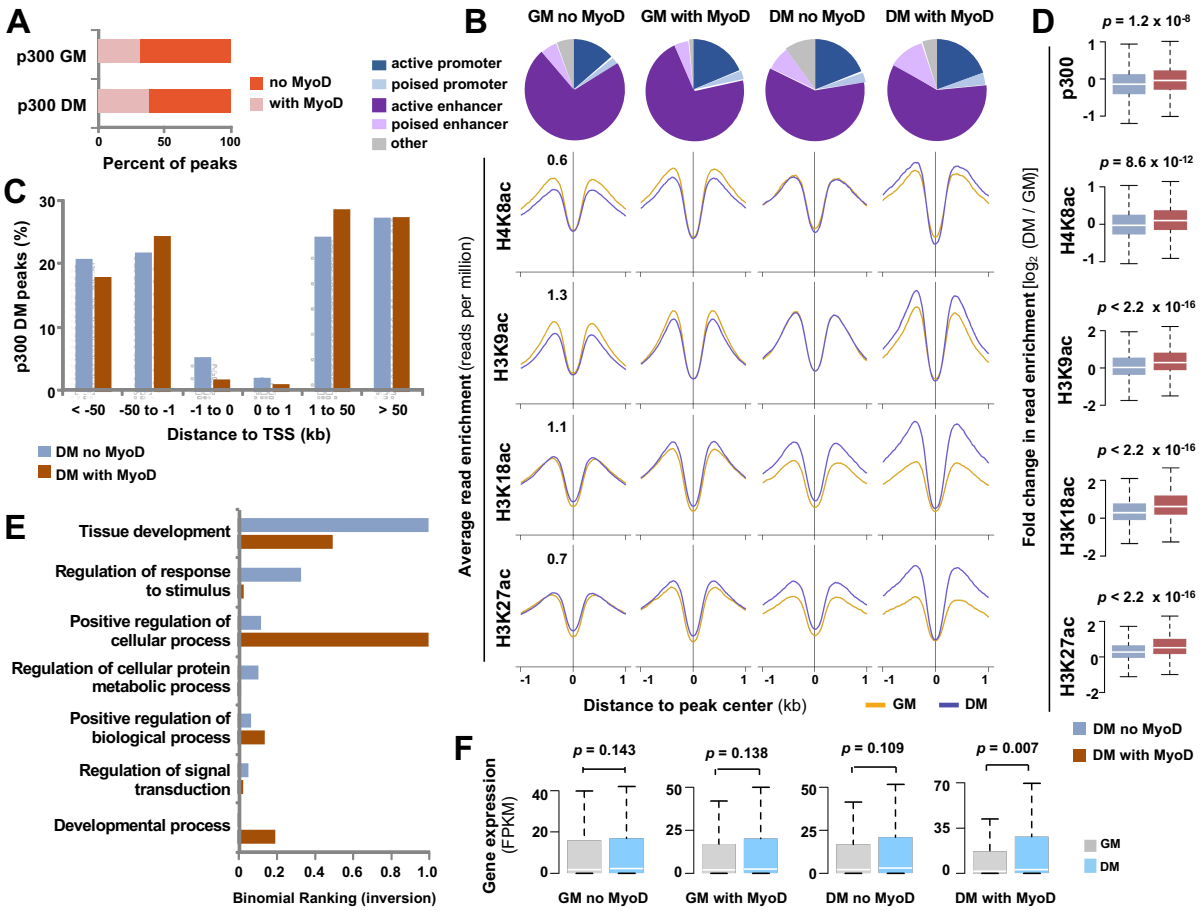

Figure 2.4 MyoD and p300 overlap in early myoblast differentiation.

(A) The magnitude of overlap between p300 and MyoD peaks in proliferating myoblasts (GM) and myoblasts differentiated for 24 hours (DM) is presented as a percentage of total p300 peaks in each condition. (B) Chromatin state distribution of p300 loci with or without a MyoD overlap. The average read density of histone acetylation spanning 2 kb across corresponding p300 loci is presented below. (C) The distance of p300 peaks with and without a MyoD overlap in relation to the closest TSS is presented as a bar graph. (D) Boxplots present $\log_2$-fold change in signal enrichment between differentiating and proliferating conditions at the indicated category of p300 loci. (E) GO analysis of p300 loci with or without a MyoD overlap is plotted as an inversion of binomial ranking as output by GREAT. (F) The expression levels of ENSEMBL genes associated to the indicated categories of p300 peaks are plotted as FPKM measured by RNA-seq analysis (Wilcoxon signed-rank test, $p < 0.05$).

Regulation of myogenic enhancers by p300 and MyoD during early differentiation

Since it appears that p300 and MyoD function together to promote early myoblast differentiation and enrichment of both regulators correlates to a specific chromatin state (Fig. 2.4B), we aimed to explore the dynamics of p300 co-localization with MyoD. By unravelling the profiles of histone acetylation at p300 loci with and without a MyoD overlap, we found that, in the absence of MyoD, an increase in the level of H4K8ac and H3K9ac was only observed at loci classified as poised enhancers between proliferation and differentiation (Fig. 2.5A). However, an increase in the levels of all histone acetylation marks examined was detected at p300 associated active enhancers in the presence of MyoD (Fig. 2.5A). Nevertheless, enrichment of these histone acetylation marks was more pronounced at poised enhancers compared to active enhancers, particularly for H3K9ac and H4K8ac, the signal read density of which increased by about 2-fold (Fig. 2.5A, B). Interestingly, at the regions surrounding the TSS, histone acetylation appeared to decline overall during early differentiation, with the exception of H3K18ac and H3K27ac at genes that were upregulated during differentiation (Fig. S2.2). Thus, H3K9ac and H4K8ac enrichment may be a specific signature of myogenic enhancers since no such enrichment was observed at the TSS of myogenic programs.

We next examined the association of p300 and MyoD to selected target loci based on the ChIP-seq read coverage and chromatin state association (Fig. 2.5C), using ChIP-qPCR analysis with normal IgG antiserum and a random locus used as negative controls. As shown in figure 2.5D, the occupancy of p300 to the putative regulatory loci of Tnnt1, Igsf3, Asb2, and Gpc6 was significantly enriched by 24 hours of differentiation, corresponding to a concurrent augmentation in MyoD binding, in addition to the differentiation- and p300-dependent expression pattern of

these genes (Fig. 2.2C). As poised/inactive lineage-specific enhancers play a determinant role in stem cell differentiation (Xu et al., 2009) and MyoD interacts with p300 (Puri et al., 1997b; Sartorelli et al., 1997), the recruitment of p300 by MyoD to target loci may thus be important for the expression of muscle-related genes. Therefore, examining the chromatin state associated with differentiation-specific regulators can be applied to delineate the molecular mechanisms by which gene expression is facilitated in a condition-specific manner.

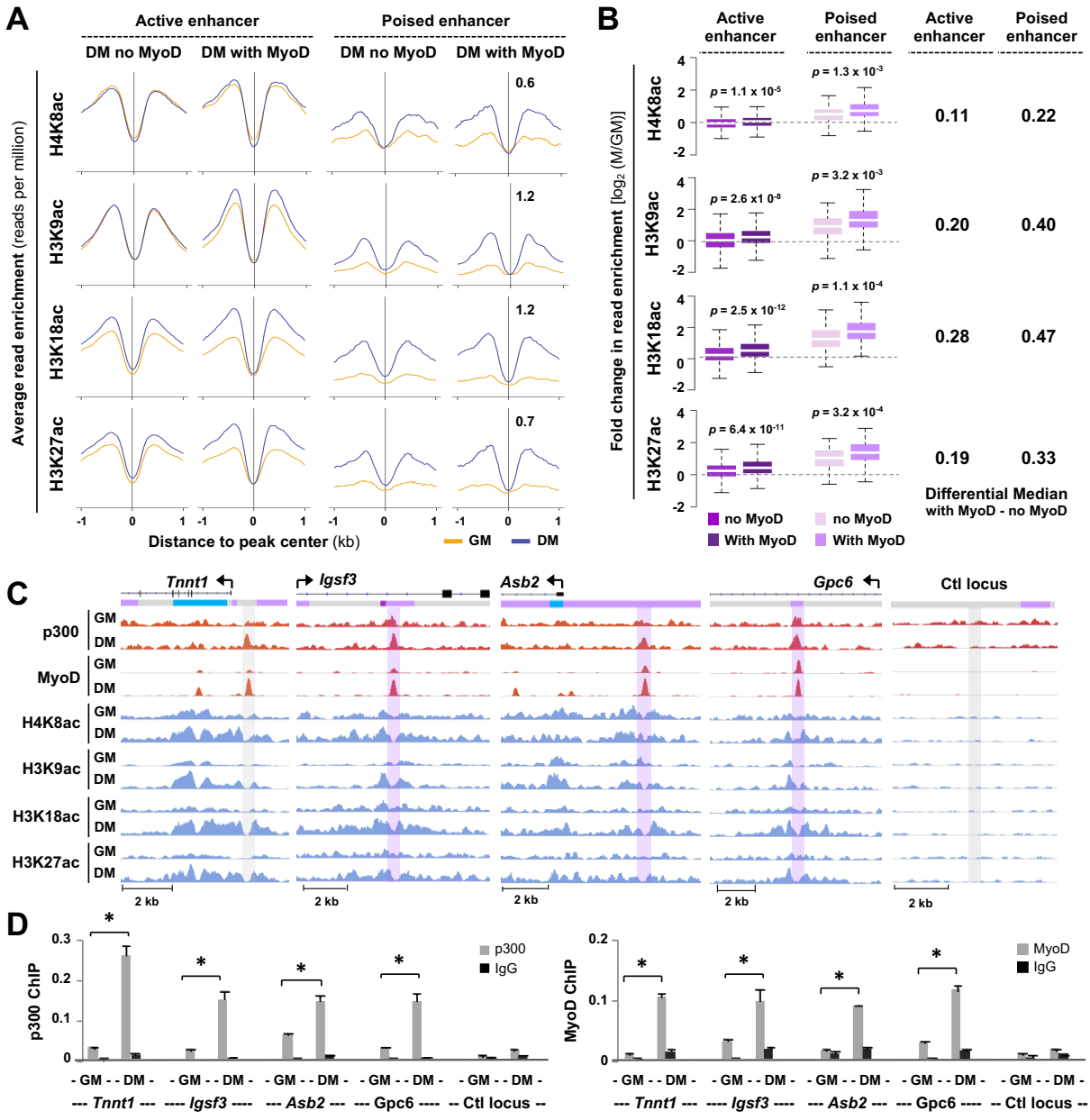

Figure 2.5 Overlap of p300 and MyoD at distinct chromatin state.

(A) Normalized average H4K8ac, H3K9ac, H3K18ac, and H3K27ac read density in proliferating myoblasts (GM) and myoblasts differentiated for 24 hours (DM) was plotted 2 kb across p300 loci with or without a MyoD overlap at active or poised enhancers. (B) Quantification of $\log_2$-fold difference in histone acetylation between differentiation and proliferation as categorized in Panel A. The differential median for signal enrichment is displayed to the right. (C) Genome browser view of p300, MyoD and histone acetylation read density at *Tnnt1, Igsf3*, *Asb2*, and *Gpc6* loci. Blue bars show Refseq gene position and the colors of ChromHMM track below

correspond to that designated to each chromatin state as illustrated in Fig. 2.4B. (D) ChIP-qPCR analysis was performed for identified target loci, using antibodies against p300 and MyoD. Normal IgG antiserum and a random locus (Ctl) were used as negative controls. Quantification is presented as the percentage of enrichment in relation to input chromatin DNA (error bars: SEM; $n = 3$; *, $p < 0.05$).

Discussion

Differentiation signaling pathways are affected by both genetic and epigenetic determinants. Given the role of enhancers in driving cell-fate specific gene programs, it is imperative to understand the mechanistic action of enhancers that contribute to cellular differentiation. Here, we utilize genome-wide chromatin state association to delineate the functional mode of transcription regulators in early myogenic differentiation. We define a role of transcriptional coactivator p300, when recruited by MyoD, in the establishment and regulation of myogenic loci during early myoblast differentiation. In addition, we reveal a significant enrichment of loci-specific histone acetylation, particularly of H4K8 and H3K9, at p300 associated active enhancers, but only when enlisted by MyoD. Our studies provide novel mechanistic insights into the action of p300 as a coactivator in early differentiation and its functional mode in the regulation of myogenic enhancers.

Epigenetic modifications of histone tails can be considered an additional evolutionary tool to regulate gene programs. Transient cycles of acetylation and deacetylation of the genes primed by H3K4 methylation create a poised state equipped for future activation (Wang et al., 2009). Thus, acetylation of histone tail contributes to the determination of lineage specification and is regulated by several HATs including p300 (Gan et al., 2007). Previous studies have examined the role of p300 in myotube formation by comparing global p300 occupancy and histone modification of mature myotubes generated from C2C12 myoblasts (Blum et al., 2012). Although an in vitro system, it mirrors the molecular processes of primary myoblasts, but more synchronized to differentiate and fuse into post-mitotic myotubes (Asp et al., 2011; Blais et al., 2005). Comprehensive gene expression analyses have also shown that myogenic differentiation

ensues in a stepwise fashion, where sequential activation of a specific set of genes restructures the cells one step at a time toward the differentiated phenotype (Delgado et al., 2003). Nonetheless, at the early stage of the differentiation, thousands of genes are differentially expressed (Doynova et al., 2017; Hamed et al., 2017; Trapnell et al., 2010), mostly within 24 hours of differentiation. As a result, epigenetic changes reflecting the alteration of gene programs should occur. Therefore, the focus of our study is not only to examine the transient chromatin dynamics that initiate and drive early myoblast differentiation, but also to explore the functional mode of p300 in regulating gene expression coupled to specific chromatin states.

By mapping globally p300-associated loci, we show that a majority of p300 peaks are localized to the enhancer regions (Fig. 2.1), in agreement with previous reports (Blum et al., 2012; Wang et al., 2008b). However, a substantial fraction of p300 peaks distribute specifically to the poised enhancer, accompanied particularly by loci-specific histone acetylation in early myoblast differentiation (Fig. 2.1). Binding of MyoD to myogenic enhancers in proliferating myoblasts leads to concomitant recruitment of p300 and deposition of H3K27ac (Blum et al., 2012). The recruitment of p300 principally by MyoD in early differentiation (Fig. 2.2) suggests that enhancers identified through chromatin state association reflect the development of skeletal lineage, which forms the rationale for us to explore the genome-wide presence of MyoD in proliferating and differentiating myoblasts. Interestingly, the number of MyoD binding sites increases significantly in early differentiation (Fig. 2.3), in line with previous studies (Cao et al., 2010; Cui et al., 2017). Similar to p300, the MyoD peaks tend to be wider while switching from proliferation to differentiation (Fig. 2.1 and 2.3), possibly due to a broader DNA coverage by

MyoD in early differentiation or a simple reflection of the difference in chromatin organization between the two cell stages.

In addition, a greater number of MyoD sites localized to poised enhancers in early differentiation (Fig. 2.3). By comparing MyoD peaks specific to differentiation and proliferation, we reveal an increase in loci-specific histone acetylation, but H4K8 and H3K9 acetylation are distinct in that their enrichments are differentiation-dependent (Fig. 2.3). We also show that the distance of p300 peaks to the nearest TSS increases with a MyoD overlap, implying that p300 recruited by MyoD occurs to distal regulatory regions possibly for potential enhancer activities. Intriguingly, the average histone acetylation profiles spanning MyoD peaks between differentiation in general and unique to differentiation are rather similar, which may be due to the large number of differentiation unique peaks encapsulated within the total differentiation peaks, in addition to perhaps a differentiation related requirement for MyoD peaks maintained between differentiation and proliferation (Fig. 2.3).

More importantly, there is an apparent increase in the occupancy of poised enhancers by p300 in differentiating myoblasts coinciding with MyoD, whereas no such increase is found in the proliferating stage, suggesting a functional relationship between p300 and MyoD in the establishment or activation of poised enhancers during differentiation (Fig. 2.5). This relationship is further signified by an enrichment of H4K8ac and H3K9ac, largely in the presence of MyoD in contrast to H3K18ac and H3K27ac, which were enriched at p300 loci in the absence of MyoD as well. The augmentation of H4K8ac and H3K9ac persists at p300 associated active enhancers, however, only when p300 overlaps with MyoD (Fig. 2.5). While

H3K9ac has been correlated to active enhancers (Karmodiya et al., 2012), H4K8ac and H3K9ac are generally considered as global marks of promoter activity (Wang et al., 2008b). Our study identifies these acetylation marks at both poised and active enhancers coupling with MyoD at the early stage of differentiation. Collectively, our data suggest a role for MyoD in p300 recruitment at lineage-specific enhancers to regulate muscle-related genes, as exemplified by muscle-specific target, Tnnt1 (Fig. 2.2, 2.5).

In this study, we have identified key lineage specific regulatory signature and present a blueprint to explore novel regulators of myogenic differentiation. We provide evidence for the enrichment of not only H3K27ac, but also H4K8ac and specifically H3K9ac at MyoD associated enhancers specific to myoblast differentiation (Fig. 2.3E). While some parallels between our data and previous genome-wide studies in myotubes (Asp et al., 2011; Blum et al., 2012) exist, our studies present critical new findings. An example relates to the state of global histone acetylation of H3K9 and H3K18. The previous study comparing myotubes to proliferating myoblasts (Asp et al., 2011) presents a decrease in global histone acetylation levels following 3 days of differentiation, whereas our studies show no significant change in global histone acetylation in myoblasts differentiated for 24 hours. We provide evidence that the differentiation process is mediated by transformations in residue-specific histone acetylation at lineage-specific loci, rather than global histone acetylation events. Our data compilation thus reflects the transformations required to move the proliferating myoblasts into differentiation and provide greater insights into epigenetic changes that govern myogenic differentiation.

Here, we offer a novel molecular insight into the modification of myogenic enhancers by loci-specific histone acetylation in concert with p300 and muscle master regulator MyoD. Our data suggest the intriguing possibility that cellular stage may be regulated through alteration of distinct chromatin states. It thus presents a valuable potential of driving chromatin state pharmacologically for the treatment of tissue-specific diseases. Future prospects will therefore be to determine the functional capacity of the myogenic enhancers identified in a specific physiological context. The model of p300-associated cellular stage-specific enhancers provides an excellent system to initiate the identification of additional myogenic targets and molecular interactions for therapeutic development towards muscle-related diseases.

Materials and Methods

Cell Culture and Western blot analysis

C2C12 myoblasts (ATCC) and the p300 shRNA knockdown cells (Chen et al., 2015) were maintained in proliferating conditions at a confluency less than 70% in Dulbecco's Modified Eagle Medium (DMEM) supplemented with 10% FBS (GM) at 37ºC with 5% CO_2. Myoblasts were induced to differentiate at about 80% of confluence using differentiation medium (DM, DMEM medium containing 2% horse serum). Whole cell extracts were prepared for protein immunoblotting as described previously (Chen et al., 2005), and Scion Image software (Scion Corp.) was used for protein band quantification where band intensities were measured and corrected for against the background of the images. The antibodies used in this study for H4K8ac, H3K9ac, H3K18ac, and H3K27ac were obtained from Abcam (ab15823, ab4441, ab1191, ab4729), while anti-p300 and anti-MyoD were from Santa Cruz (sc-584x, sc-32758x respectively). Myogenin antibody was from hybridoma F5D and anti-tubulin from hybridoma E7 (Le May et al., 2011).

ChIP-seq and data processing

Chromatin immunoprecipitation was performed by standard procedures as previously described (Hamed et al., 2013), followed by sonication with a Covaris S220 Ultra-Sonicator system. Chromatin DNA was purified using the MinElute Spin Columns Kit (Qiagen). ChIP-seq library preparation and sequencing was performed by the McGill University Genome Quebec Innovation Centre with Illumina HiSeq 2000 as single-end 50 nucleotide reads, according to Illumina instructions with input chromatin DNA used as control. Sequencing data was mapped to the mm9 assembly of the mouse genome with BWA-MEM (Li and Durbin, 2009), marking

shorter split hits as secondary, and processed for visualization of ChIP-seq signals as previously described (Hamed et al., 2017). Peak detection was performed using the MACS software (Zhang et al., 2008), whereas *de novo* motif discovery was completed with Homer (Heinz et al., 2010) on the 100 base pairs surrounding the centre of the peaks. Homer was employed to classify overlapping peaks that were defined as being co-localized within 100 bp of one another. Peak annotation followed by gene ontology (GO) was performed by GREAT *v3.0.0* (McLean et al., 2010) utilizing the whole genome as background and the single nearest gene association rule.

Quantification of histone acetylation profiles and transcription factor binding sites

The average ChIP-seq enrichment was calculated and visualized by ngs.plot (Shen et al., 2014) with respect to specific genomic features or defined regions. The analysis tool calculates the coverage vectors for each alignment file followed by normalization and transformation to generate an average profile which displays the average number of reads normalized to the total number of mapped reads (in millions), centred at a specified region. Significance between conditions was calculated with the Two-sided Wilcoxon signed-rank test.

Reverse transcription qPCR and qChIP analysis

For RT-qPCR, total RNA was isolated using the GeneJET RNA Purification kit (ThermoFisher Scientific) and equal amounts of RNA was reverse-transcribed using a High-Capacity cDNA Reverse Transcription kit (Applied Biosystems). RT-PCR amplification was conducted using SYBR® Green PCR Master Mix and HotStarTaq DNA polymerase (Qiagen) on a CFX96 Touch Real-Time PCR Detection System (BioRad). Quantification of the targets, normalized to endogenous reference and relative to a calibrator control, was calculated using the formula 2^{-}

$^{\Delta\Delta CT}$. Data are presented as the mean ± S.E.M, where *p* values were determined using a student's t-test. All relevant primers are listed in Table S2.2 (D'Angelo et al., 2012; Di Padova et al., 2007; Usardi et al., 2017). For qChIP, purified chromatin DNA was amplified in triplicate real-time PCR reactions with locus-specific primers described in Table S2.2. A standard curve was created for each set of primers with input DNA, followed by quantification as the abundance of locus-specific DNA as a percentage of input DNA.

Availability of Data

The ChIP-seq data generated and analysed for this study (Table S2.1) are deposited in the Gene Expression Omnibus (GEO) database and are accessible through GEO Series accession number GSE109636. Supplemental data for this article can be accessed on the publisher's website.

Disclosure Statement

The authors declare no conflict of interest.

Acknowledgements

We thank Mr. Yan Mach for excellent assistance in data processing and our colleagues for a supportive research environment.

Funding

This work was supported by an Operating Grant from the Natural Sciences and Engineering Research Council (#250174 to Q.L.); a Canada Graduate Scholarship from Natural Sciences and Engineering Research Council (to S.K.) and a scholarship from Umm Al-Qura University in Saudi Arabia (to M.H.).

Supplementary Data

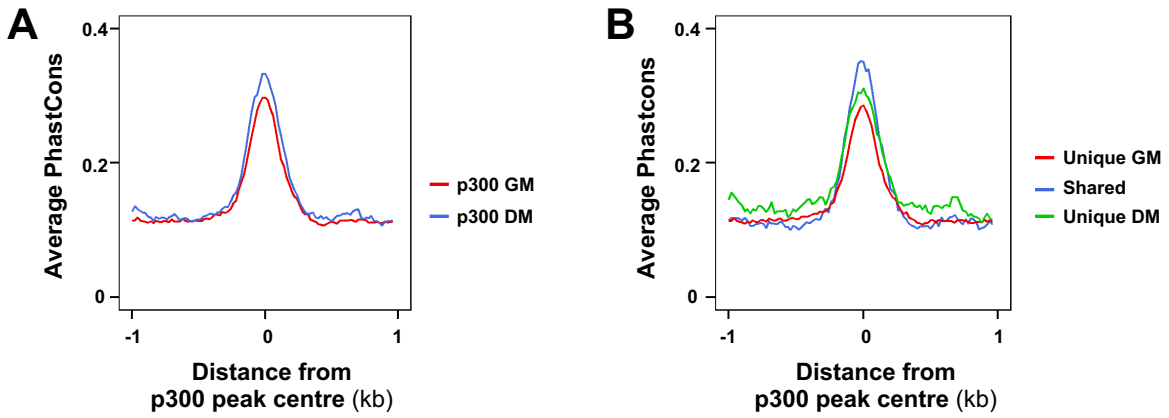

Figure S2.1 Genomic distribution of p300 in early myogenic differentiation.

(A) The average PhastCons conservation scores of p300 peaks in proliferating myoblasts (GM) and myoblast differentiated for 24 hours (DM). (B) The average PhastCons conservation scores of the unique and shared p300 peaks.

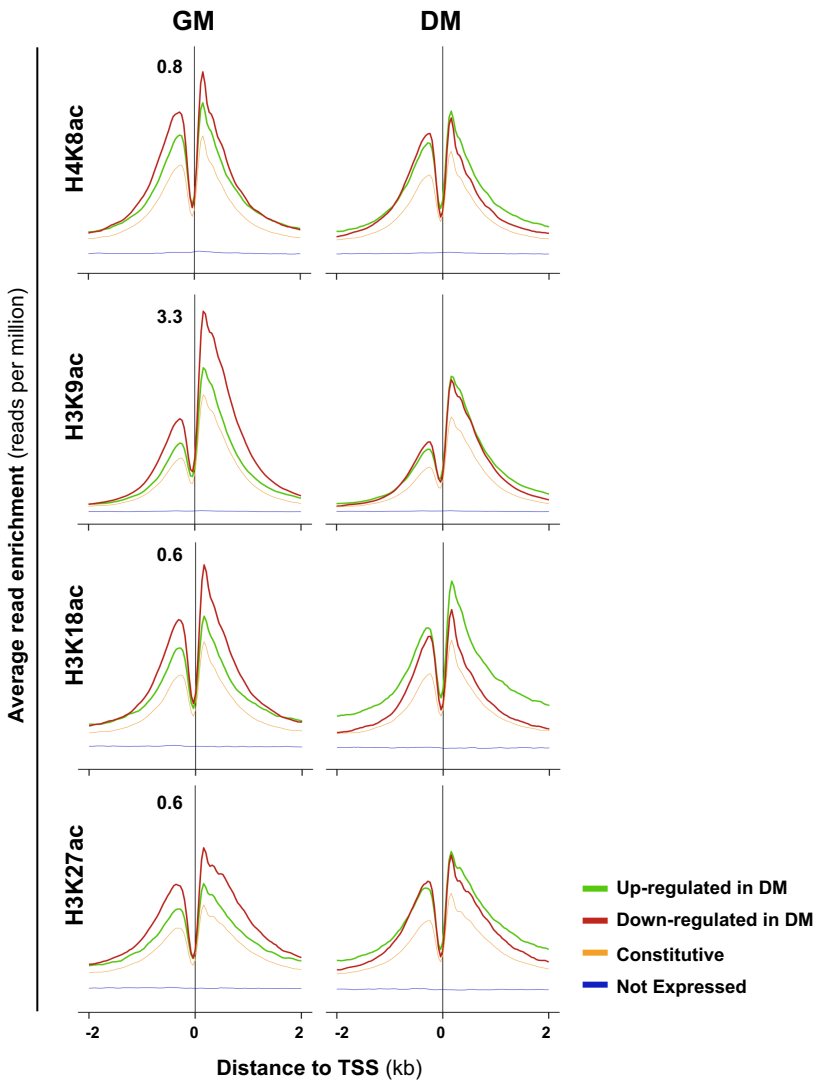

Figure S2.2 Histone acetylation associated to gene promoters in early myogenic differentiation.

The total population of ENSEMBL genes were categorized in four expression groups as determined by RNA-seq expression profiling of proliferating myoblasts (GM) and myoblasts differentiated for 24 hours (DM). Shown are average ChIP-seq enrichment profiles for H4K8ac, H3K9ac, H3K18ac, and H3K27ac spanning 4 kb across the TSS of genes in the four expression groups.

Table S2.1 ChIP-seq Dataset Access within the NCBI

Organism	Cell line	Condition	Antibody	Data Type	GEO Accession	Reference
mus-musculus	C2C12	Input		ChIP-seq	GSM2947736	This study
mus-musculus	C2C12	Proliferating	p300	ChIP-seq	GSM2947737	This study
mus-musculus	C2C12	Differentiating / 24h	p300	ChIP-seq	GSM2947738	This study

Table S2.2 Primer Sets Used for RT-qPCR and qChIP Analyses

RT-PCR Primers

Gene	Accession #	Forward Primer	Reverse Primer	Reference
Tnnt1	NM_001277903.1	5'-TCCTGCAGCAAGCCTACC-3'	5′-ATCGCACCAATATCCTCACC-3′	Puri *et al*., *Mol. Cell*., 1997
Igsf3	NM_207205.2	5′-AAGTACAGATCGTTAGCACGGT-3′	5′-GGTGTGACATTCATACTCGCC-3′	Sartorelli *et al*., *Mol. Cell Biol*., 1997.
Asb2	NM_023049.1	5′-TCCTGCAGCAAGCCTACC-3′	5′-ATCGCACCAATATCCTCACC-3′	Wang *et al*., *Cell*, 2009.

ChIP Primers

Gene	Locus	Forward Primer	Reverse Primer	Reference
Tnnt1	-600 bp	5′-GTGGTGACAACAGGCAGCTA-3′	5′-GTTAGAAAGAGGAGGGGCTGG-3′	This study
Igsf3	+46 kb	5′-GCTCATCTAGGCCACTCAACA-3′	5′-GGACCCCGTCTGATGCAAT-3′	This study
Asb2	-4 kb	5′-ACCCATTTGGCCCTCTTCAG-3′	5′-GGATGCTGTATCTCTGGCCC-3′	This study
Control	Intergenic	5′-ACAGACAACGCAGAGTACCG-3′	5′-GCCACACTCCAGACAAGATAGT-3′	Hamed *et al*., *Nucleic Acids Res.,* 2017.

Chapter Three: Insights into interplay between rexinoid signaling and myogenic regulatory factor-associated chromatin state in myogenic differentiation

---

Hamed M., Khilji S., Dixon K., Blais A., Ioshikhes I., Chen J., Li Q. *Nucleic Acids Res.* 2017;45(19):11236–11248

Insights into interplay between rexinoid signaling and myogenic regulatory factor-associated chromatin state in myogenic differentiation

Munerah Hamed[1*], Saadia Khilji[1*], Katherine Dixon[1], Alexandre Blais[3,4], Ilya Ioshikhes[3,4], Jihong Chen[2] and Qiao Li[1,2,5]

[1] Department of Cellular and Molecular Medicine, [2] Department of Pathology and Laboratory Medicine, [3] Department of Biochemistry, Microbiology and Immunology, and [4] the Ottawa Institute of Systems Biology, Faculty of Medicine, University of Ottawa, Ottawa, Ontario, Canada K1H 8M5

[*] Co-first authors

[5] Corresponding Author: Q. L. (Qiao.Li@uOttawa.ca)

Abstract

While skeletal myogenesis is tightly coordinated by myogenic regulatory factors including MyoD and myogenin, chromatin modifications have emerged as vital mechanisms of myogenic regulation. We have previously established that bexarotene, a clinically approved agonist of retinoid X receptor, promotes the specification and differentiation of skeletal muscle lineage. Here, we examine a genome-wide impact of rexinoids on myogenic differentiation through integral RNA-seq and ChIP-seq analyses. We found that bexarotene promotes myoblast differentiation through the coordination of exit from the cell cycle and the activation of muscle-related genes. We uncovered a new mechanism of rexinoid action which is mediated by the nuclear receptor and largely reconciled through a direct regulation of MyoD gene expression. In addition, we determined a rexinoid-responsive residue-specific histone acetylation at a distinct chromatin state associated to MyoD and myogenin. Thus, we provide novel molecular insights into the interplay between retinoid X receptor signaling and chromatin states pertinent to myogenic programs in early myoblast differentiation.

Introduction

While functional DNA sequences in the non-coding portion of the genome offer an important framework for gene regulation, the epigenome exhibits remarkable lineage-specificity and plays a critical role in differential gene expression (Nord et al., 2013; Thurman et al., 2012; Zhou et al., 2011). The findings in recent years that certain DNA elements are associated with distinct histone modifications have provided a new pathway to identify networks of regulatory loci whose activities underpin the control of gene expression. As such, lineage-specific enhancers can be identified by promoter-distal enrichment in H3K4me1 and/or the recruitment of histone acetyltransferases (HATs) (Hon et al., 2009; Krebs et al., 2011). Furthermore, two classes of enhancers have been described, active enhancers marked additionally by H3K27ac and poised enhancers marked by the presence of H3K4me1 but lack of H3K27ac (Creyghton et al., 2010; Rada-Iglesias et al., 2011). These studies also reveal that poised enhancers can be activated during differentiation by gaining H3K27ac, and as a result are able to mediate the expression of proximal genes. Therefore, enhancers marked by histone acetylation upon differentiation may reflect the activation of distinct gene programs regulated by lineage-specific transcription factors.

During myogenic differentiation, the commitment and development of skeletal muscle lineage is regulated by complex signaling pathways that induce a sequential expression of the muscle regulatory factors (MRFs). Myf5 and MyoD are the first MRFs to be expressed during development and have overlapping roles in the commitment of progenitor cells into the skeletal muscle cell lineage (Buckingham, 2001; Davis et al., 1987; Rudnicki et al., 1993). Myogenin functions downstream of Myf5 and MyoD, and has been identified in particular as a fundamental regulator of myoblast differentiation (Edmondson and Olson, 1989). The MRFs generally

recognize a highly similar DNA motif, referred to as the E-box, to which they bind and dimerize with other basic helix-loop-helix (bHLH) transcription factors (Buckingham, 2001). How MRFs regulate gene expression during early myoblast differentiation is consequently affected by their DNA binding partner and through their association with the HATs (Puri et al., 1997b; Roth et al., 2003; Sartorelli et al., 1997).

C2C12 is a non-transformed myogenic cell line obtained by continuous passaging of primary myoblasts isolated from mouse limb muscle (Yaffe and Saxel, 1977). They not only closely resemble proliferating myoblasts that express the MyoD determination factors, abide genetic manipulation in that selected stable clones retain their ability to differentiate, but also provide a more homogenous population compared to primary myoblasts (Asp et al., 2011; Burattini et al., 2004). Furthermore, studies of gene expression in this well characterized and widely used model of myogenesis provide results consistent with that obtained from primary tissue cells (Blais et al., 2005; Cao et al., 2010).

Retinoid X receptors (RXRs) belong to the nuclear receptor (NR) superfamily. There are three subtypes of RXRs, namely RXRα, RXRβ and RXRγ, which are bound constitutively to DNA, regardless of ligand, but act as transcriptional activators upon agonist activation (Chambon, 2005; Gampe et al., 2000; Mangelsdorf et al., 1995). The function of RXRα is very important for early development (Kastner et al., 1994; Sapin et al., 1997; Sucov et al., 1994). Specifically, RXRα null mice die in utero and present with myocardial and ocular malformation (Kastner et al., 1994; Krezel et al., 1996). We have previously reported that bexarotene, a selective RXR agonist, promotes the specification and differentiation of skeletal myoblasts through the function

of RXRα (AlSudais et al., 2016; Le May et al., 2011). As a potential dimerizing partner of many nuclear receptors, RXR is involved in the regulation of a wide array of genetic targets, but it is unclear how rexinoids affect global myogenic expression.

In this study, we examined rexinoid responsive transcriptional program and the interplay of rexinoid signaling with myoblast-specific chromatin state. We found that bexarotene coordinates muscle-related gene expression and bexarotene-promoted myoblast differentiation is largely transmitted through MyoD expression and coupled with MyoD- and myogenin-associated residue-specific histone acetylation at a distinct subset of enhancers. Our study thus provides novel molecular insights into the regulation of myogenic expression at the early stage of myoblast differentiation.

Materials and Methods

Cell Culture and Reagents

Cells of the murine myoblasts cell line C2C12 (ATCC) were maintained in growth medium (GM), Dulbecco's Modified Eagle Medium (D-MEM) supplemented with 10% FBS, at 37ºC with 5% CO_2. To induce differentiation, the medium of 80% confluent cell cultures was changed to differentiation medium (DM), D-MEM supplemented with 2% HS (Hamed et al., 2013) and 50 nM of bexarotene was used for treatment conditions. Bexarotene was purchased from the LC Laboratories and UVI 3003 was from Tocris. The RXRα shRNA knockdown cells have been described previously (AlSudais et al., 2016).

RNA-seq and data processing

Total RNA was extracted using RNeasy kit (Qiagen) according to manufacturer's instructions and sequenced by the McGill University Genome Quebec Innovation Centre in two biological repeats. Sequencing reads were aligned to the mouse genome build mm9 using Tophat (Trapnell et al., 2009) and guided by transcripts from the Ensembl 67 database. Transcript assembly was performed using Cufflinks and was followed by Cuffdiff (Trapnell et al., 2010) to estimate normalized gene expression and perform differential expression testing. To identify genes showing differential expression between conditions for downstream analysis, genes with a fold change in expression greater than ±1.5-fold and below a false discover rate (FDR) of 5% were selected. GO (gene ontology) terms significantly associated (p-value ≤ 0.05, Bonferroni) with genes that were differentially expressed were identified using the database for annotation, visualization and integrated discovery (DAVID) (Huang et al., 2008). For visualization and hierarchical clustering, z-scores were calculated from raw FPKM values (Fragments Per

Kilobase of transcript per Million mapped reads), which were $\log_2$-transformed and scaled to the row mean and standard deviation using the following formula: [$\log_2$ (FPKM)-mean of row]/(standard deviation of row). These z-scores were also used to calculate the Pearson correlation coefficients between conditions.

ChIP-seq and data processing

Cells were crosslinked and sonicated followed by chromatin immunoprecipitation as previously described (Hamed et al., 2013). Antibodies against H3K9ac, H3K18ac, H3K27ac, H4K8ac and H3K27me3 were obtained from Abcam (ab4441, ab1191, ab4729, ab15823, and ab6002), RXRα, and p300 from Santa Cruz (sc-553x and sc-584x). DNA was purified using the MinElute Spin Columns Kit (Qiagen) and input chromatin DNA was used as control. Purified DNA was sequenced by the McGill University Genome Quebec Innovation Centre with Illumina HiSeq 2000. Sequencing reads were mapped to the mouse genome build mm9 using Bowtie, allowing for 3 mismatches and reporting the single best alignment per 50 bp read. Picard was used to filter out replicated reads (http://picard.sourceforge.net/), and BAM files were converted into BED files with the BEDTools suite (Quinlan and Hall, 2010). For visualization of ChIP-seq signals in the Integrative Genomics Viewer, aligned reads were extended by 125 bp at their 3' end and basewise signal intensity was computed. Local peaks in read enrichment were identified using MACS (Zhang et al., 2008) (*v*1.0.0) with a *p*-value threshold of $1x10^{-5}$.

Chromatin state model

ChIP-seq data sets were obtained from the NCBI Gene Expression Omnibus (GEO) for RNA Pol II under the accession number GSM721286 and for H3K4me1 under GSM721288 (Asp et al.,

2011), while for H3K4me3 under GSM918415 and for H3K36me3 under GSM918417 (Yue et al., 2014). The corresponding input for Pol II and H3K4me1 were obtained under GSM721306 (Asp et al., 2011), and for H3K4me3 and H3K36me3 under GSM918421 (Yue et al., 2014). Genome-wide binding sites for MyoD and myogenin were obtained for MyoD_GM under accession number GSM 915186, for MyoD_24h under GSM915183 and for myogenin_24h under GSM915159 (Yue et al., 2014). The chromatin state model was generated using ChromHMM (Ernst and Kellis, 2012). The enrichment of TSSs, Pol II binding sites and highly conserved non-coding elements (HCNCEs) was calculated as a ratio between the fraction of nucleotides overlapping between the feature and state and the joint probability of observing the feature and state. HCNCEs for the mm9 build were identified using genomic evolutionary rate profiling and obtained from http://mendel.stanford.edu/SidowLab/downloads/gerp/ (Davydov et al., 2010).

Analysis of histone enrichment and transcription factor binding sites

The enrichment of histone acetylation at the MRF binding sites was calculated with ngs.plot (Shen et al., 2014), which calculates the coverage vectors for each query region based on specified alignment files. Following normalization and transformation on the coverage, an average profile is created as the number of reads in 20 bp bins within a 2 kb region, centered at the peaks and normalized to the total number of mapped reads (in millions) in the dataset. Two-sided Wilcoxon signed-rank test was used for statistical analysis. Homer (Heinz et al., 2010) was used to perform d*e novo* motif analysis for RXR ChIP-seq peaks, allowing for motif identification within 100 bp region from the peak center. Overlapping peaks were calculated as being located within 100 bp of one another with the *mergePeaks* tool within Homer.

Reverse transcription qPCR analysis

Reverse transcription was performed using a High-Capacity cDNA Reverse Transcription kit (Applied Biosystems). Real-time PCR was conducted using SYBR® Green PCR Master Mix and HotStarTaq DNA polymerase (Qiagen) on a CFX96 Touch Real-Time PCR Detection System (BioRad). Quantification of the targets, normalized to endogenous reference and relative to a calibrator control was calculated using the formula $2^{-\Delta\Delta CT}$. MyoD, myogenin, Akt2 and Angptl4 gene specific primers have been described previously (AlSudais et al., 2016; Hamed et al., 2013; Kaplan et al., 2002; Kersten et al., 2009) and primers for Cdkn1a, Sntb1, Tnnc1 and Tmem38a are listed in Table S3.2.

Quantitative ChIP analysis

Following ChIP, purified DNA was amplified in triplicate real-time PCR reactions with locus-specific primers described previously (AlSudais et al., 2016; Asp et al., 2011; Daniel et al., 2014; Hamed et al., 2013) or in Table S3.2. Input DNA was used to create a standard curve in the PCR amplification for each set of primers. Quantification was analyzed as the abundance of locus-specific DNA in percentage of input DNA (enrichment as the percentage of input). MyoD antibody was from Santa Cruz (sc-32758x) and myogenin from the Developmental Studies Hybridoma Bank (F5D).

Western analysis

Whole cell extracts were prepared as described previously (Chen et al., 2005). Bio-Rad ChemiDoc MP System was used to capture chemiluminescent images, and ImageJ software was used for densitometry quantification.

Results

Rexinoids promote distinct transcriptional programs during myoblast differentiation

Given that little is known about the gene programs modulated by rexinoid signaling during myogenesis, we interrogated the transcriptome associated with the action of bexarotene, a selective RXR agonist. C2C12 myoblasts were differentiated in the presence of bexarotene for 12 or 24 hours with untreated differentiating or proliferating myoblasts as controls, and then subjected to RNA-seq analysis in two biological repeats (GSE94560, Table S3.1). Cuffdiff analysis revealed that in untreated differentiating myoblasts, several thousand genes were up- or downregulated in comparison to their expression in proliferating myoblasts (FC $\geq \pm 1.5$-fold, FDR $\leq 5\%$) (Fig. 3.1A, B).

Consistent with previous microarray studies (Lionikas et al., 2010; Moran et al., 2002), many of the upregulated genes were involved in muscle development and function, including myogenin (*Myog*) and skeletal muscle specific myosin heavy chain (*Myh1*), while downregulated genes were involved largely in cell cycle regulation and progression, such as *Ccnd1*, reflecting simultaneous exit from the cell cycle and the activation of myogenic expression (Fig. 3.1A and S3.1). Notably, much of the differential expression occurring over the 24 hours of differentiation took place during the first 12-hour period, indicating a rapid switch in transcriptional programs at the onset of myoblast differentiation (Fig. 3.1B).

We also identified 533 genes that were differentially expressed in bexarotene-treated differentiating myoblasts compared to the untreated by 24 hours of differentiation (Fig. 3.1C, D). Hierarchical clustering of the bexarotene responsive genes on standardized values of expression

revealed distinct groups of genes that appeared to be differentially coregulated across treated and untreated conditions (Fig. 3.1C). Evidently, most of the bexarotene responsive genes were not affected during the first 12-hour period of differentiation, suggesting that the majority of these genes may be regulated as an indirect response to bexarotene treatment (Fig. 3.1D).

Nonetheless, MyoD, a key regulator of myogenic differentiation, was identified as an early genetic target of bexarotene through our RNA-seq analysis. Time course of RT-qPCR analysis revealed that MyoD transcripts were significantly upregulated by bexarotene starting from the 6-hour time-point, while myogenin transcripts from the 12-hour (Fig. 3.1E). The levels of MyoD and myogenin protein emulated their sequential upregulation during early differentiation and were further augmented following bexarotene treatment (Fig. 3.1F, G). In comparison, levels of RXRα protein remained largely steady (Fig. 3.1F).

Interestingly, GO analysis illustrated that bexarotene affected the expression of many genes that are associated with muscle cell differentiation and cell cycle regulation, indicative of targeted genes involved in the coordinated progression of myoblast differentiation (Fig. 3.1H, I). For example, Cdkn1a, a gene that was upregulated at the onset of myoblast differentiation, was further augmented by bexarotene as validated by RT-qPCR analysis (Fig. 3.1J). More importantly, co-treatment of differentiating myoblasts with RXR antagonist UVI 3003 (AlSudais et al., 2016) attenuated bexarotene-enhanced Cdkn1a expression (Fig. 3.1J). Similarly, the RXR antagonist also impeded the positive effects of bexarotene on gene expression of Akt2 and myogenin which have been identified previously as rexinoid responsive genes (AlSudais et al., 2016). Taken together, our data suggests that bexarotene-enhanced myogenic expression is

mediated through RXR selective signaling and rexinoid action occurs through the coordination of myoblast differentiation, from the exit of the cell cycle to the activation of myogenic expression.

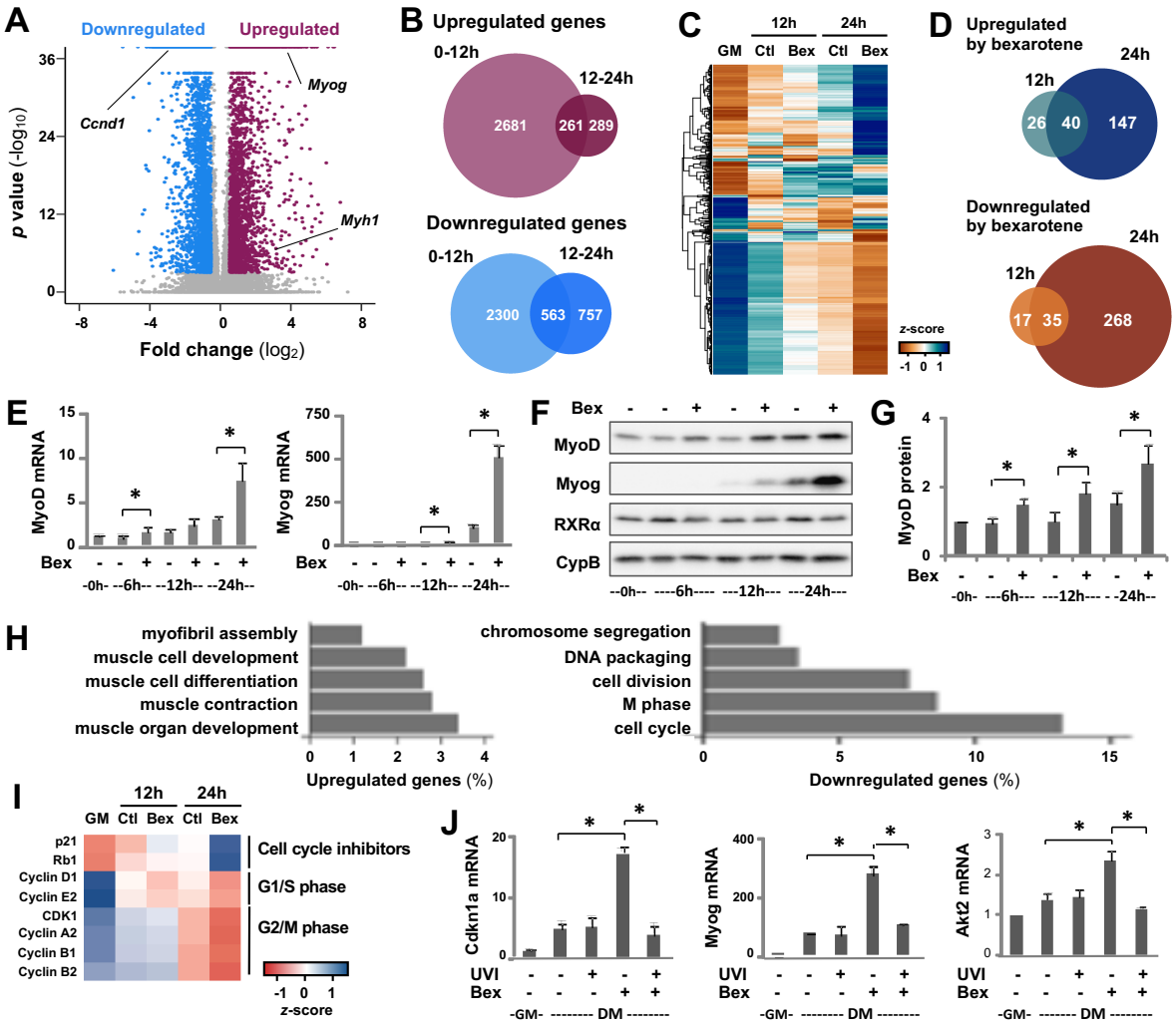

Figure 3.1 Bexarotene coordinates differentiation-related gene expression.

(A) C2C12 myoblasts were differentiated for 12 or 24 hours and subjected to RNA-seq analysis with proliferating myoblasts as control. Volcano plot analysis of differentially expressed genes by 24 hours of differentiation among all annotated Ensembl genes. Genes with a significant fold change in expression greater than 1.5-fold are shown in magenta (upregulated) and blue (downregulated), while the remaining genes are in gray. (B) Union analysis for genes

differentially expressed during the first 12 hours (0-12h) and/or between 12 and 24 hours (12-24h) of differentiation. (C) Hierarchical clustering of bexarotene responsive genes on standardized values of expression in proliferating myoblasts (GM) and myoblasts differentiated for 12 or 24 hours in the absence or presence of bexarotene (Ctl or Bex 50 nM). FPKM values were log_2-transformed and scaled to the mean and standard deviation of the row to give row-based *z*-scores. (D) Overlap between genes that were responsive to bexarotene. (E) Levels MyoD and myogenin transcripts were examined by a time course of RT-qPCR and presented as fold change relative to proliferating myoblasts (0h), normalized to internal control (error bars: SEM; n = 3; *, $p < 0.05$). (F) Western analysis of MyoD, myogenin and RXRα protein with cyclophilin B as a loading control. (G) Quantification of MyoD blots was presented as fold change relative to proliferating myoblasts (error bars: SEM; n = 5). (H) GO terms associated with genes that were responsive to bexarotene. (I) Heat map of bexarotene-responsive cell cycle-related genes presented as standardized *z*-scores in proliferating myoblasts (GM), and myoblasts differentiated with or without bexarotene for 12 or 24 hours. (J) C2C12 myoblasts were differentiated with bexarotene in the presence or absence of RXR antagonist UVI 3003 (UVI, 1 μM) for 24 hours. The mRNA levels of myogenin, Akt2, Tmem8c, and p21 were determined by RT-qPCR and presented as the fold change in relation to proliferating myoblasts (error bars: SEM; n = 3).

RXR signaling regulates MyoD directly to promote myoblast differentiation

We have previously shown that bexarotene acts through the function of RXRα to enhance muscle-related gene expression (AlSudais et al., 2016). To identify direct genetic targets of RXR signaling in early myoblast differentiation, we performed RXRα ChIP-seq analysis with myoblasts differentiated for 24 hours in the absence or presence of bexarotene (GSE94558, Table S3.1). To profile histone acetylation coupled with rexinoid action, we also performed ChIP-seq for H4K8ac, H3K9ac, H3K18ac and H3K27ac in matching conditions (GSE94558, Table S3.1).

Through MACS analysis of the RXRα read enrichment signals, 627 and 1,207 high confidence peaks were identified in treated and untreated condition, respectively (Fig. 3.2, S3.2). As determined by *de novo* motif analysis, the nuclear receptor motif was found to be the top ranking binding motif amongst the RXRα peaks in both treated and untreated conditions (Fig. 3.2A), in agreement with previous studies that RXRs are bound to their DNA sites constitutively, despite of ligand (Pazin and Kadonaga, 1997; Torchia et al., 1998). Particularly, RXRα occupancy was evident at previously identified locus of the gene encoding angiopoietin-like factor 4 (*Angptl4*), a model target of RXR signaling (Yoon et al., 2000), and the *Angptl4* locus exhibited an apparent increase in H3K18ac enrichment following bexarotene treatment compared to untreated myoblasts (Fig. 3.2B).

Interestingly, the core enhancer region (CER) of *Myod1* (Goldhamer et al., 1992, 1995), approximately 20 kb upstream of the transcription start site (TSS), as well as three additional regions (about 26, 34 and 38 kb upstream of the TSS) were also occupied by RXRα (Fig. 3.2C). Moreover, H3K18ac at the CER was further enriched following bexarotene treatment as compared to untreated condition (Fig. 3.2C). ChIP-qPCR analysis validated that H3K18ac signals at the *Angptl4* and *Myod1* loci increased significantly following bexarotene treatment (Fig. 3.2D), which is consistent with previous reports that H3K18ac is often associated with nuclear receptor signaling and rexinoid action (AlSudais et al., 2016; Jin et al., 2011).

Additionally, the mRNA levels of Angptl4 and MyoD in differentiating myoblasts were indeed augmented after 24 hours of bexarotene treatment and the positive effects of bexarotene on their gene expression were impeded by RXRα shRNA knockdown, indicating that bexarotene-

enhanced gene expression is mediated through the function of RXRα as a transcription factor (Fig. 3.2E, S3.2B). On average, the expression levels of RXRα-associated bexarotene responsive genes increased significantly following bexarotene treatment, whereas that of ENSEMBL genes assigned to RXRα en bloc was rather comparable in treated and untreated conditions (Fig. 3.2F). Taken together, our data suggests that a common mode of molecular regulation may mediate differential gene expression observed in rexinoid-enhanced myoblast differentiation, in that it may be reconciled largely through the regulation of MyoD gene expression.

Pearson correlation analysis revealed that the expression levels of bexarotene responsive genes at 12-hour of untreated condition not only positively correlated to treated condition at the same time point, but also to the proliferating state (Fig. 3.2G), suggesting that these genes may be globally coregulated at the early stage of differentiation. Likewise, the lack of positive correlation between 24-hour treated condition with the 12-hour untreated and proliferating state again suggests that the late response to bexarotene treatment may be an indirect outcome. We therefore analyzed in greater detail the association of MyoD with bexarotene responsive genes to explore the potential of rexinoid signaling through MyoD to enhance myogenic expression, since MyoD is a direct target of RXRα (Fig. 3.2C).

We found that 86% of the late bexarotene upregulated genes (12-24 hours) were associated with MyoD (Fig. 3.2H). In comparison, only 50% of the genes upregulated during the 12-24 hour period of differentiation but not affected by bexarotene, were associated with MyoD (Fig. 3.2I). In addition, 57% of MyoD associated bexarotene upregulated genes were significantly inhibited (FC $\geq$ 0.5) by MyoD siRNA knockdown (Chakroun et al., 2015), whereas only 23% of the

differentiation-dependent bexarotene-nonresponsive genes were impacted in the same degree (Fig. 3.2I). Finally, the expression of bexarotene upregulated genes was inhibited more significantly by MyoD siRNA in comparison to the differentiation dependant genes (Fig 3.2J). Taken together, our study suggests that MyoD is a major mediating factor in rexinoid responsive gene expression at the early stage of myoblast differentiation.

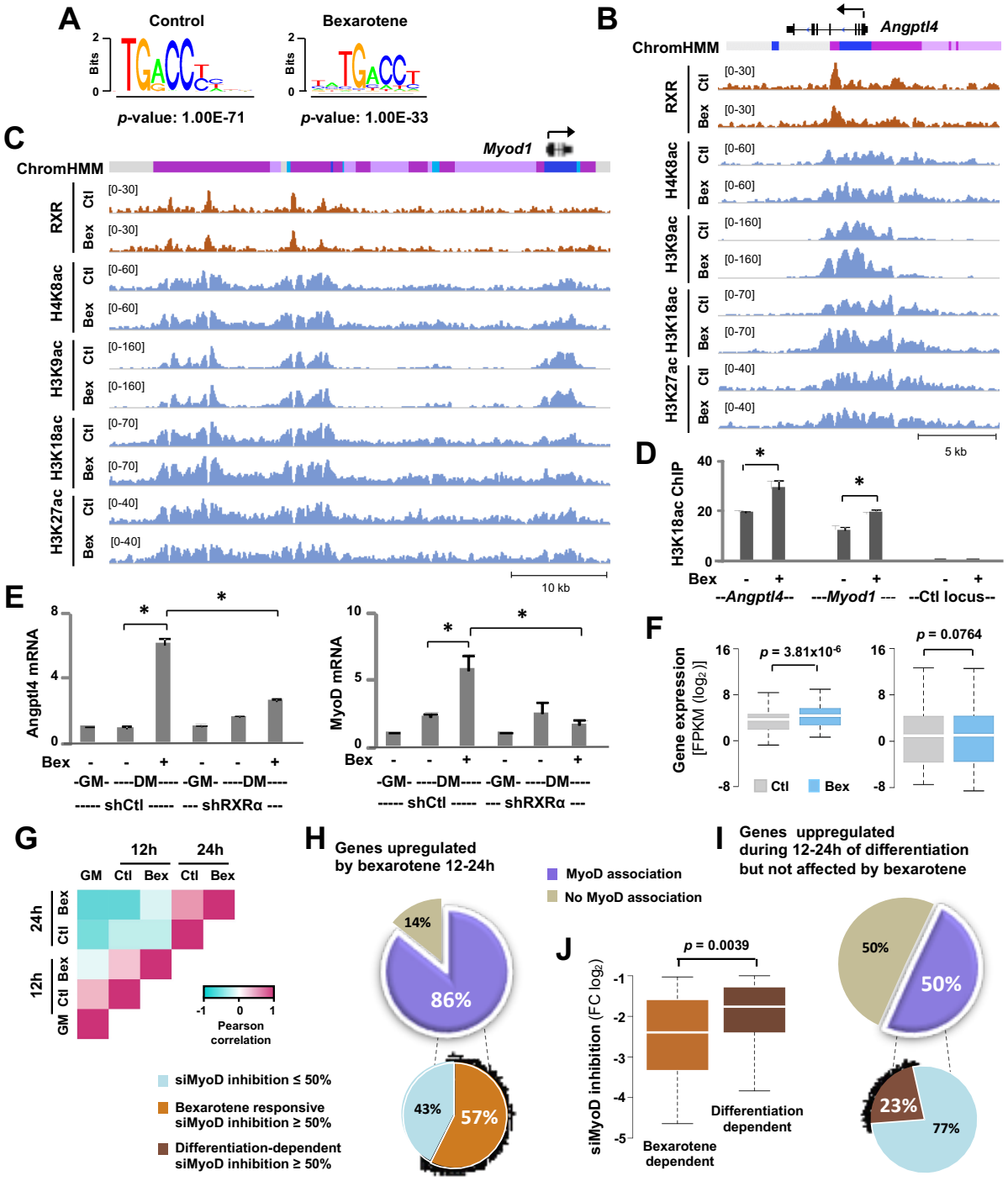

Figure 3.2 RXR regulations MyoD expression.

(A) Consensus binding sequences of nuclear receptors were discovered through *de novo* motif analysis of RXRα peaks in myoblasts differentiated for 24 hours in the absence or presence of

bexarotene (Ctl or Bex 50 nM). (B) Genome browser view of RXRα and histone acetylation signals at the *Angptl4* locus. Black bars show Refseq gene position and ChromHMM track colors correspond to color designated to each chromatin state as in Fig. 3.3A. (C) Genome browser view of the *Myod1* locus. (D) H3K18ac enrichments at the *Angptl4* and *Myod1* locus were examined by qChIP analysis with an intergenic region as control. Enrichment was quantified as percentage of input (error bars: SEM; n = 3; *, $p < 0.05$). (E) RXRα-knockdown (shRXRα) myoblasts were differentiated with or without bexarotene for 24 hours with proliferating myoblasts (GM) as controls. A non-silencing shRNA (shCtl) was used in parallel as control. The mRNA levels of Angptl4 and MyoD were assessed by RT-qPCR and plotted as fold change in relation to proliferating myoblasts (error bars: SEM; n = 3). (F) Expression levels of bexarotene responsive genes assigned to the RXRα peaks in differentiating myoblast and that of all genes is presented as FPKM measured by the RNA-seq. (G) The heatmap of Pearson correlation coefficients calculated between the row-based *z*-scores for bexarotene responsive genes. (H, I) MyoD association is categorized for the 147 genes upregulated by bexarotene between 12-24 hours of differentiation and the 246 genes upregulated in the same period but not affected by bexarotene. A pie chart below displays percentage of genes exhibits a greater than 50% of inhibition in C2C12 myoblasts differentiated for 24 hours following siMyoD knockdown, compared to a non-specific silencing control. (J) Expression of MyoD-associated genes (the 86% and 50% group respectively) from the siMyoD knockdown microarrays is presented as fold change in relation to a non-specific silencing control.

Mapping of genomic loci through chromatin states in proliferating myoblasts

To further delineate the molecular pathways of rexinoid signaling in myogenic modulation, we generated a chromatin state model based on genome-wide co-occurrence of different epigenetic marks in committed proliferating myoblasts, using a hidden Markov model-based method. Incorporating published ChIP-seq datasets for the promoter-associated mark H3K4me3 and RNA polymerase II (RNA Pol II), enhancer-associated mark H3K4me1, transcription-associated mark

H3K36me3 and the repressive mark H3K27me3 together with our own H3K9ac, H3K18ac, H3K27ac and H4K8ac ChIP-seq data in proliferating C2C12 myoblasts (GSE94558, Table S3.1), we established a model with 14 chromatin states reflecting diverse activities in gene expression prior to onset of myoblast differentiation (Fig. 3.3).

These chromatin states were categorized as promoters, transcribed regions, enhancers and regions that were either inactive or repressed (Fig. 3.3A). Briefly, promoter states were identified by enrichment of H3K4me3, TSSs, RNA Pol II and histone acetylation (Fig. 3.3A). Such is the case of *Ccnd1* promoter (Eto, 2000), reflecting the fact that *Ccnd1*is readily accessible to transcriptional machinery and actively transcribed in proliferating myoblasts (Fig. 3.3B, C). On the other hand, enhancers were identified by the presence of H3K4me1 and absence of H3K4me3 and H3K36me3, and further classified as active or poised based on levels of histone acetylation (Fig. 3.3A). For example, upstream region of the gene encoding Ccnd1 (Eeckhoute et al., 2006), a critical regulator of cellular proliferation, were marked by abundant of H3K4me1 and histone acetylation coupled to a high level of Ccnd1 transcripts, in contrast to neighbouring genes (Fig. 3.3B, C).

As previously reported for other cell types (Ernst et al., 2011), the majority of the myoblast genome (~80%) was devoid of histone modifications analyzed (Fig. 3.3A). Promoter and enhancer regions covered about 1% and 8% of the genome respectively, and had shorter median lengths than inactive or repressed regions, indicating that only a small portion of the genome is utilized to actively regulate gene expression within proliferating myoblasts (Fig. 3.3A). Active promoters and enhancers were also enriched in HCNCEs (Fig. 3.3A), as previously identified

through genomic evolutionary rate profiling (Davydov et al., 2010). Thus, distinct chromatin states characterized in proliferating myoblasts may be used to identify lineage-specific regulatory loci pertinent to myogenic differentiation.

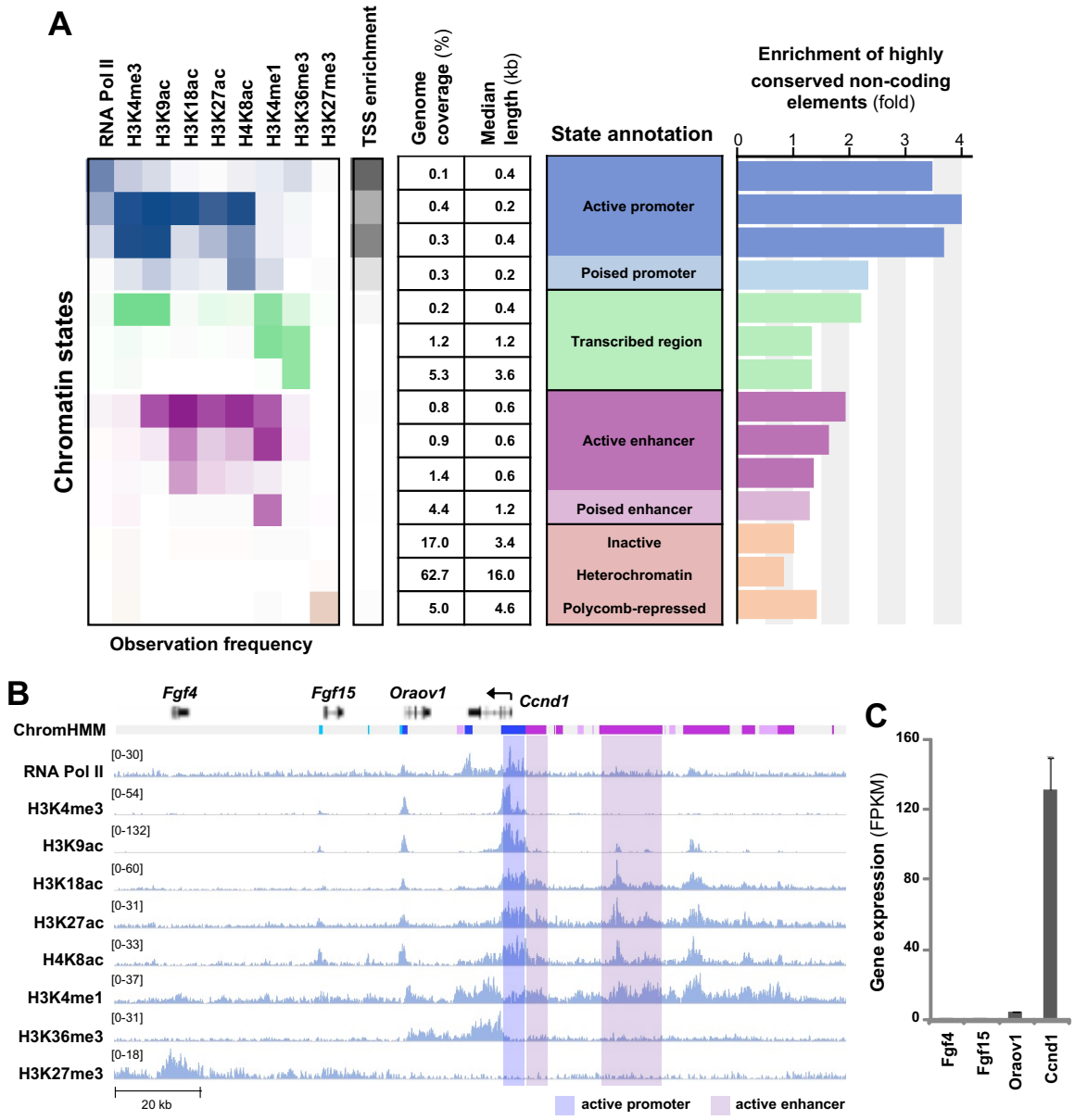

Figure 3.3 Characterization of the epigenome in proliferating myoblasts.

(A) 14-state chromatin state model was generated based on global ChIP-seq read enrichment for RNA Pol II, H3K4me3, H3K9ac, H3K18ac, H3K27ac, H4K8ac, H3K4me1, H3K36me3 and

H3K27me3. TSS enrichment was calculated as the ratio between the fraction of bases in the genome overlapping the feature and state and the joint probability that a base would overlap with the feature and state. Enrichment of highly conserved non-coding elements was calculated similarly. (B) Genome browser view of the ChIP-seq signals and chromatin states at the *Ccnd1* locus. Black bars show Refseq gene positions and ChromHMM track colors correspond to the colors designated for each chromatin state as in panel A. (C) Expression levels of the Refseq genes in proliferating myoblasts is presented as FPKM measured by RNA-seq analysis.

MyoD and myogenin associate with distinct chromatin states

Since rexinoids appear to act through MyoD expression and MyoD and myogenin play sequential roles in the control of myogenic differentiation, we used published datasets (Yue et al., 2014) on genome-wide myogenin- and MyoD binding sites (Table S3.1) in differentiating myoblasts to exam change in residue-specific histone acetylation that may be linked to rexinoid signaling during early myogenic differentiation. As predicted by our 14 chromatin state model for proliferating myoblasts, 33% and 36% of myogenin peaks were associated to the promoter and enhancer regions respectively, whereas MyoD binding sites (~61%) were largely found at the enhancer regions (Fig. 3.4A). Although myogenin and MyoD sites at active enhancers displayed a differentiation-dependent increase in H3K18ac and H3K27ac signals, their binding sites at poised enhancers exhibited an apparent enrichment in each of the acetylation marks profiled including H4K8ac and H3K9ac (Fig. 3.4B). Most interestingly, H4K8ac, H3K9ac, H3K18ac and H3K27ac were further enriched following bexarotene treatment at MyoD- and myogenin-associated poised enhancers, while no such increase was found at the active enhancers (Fig. 3.4B). Our analyses thus suggest a possible role for MyoD and myogenin in the regulation of poised enhancers particularly in the context of rexinoid signaling.

In differentiating myoblasts, the activation of myogenin expression is coupled with the binding of MyoD to the promoter and upstream enhancer regions of *Myog* locus (Faralli and Dilworth, 2012) which was characterized as poised or inactive regions in proliferating myoblasts based on our 14 chromatin state model (Fig. 3.4C). While myogenin has been identified previously (AlSudais et al., 2016) as a bexarotene responsive gene (Fig. 3.1), RXR occupancy was not detected at the *Myog* locus (GSM2478304, GSM2478305). However, MyoD associated H4K8ac, H3K9ac, and H3K18ac signals at the poised enhancers were not only enriched by 24 hours of differentiation, but also further augmented following bexarotene treatment (Fig. 3.4C). To delineate the potential mechanisms of MyoD mediated rexinoid responsive gene expression, we conducted ChIP-qPCR analysis to examine the association of MyoD and p300 to multiple poised enhancers as indicated by our chromatin state model, including a previously identified *Myog* enhancer (Asp et al., 2011). Normal IgG antiserum and random locus were used as negative controls in the analysis. As shown in figure 3.4D, the association of MyoD and p300 to these poised enhancers were markedly enriched by 24 hours of differentiation. More importantly, the enrichment of MyoD and p300 at these posed enhancers were further significantly augmented with the addition of bexarotene (Fig. 3.4D). Interestingly, myogenin was also significantly enriched at these poised enhancers to a similar degree following bexarotene treatment of the differentiating myoblasts (Fig. 3.4E). RT-qPCR revealed that the expression of genes associated to these poised enhancers emulated the degree of MyoD, myogenin and p300 enrichments (Fig. 3.1 and S3.1). Thus, bexarotene responsive gene expression is mediated through the activation of poised enhancers by MyoD and myogenin as transcription factors and p300 as a HAT.

By and large, 51% of the MyoD peaks associated with the late bexarotene upregulated genes (12-24 hours) were found at poised enhancers (Fig 3.4F). In comparison, only 32% of MyoD peaks associated with genes upregulated during the 12-24 hour period of differentiation but not affected by bexarotene were found at the poised enhancers, which was similar to the chromatin state distribution of all MyoD peaks (compare Fig. 3.4F to 3.4A). Taken together, our results highlight the importance of MyoD-coupled histone acetylation for the activation of myogenic expression at the onset of myoblast differentiation and for transmitting rexinoid signaling in differentiating myoblasts through poised enhancers, as MyoD is a direct genetic target of RXRα (Fig. 3.2C) and important for myogenin expression (Faralli and Dilworth, 2012; Rudnicki et al., 1993).

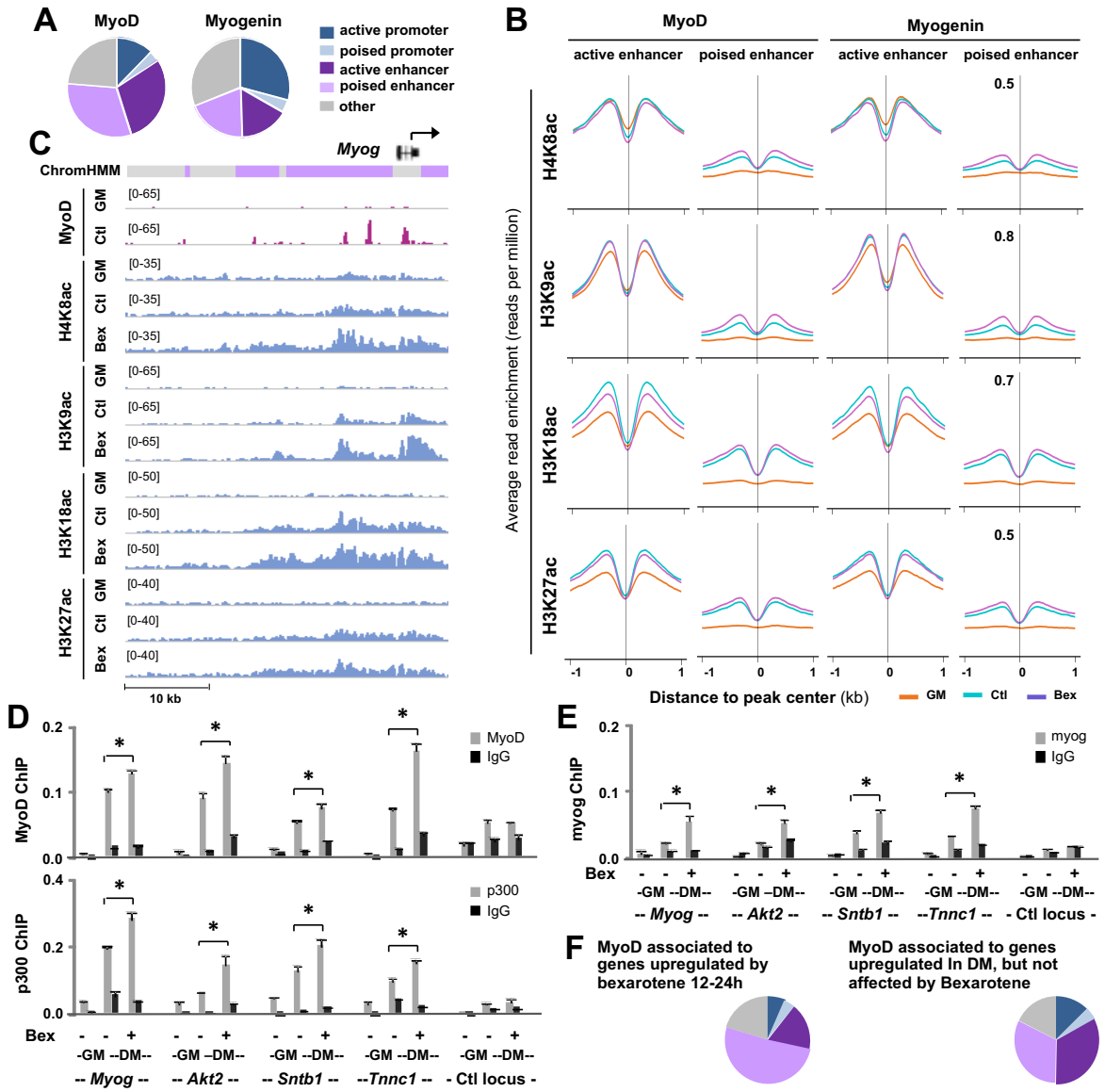

Figure 3.4 Association of MyoD and myogenin with distinct chromatin states.

(A) Genome wide MyoD and myogenin binding sites in myoblasts differentiated for 24 hours were associated with distinct chromatin states. (B) The average read enrichment profiles for H4K8ac, H3K9ac, H3K18ac, and K3K27ac corresponding to ± 1 kb of the MyoD and myogenin peaks associated to active and poised enhancers in proliferating myoblasts (GM), and myoblasts differentiated for 24 hours in the absence or presence bexarotene (Ctl or Bex 50 nM). (C) The genome browser view of the ChIP-seq signals for MyoD and indicated histone acetylation at the *Myogenin* locus. Black bars show Refseq gene position and ChromHMM track colors correspond to the color designated for each chromatin state. (D, E) ChIP-qPCR analysis was performed for

poise enhancers identified for *Myog, Akt2, Sntb1* and *Tnnc1* using antibodies against MyoD, p300 or myogenin. Normal IgG antiserum and a random locus (Ctl) were used as negative controls. Quantification is presented as the percentage of enrichment in relation to the input chromatin DNA (error bars: SEM; n = 3; *, $p < 0.05$). (F) Chromatin state distribution of MyoD peaks associated with genes upregulated by bexarotene and with genes upregulated during differentiation but not affected by bexarotene (the 86% and 50% group in Fig. 3.2H and I respectively).

Overlapping of myogenin and MyoD in bexarotene responsive histone acetylation

Since bexarotene responsive genes may be globally coregulated at the early stage of differentiation and MyoD and myogenin play critical roles in muscle development, we explored further their interplay with rexinoid signaling. We first grouped genome-wide myogenin binding sites based on their colocalization with MyoD and found that approximately 39% of myogenin sites overlapped with MyoD (Fig. 3.5A, B), similar to a previous observation in which about 42% of myogenin sites overlap with MyoD at promoter regions (Blais et al., 2005). Interestingly, about 38% of myogenin-only sites were found in active promoters, but only 12% were found in poised enhancers (Fig. 3.5C). On the other hand, approximately 31% of MyoD sites were associated with poised and active enhancers, regardless of their colocalization with myogenin (Fig. 3.5C). Additionally, the pattern of chromatin state association for sites overlapped by myogenin and MyoD is similar to that bound by MyoD-only but markedly different from that bound by myogenin-only (Fig. 3.5C). Collectively, these results suggest that while myogenin and MyoD may share some overlapping targets, they each bind to a distinct set of loci associated with different chromatin states.

More interestingly, poised enhancers bound by MyoD-only or overlapped by MyoD and myogenin showed a similar increase in differentiation-dependent histone acetylation (Fig. 3.5D). However, histone acetylation in the two classes of binding sites differed in their response to rexinoid signaling. The MyoD binding sites overlapped by myogenin displayed a more pronounced increase in histone acetylation following bexarotene treatment as compared to those bound by MyoD-only, particularly in H3K9ac (Fig. 3.5D, E). Taken together, our analyses suggest that while MyoD may lead the localization of MyoD-myogenin complexes across the enhancer regions, myogenin possibly cooperates with MyoD in rexinoid responsive histone acetylation at the poised enhancers.

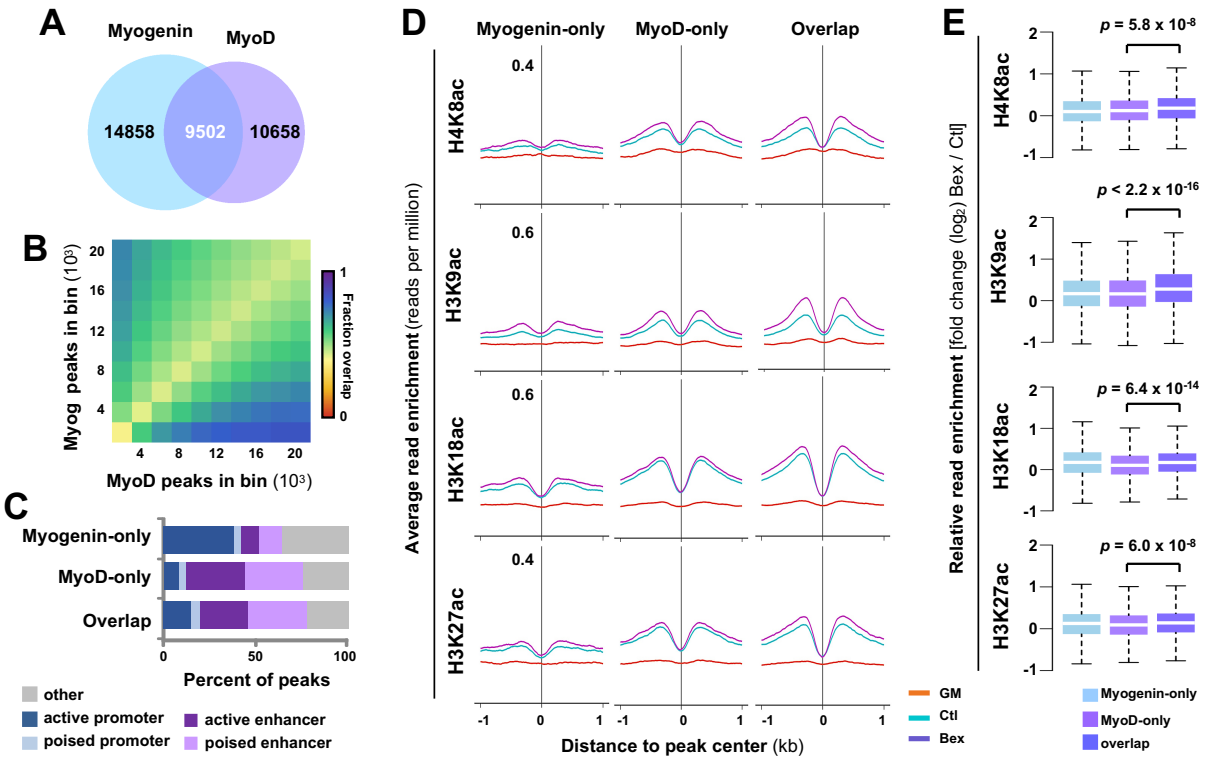

Figure 3.5 Overlapping of myogenin with MyoD in histone acetylation.

(A) Union analysis of MyoD and myogenin ChIP-seq signals in myoblasts differentiated for 24 hours. (B) The top 20,000 MyoD and myogenin peaks were ranked by read enrichment, and grouped into bins with increments of 2,000. Each box represents the fraction of sites bound by MyoD and myogenin in that bin. (C) The association of unique and overlapping MyoD and myogenin peaks with distinct chromatin states. (D) The average ChIP-seq signal profiles for H4K8ac, H3K9ac, H3K18ac, and H3K27ac at poised enhancers bound by MyoD- or myogenin-only, or both in proliferating myoblasts (GM), and myoblasts differentiated for 24 hours in the absence or presence bexarotene (Ctl or Bex 50 nM). (E) Quantification of $\log_2$-fold change in histone acetylation.

Discussion

We have examined the molecular pathways associated with rexinoid-enhanced myogenic differentiation using integral RNA-seq and ChIP-seq analyses. Our findings show that rexinoid signaling acts through the coordination of myogenic expression, from the exit of the cell cycle to the activation of muscle-related genes. Interestingly, bexarotene-responsive gene expression is mediated through RXR as a transcription factor and reconciled largely through a direct regulation of MyoD gene expression. While histone acetylation increases with differentiation at MyoD binding sites associated with different chromatin states, bexarotene augments the enrichments of H3K9ac and H4K8ac particularly at poised enhancers. Our studies thus provide novel molecular insights into the interplay between rexinoid signaling and MRFs-associated chromatin states during early myogenic differentiation.

Intercellular signaling is vital for the intricate coordination of cell cycle regulation and muscle-specific expression at the early stages of myoblast differentiation. The transition between proliferation and differentiation is dependent on a rapid exit from the cell cycle and simultaneous expression of early MRFs. We found that *Myod1* is an early rexinoid responsive gene, the active enhancer regions of *Myod1* are occupied by RXRα, and knockdown of RXRα impedes MyoD gene expression (Fig. 3.1, 3.2), suggesting that MyoD is a direct genetic target of RXR in early myogenic differentiation. At the onset of differentiation, MyoD activates the expression of both muscle-specific genes and cell cycle inhibitors, allowing irreversible exit from the cell cycle and progression into differentiation (Halevy et al., 1995; Weintraub et al., 1989). Given that the expression of MyoD is upregulated by bexarotene and RXRα is important for the positive effect of bexarotene on MyoD expression (Fig. 3.1, 3.2) and myoblast differentiation (AlSudais et al.,

2016), a common mode of molecular regulation may mediate differential gene expression observed in bexarotene-enhanced myoblast differentiation.

Characterization of the chromatin states in proliferating C2C12 myoblasts reveals a muscle-specific usage of regulatory DNA elements, and the activity of muscle-specific enhancers is marked by local changes in residue-specific histone acetylation at the early stage of myoblast differentiation (Fig. 3.3-3.5). While H3K9ac is generally considered as a global mark of promoter activity, we identify an enrichment of H3K9ac at poised enhancers coupled by MyoD at the early stage of differentiation (Fig. 3.4, 3.5). Interestingly, this enrichment of H3K9ac was further augmented at myogenin and MyoD overlapping sites following bexarotene treatment (Fig. 3.5). Thus, H3K9ac may reflect the control of a discrete set of genes through the function of MyoD with cooperation of myogenin in early myogenic expression and MyoD plays important roles in the activation of poised enhancers particularly in milieu of rexinoid action. Besides H3K9ac, the enrichments of H4K8ac are also strongly coupled with MyoD and myogenin at the poised enhancers (Fig. 3.4, 3.5), suggesting that MyoD and myogenin may play important roles in residue-specific histone acetylation.

A recent study found that although Myf5 and MyoD bind to a largely shared set of DNA binding sites, they differ in their potential to activate gene transcription (Conerly et al., 2016). We found here that myogenin is preferentially associated with promoters, while MyoD has an affinity to enhancers (Fig. 3.4). In addition, MyoD appears to be governing the localization of myogenin and MyoD complexes across enhancers, and myogenin may cooperate with MyoD in rexinoid responsive histone acetylation at poised enhancers primed with MyoD binding (Fig. 3.5). More

interestingly, rexinoid-upregulated genes are preferentially associated with MyoD as compared to genes that are upregulated during the same period but not affected by rexinoid, while only a subset of MyoD associated genes are affected by rexinoids (Fig. 3.2). Taken together, our findings support a role for MyoD in the activation of poised enhancers at the onset of myogenic differentiation and in the interplay with rexinoid signaling to further promote myoblast differentiation.

A variety of tissue-related diseases are characterized by muscle wasting, including cerebral palsy, inflammatory myopathies, muscular dystrophies (Carpenter and Karpati, 1979; Meryon, 1852; O'Dwyer et al., 1989). Particularly in Duchenne muscular dystrophy (DMD) patients, the type II skeletal muscle fibers are more prone to damage (Webster et al., 1988). Interestingly, nuclear receptors, such as PPARδ which regulate transcription by heterodimerizing with RXR, play a key role in the regulation of mitochondrial respiration (Luquet et al., 2003), skeletal muscle lipid oxidation as well as the determination of skeletal muscle fiber types, where an activated form of PPAR was shown to increase the proportion of type I fibers (Wang et al., 2004), suggesting that RXR agonists may be able to promote muscle generation. Thus, the application of specific nuclear receptor agonists may be explored in muscle-related diseases to promote myofiber numbers and oxidative capacity (Gaudel et al., 2008).

In this study, we demonstrate that specific targeting of RXR signaling promotes normal regulation of gene expression occurring during myoblast differentiation, and describe a novel molecular regulation of MyoD gene expression through the activation of RXR. A potential direction will be therefore to determine if rexinoids are able to similarly regulate myogenic

transcription in a specific physiological context or disease models. Moreover, the model of rexinoid-enhanced myogenesis also offers an excellent system to identify additional genetic targets and molecular interactions for therapeutic development towards muscle-related diseases.

Data Availability

All RNA-seq and ChIP-seq data from this study have been deposited in the National Center for Biotechnology Information Gene Expression Omnibus (GEO) database, assigned as SuperSeries GSE94561. This SuperSeries is composed of two SubSeries assigned as GSE94560 (RNA-seq data) and GSE94558 (ChIP-seq data), respectively.

Funding

This work was sponsored by an operating grant from the Cancer Research Society to Q.L. (#21126). S.K. was a recipient of a Graduate Scholarship from the Natural Sciences and Engineering Research Council of Canada, and M.H. from the Umm Al-Qura University of Saudi Arabia.

Acknowledgements

We thank Drs. C. Porter and T. Perkins for assistance in transcript assembly of the RNA-seq reads and Mr. H. AlSudais for RNA isolation.

Supplementary Data

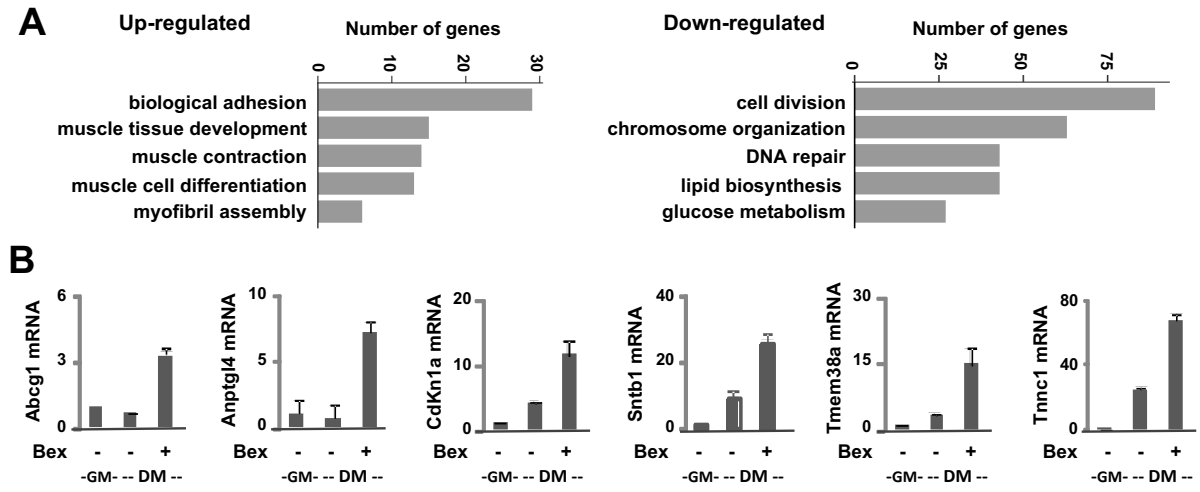

Figure S3.1 Expression of muscle-related genes during the early stage of differentiation.

(A) GO terms associated with genes differentially expressed between 12 and 24 hours of differentiation in untreated conditions. (B) RT-qPCR validation of bexarotene responsive gene expression in myoblasts differentiated in the absence or presence of bexarotene (Ctl or Bex 50 nM) for 24 hours. Quantification is presented as fold change relative to proliferating myoblasts (GM; Error bars: SEM; n = 3).

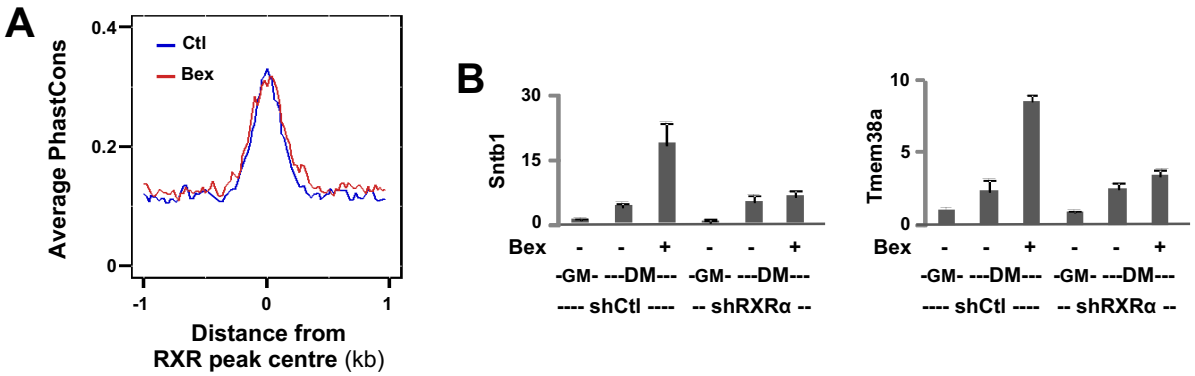

Figure S3.2 Role of RXR in myogenic regulation.

(A) The average PhastCons conservation scores of RXRα peaks in myoblasts differentiated in the absence or presence of bexarotene (Ctl or Bex 50 nM) for 24 hours. (B) RT-qPCR analysis of bexarotene responsive genes in RXRα knockdown cells (shRXR). A non-silencing shRNA (shCtl) was used as control. Quantification is presented as fold change relative to proliferating myoblasts (GM; error bars: SEM; n = 3).

Table S3.1 RNA-seq and ChIP-seq Dataset Access

A compilation of the ChIP-seq and RNA-seq datasets generated in this study which have been deposited within the NCBI Gene Expression Omnibus (GEO), as well as the publicly available ChIP-seq datasets.

Organism	Cell line	Condition	Antibody	Data Type	Replicate	GEO Accession	Citation
mus-musculus	C2C12	GM		RNA-seq	#1	GSM2478318	This study
mus-musculus	C2C12	Differentiating / 12h_Ctl		RNA-seq	#1	GSM2478320	This study
mus-musculus	C2C12	Differentiating / 12h_Bex		RNA-seq	#1	GSM2478322	This study
mus-musculus	C2C12	Differentiating / 24h_Ctl		RNA-seq	#1	GSM2478324	This study
mus-musculus	C2C12	Differentiating / 24h_Bex		RNA-seq	#1	GSM2478326	This study
mus-musculus	C2C12	GM		RNA-seq	#2	GSM2478319	This study
mus-musculus	C2C12	Differentiating / 12h_Ctl		RNA-seq	#2	GSM2478321	This study
mus-musculus	C2C12	Differentiating / 12h_Bex		RNA-seq	#2	GSM2478323	This study
mus-musculus	C2C12	Differentiating / 24h_Ctl		RNA-seq	#2	GSM2478325	This study
mus-musculus	C2C12	Differentiating / 24h_Bex		RNA-seq	#2	GSM2478327	This study
mus-musculus	C2C12	Input for RXRα		ChIP-seq	1	GSM2478303	This study
mus-musculus	C2C12	Differentiating / 24h_Ctl	RXRα	ChIP-seq	1	GSM2478304	This study
mus-musculus	C2C12	Differentiating / 24h_Bex	RXRα	ChIP-seq	1	GSM2478305	This study
mus-musculus	C2C12	Input for histone marks		ChIP-seq	1	GSM2478289	This study
mus-musculus	C2C12	GM	H4K8ac	ChIP-seq	1	GSM2478290	This study
mus-musculus	C2C12	Differentiating / 24h_Ctl	H4K8ac	ChIP-seq	1	GSM2478291	This study
mus-musculus	C2C12	Differentiating / 24h_Bex	H4K8ac	ChIP-seq	1	GSM2478292	This study
mus-musculus	C2C12	GM	H3K9ac	ChIP-seq	1	GSM2478293	This study
mus-musculus	C2C12	Differentiating / 24h_Ctl	H3K9ac	ChIP-seq	1	GSM2478294	This study
mus-musculus	C2C12	Differentiating / 24h_Bex	H3K9ac	ChIP-seq	1	GSM2478295	This study
mus-musculus	C2C12	GM	H3K18ac	ChIP-seq	1	GSM2478296	This study
mus-musculus	C2C12	Differentiating / 24h_Ctl	H3K18ac	ChIP-seq	1	GSM2478297	This study
mus-musculus	C2C12	Differentiating / 24h_Bex	H3K18ac	ChIP-seq	1	GSM2478298	This study
mus-musculus	C2C12	GM	H3K27ac	ChIP-seq	1	GSM2478299	This study

mus-musculus	C2C12	Differentiating / 24h_Ctl	H3K27ac	ChIP-seq	1	GSM2478300	This study
mus-musculus	C2C12	Differentiating / 24h_Bex	H3K27ac	ChIP-seq	1	GSM2478301	This study
mus-musculus	C2C12	GM	H3K27me3	ChIP-seq	1	GSM2478302	This study
mus-musculus	C2C12	Input for RNA Pol II, H3K4me1		ChIP-seq	1	GSM721306	Asp *et al.*, *Proc. Natl. Acad. Sci. U.S.A.*, 2011.
mus-musculus	C2C12	GM	RNA Pol II	ChIP-seq	1	GSM721286	Asp *et al.*, *Proc. Natl. Acad. Sci. U.S.A.*, 2011.
mus-musculus	C2C12	GM	H3K4me1	ChIP-seq	1	GSM721288	Asp *et al.*, *Proc. Natl. Acad. Sci. U.S.A.*, 2011.
mus-musculus	C2C12	Input for H3K4me3, H3K36me3		ChIP-seq	1	GSM918421	Yue *et al.*, *Nature*, 2014.
mus-musculus	C2C12	GM	H3K4me3	ChIP-seq	1	GSM918415	Yue *et al.*, *Nature*, 2014.
mus-musculus	C2C12	GM	H3K36me3	ChIP-seq	1	GSM918417	Yue *et al.*, *Nature*, 2014.
mus-musculus	C2C12	GM	MyoD	ChIP-seq	1	GSM915186	Yue *et al.*, *Nature*, 2014.
mus-musculus	C2C12	Differentiating / 24h	MyoD	ChIP-seq	1	GSM915183	Yue *et al.*, *Nature*, 2014.
mus-musculus	C2C12	Differentiating / 24h	Myogenin	ChIP-seq	1	GSM915159	Yue *et al.*, *Nature*, 2014.

Table S3.2 Primer sets used for RT-qPCR and ChIP-qPCR analyses

RT-PCR Primers

Gene	Accession #	Forward Primer	Reverse Primer
Cdkn1a	NM_007669.5	5′-CGCGGTGTCAGAGTCTAGG-3'	5'-GGACATCACCAGGATTGGAC-3'
Sntb1	NM_016667.3	5′-GAAGGAGAGATTCAACTGGACC-3′	5′-CCAAGCCCAGTCGTGTTATC-3′
Tmem38a	NM_144534.1	5′-GCCTCTGGAGTGTGGTACTTG-3′	5′-CAGCGATCTTTCGGACCCTC-3′
Tnnc1	NM_009393.2	5′-GGAGCTGCAGGAGATGATTG-3′	5′-CCTCAGACTTCCCTTTGCTG-3′

ChIP Primers

Gene	Forward Primer	Reverse Primer
Akt2	5′-AAGTGCCCTTCTCTGCACTC-3′	5′-TGCTTTGGCAGCTCAGAGG-3′
Sntb1	5′-AGTCAGTTTTCTCCCTGCCC-3′	5′-TACCACATGTGTGGGACAGC-3′
Tnnc1	5′-AGTTGGGGGCTTTCAAGGAA-3′	5′-AATACAGTCACAGGGCGGAG-3′
Control	5′-ACAGACAACGCAGAGTACCG-3′	5′-GCCACACTCCAGACAAGATAGT-3′

Chapter Four: Dissecting myogenin-mediated retinoid X receptor signaling in myogenic differentiation

---

Khilji S., Hamed M., Chen J., Li Q. *Commun. Biol.* 2020;3(1):315.

Dissecting myogenin-mediated retinoid X receptor signaling in myogenic differentiation

Saadia Khilji[1], Munerah Hamed[1], Jihong Chen[2] and Qiao Li[1,2 *]

[1]Department of Cellular and Molecular Medicine and [2]Department of Pathology and Laboratory Medicine, Faculty of Medicine, University of Ottawa, Ottawa, ON, Canada

[*] Correspondence should be addressed to Q. L. (Qiao.Li@uOttawa.ca)

Abstract

Deciphering the molecular mechanisms underpinning myoblast differentiation is a critical step in developing the best strategy to promote muscle regeneration in patients suffering from muscle-related diseases. We have previously established that a rexinoid x receptor (RXR)-selective agonist, bexarotene, enhances the differentiation and fusion of myoblasts through a direct regulation of MyoD expression, coupled with an augmentation of myogenin protein. Here, we found that RXR signaling associates with the distribution of myogenin at poised enhancers and a distinct E-box motif. We also found an association of myogenin with rexinoid-responsive gene expression and identified an epigenetic signature related to histone acetyltransferase p300. Moreover, RXR signaling instigates residue-specific histone acetylation at enhancers co-occupied by p300 and myogenin. Thus, genomic distribution of transcriptional regulators is an important designate for identifying novel targets as well as developing therapeutics that modulate epigenetic landscape in a selective manner to promote muscle regeneration.

Introduction

Recent large-scale functional genomic studies have elucidated the impact of epigenetic control on stem cell fate decision. Histone acetylation is one form of epigenetic regulation that affects DNA accessibility for lineage-specific transcription factors to direct the differentiation of stem cells into distinct lineages, including skeletal myoblasts (Zhang and Pradhan, 2014).

The formation of skeletal muscle requires temporal-spatial expression of myogenic regulatory factors (MRFs) that overlap in their ability to convert stem cells into the myoblast lineage (Zammit, 2017). Amongst the MRFs, Myf5 and MyoD are considered as determination factors since they regulate the proliferation and early differentiation of myoblasts, while myogenin functions downstream of MyoD to activate muscle gene expression and is critical for the differentiation and fusion of myoblasts into multinucleated myotubes (Rudnicki and Jaenisch, 1995; Zammit, 2017). While Myf5 and MyoD collaborate with partial redundancy in the development of open chromatin formation at muscle-specific loci, myogenin has a unique role in transcription from genes that have been primed (Singh and Dilworth, 2013). At the structural level, MRFs are a family of basic helix-loop-helix (bHLH) transcription factors that bind to a conserved core hexanucleotide motif (CANNTG) known as E-box (Asfour et al., 2018). MRF binding are modulated by E-box accessibility, central dinucleotide pair and flanking sequences, which may vary between biological systems and conditions (Cao et al., 2010; Fong et al., 2012; Li et al., 2019). As such, the myogenic program is genetically governed by E-box components, whereas E-box accessibility is controlled epigenetically (Fong et al., 2012, 2015).

Genome-wide profiling of histone marks has allowed segmentation of the myoblast genome into distinct chromatin states characterized by a combination of histone modification patterns present in those regions (Hamed et al., 2017). During myoblast differentiation, an overall decrease in acetylation of H3K9, H3K18, and H3K27 (Asp et al., 2011; Khilji et al., 2018) is accompanied by an increase in H4 acetylation, specifically at MyoD targets (Cao et al., 2010; Khilji et al., 2018). Overexpression of myogenin in differentiating C2C12 myoblasts correlates to hyperacetylation of H4, which is associated specifically to late muscle genes (Du et al., 2012). The global decrease in histone acetylation during myoblast differentiation likely reflects a down-regulation of proliferation genes, whereas histone acetylation increases at loci important for differentiation. For example, the regulatory regions of *Myod* and *Myf5* are associated with an increase in H3K18 and H3K27 acetylation, connected specifically to the histone acetyl-transferase (HAT) activity of p300 (Francetic et al., 2012; Hamed et al., 2013).

Initially identified as an E1A-associated protein (Arany et al., 1995), p300 is a critical transcriptional co-activator of a myriad of transcription factors involved in many cellular processes including proliferation and differentiation (Goodman and Smolik, 2000). It instigates chromatin remodeling as a HAT, but acts also as a molecular scaffold, bridging different DNA-binding proteins and activators with the basal transcriptional machinery (Chen et al., 2015; Ogryzko et al., 1996; Vo and Goodman, 2001). Particularly, H3K18 and H3K27 are the acetylation targets of p300 prior to RNA polymerase II recruitment (Jin et al., 2011). While p300 can be found at the promoter regions (Wang et al., 2009), its occupancy is regarded as the best chromatin signature of enhancers (Hnisz et al., 2013; Visel et al., 2009) which can be further categorized as poised, marked by H3K4me1/2, or active, signified by H3K27ac in addition to

H3K4me1/2 (Creyghton et al., 2010; Heintzman et al., 2007). In contrast, H3K27me3 is tightly associated with inactive genes and has a predictive nature of gene silencing (Barski et al., 2007). We have recently utilized different histone marks within the proliferating myoblasts to generate a 14-state chromatin state model to characterize loci-specific histone acetylation at p300-associated enhancers in early myoblast differentiation, particularly when it is recruited by MyoD (Hamed et al., 2017). Our data presents a model of histone acetylation increases at distinct genomic loci despite a global decrease in histone acetylation as myoblasts differentiate (Khilji et al., 2018).

Nuclear receptor superfamily of transcription factors regulate gene expression in response to steroids, lipids, and other small molecule ligands (Shulman and Mangelsdorf, 2005). As a member of this family, retinoid X receptor (RXR) binds to DNA either as a homodimer or heterodimer with other family members, making it a partaker of a large array of signaling pathways and a significant modulator of drug targets. We have previously reported that a RXR-selective agonist, bexarotene, enhances the differentiation and fusion of myoblasts through the function of RXR as a transcription factor (AlSudais et al., 2016). In addition, this enhancement is mediated largely through a direct regulation of MyoD gene expression and coupled with an augmentation of myogenin protein (Hamed et al., 2017). While MyoD is required for early myogenic differentiation, the activation of a subset of late muscle-specific genes occurs most efficiently in the presence of myogenin that amplifies the expression of genes previously primed by MyoD (Cao et al., 2006).

Nonetheless, the molecular pathways of transcription partners, co-activators and chromatin state dynamics underlying myogenin-mediated myoblast differentiation in response to RXR signaling remain an important but poorly understood issue. Here, we delineate how RXR-selective signaling affects genome-wide myogenin binding characteristics and dissect the molecular pathways through which RXR-selective signaling promotes myoblast differentiation.

Results

Genome-wide localization of myogenin in RXR signaling

We have previously reported that a RXR-selective agonist, bexarotene, enhances the differentiation and fusion of skeletal myoblasts into mature myotubes, while augmenting the protein level of myogenin, a terminal differentiation factor (AlSudais et al., 2016; Hamed et al., 2017). To study the molecular pathways underlying myogenin-mediated myoblast differentiation in the context of RXR signaling, we examined genome-wide myogenin localization using chromatin immunoprecipitation coupled with deep-sequencing (ChIP-seq), in the well-established myoblast model (Asp et al., 2011; Blais et al., 2005; Burattini et al., 2004). As shown in Fig. S4.1a and b, the expression of myogenin was induced upon 24-hour of differentiation, which was significantly augmented furthermore by over 3-fold following the addition of bexarotene. The myoblasts were subsequently subjected to myogenin ChIP-seq experimentation.

The quality metrics of myogenin ChIP-seq data were falling within the high confidence range for base quality, as represented by the average base quality score for myoblasts differentiated with or without bexarotene (score of 30–40, Fig. S4.1c). Fingerprint analysis with the deepTools suite showed an enriched but localized ChIP-seq read signal, 10% of the myoblast genome was enriched with 70% of uniquely aligned reads (Fig. S4.1d). Additionally, 98% of reads were successfully aligned to the mm9 genome with an IP efficiency of 2.9% and 3.1% for myoblasts differentiated with or without bexarotene, respectively, as projected by Hypergeometric Optimization of Motif EnRichment (HOMER) program analysis. Following peak calling of the sequencing data, about 9,500 confident myogenin peaks were obtained across both conditions (Fig. 4.1a), where the center of peaks displayed higher phylogenetic conservation (PhastCons)

scores than the surrounding regions, signifying well-aligned and ChIP-ed binding sites (Fig. S4.1e). In addition, Integrated Genome Viewer (IGV) (Robinson et al., 2011) of myogenin read signals displayed a distinct enrichment at myogenic loci (Fig. 4.1b), including regions flanking ADORA1 loci implicated previously in skeletal muscle injury and repair (Blum et al., 2012; Chandra et al., 2015; Zheng et al., 2007).

RXR signaling directs myogenin to poised enhancers

When categorizing the events of myogenin binding, we found approximately 55% of the peaks from myoblasts differentiated with bexarotene to be unique to bexarotene (Fig. 4.1a), although the length of peaks was similar between bexarotene and control conditions (Fig. S4.1f). There was a distinct increase in the number of myogenin peaks unique to bexarotene (3645) in comparison with unique to control (2920). In addition to the increase in the number of peaks, there was an increase in peak signal intensity in response to RXR signaling, as demonstrated by the heatmaps (Fig. 4.1c). Quantification of tag density from each category showed that myogenin peaks unique to bexarotene consist of a significantly greater number of tags per peak compared to peaks unique to control (Fig. 4.1d).

Given that myogenin is mainly associated with promoter regions (Blais et al., 2005; Hamed et al., 2017), we analyzed if RXR signaling affects the distance of myogenin peaks to the nearest transcription start site (TSS). Comparing to 40% of myogenin loci unique to control, only 15% of loci unique to bexarotene were found to be within 1 kb of a promoter (Fig. 4.1e). Therefore, the majority of loci unique to bexarotene were located distal to the promoters (> 1kb), suggesting that RXR signaling yields a preference for myogenin to bind regions likely to be enhancers (Fig.

4.1e). We also utilized an established chromatin state model based on genome-wide co-occurrence of different epigenetic marks in proliferating myoblasts (Hamed et al., 2017), to classify the chromatin state distribution of myogenin loci in differentiation. As previously reported (Blais et al., 2005; Hamed et al., 2017), myogenin loci unique to control were largely associated to active promoters (45%, Fig. 4.1f), in line with the close TSS proximity of a large proportion of myogenin peaks (Fig. 4.1e). However, in response to RXR signaling, the proportion of myogenin loci falling within enhancer regions increased from 38% to 60%, and especially to poised enhancers where myogenin association doubled from 13% to 30% (Fig. 4.1f). In contrast, the association of myogenin to active promoters diminished from 45% to 19% (Fig. 4.1f). Thus, a genome-wide shift in myogenin association from promoter to enhancer regions may be a functional signature of RXR signaling in myogenic differentiation.

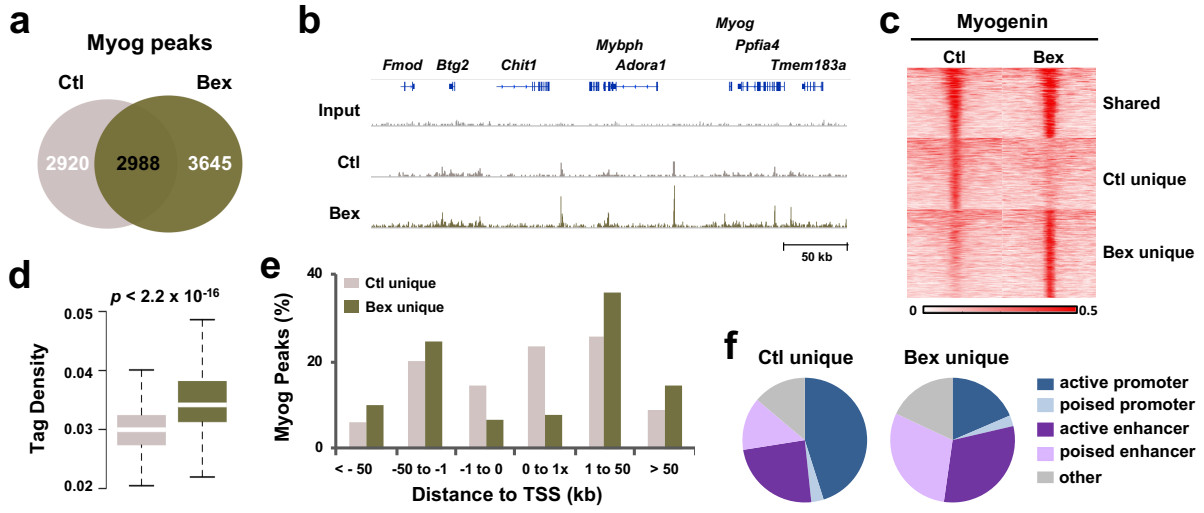

Figure 4.1 Characterization of myogenin localization in response to RXR signaling.

(a) Venn diagram depicts the overlap of myogenin ChIP-seq peaks between C2C12 myoblasts differentiated in the absence or presence of bexarotene (Ctl or Bex) for 24-hour. (b) Myogenin ChIP-seq read signals surrounding the *Adora1* locus. (c) Myogenin signal intensity was centered

around myogenin peaks (±1 kb), categorized into sites that were unique to control or bexarotene, and those shared between the two conditions. (d) Quantification of peak tag density (total number of tags in the peak region/ length of the peak) for the myogenin peaks (Wilcoxon rank sum test). (e) Distribution of peak distance to the nearest TSS. (f) Myogenin peaks were associated with distinct chromatin states.

RXR signaling promotes myogenin binding preference

To determine if RXR signaling affects myogenin binding site preferences, we performed *de novo* motif analysis on myogenin loci unique to bexarotene or control, covering sequences ± 50 bps to the center of peaks. The most enriched and significant primary motif across both categories was a canonical CANNTG E-box (Fig. 4.2a). Although E-box was the most significant motif identified across both categories, approximately 63% of myogenin loci unique to bexarotene harbored an E-box compared to only 21% of loci unique to control (Fig. 4.2a). Additionally, quantification of motif enrichment revealed that the E-box was enriched more than 4-fold at myogenin loci unique to bexarotene, compared to loci unique to control, while little changing in the enrichment of other identified motifs (Fig. S4.2).

Interestingly, while myogenin loci from both categories harbored an E-box with a GC at its core, E-box unique to bexarotene displayed a lower degree of consensus at the central G nucleotide (Fig. 4.2a), reflecting possibly an increased adaptability of myogenin recognition in response to RXR signaling. Furthermore, distinct from unique to control, E-box unique to bexarotene contained two additional consensus flanking nucleotides (Fig. 4.2a), potentially increasing the stringency of myogenin recognition upon RXR signaling, since nucleotides outside the E-box

determine binding specificity by influencing the three-dimensional structure of DNA binding sites (Gordân et al., 2013).

To further understand the impact of RXR-selective signaling on myogenin binding site preferences in early differentiation, we analyzed publicly available myogenin ChIP-seq data from C2C12 myoblasts differentiated for 24-, 60-hour, and 7 days. *De novo* motif analysis revealed that an increasing proportion of myogenin loci (from 45% to 77%) harbor the E-box motif as differentiation proceeds from 24-hour to 7-day, similar to myoblasts differentiated with bexarotene for 24-hour (Fig. 4.2a, Fig. S4.3a). We also analyzed myogenin ChIP-seq data from primary myoblasts isolated from gastrocnemius of C57BL/6 mice and differentiated for 24-hour (Umansky et al., 2015a). Interestingly, the central and flanking nucleotides of the E-box bound by myogenin in differentiating primary myoblasts were most similar to C2C12 myoblasts differentiated for 7-day or with bexarotene for 24-hour (Fig. 4.2a, Fig. S4.3a). In addition, it is only in primary myoblasts differentiated for 24-hour or C2C12 myoblasts for 7-day, we discerned two additional consensus flanking nucleotides, mirrored by myoblasts differentiated with bexarotene for 24-hour (Fig. 4.2a, Fig. S4.3a).

Next, we quantified the number of E-box motifs per myogenin peak, and found that 47% of myogenin loci in myoblasts differentiated with bexarotene for 24-hour contained 2 or more E-boxes similar to 58% and 43% of myogenin loci in 7-day C2C12 and 24-hour primary myoblast differentiation respectively (Fig. 4.2b, Fig. S4.3b). In contrast, only 13% of myogenin loci unique to control contained 2 or more E-boxes per peak, comparable to the public data from myoblasts differentiated for 24- and 60-hour (Fig. 4.2b, Fig. S4.3b). Quantification of motif

density also revealed greater E-box density at myogenin peaks from 7-day C2C12 and 24-hour primary myoblast differentiation than myoblasts differentiated for 24- and 60-hour (Fig. S4.3c). Thus, RXR signaling modulates myogenin binding preferences in terms of E-box identity and density, reflecting a dynamic environment representative of an *ex vivo* context and mature myotubes.

As gene expression is often controlled by regulatory circuits consisting of multiple transcription factors, we explored regions proximal to the primary E-box for neighboring transcription factor motifs using MEME secondary motif analysis. Runx1 motif was the most significant motif associated with E-box unique to control (Fig. 4.2c), consistent with previous observation that Runx1 cooperates with MRFs and the AP-1 family of transcription factors to regulate myoblast proliferation and differentiation (Umansky et al., 2015a). However, among myogenin loci unique to bexarotene, we identified a double-E-box, two canonical E-boxes, separated by 4 bp or 6 bp (Fig. 4.2c, d). Previous characterization of double E-box has modeled a spacing of 5 bp as optimal for a full turn of the DNA double helix, such that the nucleotides in each E-box face the same spatial direction of DNA (Chang et al., 2015). Taken together, our results suggest that RXR signaling not only modulates the preference of myogenin for E-box component, but may also promote its cooperation with flanking E-box binding protein for complex formation.

Next, we discerned in detail the population of myogenin loci unique to bexarotene containing a single E-box or double E-box. While about 28% of single E-box associated loci displayed a fold change greater than 10 in the enrichment of myogenin over input, approximately 42% of double E-box peaks fell into this category (Fig. 4.2e). Moreover, myogenin loci associated with single

E-box generally appeared as sharper and narrower peaks compared to a broader compilation of read signals at loci containing the double E-box, shown by IGV snapshots of representative myogenin ChIP-seq tracks (Fig. 4.2f, g). Taken together, E-box components in central dinucleotide, flanking sequences and density, as well as flanking motif composition may all contribute to myogenin binding as a functional avenue of RXR signaling in myogenic differentiation.

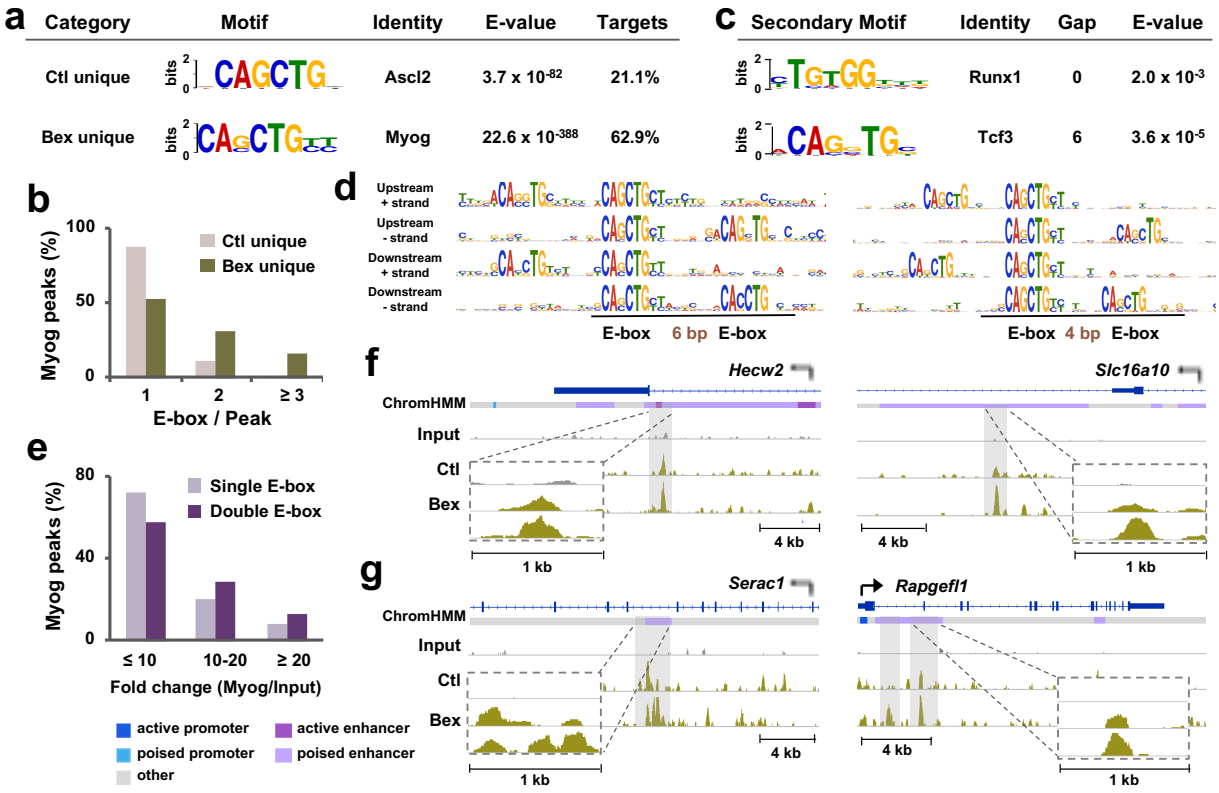

Figure 4.2 RXR signaling influences myogenin binding site specificity.

(a) The most significant and centrally distributed consensus motif, its associated identity, E-value, and the percentage of myogenin loci associated to each motif as revealed by *de novo* motif analysis of myogenin peaks unique to control or bexarotene (Ctl or Bex) following 24-hour of differentiation. (b) Bar graph displays the distribution of myogenin peaks associated to the indicated number of E-box motifs. (c) The predicted secondary motif, its associated identity, E-value, and base pair spacing between the primary and secondary motifs by MEME secondary

motif analysis. (d) Presentation of the primary and secondary motifs for myogenin loci unique to bexarotene. (e) Myogenin enrichment over input for myogenin peaks unique to bexarotene, categorized as those associated to single E-box motifs or double E-box motifs. (f, g) Genome browser view of *Hecw2*, and *Slc16a10* with myogenin peaks associated to single E-box, and *Serac1* and *Rapgefl1* with myogenin peaks associated to double E-box. Dashed boxes show a zoomed in view of the regions boxed in grey. Blue bars show Refseq gene positions.

Epigenetic features associated to myogenin loci

As transcription factor occupancy is an important indicator of lineage-specific gene expression, we integrated genome-wide myogenin loci with differential RNA-seq of myoblasts in matching conditions (Hamed et al., 2017). To this end, genes upregulated between proliferation and differentiation were subdivided into groups affected by differentiation only or bexarotene additionally, and each group of genes was then examined for myogenin association in response to RXR signaling. Approximately 25% of genes upregulated in differentiation only were associated to myogenin, whereas about 70% of bexarotene-responsive genes displayed an association to myogenin (Fig. 4.3a). Furthermore, 57% of bexarotene-responsive genes were associated with two or more myogenin peaks compared to 45% of genes in differentiation only (Fig. 4.3b). Taken together, our results suggest that myogenin is intimately connected to rexinoid-responsive gene expression in early myoblast differentiation.

Since RXR signaling modifies genomic localization of myogenin (Fig. 4.1g), we explored the chromatin state distribution of myogenin associated with genes upregulated in differentiation only or by bexarotene additionally. Approximately 53% of myogenin loci associated with bexarotene-responsive genes were found in poised enhancers, compared to about 33% of

myogenin loci associated with genes upregulated in differentiation only (Fig. 4.3c). Since histone acetylation and methylation are important for gene expression, we also analyzed H4K8ac, H3K9ac, H3K18ac, and H3K27ac centered at myogenin loci associated with each group of genes. H3K27me3, associated with transcriptional repression (Barski et al., 2007), was used as control (Fig. S4.4). Interestingly, myogenin loci associated to rexinoid-responsive genes displayed an overall increase in histone acetylation following addition of bexarotene, in contrast to loci associated to genes upregulated in differentiation only where no change in histone acetylation was observed (Fig. 4.3d, e). Moreover, the largest increase in histone acetylation in response to bexarotene was H4K8ac and H3K9ac, whereas H3K27me3 signal was minimum (Fig. 4.3d, e). Therefore, myogenin-mediated RXR signaling may be reflected by residue-specific acetylation in bexarotene-responsive gene expression.

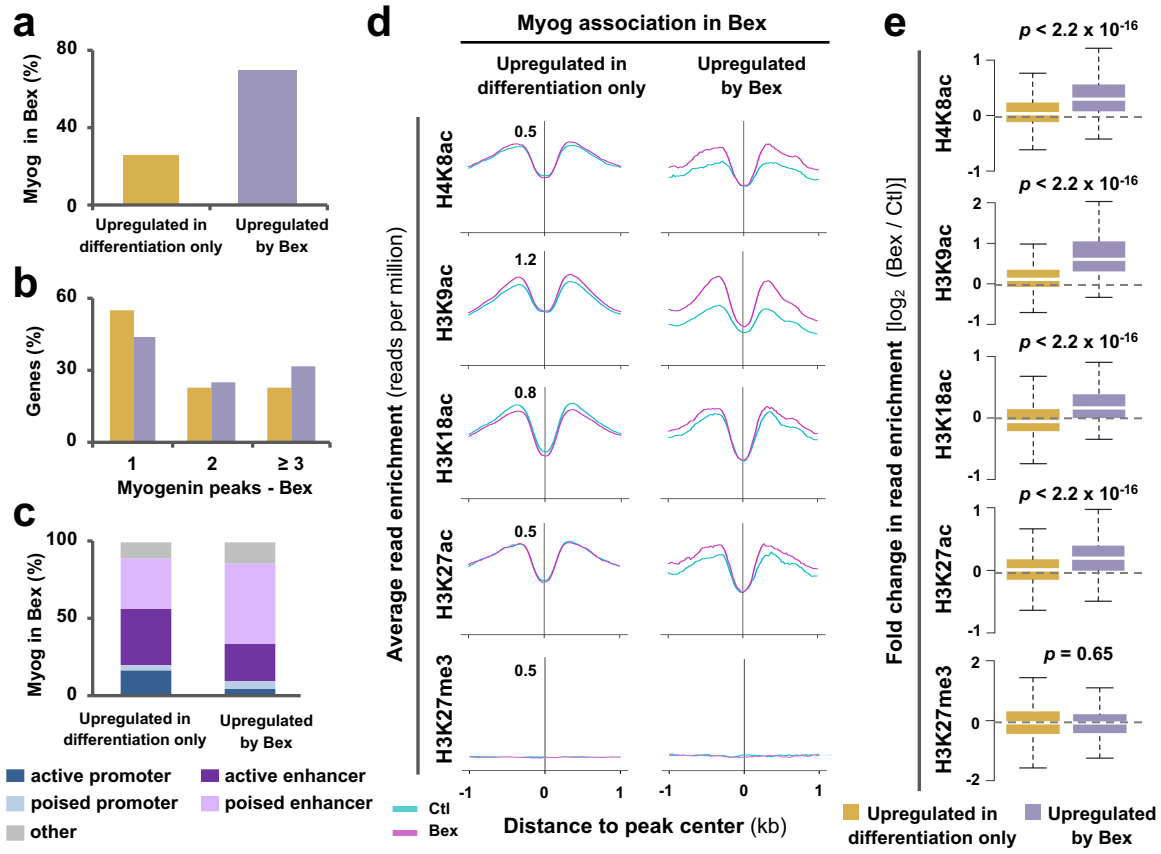

Figure 4.3 Myogenin is associated with bexarotene-responsive gene expression.

(a) Myogenin loci from myoblasts differentiated with bexarotene (Bex) for 24-hour were associated with genes upregulated in differentiation only or additionally by bexarotene. (b) Quantification of the number of peaks per gene. (c) Chromatin state distribution of myogenin loci. (d) Average read density for acetylation of H4K8, H3K9, H3K18, and H3K27 in addition to H3K27 trimethylation from myoblasts differentiated in the absence (Ctl) or presence of bexarotene. (e) Quantification of log2-fold difference in the histone acetylation and methylation read signal at myogenin loci categorized in Panel d (Wilcoxon rank sum test).

Genomic distribution of p300 in response to RXR signaling

Since myogenin-mediated rexinoid-responsive gene expression is associated with a histone acetylation signature and p300 is a critical HAT required for skeletal muscle development (Chen

et al., 2015; Polesskaya et al., 2001; Roth et al., 2003), we next examined in detail p300 and histone modification in early myoblast differentiation. Interestingly, the global levels of cellular p300 protein and histone modifications were relative stable in differentiation and in the presence of bexarotene (Fig. 4.4a, b). We next conducted p300 ChIP-seq in matching conditions of myogenin ChIP-seq to dissect the role of p300 and residue-specific histone acetylation in response to RXR signaling. As shown in figure 4.4c, the proportion of p300 peaks unique to bexarotene was considerably less than the 14,849 peaks unique to control or the 7,198 peaks shared regardless of treatment. When assessing the chromatin state distribution of p300, we found that p300 loci unique to control mainly associated to enhancers with only 20% to the promoter regions (Fig. 4.4c), similar to previous reports (Heintzman et al., 2007; Visel et al., 2009). The addition of bexarotene, however, led to a distinct change in chromatin state distribution with nearly 40% of p300 loci unique to bexarotene found in the promoter regions (Fig. 4.4c).

As p300 displayed a preference for promoter association in response to RXR signaling (Fig. 4.4c), we examined motif composition underlying p300 loci for which active and poised promoters as well as active and poised enhancers were simply grouped into promoters and enhancers. *De novo* motif analysis of p300 associated promoters revealed the presence of binding motifs for Atf1, Sp1 and bZIP transcription factors (Fig. 4.4d-f). Binding motif for Sp1, a ubiquitously expressed transcription factor involved in the formation of pre-initiation complex (PIC) in communication with coactivators including p300 (Emili et al., 1994; Kim et al., 2005; Visel et al., 2009), was particularly enriched in unique to control (Fig. 4.4e, f). However, bexarotene promoted an increase in the Atf1 motif (Fig. 4.4e, f), suggesting RXR signaling may

promote the distribution of p300 to promoters as well as affect the identity of the recruiting factor.

In contrast to enrollment of p300 at the promoters, p300 occupancy at the enhancers correlated not only with binding motifs for bZIP transcription factor, but also for E-box binding proteins, Tead4, and Runx (Fig. 4.4g, h). In addition, E-box enrichment increased over 2-fold in response to bexarotene, and it was the only motif to which p300 association increased in RXR signaling (Fig. 4.4g, h). Additionally, nearly 40% of p300 loci unique to bexarotene were associated to an E-box in contrast to only 16% of loci unique to control (Fig. 4.4h), suggesting that RXR signaling promotes the recruitment of p300 by E-box binding proteins to the enhancers. Taken together, p300 is differentially recruited to promoters and enhancers in that p300 may mediate RXR signaling through distinct functional modes.

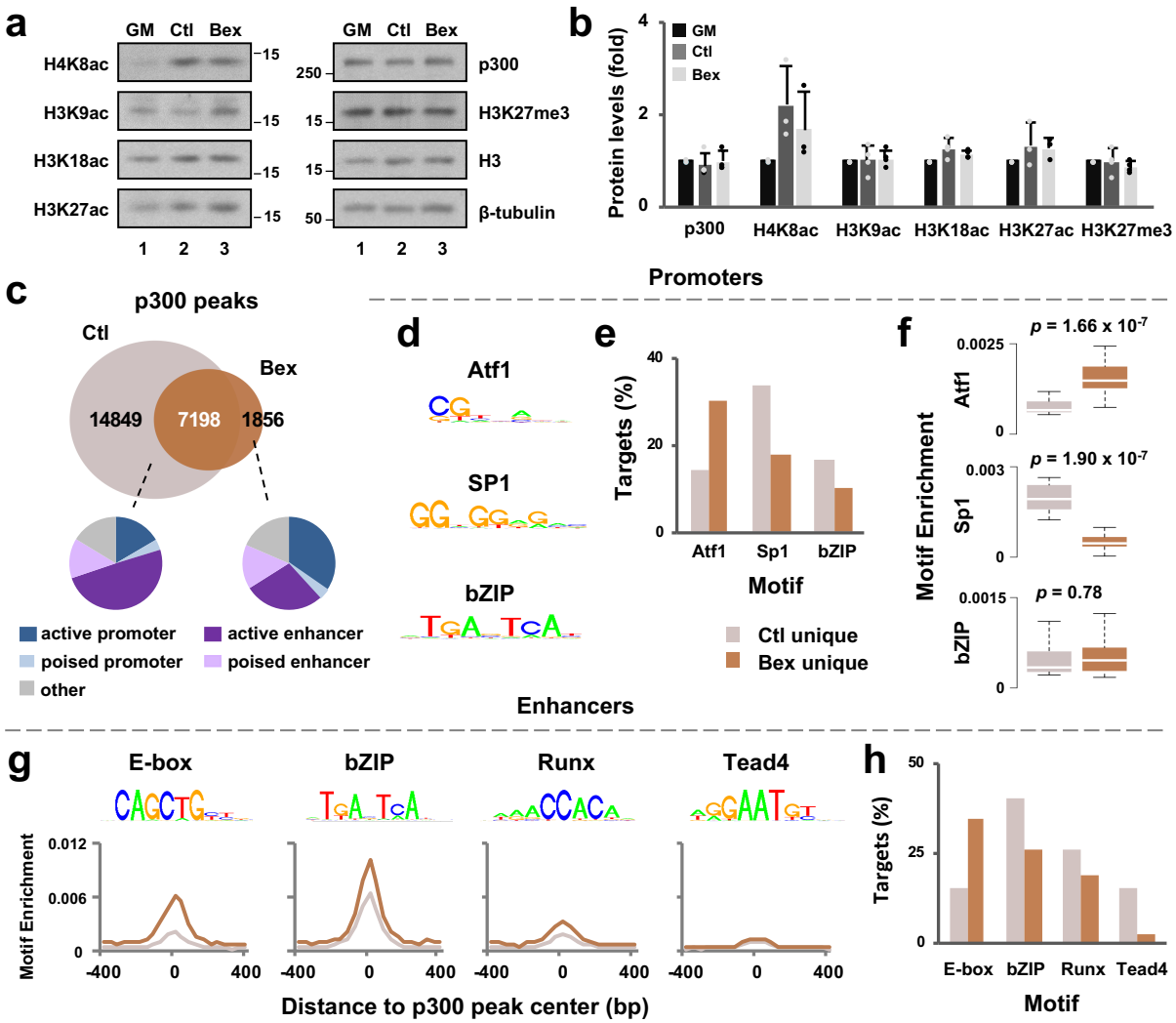

Figure 4.4 Genomic distribution of p300 in RXR signaling.

(a) Western analysis of p300, and indicated histone marks with β-tubulin as a loading control in proliferating C2C12 myoblasts (GM) and myoblasts differentiated in the absence or presence of bexarotene (Ctl or Bex) for 24-hour. (b) Quantification of the Western blots is presented as fold change in relation to proliferating myoblasts (error bars: SD; n = 3). (c) Venn diagram depicts unique and shared p300 loci between myoblasts differentiated without or with bexarotene. Chromatin state distribution of p300 loci unique to each condition is also shown. (d) *De novo* motif analysis of p300 loci in the promoter regions. (e) The percentage of p300 loci harboring motifs displayed in Panel d. (f) Boxplots represent the enrichment of each motif shown in Panel d (Wilcoxon rank sum test). (g) *De novo* motif analysis of p300 loci in the enhancer regions with

the corresponding motif enrichment shown. (h) The percentage of p300 loci harboring the motifs from Panel g.

Histone acetylation associated to bexarotene-responsive genes

Previous studies have found that the level of histone acetylation at promoters decreases during myoblast differentiation regardless if gene expression is up- or down-regulated (Asp et al., 2011; Blum et al., 2012). We thus examined the profiles of H4K8ac, H3K9ac, H3K18ac and H3K27ac, with H3K27me3 as control, across the promoters of bexarotene-responsive genes. Interestingly, the average signal of H3K9ac at the TSS of bexarotene-responsive genes was significantly enriched following bexarotene treatment (Fig. 4.5a, b). However, there was no such enrichment observed at the TSS of genes upregulated in differentiation only (Fig. 4.5a, b). Additionally, there was little detectable H3K27me3 signal at the promoters (Fig. 4.5a, b). Evidently, the increase in the level of H3K9ac at the TSS of bexarotene-responsive genes was correlated to the transcriptional activity of those genes, suggesting that residue-specific histone acetylation at distinct promoters may play a key role in rexinoid-responsive gene expression.

Since rexinoid-responsive gene expression is linked to residue-specific histone acetylation, we examined the role of p300 in the regulation of myomixer, a microprotein essential for myoblast fusion and muscle formation (Bi et al., 2017; Quinn et al., 2017; Zhang et al., 2017), along with the aforementioned histone acetylation. IGV track of ChIP-seq read signal coverage displayed a constitutive presence of p300 at the promoter, accompanied by residue-specific histone acetylation, particularly H3K9ac (Fig. 4.5c). ChIP-qPCR analysis demonstrated that p300 occupancy at the myomixer locus was enriched by about 2-fold upon 24-hour of differentiation,

and further increased following bexarotene treatment (Fig. 4.5d). We also used a previously established p300 shRNA knockdown myoblast system (Chen et al., 2015) to determine the requirement of p300 for myomixer expression. As shown in figure 4.5e, in shRNA control myoblasts, myomixer expression was markedly induced in differentiating myoblasts and augmented further by bexarotene. However, shRNA knockdown of p300 attenuated myomixer gene expression in differentiating myoblasts regardless of treatment, suggesting a critical role for p300 in myomixer gene regulation.

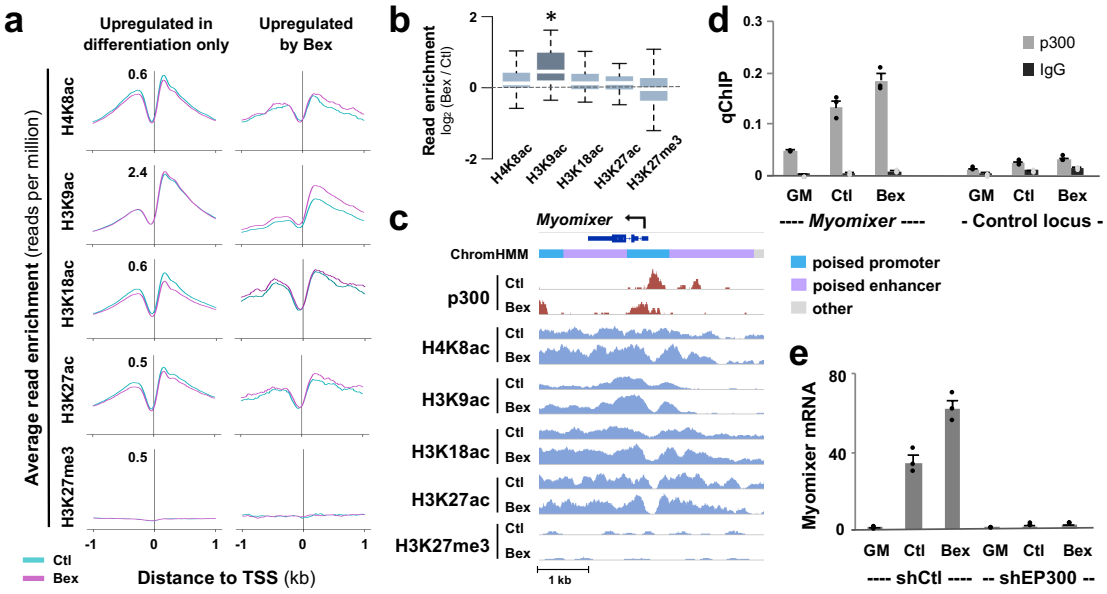

Figure 4.5 Bexarotene-responsive gene promoters are marked by residue-specific histone acetylation.

(a) Average enrichment profiles of H4K8ac, H3K9ac, H3K18ac, H3K27ac and H3K27me3 from myoblasts differentiated in the absence or presence of bexarotene (Ctl or Bex) for 24-hour. The profiles span 2 kb across the TSS of genes upregulated in differentiation only and by bexarotene additionally. (b) Boxplots present fold change in enrichment of histone modifications between treated and control myoblasts at bexarotene responsive promoters shown in Panel a (*, $p \leq 0.05$, Wilcoxon rank sum test). (c) IGV view of p300 and indicated histone marks at the *Myomixer* locus. Blue bars show Refseq gene position. (d) Enrichment of p300 at the *Myomixer* promoter

was determined by qChIP analysis in proliferating (GM) and differentiating myoblasts. Normal IgG antiserum and a random locus were used as control. Quantification is presented as percentage of enrichment in relation to input chromatin DNA (error bars: SEM; n = 3). (e) RT-qPCR analysis of *Myomixer* gene expression following the introduction of p300 shRNA (shEP300). Quantification is presented as fold change relative to proliferating myoblasts, after normalization to an internal control. A nonsilencing shRNA (shCtl) was used as control (error bars: SEM; n = 3).

Genomic overlap of p300 with myogenin

Since p300 can be recruited by E-box binding proteins (Fig. 4.4), we analyzed the overlap of myogenin loci in differentiating myoblasts with p300 loci in promoters or enhancers unique to control or bexarotene. As shown in Figure 4.6a, approximately 5% of p300 loci unique to control displayed an overlap with myogenin at either promoters or enhancers. Although the addition of bexarotene did not affect the degree of p300 and myogenin overlap at the promoters, their overlap increased from 5% to 23% at the enhancer regions (Fig. 4.6a). Furthermore, it was only in response to RXR signaling, enhancers associated with both myogenin and p300 displayed a significant increase in H4K8ac and H3K9ac (Fig. 4.6b, c). Figure 4.6d shows an IGV snapshot of the sarcomeric gene *Mybph* locus, where the enrichment of p300 and myogenin increased at putative enhancer regions following the addition of bexarotene. As demonstrated by qChIP analysis, myogenin and p300 enrichment was evident at the putative enhancer in differentiating myoblasts and further increased markedly by bexarotene (Fig. 4.6e). The enrichment of p300 and myogenin at the *Mybph* locus also correlated with an activation of Mybph gene expression as revealed by RT-qPCR analysis in matching conditions (Fig. 4.6f). Moreover, differentiation-dependent and bexarotene-responsive Mybph gene expression was attenuated following shRNA

p300 knockdown (Fig. 4.6f), designating *Mybph* as a p300 target gene and signifying a role for p300 in mediating rexinoid signaling.

Taken together, our results suggest that RXR signaling modulates the global binding dynamics and motif recognition of myogenin, an important myogenic regulatory factor, which cooperates with p300, in the installation of an epigenetic signature associated to rexinoid-responsive gene expression in early myogenic differentiation (Fig. 4.7).

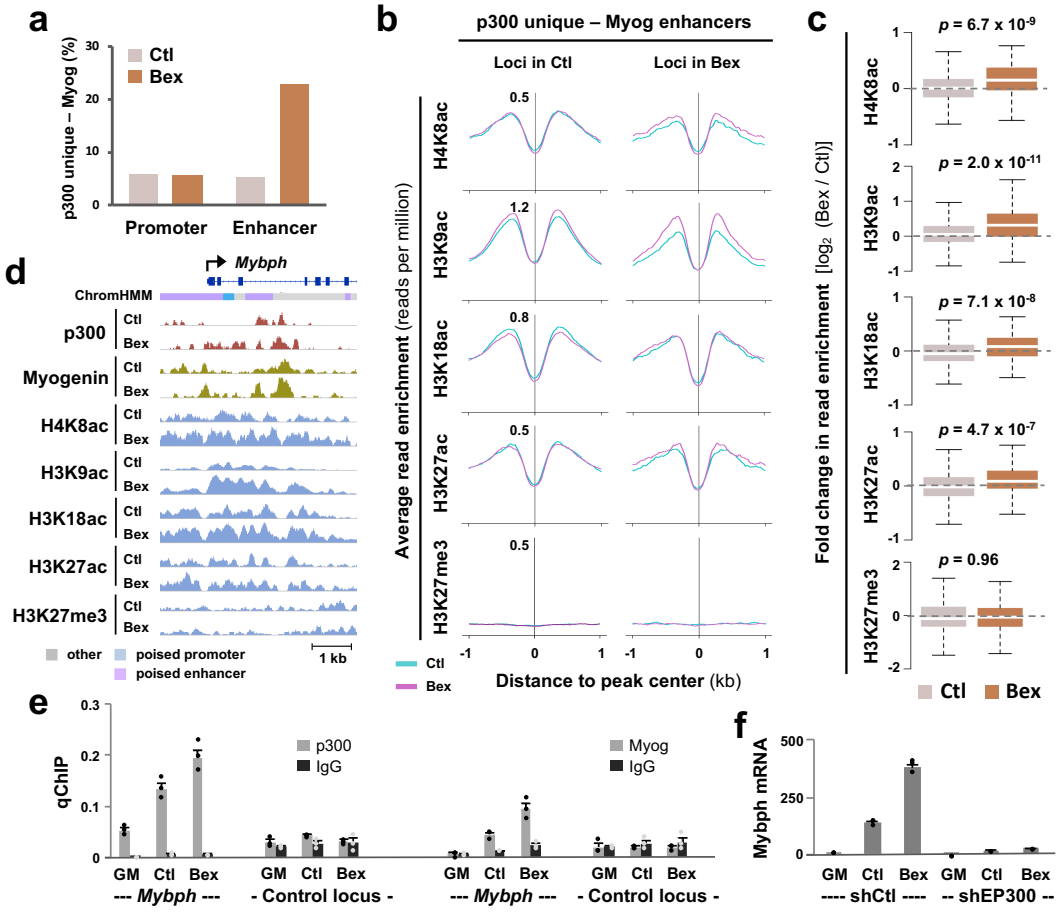

Figure 4.6 Overlap between p300 and myogenin in RXR signaling.

(a) p300 loci unique to myoblasts differentiated in the absence or presence of bexarotene (Ctl or Bex) were associated to promoters or enhancers and co-localized with myogenin loci from myoblasts differentiated with bexarotene. (b) Average read signal profiles for indicated histone marks at enhancers associated with p300 and myogenin. (c) Boxplots present the fold change in enrichment between control and bexarotene for histone modifications shown in Panel b (Wilcoxon rank sum test). (d) IGV view of p300, myogenin and histone modification read density at the Mybph locus. Blue bars show Refseq gene position. (e) Occupancy of p300 at the Mybph locus was determined by qChIP analysis in proliferating myoblasts (GM) and myoblasts differentiated for 24-hour. Normal IgG antiserum and a random locus were used as controls. Quantification is presented as percentage of enrichment in relation to input chromatin DNA (error bars: SEM; n = 3). (f) RT-qPCR analysis of Mybph gene expression following the introduction of p300 shRNA (shEP300). A nonsilencing shRNA (shCtl) was used as control.

Quantification is presented as fold change relative to proliferating myoblasts normalized to an internal control (error bars: SEM; n = 3).

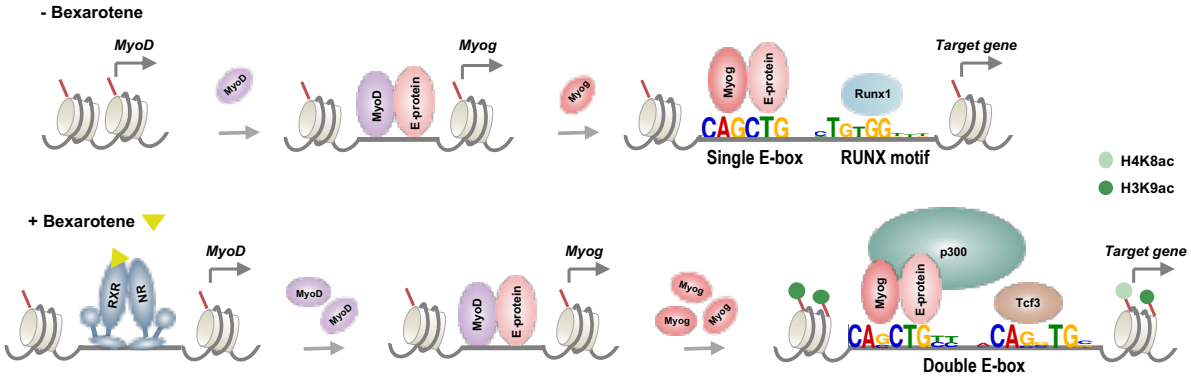

Figure 4.7 A model of the regulatory events underlying myogenin-mediated RXR signaling in myoblast differentiation.

In the absence of rexinoid, a single canonical E-box with RUNX as the most significant neighboring motif is found in myogenin loci. RXR signaling augments directly MyoD gene expression, which in turn enhances the expression of myogenin. Nevertheless, RXR signaling promotes myogenin binding preference to a distinct double E-box motif with a lower degree of consensus at the central G nucleotide but two additional consensus flanking nucleotides. In addition, p300 occupancy as well as an increase in H3K9 and H4K8 acetylation overlap with rexinoid-responsive myogenin loci, important to myogenin-mediated RXR signaling in myoblast differentiation.

Discussion

We have previously established that a selective RXR agonist, bexarotene, enhances the differentiation and fusion of myoblasts, while augmenting myogenin expression (AlSudais et al., 2016). Here, we delineate myogenin-mediated RXR signaling in early myoblast differentiation using OMICs approaches. We have found that RXR signaling leads to myogenin occupancy at poised enhancers and a specific "double E-box" with consensus flanking sequences. We have also found a close association of myogenin with rexinoid-responsive gene expression. Furthermore, we have identified an epigenetic signature related to p300 and rexinoid-responsive promoters on connection with residue-specific histone acetylation. Thus, RXR signaling-promoted genomic distribution of transcription regulators presents distinct dynamics which may be utilized to identify novel genetic targets, as well as the potential of pharmaceutical modification of the epigenetic landscape to promote muscle development and regeneration.

Characterization of genome-wide transcription factor distribution and binding motifs is an important avenue for understanding regulatory networks that govern stem cell differentiation. Using a ChIP-seq approach, we have found that RXR signaling shifts the distribution of myogenin from promoter to poised enhancer regions (Fig. 4.1). As poised enhancers play a crucial role within gene programs that remain in an inactive state until onset of differentiation (Creyghton et al., 2010), myogenin may contribute to the initiation of these pathways to elicit myoblast differentiation in response to RXR signaling. Interestingly, myogenin loci unique to rexinoids have a greater association to a distinct E-box with two flanking nucleotides consisting of CASCTGYY, whereas loci unique to control are associated with a shorter motif of CAGCTG (Fig. 4.2). DNA sequences flanking the core motif exert an impact on transcription factor

binding, as they affect DNA topology and as a result binding affinity (Dror et al., 2015; Levo et al., 2015). For example, yeast bHLH binding specificity is determined by nucleotides outside the E-box motifs due to 3D structure of the DNA binding sites (Gordân et al., 2013). Thus, the flanking sequences of E-box represent an important mechanism in loci selection of nearly 63% of myogenin occupancy in rexinoid-enhanced myoblast differentiation (Fig. 4.2). Nonetheless, myogenin binding may also be influenced by factors beyond consensus sequences including chromatin accessibility, DNA topology, protein interactions, and epigenetic regulation such that characterizing consensus motifs is an important first step to further understand gene regulatory networks (Inukai et al., 2017; Spitz and Furlong, 2012).

Apart from the primary motif, RXR signaling also favors a secondary motif proximal to the primary E-box. Runx1, a well-known component of regulatory complexes within the muscle lineage (Umansky et al., 2015b, 2015a), is a potential partner for myogenin at loci unique to control (Fig. 4.2). However, myogenin loci unique to rexinoids harbor a double E-box, as well as an overall increase in the number of E-box motifs per locus (Fig. 4.2). Casey and colleagues (Casey et al., 2018) have suggested that an increase in E-box density may be important for improving DNA accessibility in the context of a closed chromatin conformation, where based on the length of spacing, a series of motifs may serve as a platform on the surface of a nucleosome, to promote bHLH factor binding. Thus, the presence of secondary E-box in close proximity to the primary E-box, suggests that a bHLH dimer as well as E-box density may both play roles in increasing the binding intensity of myogenin in rexinoid-enhanced myoblast differentiation.

Interestingly, the presence of multiple E-box motifs on adjacent helical turns can create a platform permissible for a tetrameric bHLH complex. Chang et al. (Chang et al., 2015) recently illustrated the formation of an intramolecular tetramer within the TWIST family of bHLH transcription factors with a spatial configuration of a double E-box separated by 5 nucleotides. The spacing allows a full turn of the DNA double helix such that the E-boxes are facing the same spatial direction, with minimal steric hindrance between the E-boxes, providing efficient co-factor interactions to promote enhancer function (Chang et al., 2015). Furthermore, we have observed a difference in the length of peaks associated to single or double E-box where the latter contained broader span of read signals (Fig. 4.2), which may translate to functional relevance as studies have shown that peak shape analysis can reveal information regarding the binding of neighboring proteins and in certain instances, is correlated with gene expression (Cremona et al., 2015). Taken together, rexinoid-promoted loci recognition and selection may contribute to the overall increase in myogenin binding intensity and capacity.

Importantly, the majority of rexinoid-responsive genes are associated with a myogenin peak, accompanied by an increase in H4K8 and H3K9 acetylation in contrast to genes upregulated in differentiation only (Fig. 4.3). An overexpression of myogenin in C2C12 myoblasts has been shown to increase hyperacetylation of H4 associated directly to late muscle genes, such that myogenin induces chromatin remodeling of MyoD-initiated late muscle genes, and shifts the transcriptional activation of these genes to an earlier time period (Du et al., 2012). Since RXR signaling increases the level of myogenin protein (Hamed et al., 2017), it may promote loci-specific histone acetylation of late muscle genes, leading to an earlier expression of rexinoid-responsive genes and thus enhance the differentiation and fusion of myoblasts.

We have also examined the genomic dynamics of p300, a HAT crucial for myogenic differentiation, due to the coupling of histone acetylation with rexinoid-responsive gene expression. While p300 and its functional homologue CBP share many functional parallels, they have distinct cellular functions (Eid et al., 2000; Kung et al., 2000; Yao et al., 1998). Severe myogenic abnormalities are found in p300 knockout mice, but not in CBP knockout (Tanaka et al., 1997; Yao et al., 1998). In addition, ES cells from p300 knockout mice are unable to express MyoD or Myf5, whereas $CBP^{-/-}$ ES cells can develop into multinucleated myotubes, demonstrating that compared to CBP, p300 is required for muscle development (Roth et al., 2003).

Interestingly, we have found that p300 is mainly associated with active promoters in response to RXR signaling (Fig. 4.4), contrasting to its large association to enhancers in the absence of rexinoids (Khilji et al., 2018). Also, p300 may be recruited to the promoters by Atf1, Sp1 and bZIP binding proteins, where Atf1 motif displayed the largest enrichment at p300 associated promoters unique to rexinoid (Fig. 4.4). Combinations of Jun, Fos and Atf heterodimers are part of a large family known as the activating protein-1 (AP-1) transcription complex, in that the composition of AP-1 dimers, their relative abundance, and cell type determine cellular fate outcome (Hess et al., 2004). Motif analysis of p300-associated promoters suggests recruitment of p300 by AP-1 family members during rexinoid-enhanced differentiation, with a predisposition by Atf1 binding protein in particular (Fig. 4.4). On the other hand, Sp1 motif displays the greatest enrichment at promoters unique to control (Fig. 4.4). Many studies have shown the interaction of Sp1 with p300 within the same regulatory complex on promoters of genes which

they regulate, such as p21 (Xiao et al., 2000), IL-12 (Sun et al., 2006) and IQGAP (Jin et al., 2019). The presence of p300 allows for assembly of the transcription complex in which it acts as a bridging factor to connect transcription factors to the basal transcription machinery, but also leads to targeted histone acetylation to open up the chromatin environment and to ¨bookmark¨ the promoters for rapid transcription re-initiation. As such, the promoters of rexinoid-responsive genes exhibit a significant increase in H3K9 acetylation, which is not the case for promoters of genes upregulated in differentiation only (Fig. 4.5). More importantly, knockdown of p300 diminishes the expression of myomixer, a rexinoid-responsive myogenic target (Fig. 4.5). Therefore, RXR signaling is exemplified by the association of p300 to promoters and an enrichment in H3K9 acetylation in particular (Fig. 4.5). Taken together, p300 function as a scaffold for protein complexes and a HAT for residue-specific histone acetylation at promoters may together facilitate rexinoid-responsive gene expression.

Apart from promoters, enhancers also play a key role in determining cell-type specific gene regulation, as the chromatin marks at enhancers are cell-type-specific and a functional signature of cellular fate (Heintzman et al., 2009; Komashko et al., 2008; Pennacchio et al., 2007). We have identified binding motifs for Ap-1, Runx and Tead4 within p300 associated enhancers (Fig. 4.4), all of which are known myogenic enhancer regulators (Andreucci et al., 2002; Joshi et al., 2017; Umansky et al., 2015b). However, p300 may largely be recruited to the enhancer regions by E-box binding proteins (Fig. 4.4), following RXR signaling where a considerable overlap between p300 and myogenin loci occurs (Fig. 4.6). Enhancers co-occupied by p300 and myogenin are also marked by an enrichment of H4K8 and H3K9 acetylation (Fig. 4.6), such that

the recruitment of p300 by E-box binding proteins and residue-specific histone acetylation may be a signature of rexinoid-responsive gene expression (Fig. 4.7).

In conclusion, we have provided molecular insights into the role of myogenin-mediated RXR signaling in skeletal myoblast differentiation. (Fig, 4.7). A thorough understanding of the epigenetic mechanisms that regulate myogenic fate transitions will allow the development of novel therapeutics to treat muscle-related diseases, as the ability to control endogenous epigenetic modifiers will enable specific changes in transcriptional activity of genes important for myogenesis.

Methods

Cell Culture

C2C12 mouse myoblasts (ATCC) were maintained in growth medium (GM), consisting of Dulbecco's modified Eagle medium (DMEM) supplemented with 10% fetal bovine serum, 100 units/ml penicillin and 100 μg/ml streptomycin, at 37°C with 5% CO_2. To induce differentiation, cells at 70-80% confluence were switched to differentiation medium (DM), DMEM supplemented with 2% horse serum, and cultured for 24 hours. Bexarotene (LC Laboratories) was added to DM at a final concentration of 50 nm for treatment.

Western Blot Analysis

Cells were lysed in whole cell extract buffer (10% glycerol, 50 mM Tris-HCl pH 7.6, 400 mM NaCl, 5 mM EDTA, 1mM DTT, 1 mM PMSF, 1% NP-40), at 4ºC for 30 minutes with rotation. Cell extracts were prepared as previously described (Chen et al., 2005). Protein concentrations were determined by the Bradford Method (Bio-Rad). The proteins were then separated by SDS-PAGE and transferred to an Immun-Blot PVDF membrane. Bio-Rad ChemiDoc MP System was used to capture chemiluminescent images, and the protein bands were quantified using Scion Image (Scion Corporation). The primary antibodies used for western analysis were from hybridoma E7 for β-tubulin and hybridoma F5D for myogenin.

Reverse transcription qPCR analysis

Total RNA from C2C12 cells was isolated by using the GeneJET RNA Purification Kit (ThermoFisher Scientific) and quantified by Nanodrop (ND-1000). An equal amount of RNA was reverse transcribed into cDNA by using a High-Capacity cDNA Reverse Transcription Kit

(Applied Biosystems) in accordance with the manufacturer's instructions. SYBR® Green PCR Master Mix and HotStarTaq DNA polymerase (Qiagen) were used for qPCR on a CFX96 Touch Real-Time PCR Detection System (BioRad). The data was analyzed by using the threshold cycle comparative method, normalized to the expression of TATA-Binding Protein (TBP), using the formula $2^{-\Delta\Delta CT}$. Experiments were repeated at least three times. The following primers were used: myomixer primer forward, GTTAGAACTGGTGAGCAGGAG and reverse, CCATCGGGAGCAATGGAA; Mybph primer forward, ACTTAGCCACCACCACCAAG and reverse, GGAGTGGAGGTATGGTCAGC; TBP primer forward, TCATGGACCAGAACAACAGC, and reverse, GCTGTGGAGTAAGTCCTGTGC.

ChIP-seq and data processing

Following 24 hours of differentiation, cells were fixed, crosslinked, and sonicated with a Bioruptor as previously described (Higazi et al., 2011). Chromatin immunoprecipitation was performed with antibodies obtained from Santa Cruz against myogenin (sc-12732) and p300 (sc-584). The immunoprecipitants were purified using a MiniElute PCR Purification kit (Qiagen). ChIP-seq libraries were prepared and sequenced on an Illumina HiSeq 2000 (p300 and H3K27me3) or Illumina HiSeq 4000 (myogenin) as single-end 50 bp reads. For p300 and H3K27me3, reads were mapped to the mm9 genome using Bowtie (Langmead et al., 2009) v0.12.7 allowing for three mismatches and reporting the single best alignment per 50 bp read. For myogenin, sequence reads were aligned to the mouse mm9 reference genome build using BWA-Mem (Li and Durbin, 2009) v0.7.10 with default parameters. Duplicate reads were removed utilizing the Picard package v2.6.0. Genome-wide read coverage and enrichment was assessed using deepTools (Ramírez et al., 2016) fingerprint plots where the corresponding x- and

y-axes for a point of intersection, denote the percentage of genome coverage and the percentage of all uniquely aligned reads, respectively. Peak calling was performed with HOMER (Heinz et al., 2010) v4.10 with -style factor and FDR of 1.0×10^{-4}. The approximate IP efficiency calculated by HOMER describes the fraction of tags found in peaks compared to the genomic background and is utilized as one measure of ChIP efficacy.

De novo motif discovery was performed with MEME using the "meme-pal" command with input sequences of 500 bps surrounding the peak center. The mergePeaks tool from HOMER was utilized for co-localization of peaks (-d given) and the findMotifsGenome tool for *de novo* motif discovery on the 200 bp surrounding the peak centers. The annotatePeaks.pl script was employed for quantification of motif enrichment and for peak annotation, where HOMER compares the distance from a peak to the RefSeq catalog of transcription start sites of nearby genes, and reports the closest TSS as the associated gene.

The enrichment of histone acetylation at specified loci or TSSs was calculated with ngs.plot (Shen et al., 2014) which calculates the coverage vectors for each query region based on specified alignment files. Coverage data is normalized for equal length and vectors are normalized against the corresponding library size, to allow comparisons of datasets with differences in sequencing depth. Default values for all analyses were used unless specified. IGV v2.3.97 was used for data browsing and representative snapshots.

Quantitative ChIP analysis

Following ChIP, qPCR was performed in triplicate reactions using the SYBR green method with locus specific primers. A standard curve was created for each set of primers with input DNA, followed by quantification of the abundance of immunoprecipitated target DNA in relation to input chromatin DNA. Each qChIP was repeated at least three times. Antibodies against p300 and myogenin were the same as for Western. Primer pairs used for qPCR amplification were as follows: *myomixer* locus forward, GAACAGCTGTGTTCTGGCAC and reverse, TGGGGAATTCCTGCACATGG; *Mybph* locus forward, AGTGCCTGCTCAGCTAATCC and reverse, CTGAGCCTCCTAAGCAGCAA.

Statistics and reproducibility

All statistical analyses were performed using The R Project for Statistical Computing or Microsoft Excel. Normally distributed data were analyzed by a two-tailed Student's t-test. Non-normally distributed data were analyzed by non-parametric two-sided Wilcoxon rank sum tests. A $p < 0.05$ was considered statistically significant. Statistical details and number of replicates are indicated in the figure legends.

Data Availability

All ChIP-seq datasets have been deposited in the NCBI Gene Expression Omnibus (GEO) under accession number GSE139942. Source data are available as Supplementary Data 1.All other relevant data supporting the key findings of this study are available within the article and its Supplementary Information or from the corresponding author upon reasonable request.

Acknowledgements

This research was supported by an Operating Grant from the Natural Sciences and Engineering Research Council of Canada (NSERC #250174 to Q.L.). S.K. is a recipient of Canada Graduate Scholarship from the NSERC, and M.H. a scholarship from Umm Al-Qura University in Saudi Arabia.

Author Contributions

S.K. and Q.L., data analysis and manuscript preparation; M.H., data collection; J.C., and Q. L. conception and final approval of the manuscript. All authors reviewed the manuscript.

Competing Interests

The authors declare no competing interests.

Supplementary Data

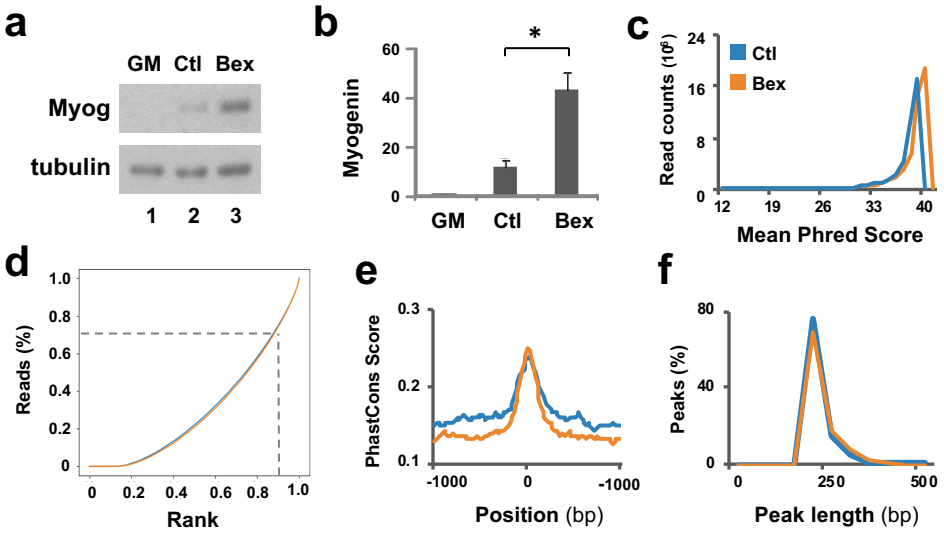

Figure S4.1 Quality control of myogenin ChIP-seq.

(a) C2C12 myoblasts were differentiated for 24-hour in the absence (Ctl) or presence of bexarotene (Bex), followed by Western blotting of myogenin protein levels. Proliferating myoblasts (GM) were included with β-tubulin as a loading control. (b) Quantification of myogenin protein levels as a fold change relative to proliferating myoblasts (error bars: SD; n = 4; *, $p \leq 0.05$, Student's t-test). (c) Base quality scores for myogenin sequencing data. (d) ChIP enrichment plot shows the percentage of reads in a given percent of mappable genome, where rightward deflection indicates the extent of ChIP signal enrichment. (e) The average PhastCons conservation scores of myogenin peaks. (f) Distribution of the length of myogenin peaks.

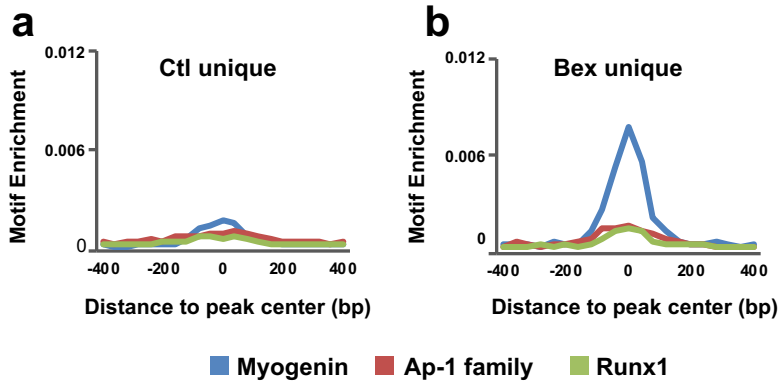

Figure S4.2 Motif enrichment at myogenin loci.

(a) Motif enrichment at myogenin loci unique to C2C12 myoblasts differentiated for 24-hour in the absence or (b) presence of bexarotene (Ctl or Bex).

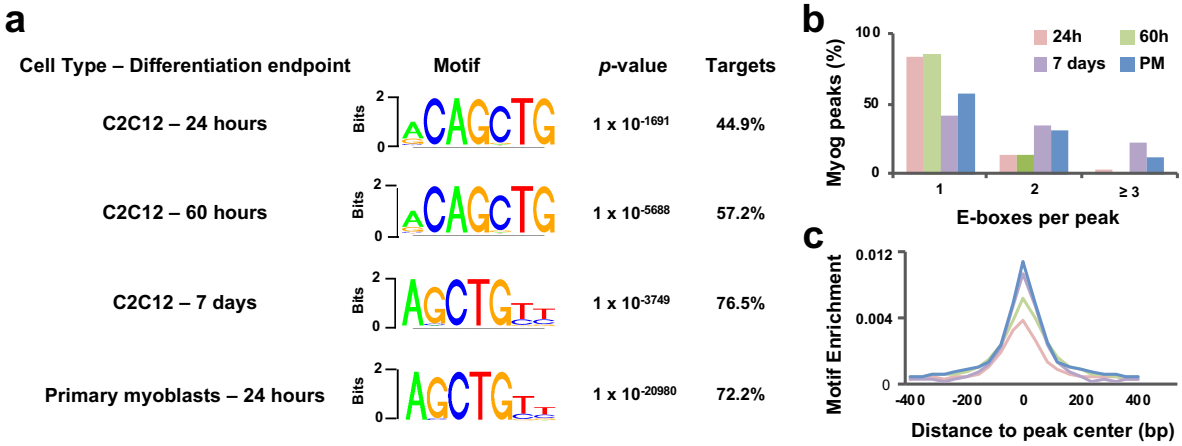

Figure S4.3 Motif analysis of publicly available myogenin ChIP-seq.

(a) Myogenin loci in myoblasts differentiated for 24-, 60-hour, and 7 days as well as primary myoblasts (PM) differentiated for 24-hour were subjected to *de novo* motif analysis. The most significant motif in each condition, its associated *p*-value and the percentage of target loci harboring the motif are shown. (b) Bar graph displays the percentage of myogenin peaks associated to a specified number of E-box per peak. (c) Enrichment of motifs shown across myogenin loci.

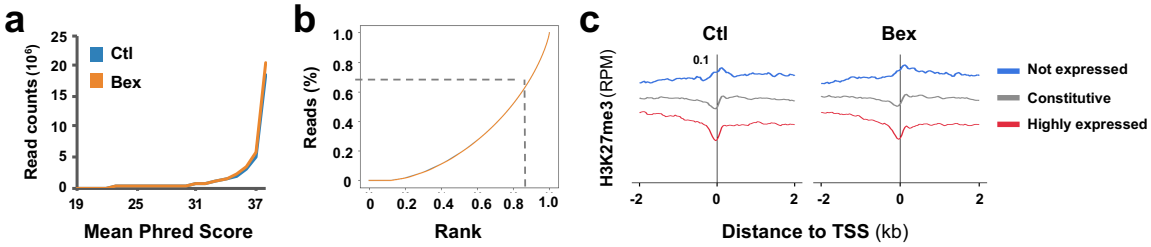

Figure S4.4 Quality control of H3K27me3 ChIP-seq.

(a) C2C12 myoblasts were differentiated for 24-hour in the absence (Ctl) or presence of bexarotene (Bex) and subjected to H3K27me3 ChIP-seq. Quality score distribution shows majority of reads were attributed with a Phred score above 30, equating to 99.9% base call accuracy. (b) ChIP enrichment plot presents the percentage of reads in a given percent of mappable genome. Rightward deflection of the curve indicates ChIP enrichment. (c) The total population of ENSEMBL genes from RNA-seq expression profiling of proliferating myoblasts and myoblasts differentiated for 24-hour were categorized into three groups (GSE94560). The average enrichment of H3K27me3 (reads per million) with respect to the TSS of each gene group is shown. H3K27me3 was prominently enriched around the TSS of inactive genes, consistent with its role in gene silencing.

Chapter Five: Functional and regulatory characterization of novel myogenic target, Tmem182 in the context of RXR signaling

---

Khilji S., Hamed M., Chen J., Li Q.

Manuscript in preparation for submission to the *Journal of Biological Chemistry*

Functional and regulatory characterization of novel myogenic target, Tmem182 in the context of RXR signaling

Saadia Khilji[1], Munerah Hamed[1], Jihong Chen[2] and Qiao Li[1,2 *]

[1]Department of Cellular and Molecular Medicine and [2]Department of Pathology and Laboratory Medicine, Faculty of Medicine, University of Ottawa, Ottawa, ON, Canada

[*] Correspondence should be addressed to Q. L. (Qiao.Li@uOttawa.ca)

Abstract

We have previously established that bexarotene, a clinically approved agonist of retinoid X receptor (RXR), promotes the differentiation and fusion of skeletal myoblasts. In this study, we utilized global transcriptional profiling underlying rexinoid enhanced myogenic differentiation to identify novel myogenic targets for downstream therapeutic development. As such, we observed a significant upregulation for a transcript encoding a novel predicted transmembrane protein, Tmem182, during early C2C12 myoblast differentiation. Despite the documentation of its upregulation in skeletal muscle, the regulatory and functional characterization of Tmem182 had yet to be explored. Here, we show that Tmem182 is a target of RXR signaling via RXRα as a transcription factor and its expression is specific to muscle tissues. We also show that Tmem182 is augmented during myoblast differentiation and our results indicate that its levels may be directly regulated by differentiation-specific expression of MyoD. We also report the association of p300 to the Tmem182 promoter and reveal Tmem182 as a MyoD- and p300-dependent gene. Our results display a putative epigenetic signature related to p300 and associated histone acetylation for bexarotene-responsive locus activation and transcription of myogenic targets. Importantly, using analysis of Tmem182 knockdown, we present the first report indicating a requirement for Tmem182 in myoblast differentiation and our results cumulatively provide evidence to indicate an important but distinct role for Tmem182 in skeletal muscle development.

Introduction

The proper formation of skeletal muscle requires sequential expression of muscle regulatory factors (MRFs) including Myf5, MyoD, myogenin and MRF4 (Braun et al., 1989; Davis et al., 1987; Edmondson and Olson, 1989; Rhodes and Konieczny, 1989). MRFs are a group of basic helix-loop-helix (bHLH) transcription factors that bind a conserved DNA motif known as an E-box, present in the regulatory loci of many skeletal muscle specific genes (Sartorelli and Caretti, 2005). Myf5 and MyoD regulate proliferation and early differentiation of myoblasts, diminishing in expression soon after differentiation has begun (Bergstrom and Tapscott, 2001). Myogenin is critical for the regulation of late differentiation and fusion, and MRF4 is expressed several days after fusion (Rudnicki and Jaenisch, 1995). Studies have also delineated additional functions for MyoD in terminal differentiation and of MRF4 in the commitment of MPCs suggesting that the proper development of skeletal muscle requires the coordinated interaction of MRFs within complex transcriptional regulatory networks (Kassar-Duchossoy et al., 2004; Rawls et al., 1995; Zammit, 2017).

Myogenic gene expression relies on the recruitment of histone acetyltransferases (HATs) such as the coactivator p300 and its functional homologue CREB-binding protein (CBP), which are part of multi-protein apparatuses that are recruited to the regulatory regions of target genes (Perissi and Rosenfeld, 2005). Knockout studies in mice and embryonic stem cells have delineated that the HAT activity of p300 but not CBP is essential for skeletal myogenesis and for the expression of muscle-specific genes, including Myf5 and MyoD (Francetic et al., 2012; Hamed et al., 2013; Polesskaya et al., 2001; Roth et al., 2003). Additionally, as a global co-activator of numerous cellular processes including differentiation (Ait-Si-Ali et al., 2000; Goodman and Smolik, 2000;

Iyer et al., 2004), p300 is a key chromatin signature of enhancers where H3K18 and H3K27 are its main acetylation targets (Akhtar-Zaidi et al., 2012; Blow et al., 2010; Heintzman et al., 2007; Jin et al., 2011). Although, histone acetylation decreases globally during the course of myogenic differentiation, we have characterized an increase in loci-specific histone acetylation at p300-associated enhancers in early myoblast differentiation, particularly when it is recruited by MyoD (Asp et al., 2011; Khilji et al., 2018). Taken together, these results indicate p300 is an important coactivator for myogenic expression and provides a valuable signature to identify novel regulatory elements for studies of transcriptional control.

Chromatin modifications which play an important role in differentiation have recently emerged as an avenue to identify networks of regulatory loci underlying gene expression. While histone acetylation plays an important role in the activation of gene expression (Lee et al., 1993), histone methylation associates with both gene activation and repression, dependent upon the specific lysine residue and the state of methylation (Barski et al., 2007; Kouzarides, 2007). For example, actively transcribed genes are characterized by high levels of H3K4me3 and H3K36me3 (Berger, 2007; Hon et al., 2009) whereas H3K27me3 is associated with transcriptional repression. Furthermore, H3K9ac, H3K18ac, and H3K27ac are found in regions surrounding transcription start sites (TSS) in combination with H4K8ac at promoter regions (Halsall et al., 2012; Wang et al., 2008b). Thus, genomic localization of chromatin modifications is a useful tool to identity regulatory regions and provide indications for activation of distinct gene programs.

The nuclear receptor (NR) superfamily of transcription factors broadly influence gene expression in response to steroids, lipids, and other small molecules or synthetic ligands (Shulman and Mangelsdorf, 2005). RXR belongs to the Type II NR family and has the ability to form

heterodimers with one third of the other NRs, allowing it to mediate a large array of signaling pathways. Three different isoforms of RXR have been identified (α, β, and γ), however RXRα is the predominant subtype expressed in adult skeletal muscle (Barbosa-Morais et al., 2012). RXRα-null mice died in utero due to myocardial malformations and thus the NR is critical for embryonic development. As type II NRs, RXR dimers constitutively bind a consensus sequence known as a hormone response element (HRE) in the promoters or enhancers of the genes they regulate, but require the presence of specific ligands to initiate ligand-induced transcription (Gronemeyer et al., 2004). As such, we have previously reported that bexarotene, a selective RXR agonist, promotes the specification and differentiation of skeletal myoblasts through the function of RXRα largely via a direct regulation of MyoD expression (AlSudais et al., 2016; Le May et al., 2011). Interestingly, we also found an association of myogenin with rexinoid-responsive gene expression coupled with residue-specific histone acetylation at enhancers co-occupied by p300 and myogenin (Khilji et al., 2020).

Since RXR signaling distinctly promotes myogenic gene expression, we utilized condition specific gene expression profiling in rexinoid enhanced myoblast differentiation to characterize gene activation patterns induced during the differentiation program (Hamed et al., 2017). This led us to the identification of Tmem182 as a novel myogenic target, highly upregulated during early myoblast differentiation. Tmem182 was first described by Kuninger et al. in a study of novel genes induced during growth factor-mediated muscle cell survival and differentiation (Kuninger et al., 2004). Follow-up studies have described a ~770-fold upregulation of Tmem182 transcript upon conversion of C2C12 myoblasts to myocytes and an 45-fold upregulation during brown preadipocyte to adipocyte conversion (Wu and Smas, 2008). Since Tmem182 displays a

differentiation dependent upregulation in myotube formation as well as adipogenesis, its function may be related to cellular pathways shared by both lineages (Wu and Smas, 2008). In the context of myogenesis, siRNA mediated knockdown of Tmem182 led to a reduction of myogenin transcript by approximately 30% (Wales et al., 2014). Moreover, Tmem182 knockdown in oral squamous cell carcinomal cells (OSCC) reduced cell adhesion ability towards to fibronectin and overexpression of Tmem182 led to a suppression of invasion, suggesting that Tmem182 is important for cellular mechanisms underlying cell motility in particular (Hsing et al., 2019). Collectively, the limited studies describing Tmem182 thus far indicate an important myogenic role. However, the protein sequence of Tmem182 lacks homologies with previously defined protein families and its function in any given system remains currently unknown. Thus, with this study, we aimed to characterize the regulation and the function of Tmem182 in myoblast differentiation and fusion to provide valuable insights into its potential role in skeletal muscle health and disease.

Results

Tmem182 is a rexinoid-responsive target expressed in skeletal muscle

We have previously demonstrated that RXR signaling promotes myoblast specification, differentiation and fusion of skeletal myoblasts (AlSudais et al., 2016; Hamed et al., 2017). In this study, we used an interval approach to examine the optimal time period of rexinoid treatment required to induce the myogenic program (Fig. 5.1). As such, C2C12 myoblasts were differentiated for four days in the presence of bexarotene for different time periods including during the first two days of differentiation, the last two days or throughout the entire 4-day time period. Intriguingly, only the addition of bexarotene in the first two days or throughout the four days of differentiation significantly enhanced the differentiation and fusion of myoblasts as determined by quantitative microscopy (Fig. 5.1A). The presence of bexarotene two days following initiation of differentiation failed to significantly augment differentiation or fusion of myoblasts to the extent of treatment during the first two days or throughout the 4 days (Fig. 5.1A-C). Additionally, the ability of bexarotene to enhance myogenic differentiation was also illustrated by a significant increase in muscle marker, MyHC compared with untreated myoblasts (Fig. 5.1D), suggesting that bexarotene treatment is most efficient during early differentiation as it enhances myogenesis via an augmentation of early gene expression (Fig. 5.1).

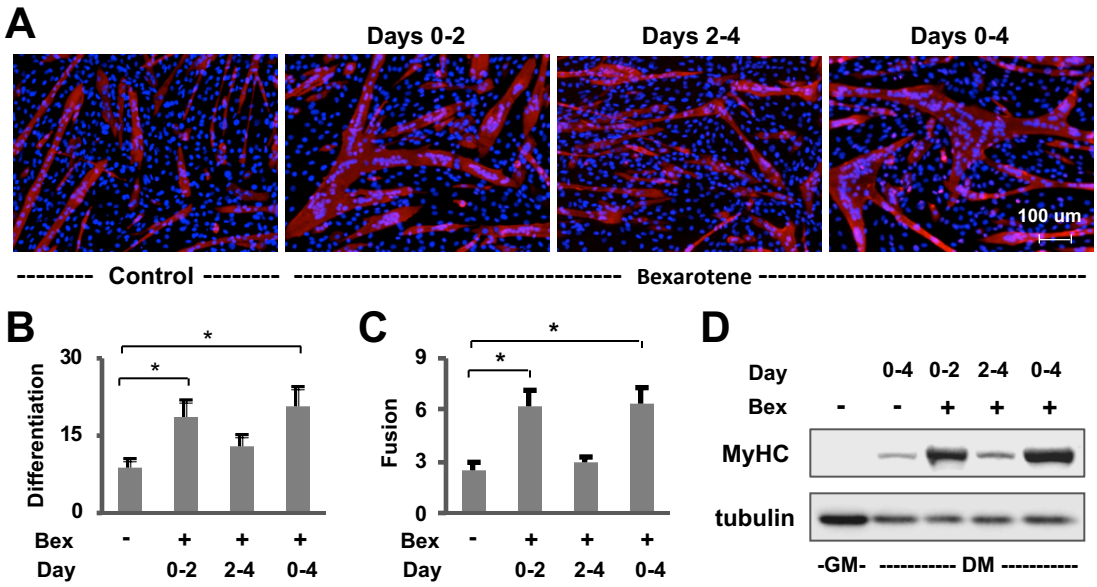

Figure 5.1 Bexarotene enhances the differentiation and fusion of C2C12 myoblasts.

(A) C2C12 myoblasts were differentiated for 4 days in the absence or presence of bexarotene (Control or Bex, 50 nM) for the periods specified, and stained for myosin heavy chain (red) and nuclei (blue). Representative microscopy images are shown. (B) Differentiation was defined as the percentage of myogenic nuclei relative to the total number of nuclei. (C) Fusion rate was defined as the number of nuclei per myocyte. Error bars are the standard deviations of three independent experiments (*, $p < 0.05$). (D) MyHC protein levels were determined by Western blotting in proliferating myoblasts (GM) and myoblasts differentiated for 4 days (DM). Tubulin was used as a loading control.

Since bexarotene promotes early myogenic gene expression, we utilized selective ligand-induced activation of myogenic programs to delineate novel myogenic targets and molecular interactions underlying skeletal myogenesis. As such, we analyzed differential gene expression in C2C12 myoblasts differentiated for 24 hours in the absence or presence of bexarotene with proliferating myoblasts as control (Hamed et al., 2017). From the list of genes with unknown functions in myogenesis, we focused upon Tmem182, a novel transmembrane protein that is upregulated

nearly 5-fold during the first 24 hours of differentiation, similar to other muscle-specific genes such as *myomaker* (Millay et al., 2013) (Fig. 5.2A). Tmem182 mRNA and protein levels were significantly augmented further following the addition of bexarotene, exhibiting Tmem182 as a rexinoid-responsive target (Fig. 5.2B-C). Due to the lack of functional information regarding Tmem182, we also assessed its tissue-specificity across nine mouse tissues which displayed the highest Tmem182 expression in muscle tissue including cardiac and skeletal muscle (Fig. 5.2D). Since our results indicate that Tmem182 is expressed in skeletal muscle, we examined whether its levels are also modulated during skeletal muscle regeneration *in vivo* via a cardiotoxin (CTX) injured model of myonecrosis and subsequent muscle regeneration (Fig. 5.2E). Microarray data from injured TA muscle over 21 days following injury displayed a drastic increase in Tmem182 expression which peaked at day 3 following injury, a period of rapid regeneration, after which its levels gradually returned to control 21 days post-injury. Thus, similar to other myogenic targets including MyoD and myomaker, Tmem182 is a muscle-specific protein that may be required for muscle development, maintenance, and regeneration (Fig. 5.2).

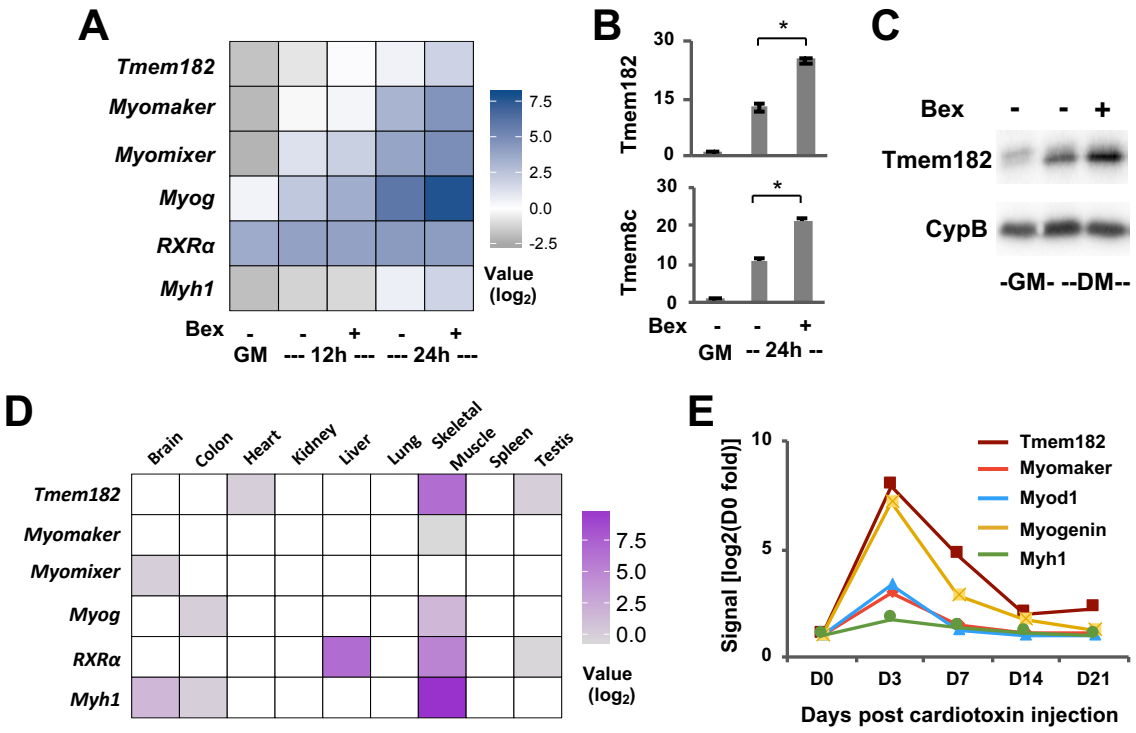

Figure 5.2 Tmem182 is expressed in skeletal muscle.

(A) The heatmap displays expression profiles for the indicated genes as determined by RNA-seq analysis of proliferating C2C12 myoblasts (GM) and those differentiated in the absence or presence of bexarotene (Bex, 50 nM). (B) The expression levels of Tmem182 and Tmem8c were determined by RT-qPCR in primary myoblasts differentiated in the absence or presence of bexarotene (30 nM). Expression values are presented as fold change relative to proliferating myoblasts (n = 3). (C) Western analysis of Tmem182 and cyclophilin B (CypB) following 2 days of differentiation (DM) in C2C12 myoblasts. (D) The heatmap presents relative expression levels collected from strand-specific RNA-seq for nine CD1 mouse tissues with an expression level cut-off of 0.5 [GSE41637]. (E) Tmem182 expression in cardiotoxin-injured TA muscle from 12-week old C57BL/6J mice, as determined by microarray analysis [GSE45577]. Signal Intensity is presented as the fold change relative to uninjured muscle (D0).

The regulation of Tmem182 expression

As bexarotene enhances myoblast differentiation and fusion largely via a direct regulation of MyoD (Hamed et al., 2017), we assessed the role of MyoD for Tmem182 expression. As shown in Figure 5.3A, microarray data from overexpression of MyoD to induce myogenic conversion of C3H/10T1/2 fibroblasts displayed a substantial upregulation of Tmem182 expression, similar to myomaker and myogenin, both of which are known targets of MyoD. Interestingly, loss of MyoD in C2C12 myoblasts dramatically reduced Tmem182 mRNA expression during the differentiation process but remained largely unaffected in proliferating conditions (Fig. 5.3B). Collectively, these results indicate that Tmem182 is augmented during the differentiation process and its levels may be regulated by differentiation-specific expression of MyoD (Fig. 5.3).

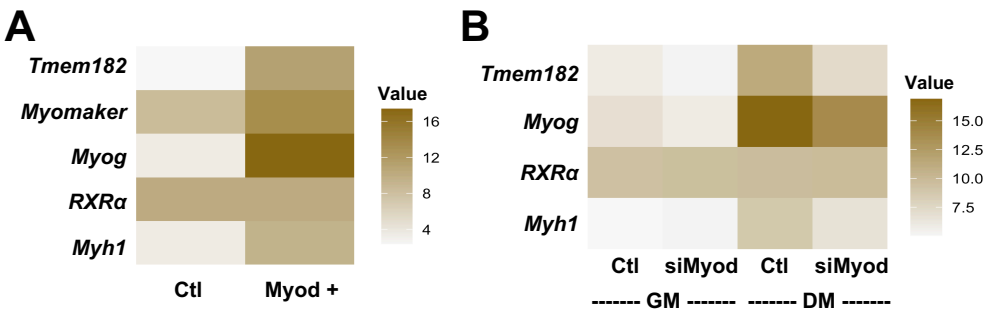

Figure 5.3 Tmem182 expression is MyoD dependant.

(A) Gene expression data from microarray analysis of C3H10T1/2 fibroblasts in untreated control (Ctl) and in fibroblasts following 48 hours of myogenic conversion and 24 hours after induction of differentiation (Myod +). (B) Gene expression values obtained from microarray analysis of proliferating C2C12 myoblasts (GM) and myoblasts differentiated for 24 hours (DM) subjected to siRNA-mediated knockdown of MyoD or a non-silencing control [GSE66319].

Given that Tmem182 is a bexarotene-responsive target (Fig. 5.2), we also assessed the requirement of RXR for Tmem182 expression (Fig. 5.4A-B). We utilized a known and potent RXR antagonist, UVI3003 (Nahoum et al., 2007), in C2C12 myoblasts differentiated with bexarotene in the absence or presence of UVI3003. Intriguingly, the RXR antagonist did not considerably effect Tmem182 gene expression in untreated controls, but significantly attenuated the enhancement effect of bexarotene for Tmem182 and myogenin expression (Fig. 5.4A-B). Furthermore, since bexarotene enhances myoblast differentiation via the activation of RXRα specifically, we utilized a subtype-specific shRNA system to reveal that enhancement of Tmem182 by bexarotene was inhibited in shRXRα stable cells compared to control cells (Fig. 5.4C). Interestingly, the loss of RXRα in the absence of treatment also inhibited Tmem182 expression compared to control cells, possibly suggesting a role for unliganded RXRα for the expression of Tmem182 as it may disrupt RXR-mediated chromatin modifications at regulatory loci. Taken together, Tmem182 is a target of RXR signaling in the enhancement of myogenic differentiation via RXRα as a transcription factor (Fig. 5.4).

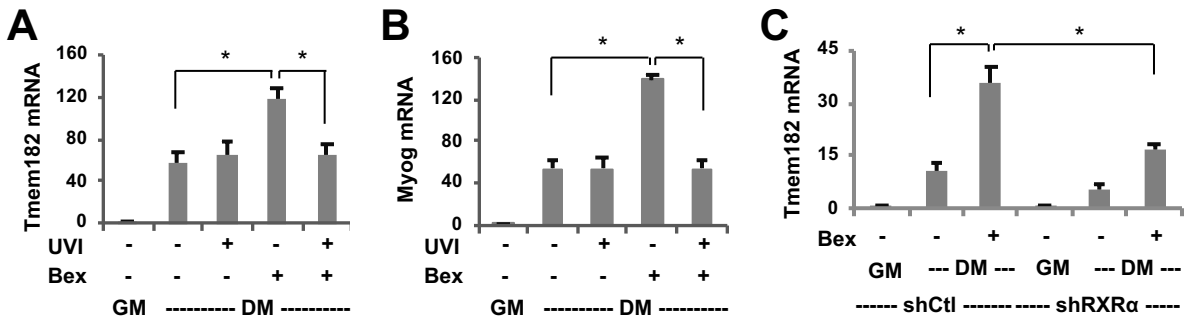

Figure 5.4 Role of RXR in bexarotene-enhanced myogenic expression.

(A-B) C2C12 cells were differentiated with bexarotene (Bex, 50 nM) in the presence of RXR antagonist UVI 3003 (1um) for 24 hours (DM). The mRNA levels for Tmem182 and myogenin were assessed by RT-qPCR and presented as the fold change in relation to proliferating

myoblasts (GM) (error bars: SEM; n = 3; *, $p < 0.05$). (C) RXRα knockdown cells (shRXRα) were differentiated in the absence or presence of bexarotene for 4 days with a non-silencing shRNA used as control (shCtl). Tmem182 expression levels were determined by RT-qPCR and presented as the fold change in relation to proliferating myoblasts.

Tmem182 expression is MyoD- and p300-dependent

Having identified Tmem182 as a putative target of MyoD in early myoblast differentiation, we delved further into its regulation as a rexinoid-responsive target. As ChIP-seq is widely used to analyze the locations of transcriptional co-regulators and histone modifications within the genome we analyzed ChIP-seq for the HAT p300, and various histone modifications representative of promoter and enhancer markers including H3K9ac, H3K18ac, H3K27ac, and H4K8ac in C2C12 myoblasts differentiated in the absence or presence of bexarotene (Fig. 5.5A). Interestingly, the promoter region of *Tmem182*, signified by increased enrichment of RNA Polymerase II (RNA Pol II) with differentiation, displayed increased enrichment of p300 as well as the MRF, myogenin following the addition of bexarotene (Fig. 5.5A). Relatedly, the histone acetylation marks generally associated with gene expression were enriched around the TSS in differentiating myoblasts but were highly augmented following the addition of bexarotene, particularly H3K9ac and H3K18ac. Notably, the levels of H3K27me3, the polycomb repressive mark associated with repressed chromatin, were almost negligible in both conditions. Additionally, since mammalian conservation scoring displays a highly conserved region across vertebrate species including humans, the promoter region of *Tmem182*, characterized by an enrichment of histone acetylation, is likely an important putative regulatory region (Fig. 5.5A).

As rexinoid-responsive gene expression is linked to residue specific histone acetylation and an epigenetic signature related to histone acetylation (Khilji et al., 2020), we also examined the role of p300 in the regulation of Tmem182. We employed p300 qChIP to quantify the enrichment of p300 at the promoter region of *Tmem182*. As seen in Fig. 5.5B, p300 association to the *Tmem182* locus was significantly enriched following 24 hours of differentiation and further increased markedly by bexarotene. This trend was similar to the increasing association of MyoD to the same region which is known to recruit p300 to myogenic regulatory loci, indicating that MyoD and p300 may cooperate to in the regulation of Tmem182 during rexinoid-enhanced myogenic differentiation (Fig. 5.5B). We also used a previously established p300 shRNA knockdown myoblast system to determine the requirement of p300 for Tmem182 expression (Chen et al., 2015). As shown in Fig. 5.5C, Tmem182 expression was considerably induced in shRNA control differentiating myoblasts and augmented further by bexarotene. However, shRNA knockdown of p300 attenuated Tmem182 gene expression in differentiating myoblasts regardless of treatment, suggesting a critical role for p300 in Tmem182 gene regulation and for its rexinoid-mediated augmentation, similar to the regulation of muscle-specific marker, myogenin (Fig. 5.5C). Therefore, Tmem182 expression is dependent upon the activities of MyoD and p300 in early myogenic differentiation.

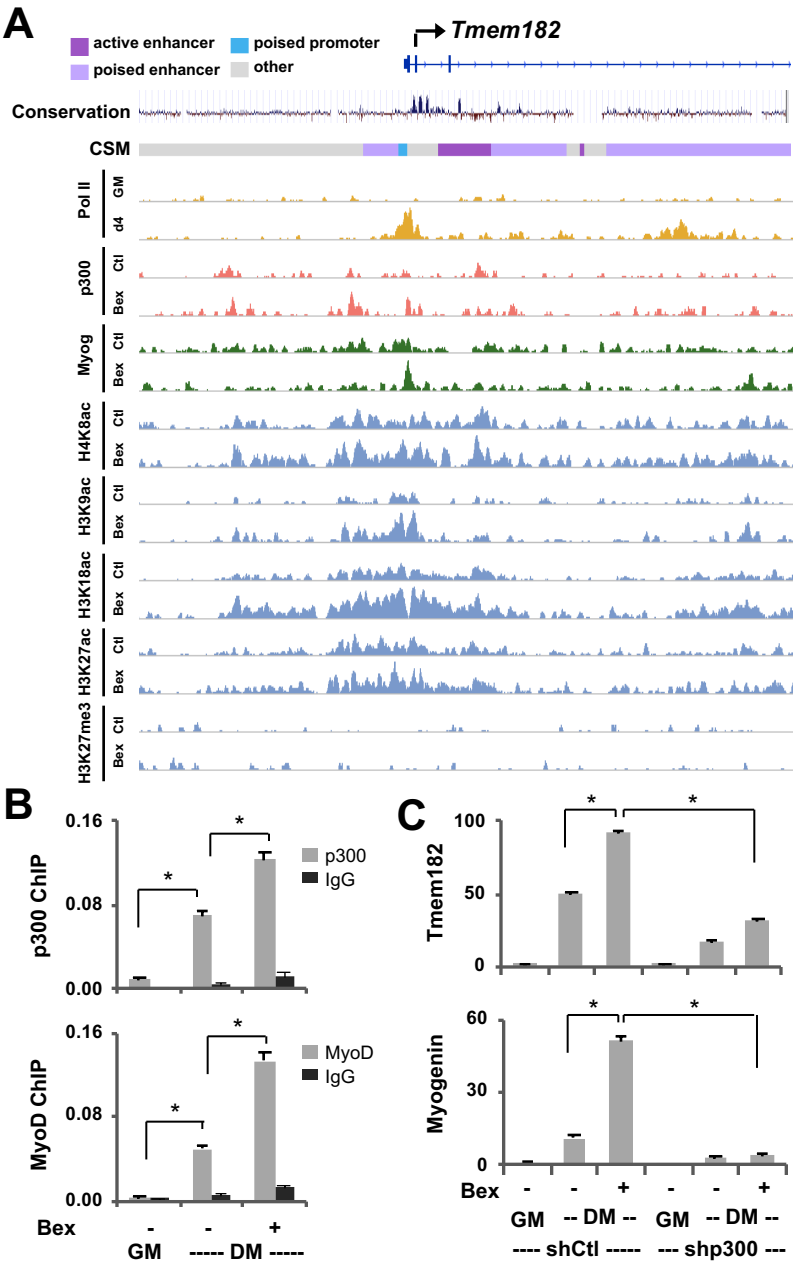

Figure 5.5 Regulation of Tmem182 expression.

(A) C2C12 myoblasts were differentiated in the absence or presence of bexarotene (Ctl or Bex) for 24 hours. Genome browser view for enrichment of p300 and various histone modifications is shown at the *Tmem182* locus. RNA Polymerase II (Pol II) enrichment was obtained from proliferating C2C12 myoblasts (GM) and myoblasts differentiated for 4 days (d4) [GSE25308]. Blue bars show Refseq gene position and the panel below presents mammalian conservation of

the locus as quantified by the UCSC genome browser. (B) C2C12 cells were differentiated for 24 hours (DM) in the presence or absence of bexarotene with proliferating myoblasts as controls. ChIP-qPCR analysis was performed at the *Tmem182* promoter using antibodies against p300 or MyoD. Normal IgG antiserum was used as a negative control. Quantification is presented as the percentage of enrichment in relation to input chromatin DNA (error bars: SEM; n = 3; *, $p < 0.05$). (C) Tmem182 and myogenin mRNA levels were examined by RT-qPCR and presented as the fold change in relation to proliferating myoblasts following p300 knockdown (shp300), with a non-silencing shRNA (shCtl) used as a control.

Tmem182 is important for myoblast differentiation

Since Tmem182 is a muscle-specific gene and is highly upregulated during myoblast differentiation, we used a shRNA approach to knockdown Tmem182 in C2C12 myoblasts to delineate the role of Tmem182 during this process (Fig. 5.6A). Interestingly, loss of Tmem182 led to a nearly 40% reduction in both differentiation and fusion of myoblasts as determined by quantitative microscopy (Fig. 5.5B-D). Following differentiation of the pooled stable cells in the presence of bexarotene, we observed a bexarotene mediated augmentation in control and Tmem182 knockdown cells, however, the augmentation was notably reduced in shTmem182 stable cells. Moreover, loss of Tmem182 also encumbered bexarotene-enhanced MyHC gene expression as determined by Western analysis (Fig. 5.5E). The impaired MyHC expression was not reflected by a change in the levels of myogenin protein, indicating that Tmem182 likely plays a structural role in myoblast differentiation (Fig. 5.5). Taken together, our results thus far suggest that Tmem182 may be important for early myoblast differentiation and as a rexinoid target, may be utilized to improve the muscle phenotype in cases of muscle-related disease.

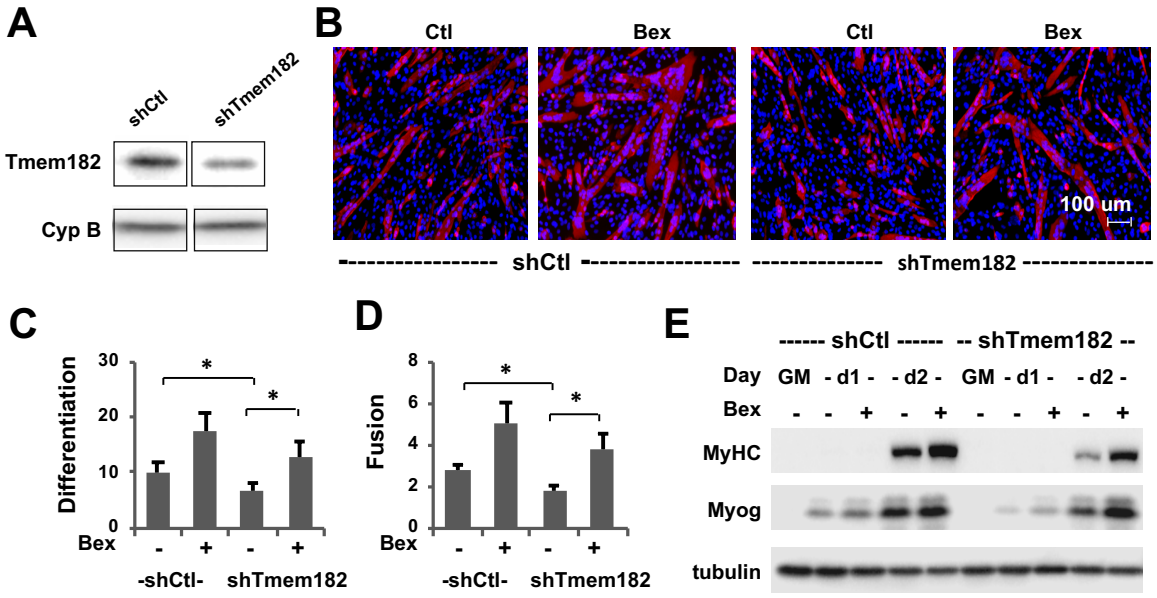

Figure 5.6 Tmem182 is important for myoblast differentiation and fusion.

(A) Tmem182 protein levels were examined by Western blotting following Tmem182 knockdown (shTmem182) in C2C12 myoblasts with a non-silencing shRNA (shCtl) used as control. (B) Tmem182 knockdown cells were differentiated in the absence or presence of bexarotene (50 nM) for 4 days. Representative images are stained for myosin heavy chain (red) and nuclei (blue). (C) Differentiation was defined as the percentage of myogenic nuclei relative to the total number of nuclei. Error bars represent the standard deviations of three independent experiments (*, $p < 0.05$). (D) Fusion rate was defined as the average number of nuclei per myocyte. (E) The protein levels of MyHC and myogenin protein were examined by Western blotting with tubulin as a loading control.

Discussion

We have previously established that a selective RXR agonist, bexarotene, enhances the differentiation and fusion of myoblasts via a direct regulation of MyoD (AlSudais et al., 2016; Hamed et al., 2017). Here we show that bexarotene addition is required during the first 48 hours of differentiation specifically such that rexinoid signaling augments existing myogenic pathways during the early stages of differentiation. Importantly, we utilized the global profiling of transcriptional regulators underlying rexinoid enhanced myogenic expression to identifying novel myogenic targets, leading us to a transmembrane protein termed Tmem182. We have shown that Tmem182 is a rexinoid responsive and muscle specific target that is upregulated during the differentiation process (Fig. 5.2, Fig. 5.6). Additionally, we delved into the regulation of Tmem182 which indicated that p300 and MyoD may cooperate in the regulation of Tmem182 expression within the context of rexinoid-responsive myogenic differentiation (Fig. 5.3-5.5). Thus, we present Tmem182 as a novel regulator of myoblast differentiation and show that the model of bexarotene-enhanced myogenic differentiation is a beneficial avenue to identify additional myogenic target genes and specific interactions that can be studied for the development of potential therapeutics in muscle regeneration and repair.

In this study, we have used C2C12 myoblasts to represent precursors of skeletal muscle cells. The C2C12 myoblast cell line consists of a pure population of myoblasts which are predetermined to differentiate and fuse with each other into myotubes (Blau et al., 1985). Following the induction of differentiation, myotubes start to appear by 24 hours of differentiation and are evident by 48 hours (Delgado et al., 2003). We have studied the role of RXR signaling in myoblast differentiation by using a treatment interval approach to compare myoblasts that are

differentiated in the presence of bexarotene during the first 48 hours of differentiation or between day 2 and day 4 (Fig. 5.1). Our results clearly indicate that bexarotene enhances myoblast differentiation by targeting early myogenic transcription and is not as effective after the first 48 hours of differentiation. Comprehensive gene expression analyses have presented a step-wise transcriptional blueprint of myogenic differentiation where thousands of genes are differentially expressed at the early stage of the differentiation, mostly within 24 hours of differentiation initiation (Doynova et al., 2017; Hamed et al., 2017; Trapnell et al., 2010). Thus this time period encapsulates epigenetic changes reflecting the alteration of gene programs and the temporal waves of gene expression that are induced prior to the transcriptional activation of myogenin which initiates terminal differentiation (Bischoff and Holtzer, 1969). Therefore, addition of bexarotene is critical at the induction of differentiation to achieve efficient enhancement of differentiation and fusion via the regulation of early myogenic genes (Fig. 5.1).

Utilizing bexarotene enhanced transcriptome profiling, we have revealed Tmem182 as a novel target in myoblast differentiation. Previous studies have characterized a requirement for Tmem182 in adipogenic conversion and OSCC motility (Hsing et al., 2019; Wu and Smas, 2008), but we show for the first time that Tmem182 is highly expressed in skeletal muscle and is upregulated during myoblast differentiation *in vitro* as well as during *in vivo* muscle regeneration (Fig. 5.2). Intriguingly, the dramatic increase in Tmem182 expression levels during in vivo regeneration were on par with the fold induction of myogenin (Fig. 5.2E). Additionally, we analyzed published microarray data, for C3H/10T1/2 fibroblasts induced to differentiate following MyoD overexpression (Chakroun et al., 2015), as well as a siRNA knockdown of MyoD in differentiating C2C12 myoblasts (Fig. 5.3) (Chakroun et al., 2015). Both studies

revealed that MyoD likely regulates Tmem182 expression, also indicated by Quinn et al. who identified Tmem182 as one of the top 100 upregulated genes in fibroblasts upon MyoD introduction (Quinn et al., 2017). Interestingly, RNA Pol II enrichment at the *Tmem182* promoter following 4 days of differentiation indicates a requirement for the protein up to the late stages of myogenesis. In combination with the observation that loss of Tmem182 impaired normal myoblast differentiation and fusion in addition to decreased levels of skeletal muscle marker, MyHC, our data collectively indicate that Tmem182 is an important player in skeletal myogenesis and future studies will be needed to outline its exact functional complexities.

In addition to the functional importance of Tmem182, we also delved into its regulation (Fig. 5.4, Fig. 5.5). We examined the role of RXR for Tmem182 expression as Tmem182 is a rexinoid-responsive target and bexarotene enhances myogenic differentiation through the activation of RXR. Interestingly, both antagonism of RXR and loss of RXR protein inhibited bexarotene-mediated enhancement of Tmem182 expression, confirming that Tmem182 is a target of RXR signaling in early myoblast differentiation. However, due to the absence of RXR enrichment associated to the *Tmem182* locus (data not shown), we suspect that Tmem182 is an indirect target of RXR and bexarotene enhances Tmem182 expression via MyoD regulation instead (Hamed et al., 2017) (Fig. 5.3, Fig. 5.5).

Since histone acetylation provides a useful baseline for gene expression, we also profiled the pattern of histone acetylation in C2C12 myoblasts differentiated in the absence or presence of bexarotene at the *Tmem182* promoter. Our results showed a distinct enrichment of histone acetylation particularly of H4K8, H3K9 and H3K18 following bexarotene treatment.

Interestingly, the increase in histone acetylation was also coupled with an augmentation of p300 and myogenin association (Fig. 5.5). Furthermore, loss of p300 led to an inhibition of Tmem182 expression as well as its bexarotene-mediated augmentation. Since p300 is recruited by Myod to myogenic loci where it acetylates histones and promotes the full transcriptional activity of Myod on chromatin-associated templates (Dilworth et al., 2004), RXR selective signaling may utilize this established transcriptional mechanism to enhance the gene expression of the myogenic program. Furthermore, we have previously shown that RXR signaling augments residue-specific histone acetylation at loci co-occupied by p300 and myogenin (Khilji et al., 2020), and thus the *Tmem182* promoter may represent a specific case of the epigenetic signature underlying rexinoid-responsive gene expression. Taken together, our study introduces a novel myogenic target and explores the regulation of a previously uncharacterized locus which is used as a model to provide molecular insights into how p300 and histone acetylation are linked to bexarotene-responsive locus activation and transcription of myogenic targets. To our knowledge, we present the first report indicating an important role for Tmem182 in myoblast differentiation and future studies will be needed to investigate its roles in skeletal muscle development and regeneration which may provide a potential target for therapeutic design towards skeletal muscle health and disease.

Experimental Procedures

Cell Culture and Reagents

C2C12 myoblasts (ATCC) were maintained in DMEM supplemented with 10% FBS (GM) at 37°C with 5% CO_2. To induce differentiation, medium of 70-80% confluent cell cultures was changed to DMEM supplemented with 2% horse serum (DM). Bexarotene was purchased from LC Laboratories and UVI3003 from Tocris.

shRNA Knockdown

C2C12 myoblasts were grown in GM to about 30% confluence and transduced at a multiplicity of infection of 6 with lentiviral particles targeting Tmem182 in the presence of Polybrene (5 μg/ml) according to the manufacturer's protocol (Santa Cruz Biotechnology). A nonsilencing shRNA was used as a negative control. Puromycin (2 μg/ml, Sigma) was used to select pooled stable clones.

Immunofluorescence Microscopy

C2C12 cells were fixed with cold methanol, rehydrated in phosphate-buffered saline (PBS), and incubated with myosin heavy chain antibody (hybridoma MF20) overnight. The next day, cells were washed with PBS, and incubated with Alexa Fluor 594 secondary antibody (Invitrogen). The cells were also incubated with 0.1 μg/ml Hoechst to stain cellular DNA. Zeiss AxioObserver D1 Microscope and AxioVision Rel 4.6 software were used to capture images via the 10X objective. Five random images were analyzed for each coverslip. ImageJ software was used for cell counting. Student's t-tests were used for the statistical analyses.

Western Analysis

Cells were washed with PBS, harvested, and centrifuged. The resulting pellet was resuspended and shaken at 4°C for 30 min in whole-cell extraction (WCE) buffer containing 50 mM Tris-HCl (pH 7.6), 400 mM NaCl, 10% glycerol, 1 mM dithiothreitol, 1 mM phenylmethylsulfonyl fluoride, and 1% Nonidet P-40 (NP-40. Lysates were centrifuged at 14,000 × *g* at 4°C for 10 min. Protein concentration was determined by a Bradford assay (Bio-Rad) and quantified with Multiscan Spectrum photospectrometer (Thermo). Equal amounts of protein were resolved on SDS-polyacrylamide gel and transferred onto an Immuno-Blot PVDF membrane (Bio-Rad). Bio-Rad ChemiDoc MP System was used to capture chemiluminescent images, and ImageJ software was used for densitometry quantification. All experiments were performed at least three times. The antibodies against Tmem182 and cyclophilin B were from Abcam (ab177360 and ab16045, respectively). Antibodies against myogenin (F5D) and β-tubulin (E7) were from Developmental Studies Hybridoma Bank.

Reverse Transcription qPCR Analysis

Total RNA was isolated from C2C12 myoblasts using the GeneJET RNA Purification Kit (ThermoFisher Scientific) and equal amounts of RNA were reverse transcribed using a High-Capacity cDNA Reverse Transcription Kit (Applied Biosystems). Real-time PCR was conducted in triplicates using a SYBR® Green PCR Master Mix and HotStarTaq DNA polymerase (Qiagen) on a CFX96 Touch Real-Time PCR Detection System (BioRad). Results were analyzed by the cycle threshold (Ct) comparative method using TATA-Binding Protein (Tbp) or Ribosomal Protein S26 (Rps26) as an internal control. The experiments were repeated at least three times. Data were presented as the mean ± S.E.M, where p values were determined using

student's t-test. The following primers were used: Tmem182 primers forward, AGTTCTGGTACACCAATCAGCC, and reverse, ATTGCGGAGTCGTAGGAGGT; myogenin primer forward, ATCCAGTACATTGAGCGCCTAC, and reverse, AGCAAATGATCTCCTGGGTTGG; myomaker primer (Millay et al., 2013) forward, ATCGCTACCAAGAGGCGTT, and reverse, CACAGCACAGACAAACCAGG.

Quantitative ChIP analysis

Cells were crosslinked and sonicated followed by chromatin immunoprecipitation as previously described (Hamed et al., 2013). Following ChIP, purified DNA was amplified in triplicate real-time PCR reactions with locus-specific primers. A standard curve was created for each set of primers with input DNA, followed by quantification of the abundance of immunoprecipitated target DNA in relation to input chromatin DNA. Each qChIP was repeated at least three times. Antibodies against p300 and MyoD were from Santa Cruz Biotechnology (sc-584x and sc-32758x, respectively). Primer pairs used for qPCR amplification were: Tmem182 promoter forward, GGGAGCAAGCAACTCCTCAA and reverse, GAGCTGTGGTGGCTTCTCAT.

Statistics and reproducibility

All statistical analyses were performed using The R Project for Statistical Computing or Microsoft Excel. Normally distributed data were analyzed by a two-tailed Student's t-test. A $p < 0.05$ was considered statistically significant. Statistical details and number of replicates are indicated in the figure legends.

Footnotes

Author Contributions

S.K and M.H performed the research and analyzed the data. S.K and Q.L designed the research and wrote the manuscript. All authors reviewed the manuscript.

Funding and additional information

This research was supported by an Operating Grant from the Canadian Institutes of Health Research (CIHR #173586 to Q.L.). S.K. is a recipient of the Canada Graduate Scholarship from the Natural Sciences and Engineering Research Council of Canada.

Conflict of Interest

The authors declare no competing interests.

Chapter Six: General Discussion

Genetic and epigenetic determinants are intimately linked during lineage formation from cellular specification and commitment to differentiation and maintenance. Accordingly, development of a particular lineage such as skeletal muscle is directed by key lineage determination factors (MyoD), which promote cell-fate specific gene programs by altering the chromatin state of distinct regulatory elements to activate spatiotemporal transcriptional programs (Berger, 2007). In addition to DNA association, the function of lineage determination factors relies upon the recruitment of other TFs and chromatin modifiers that co-regulate complex gene expression programs. As such, it is crucial to understand the functional mode of transcription regulators in early myogenic differentiation. Such studies will facilitate identification of novel myogenic targets and molecular interactions, as well as the development of therapeutics that modulate epigenetic landscape in a selective manner to promote muscle development.

In this study, we aimed to assess the role of MRFs and related epigenetic mechanisms driving early myoblast differentiation. As such, we performed comprehensive genomic profiling, including RNA-seq and ChIP-Seq, for five histone modifications in C2C12 myoblasts differentiated for 24 hours in the presence or absence of a rexinoid with proliferating myoblasts used as control. Our findings present a role for transcriptional co-activator p300, particularly when recruited by MyoD, in the enrichment of loci-specific histone acetylation at p300-associated enhancers. In addition, we show that RXR signaling enhances myoblast differentiation largely via a direct regulation of MyoD gene expression. Relatedly, rexinoid treatment promotes the coordination of exit from the cell cycle and the activation of muscle-related genes. Furthermore, we also observed a close association of myogenin with rexinoid-responsive gene expression. In exploring myogenin-mediated RXR signaling, we have described

the distribution of myogenin to poised enhancers and its association to a specific "double E-box" in RXR signaling. Similarly, we have identified an epigenetic signature related to p300 in which RXR signaling augments residue-specific histone acetylation at enhancers co-occupied by p300 and myogenin. Importantly, we utilized rexinoid enhanced myogenic gene expression to uncover a novel myogenic target, which we show is important for myoblast differentiation and fusion. Taken together, our studies provide novel molecular insights into myogenic enhancer regulation and the interplay between rexinoid signaling and MRFs-associated chromatin states during early myogenic differentiation.

6.1 Mapping genomic loci via chromatin states in proliferating myoblasts

Understanding the mechanisms governing the function of tissue-specific regulatory elements is particularly useful for the design of treatments targeting a cell's own transcriptional network. As such, we aimed to characterize the mechanistic action of p300 in the regulation of myogenic enhancers in early myoblast differentiation. To do so, we utilized a genome-wide chromatin state model, which principally clusters genomic co-occurrence of different epigenetic marks, in committed proliferating myoblasts (Fig. 3.3). The combination of multiple marks in their spatial context represents a distinct chromatin state (Ernst and Kellis, 2017). Mapping epigenomic patterns in this way is a powerful tool to annotate genomes, identify cell type-specific putative regulatory elements, study their changing activity across different cell types or to assess the differentiation potential of a cell type (Ernst and Kellis, 2017; Ernst et al., 2011; Mikkelsen et al., 2007). In our system, we established a model with 14 chromatin states which were further grouped into 5 main categories of active/poised promoters, active/poised enhancers and 'others'

which encompassed actively transcribed and repressed regions (Fig. 3.3). These five main chromatin states correlate with distinct functional elements with divergent functional properties. Although enhancers, in particular, have been historically difficult to identify and investigate due to a lack of consistent identifying signatures, recent innovations in epigenomic technologies have advanced the detection of enhancers, in addition to their categorization as poised or active states (Creyghton et al., 2010; Rada-Iglesias et al., 2011; Zentner et al., 2011). Interestingly, technological developments have also allowed utilization of chromatin state analyses in numerous systems, consistently displaying a limited number of chromatin signatures, which reflects a biological redundancy across cell types and organisms (Ernst et al., 2011; Filion et al., 2010; Kundaje et al., 2015; Lara-Astiaso et al., 2014; Roudier et al., 2011). Accordingly, we have employed distinct chromatin states, characterized in proliferating myoblasts, to portray lineage-specific regulatory loci pertinent to myogenic differentiation, as described below.

6.2 Regulation of myogenic enhancers by p300 and MyoD in early myoblast differentiation

To study the regulation of myogenic enhancers, we integrated chromatin state modeling with global localization of p300, MyoD and various histone modifications. We also correlated these ChIP-seq datasets with global transcriptomic profiling during early myogenic differentiation. In our goal to delineate the role p300 in myogenic enhancer regulation, we observed that a majority of p300 peaks are localized to enhancer regions, as expected from its identity as an enhancer marker (Fig. 2.1) (Blow et al., 2010; Spicuglia and Vanhille, 2012; Zentner et al., 2011). However, its association to poised enhancers increased with differentiation, coinciding with an

increase in MyoD association as well (Fig. 2.3). A central role of enhancers is to provide a binding platform for TFs and epigenetic regulators where environmental cues can be integrated to initiate gene programs. Poised enhancers in particular, represent a state between activation and repression as they can facilitate rapid transcription in response to differentiation cues or other cellular stimuli. Accordingly, poised enhancers are closely associated with lineage-inducing TFs that govern lineage-specification (Fueyo et al., 2018; Spicuglia and Vanhille, 2012; Wang et al., 2015). Since the increase in occupancy of poised enhancers by p300 in differentiating myoblasts coincides with increased MyoD association, these regions may represent "differentiation switches", which repress lineage commitment, until their activation, at which point they can rapidly drive muscle-specific gene programs (Fig. 2.4) (Nguyen et al., 2015). Furthermore, the presence of p300 at poised enhancers suggests that p300 activity may also be regulated to prevent premature enhancer activation (Fig. 2.1, 2.5). Interestingly, although the main acetylation targets of p300 are H3K18 and H3K27, we observed an increase in differentiation-dependent loci-specific acetylation of H4K8 and H3K9 at p300-associated enhancers, particularly when enlisted by MyoD (Fig. 2.4, 2.5). Additionally, previous studies have shown a decrease in global histone acetylation levels following terminal differentiation, whereas our study showed no significant change in global histone acetylation in myoblasts differentiated for 24 hours (Fig. 2.1) (Asp et al., 2011a). Collectively, we provide evidence that the differentiation process is mediated by transformations in residue-specific histone acetylation at lineage-specific loci, rather than global histone acetylation events. Our data indicates a role for MyoD in p300 recruitment at poised lineage-specific enhancers, which drive expression of muscle-related genes and thus reflects the molecular transformations required to transition proliferating myoblasts into differentiation.

6.3 RXR signaling directly regulates MyoD to promote myoblast differentiation

The development of distinct cell types and tissues is regulated in response to intrinsic and extrinsic stimuli. Having established that RXR signaling promotes the specification and differentiation of the skeletal muscle lineage (AlSudais et al., 2016; Le May et al., 2011), we examined the genome-wide impact of rexinoids in myoblast differentiation. Global transcriptional profiles revealed the simultaneous upregulation of muscle-specific genes, including MRFs and downregulation of cell cycle regulators (Fig. 3.1). Given that the expressions of MyoD and myogenin were distinctly upregulated in bexarotene, these results indicated that RXR signaling may be mediated by key developmental factors (Fig. 3.1). Indeed, we revealed that MyoD is a direct genetic target of RXR in early myogenic differentiation where RXR signaling is largely reconciled through a direct regulation of MyoD gene expression (Fig. 3.2). Thus, RXR activation of a single key factor that interacts with an array of molecular targets is used as a simple regulatory mechanism to drive a complex response. In contrast, although myogenin is an indirect target of RXR signaling it is also intimately associated with bexarotene-responsive gene expression (Fig. 4.3). Similarly, although MyoD and myogenin each bind to a distinct set of loci, poised enhancers associated to both MRFs exhibited increased enrichment of histone acetylation, including H4K8ac and H3K9ac (Fig. 3.4). Moreover, loci occupied by both MRFs displayed a more prominent increase in histone acetylation, particularly in H3K9ac, compared to those bound by each factor alone (Fig. 3.5). Accordingly, we used ChIP-qPCR analysis of multiple poised enhancers associated to key myogenic targets such as the troponin *Tnnc1*, to present increased enrichment of MRFs in addition to p300 (Fig. 3.5). Notably, this enrichment was further augmented following bexarotene treatment of differentiating myoblasts. Collectively, this data indicates that bexarotene responsive gene expression is mediated through

the activation of poised enhancers by MyoD and myogenin as transcription factors and p300 as a HAT.

6.4 Myogenin-mediated retinoid X receptor signaling in myogenic differentiation

While MyoD and myogenin share a set of DNA binding sites, they differ in their potential to activate gene transcription. The activation of a subset of late muscle-specific genes occurs most efficiently in the presence of myogenin, which amplifies the expression of genes previously primed by MyoD (Cao et al., 2006; Singh and Dilworth, 2013). Thus, having shown that rexinoid-responsive genes expression is largely reconciled by MyoD, we also examined how RXR-selective signaling affects genome-wide myogenin localization and the molecular pathways underlying myogenin-mediated rexinoid-enhanced gene expression. Chromatin state association of myogenin loci revealed a shift in the distribution of myogenin from promoter to poised enhancers following bexarotene treatment (Fig. 4.1). Since MyoD also displays an increased association to poised enhancers during the differentiation process, myogenin may cooperate with MyoD to drive the activation of these tissue-specific regulatory loci (Fig. 2.3, 4.1). Detailed *de novo* motif analysis of myogenin loci in bexarotene also revealed that myogenin has a greater association to a distinct E-box with two flanking nucleotides consisting of CASCTGYY, compared to the shorter motif of CAGCTG in the untreated control (Fig. 4.2). Additionally, RXR signaling also favours a secondary motif representative of an E-box, proximal to the primary E-box, characterized as a "double E-box" (Fig. 4.2). The presence of a double E-boxes is not limited to skeletal muscle and has been documented in other tissues including lung tissue, where the two E-boxes in the upstream region of *CYP3A4* were positioned two full turns of the DNA helix apart (Biggs et al., 2007). The authors of this particular study could not

identify the double E-box binding factors in their system, despite multiple attempts by DNA affinity chromatography with known double-E-box binding factors (SIP1, HEB, and δEF1), as well as single E-box binding proteins (E2A, Myc, MyoD, and E47) (Biggs et al., 2007). Thus, although secondary motif analysis predicted binding of myogenin and Tcf3 to the double E-box in a myogenic context (Fig. 4.2), future protein-DNA binding experiments such as DNA affinity chromatography and qChIP will be necessary to confirm the exact identity and molecular context of single vs. double E-box binding factors and their effects in myogenic expression.

There are over 50 known protein complexes that have the ability to recognize an E-box sequence, but the question of how protein-gene target specificity is determined remains largely unanswered. We have shown that RXR signaling promotes a specificity of myogenin for the CASCTGYY E-box, which may explain partial specificity in target gene regulation (Fig. 4.2). Relatedly, Chang *et al.* confirmed the lack of double E-box association to other bHLH transcription factors, including NEUROD1, E47, or c-MYC, suggesting that the double E-box motif may be a novel mechanism conferring myogenin target specificity (Chang et al., 2015). This mechanism is also seen in the Twist subfamily of bHLH proteins where a double E-box motif spaced by exactly 5-bp allows a full turn of the DNA double helix such that the conserved base pairs in each E-box face the same direction of the DNA with no spatial constraints (Chang et al., 2015). Thus, the prediction of two canonical E-boxes, separated by 4 or 6 bp at myogenic-associated loci in bexarotene suggests that RXR signaling not only modulates the preference of myogenin for E-box components, but may also promote its cooperation with flanking E-box binding proteins for TF complex formation (Fig. 4.2). Additionally, Twist factor ChIP-seq found that peaks with a greater number of DNA tags were more likely to contain the double E-box

motif than a single E-box (Chang et al., 2015). Similarly, we revealed that myogenin peaks associated with a double E-box were associated with a greater signal enrichment compared to input, directly indicative of the binding affinity of the factor (Fig. 4.2). Taken together, the dissection of myogenin-mediated RXR signaling during early myoblast differentiation has revealed a novel molecular mechanism by which myogenic factors may regulate target specificity and binding intensity.

6.5 Cooperation between MyoD and myogenin in rexinoid signaling

MyoD and myogenin are decisive MRFs wherein MyoD directly regulates myogenin expression to mediate terminal differentiation (Zammit, 2017). Relatedly, one of the mechanisms by which myogenin contributes to myogenic differentiation is to enhance the expression of MyoD-initiated late muscle genes via a MyoD-dependent ability to induce chromatin remodeling (Du et al., 2012). Thus, although, MyoD is sufficient to drive the expression of early target genes, it requires cooperation of myogenin to drive the expression of late muscle genes. As such, myogenin can initiate chromatin remodeling, specifically hyperacetylation of H4, to mediate the expression of genes already primed by MyoD (Cao et al., 2006; Du et al., 2012). Since rexinoid signaling augments the expression of MyoD and myogenin, our data indicate that this increase promotes residue-specific histone acetylation in a distinct chromatin state associated to MyoD and myogenin (Fig. 3.4). Importantly, RXR signaling may utilize MyoD reconciled transcriptional activation as well as myogenin-mediated chromatin remodeling of late muscle genes, cumulatively increasing the expression of rexinoid-responsive genes to enhance the differentiation and fusion of myoblasts.

6.6 The role of p300 in rexinoid signaling

The HAT activity of p300 is critical for a myriad of cellular processes, including myogenic differentiation (Hamed et al., 2013; Polesskaya et al., 2001; Puri et al., 1997a). However, apart from serving as a HAT, p300 can also act as a scaffold for TFs or serve as a bridge between TFs and the basal transcriptional machinery to activate transcription (Fig. 1.1) (Chen and Li, 2011; Goodman and Smolik, 2000). Interestingly, we have found that p300 is mainly associated with active promoters in response to RXR signaling in C2C12 myoblasts, which contrasts to its main association to enhancers in the absence of rexinoids (Fig. 4.4). Utilizing condition-specific motif analysis, we have shown that p300 may be recruited largely by AP-1 family members to promoter regions during rexinoid-enhanced differentiation, with a predisposition for Atf1 binding proteins in particular (Fig. 4.4). In contrast, recruitment of p300 to enhancers was largely mediated by E-box binding proteins, coinciding with a considerable overlap between p300 and myogenin loci (Fig. 4.4). Since MyoD is known to recruit p300 to muscle-specific loci, myogenin may also cooperate with MyoD to facilitate increased recruitment of p300 followed by deposition of H4K8 and H3K9 acetylation. As such, the recruitment of p300 by E-box binding proteins and residue-specific histone acetylation may be a signature of rexinoid-responsive gene expression. Additionally, it is important to note that MyoD loci in bexarotene remain to be determined, which will be key to resolve the true overlap between MyoD and myogenin loci in RXR signaling and shed further insights into the extent of their cooperative and unique roles.

Since RXR signaling promotes activation of muscle-related genes, we used bexarotene-enhanced transcriptome profiling to uncover novel myogenic targets such as Tmem182 (Fig. 5.2). We show for the first time that the transmembrane protein is highly expressed in skeletal muscle and

is important for myoblast differentiation and fusion (Fig. 5.2, 5.6). Moreover, a dramatic upregulation of Tmem182 mRNA during the initial phases of skeletal muscle regeneration indicates that Tmem182 may be required for the early stages of muscle formation in particular (Fig. 5.2). Since Tmem182 was exposed as a bexarotene-responsive gene, we also delved into the regulation of its promoter region. Due to the lack of RXRα enrichment associated to the Tmem182 gene (data not shown), Tmem182 is likely an indirect target of RXR. As such, bexarotene promotes Tmem182 expression via the function of MyoD, as we have shown that Tmem182 expression is indeed MyoD dependent (Fig. 5.3). Moreover, having observed an enrichment of p300 and myogenin at the Tmem182 promoter in bexarotene, the locus also reflects global trends in which myogenin cooperates with p300 in the installation of an epigenetic signature associated to rexinoid responsive gene expression in early myogenic differentiation (Fig. 4.7, 5.5). Thus, Tmem182 regulation may be further explored to delineate spatiotemporal RXR signaling regulation in specific physiological contexts.

6.7 Translation from mice to human studies

Scientific investigations in animals and their tissues have provided invaluable insights into numerous biological processes and their underlying molecular mechanisms. Our investigations thus far have utilized cultured mouse cells and tissues. However, to translate molecular findings in animals to human therapeutic development, one must consider the degree of conservation in biological processes between mice and humans. As such, it is vital to consider conservation of transcriptional mechanisms between species and their stability among different cell types. Conservation of functional genomic elements is a well-established biological concept, however

the conservation of *cis*-regulatory elements is less clear. Although, studies have reported a wide range by which transcription factor binding is conserved, perhaps reflecting diverse evolutionary dynamics (Borneman et al., 2007; Conboy et al., 2007; Mikkelsen et al., 2010; Odom et al., 2007; Schmidt et al., 2010). Accordingly, Hemberg and Kreiman assessed genomic loci of six different TFs in hepatocytes and embryonic stem cells from human and mouse and found evolutionary conservation of transcription factor binding sites within promoters is closely linked to the ability of those loci to activate gene expression (Hemberg and Kreiman, 2011). Interestingly, since only about 40% of human and mouse sequences can be aligned directly, most regulatory elements are present in non-orthologous sequences, and are predicted to contribute to functional and structural features of species-specific genomes (Bourque et al., 2008; Kunarso et al., 2010). Despite variation in positional conservation, the global fraction of regulatory elements within DNA that encode recognition sites for each TF appears to be conserved (Vierstra et al., 2014). As such, Dielh and Boyle introduced an interesting hypothesis by comparing the combination of co-bound transcription factors at a certain loci rather than the DNA sequence conservation across species (Diehl and Boyle, 2018). Distinct combinations of transcription factor binding sites or cis-regulatory modules have been implicated in specific gene expression patterns that translate across species (Borneman et al., 2007; Davidson, 2010; Gerstein et al., 2012). Thus, Dielh and Boyle proposed that the combination of transcription factor binding sites are "words" and the resulting cis-regulatory modules are "sentences" with meanings that are retained across tissues and species, where the words can be combined in many ways to produce diverse regulatory sentences/instructions (Diehl and Boyle, 2018). Similarly, as words and sentences comprise a language, the rules that dictate how transcription factor binding sites are combined into valid regulatory instructions represent the grammar of this natural "language".

Therefore, by shifting focus from the widespread divergence in positional conservation, they found that the majority of grammatical patterns, i.e., regulatory instructions, are actually shared between mouse and human cells representing stable functional signatures. Similarly, machine learning models designed to distinguish enhancers via histone marks signatures across six mammalian species, including humans showed that many short sequence patterns predictive of enhancers were largely conserved (Chen et al., 2018). Collectively, such studies suggest that despite the divergence in *cis*-regulatory element localization between mammalian genomes, cross-species enhancer prediction is often possible as sequence patterns encoding enhancer activity have been maintained across more than 180 million years of mammalian evolution (Chen et al., 2018).

In addition to genetically encoded information, histone modifications are precisely regulated to ensure that regulatory elements and associated genes are appropriately activated or repressed. Relatedly, Woo and Li demonstrated a strong association between the conservation of histone modifications between mice and humans, where modifications in promoter regions or intergenic enhancer regions were shown to be the most conserved (Woo and Li, 2012), with gene-body methylation found to be conserved among eukaryotes in general (Lee et al., 2010). Furthermore, a study examining 14 histone marks across 121 human cell types and tissues from the NIH Roadmap Epigenomics Project and mouse ENCODE Consortium found a similar number of DNA motifs that are predictive of each histone mark in humans and mice (Ngo et al., 2019). Importantly, a large portion of the found motifs were conserved indicating the presence of specific mechanisms that protect histone modifications against genetic changes (Ngo et al., 2019). Therefore, bearing in mind the functional divergence of orthologous regulatory loci,

researchers can look beyond positional conservation between species to understand common themes of regulatory control. Relatedly, insights obtained from biological processes in mice can facilitate a certain level of understanding of human physiology. As such, investigating transcriptional regulation and the molecular mechanisms of rexinoid signaling in mice as model organisms may prove fruitful in the goal of understanding human skeletal myogenesis as well as therapeutic development for the prevention and treatment of human muscle-related disease.

6.8 Epigenetic modulators in the treatment of muscle-related disease

The importance of epigenetic regulation in the development and maintenance of tissues highlights the potential for developing epigenetic therapeutics to treat diseases ranging from developmental disorders to various cancers that are characterized by defects in epigenetic regulators (Seligson et al., 2005). Moreover, the reversible nature of epigenetic modifications primes them as attractive pharmaceutical targets. Despite the development of small-molecule inhibitors for a range of chromatin modifiers including histone methyltransferases, histone demethylases, and HATS, only DNA methyltransferase and HDAC inhibitors have obtained approval by the United States Food and Drug Administration (FDA) thus far (Zhang et al., 2015). HDAC inhibitors in particular are being studied in several phase I and phase II clinical trials for their efficacy to treat solid malignancies, HIV infection and even arthritis (Lee et al., 2008; Vojinovic and Damjanov, 2011; Wightman et al., 2012). However, in the context of muscle-related disease, HDAC inhibitors have shown promise in mice models of Duchenne muscular dystrophy (DMD) (Minetti et al., 2006). DMD is defined by a lack of the dystrophin protein which links myofibers to the extracellular matrix. In the absence of this protein, muscle is

characterized by cycles of degeneration/regeneration, inflammation, fibrosis, and progressive loss of muscle mass and function, eventually leading to death in the second decade of life. Treatment with HDAC inhibitors results in increased efficiency of myoblast differentiation and fusion, without effecting proliferation (Iezzi et al., 2002, 2004). Molecularly, these inhibitors increase acetylation on the promoters of *follistatin (Fst), Myod1* and its target genes (Iezzi et al., 2002, 2004). Additionally, Mef2 and MyoD protein acetylation is boosted, promoting their recruitment to DNA (Grégoire et al., 2007; Iezzi et al., 2002). However, Fst, a glycoprotein that antagonizes the function of many transforming growth factor β members is considered the key target for HDAC inhibitors, as myofibers are non-responsive to HDAC inhibitors in the absence of this protein (Minetti et al., 2006). Notably, since HDAC inhibitors simply improve the symptomatic phenotype of the disease, a cure for the specific genetic defect is still needed.

Interestingly, HDAC inhibitors do not increase global histone acetylation, but rather target specific loci to improve myogenic differentiation (Halsall et al., 2012). Similarly, we have shown that the differentiation process is mediated by transformations in residue-specific histone acetylation at lineage-specific loci, rather than global histone acetylation events (Fig. 2.1, 2.4, 2.5). Interestingly, small molecule HAT activators have been developed which can activate the HAT activity of an enzyme by altering its structural configuration. Two of the best characterized activators of p300 include N-(4-Chloro-3-trifluoromethyl-phenyl)-2-ethoxy-6-pentadecyl-benzamide (CTPB) and nemorosone, both designed to induce structural alteration of p300, and lead to its autoacetylation. Relatedly, small molecule activator TTK21 has been used to promote maturation and differentiation of adult neuronal progenitors as it significantly induced histone acetylation in the hippocampus and frontal cortex (Chatterjee et al., 2013). Accordingly, direct

stimulation of p300 HAT activity holds therapeutic potential for the treatment of muscle-related diseases via the activation of distinct myogenic loci. As such, the epigenetic signature related to p300 underlying rexinoid enhanced myoblast differentiation provides an excellent system to identify novel myogenic targets that may be hold therapeutic potential. Taken together, a full understanding of the transcriptional mechanisms underlying tissue formation will facilitate the design of small molecule activators and inhibitors in a balanced approach to selectively target the catalytic activity of HATs for the treatment of tissue-specific disease.

6.9 Genomic localization of RXR in myogenic differentiation

Genome-wide ChIP-seq for RXRα revealed 1207 and 627 high confidence peaks in the absence and presence of bexarotene, respectively (Fig. 3.2). As RXR is a type II NR, RXR homo- or heterodimers remain nuclear and are bound to their genomic loci in the absence or presence of their ligands. As such, an important subject that must be addressed with future studies is characterization of the genomic distribution of RXRα in the absence and presence of bexarotene, specifically in a myogenic context. These studies will need to examine the mechanisms underlying a decrease in the number of RXRα loci following treatment, as well as to examine the possibility of an unliganded role for RXRα similar to other NRs. For instance, studies have indicated an unliganded VDR contributes to normal keratinocyte stem cell function and possesses intrinsic functions that control cancer cell growth via the Wnt/β-catenin pathway (Cianferotti et al., 2007; Skorija et al., 2005; Zheng et al., 2017). Furthermore, although *de novo* motif analysis revealed the nuclear receptor motif to be the top ranked binding motif amongst the RXRα peaks in both control and bexarotene conditions, approximately 60% of binding events

were not associated with a clear hormone response element (data not shown). As motif analysis is designed to predict binding to already characterized sequences, RXRα binding elements which deviate from conserved HREs may not have been identified by such analyses. Additionally, NR binding sites may be masked by the presence of other proteins or due to the recruitment of NRs by other TFs. Thus, future investigations will need to address genomic differences in RXRα localization, the influence of partner receptors, interactions with other TFs and chromatin modifiers, and the how the application of specific nuclear receptor agonists is integrated to promote skeletal myogenesis specifically.

Skeletal muscle is major target of rexinoid signaling as it also regulates sensitization of muscle to insulin via post-translational activation of several components of the insulin signaling pathway (Shen et al., 2004). Although some of the effects of rexinoids in skeletal muscles involve PPARγ–RXR heterodimers, rexinoids in skeletal muscle may also partner with other NR complexes for specific functions (Cha et al., 2001). Previous studies exploring genome-wide localization of NRs have demonstrated that RXR localization displays cell type and tissue specificity. Our study has shown differential RXRα binding following ligand activation, pertaining to a role in muscle-specific transcription (Fig. 3.1, 3.2). However, there are additional factors which influence RXR signaling including the stage of development, type of ligand, and the partner NR. Genomic profiling of RXR in adipogenic differentiation has shown that not only can the number of RXR binding sites vary throughout differentiation, but that the association of RXR to certain partners may vary as well (Nielsen et al., 2008). In contrast, cistromic examination of RXR displayed little change in RXR distribution following ligand activation in bone marrow-derived macrophages, with only an increase in RXR enrichment at predetermined

binding sites (Daniel et al., 2014). Thus, although we have shown that bexarotene enhances the differentiation and fusion of myoblasts through the function of RXRα as a transcription factor, future studies are required to examine liganded vs unliganded RXR-mediated transcriptional changes, active binding sites, partner identity and cistromic interactions in the context of the myogenic genome.

6.10 The role of RXR in health and disease

NR activation can produce a sustained pharmacological effect, making them attractive targets for drug development (Ouamrane et al., 2003; Schierle and Merk, 2019). RXRs in particular play a key role amongst NRs by participating as a heterodimer partner for several other NRs. Despite their physiological importance, only one synthetic agonist has been FDA approved and only as a second-line treatment for cutaneous T-cell lymphoma, although it has shown efficacy in the treatment of several other cancers including breast cancer, thyroid cancer, and acute myeloid leukemia (Altucci et al., 2007; Shen et al., 2018). Mechanistically, bexarotene is hypothesized to block NF-κB dependent survival signaling and enhance the pro-apoptotic potential of TNFα to produce its anti-tumor effect (Zeng et al., 2015). Additionally, RXRs are under research as promising targets for treatment of neurodegenerative diseases such as Alzheimer's disease and multiple sclerosis (Huang et al., 2008; Koster et al., 2017). However, RXR ligands are disadvantageous due to a lack of subtype specificity and tend to have various off-target effects such that bexarotene use is attributed to elevated triglyceride levels, hepatomegaly and alterations in thyroid hormone signaling, limiting its current use to a second-line cancer therapy only (Cummings et al., 2016; Farol and Hymes, 2004; Koster et al., 2017; Sherman et al., 1999).

Over the previous four years, several patents for RXR ligands have been filed for novel use in cancer, neurological disorders, and skin diseases. Io Therapeutics, a USA-based biotechnology company has proposed the use of RXR agonists in combination with the thyroid hormone thyroxine in order to improve the hypothyroidism caused by RXR agonists alone (Chandraratna and Sanders, 2017a, 2017b, 2018; Sherman et al., 1999). Interestingly, a patent for the combination of thyroxine with a molecule termed IRX4204 was filed in the treatment of muscle-wasting disorders including muscle dystrophies, stating that the combination is more effective in inducing differentiation of pluripotent stem cells to myoblasts than other rexinoids or either of the molecules alone (Chandraratna and Sanders, 2017c). Our study has set the foundation to understand the basis of RXR signaling and how it promotes the normal regulation of gene expression during early myoblast differentiation. However, it will be important to extend this research to determine if rexinoids are able to similarly regulate myogenic transcription in a specific physiological context or disease models. In summary, current RXR agonists suffer from subtype/ heterodimer selectivity, poor pharmacokinetics, and off-target effects (Schierle and Merk, 2019). However, numerous RXR ligands in development are beginning to target these issues and understanding the molecular mechanisms of rexinoid action and their specific molecular targets will provide insights into various systemic effects and eventual development of a therapeutically useful response in the context of muscle-related diseases as well as specific cell types (Burris et al., 2012).

Conclusion

In this study, we have integrated global transcriptomic profiles with genome-wide co-occurrence of MRFs and various epigenetic marks in differentiating myoblasts in the absence and presence of rexinoids. By utilizing chromatin state dynamics, we offer novel molecular insights into the regulation of myogenic enhancers by loci-specific histone acetylation at p300-associated enhancers, particularly when enlisted by MyoD. We also show that RXR signaling promotes normal regulation of gene expression occurring during myoblast differentiation, which is reconciled largely via MyoD expression. Furthermore, we present a genomic redistribution of myogenin and p300 loci in RXR signalling accompanied by a rexinoid-responsive residue-specific histone acetylation at enhancers co-occupied by p300 and myogenin. Collectively, we provide novel molecular insights into the interplay between RXR signaling and chromatin states pertinent to myogenic programs in early myoblast differentiation. Understanding the transcriptional regulators governing myogenesis and the model of rexinoid-enhanced myogenesis offers an excellent system to identify additional genetic targets and molecular interactions for therapeutic development toward muscle-related diseases. Relatedly, investigation into the use of specific pharmaceutical drugs to control endogenous epigenetic modifiers will enable specific changes in transcriptional activity of genes relevant for myogenesis.

References

Aguirre-Arteta, A.M., Grunewald, I., Cardoso, M.C., and Leonhardt, H. (2000). Expression of an alternative Dnmt1 isoform during muscle differentiation. Cell Growth Differ *11*, 551–559.

Ait-Si-Ali, S., Polesskaya, A., Filleur, S., Ferreira, R., Duquet, A., Robin, P., Vervish, A., Trouche, D., Cabon, F., and Harel-Bellan, A. (2000). CBP/p300 histone acetyl-transferase activity is important for the G1/S transition. Oncogene *19*, 2430–2437.

Akhtar-Zaidi, B., Cowper-Sal·lari, R., Corradin, O., Saiakhova, A., Bartels, C.F., Balasubramanian, D., Myeroff, L., Lutterbaugh, J., Jarrar, A., Kalady, M.F., et al. (2012). Epigenomic enhancer profiling defines a signature of colon cancer. Science *336*, 736–739.

Allfrey, V.G., Faulkner, R., and Mirsky, A.E. (1964). Acetylation and methylation of histones and their possible role in the regulation of RNA synthesis*. Proc Natl Acad Sci U S A *51*, 786–794.

AlSudais, H., Aabed, K., Nicola, W., Dixon, K., Chen, J., and Li, Q. (2016). Retinoid X Receptor-selective Signaling in the Regulation of Akt/Protein Kinase B Isoform-specific Expression. Journal of Biological Chemistry *291*, 3090–3099.

Altucci, L., Leibowitz, M.D., Ogilvie, K.M., de Lera, A.R., and Gronemeyer, H. (2007). RAR and RXR modulation in cancer and metabolic disease. Nat Rev Drug Discov *6*, 793–810.

Andreucci, J.J., Grant, D., Cox, D.M., Tomc, L.K., Prywes, R., Goldhamer, D.J., Rodrigues, N., Bédard, P.-A., and McDermott, J.C. (2002). Composition and Function of AP-1 Transcription Complexes during Muscle Cell Differentiation. J. Biol. Chem. *277*, 16426–16432.

Arany, Z., Sellers, W.R., Livingston, D.M., and Eckner, R. (1994). E1A-associated p300 and CREB-associated CBP belong to a conserved family of coactivators. Cell *77*, 799–800.

Arany, Z., Newsome, D., Oldread, E., Livingston, D.M., and Eckner, R. (1995). A family of transcriptional adaptor proteins targeted by the E1A oncoprotein. Nature *374*, 81–84.

Asfour, H.A., Allouh, M.Z., and Said, R.S. (2018). Myogenic regulatory factors: The orchestrators of myogenesis after 30 years of discovery. Exp. Biol. Med. (Maywood) *243*, 118–128.

Asp, P., Blum, R., Vethantham, V., Parisi, F., Micsinai, M., Cheng, J., Bowman, C., Kluger, Y., and Dynlacht, B.D. (2011). Genome-wide remodeling of the epigenetic landscape during myogenic differentiation. Proceedings of the National Academy of Sciences of the United States of America *108*, E149-58.

Azuara, V., Perry, P., Sauer, S., Spivakov, M., Jørgensen, H.F., John, R.M., Gouti, M., Casanova, M., Warnes, G., Merkenschlager, M., et al. (2006). Chromatin signatures of pluripotent cell lines. Nature Cell Biology *8*, 532–538.

Bannister, A.J., and Kouzarides, T. (2011). Regulation of chromatin by histone modifications. Cell Research *21*, 381–395.

Bannister, A.J., Zegerman, P., Partridge, J.F., Miska, E.A., Thomas, J.O., Allshire, R.C., and Kouzarides, T. (2001). Selective recognition of methylated lysine 9 on histone H3 by the HP1 chromo domain. Nature *410*, 120–124.

Barbosa-Morais, N.L., Irimia, M., Pan, Q., Xiong, H.Y., Gueroussov, S., Lee, L.J., Slobodeniuc, V., Kutter, C., Watt, S., Colak, R., et al. (2012). The Evolutionary Landscape of Alternative Splicing in Vertebrate Species. Science *338*, 1587–1593.

Barnes, C.E., English, D.M., and Cowley, S.M. (2019). Acetylation & Co: an expanding repertoire of histone acylations regulates chromatin and transcription. Essays Biochem *63*, 97–107.

Barski, A., Cuddapah, S., Cui, K., Roh, T.-Y., Schones, D.E., Wang, Z., Wei, G., Chepelev, I., and Zhao, K. (2007). High-Resolution Profiling of Histone Methylations in the Human Genome. Cell *129*, 823–837.

Beauchamp, J.R., Heslop, L., Yu, D.S.W., Tajbakhsh, S., Kelly, R.G., Wernig, A., Buckingham, M.E., Partridge, T.A., and Zammit, P.S. (2000). Expression of Cd34 and Myf5 Defines the Majority of Quiescent Adult Skeletal Muscle Satellite Cells. J Cell Biol *151*, 1221–1234.

Ben-Yair, R., and Kalcheim, C. (2008). Notch and bone morphogenetic protein differentially act on dermomyotome cells to generate endothelium, smooth, and striated muscle. J Cell Biol *180*, 607–618.

Berger, S.L. (2007). The complex language of chromatin regulation during transcription. Nature *447*, 407–412.

Bergstrom, D.A., and Tapscott, S.J. (2001). Molecular distinction between specification and differentiation in the myogenic basic helix-loop-helix transcription factor family. Molecular and Cellular Biology *21*, 2404–2412.

Bergstrom, D.A., Penn, B.H., Strand, A., Perry, R.L.S., Rudnicki, M.A., and Tapscott, S.J. (2002). Promoter-Specific Regulation of MyoD Binding and Signal Transduction Cooperate to Pattern Gene Expression. Molecular Cell *9*, 587–600.

Bernstein, B.E., Mikkelsen, T.S., Xie, X., Kamal, M., Huebert, D.J., Cuff, J., Fry, B., Meissner, A., Wernig, M., Plath, K., et al. (2006). A Bivalent Chromatin Structure Marks Key Developmental Genes in Embryonic Stem Cells. Cell *125*, 315–326.

Bi, P., Ramirez-Martinez, A., Li, H., Cannavino, J., McAnally, J.R., Shelton, J.M., Sánchez-Ortiz, E., Bassel-Duby, R., and Olson, E.N. (2017). Control of muscle formation by the fusogenic micropeptide myomixer. Science *356*, 323–327.

Biggs, J.S., Wan, J., Cutler, N.S., Hakkola, J., Uusimäki, P., Raunio, H., and Yost, G.S. (2007). Transcription Factor Binding to a Putative Double E-Box Motif Represses CYP3A4 Expression in Human Lung Cells. Mol Pharmacol *72*, 514–525.

Birchmeier, C., and Brohmann, H. (2000). Genes that control the development of migrating muscle precursor cells. Current Opinion in Cell Biology *12*, 725–730.

Bischoff, R., and Holtzer, H. (1969). MITOSIS AND THE PROCESSES OF DIFFERENTIATION OF MYOGENIC CELLS IN VITRO. J Cell Biol *41*, 188–200.

Blais, A., and Dynlacht, B.D. (2004). Hitting their targets: an emerging picture of E2F and cell cycle control. Current Opinion in Genetics & Development *14*, 527–532.

Blais, A., Tsikitis, M., Acosta-Alvear, D., Sharan, R., Kluger, Y., and Dynlacht, B.D. (2005). An initial blueprint for myogenic differentiation. Genes & Development *19*, 553–569.

Blais, A., van Oevelen, C.J.C., Margueron, R., Acosta-Alvear, D., and Dynlacht, B.D. (2007). Retinoblastoma tumor suppressor protein–dependent methylation of histone H3 lysine 27 is associated with irreversible cell cycle exit. J Cell Biol *179*, 1399–1412.

Blau, H.M., Pavlath, G.K., Hardeman, E.C., Chiu, C.P., Silberstein, L., Webster, S.G., Miller, S.C., and Webster, C. (1985). Plasticity of the differentiated state. Science (New York, N.Y.) *230*, 758–766.

Blow, M.J., McCulley, D.J., Li, Z., Zhang, T., Akiyama, J.A., Holt, A., Plajzer-Frick, I., Shoukry, M., Wright, C., Chen, F., et al. (2010). ChIP-Seq identification of weakly conserved heart enhancers. Nature Genetics *42*, 806–810.

Blum, R., Vethantham, V., Bowman, C., Rudnicki, M., and Dynlacht, B.D. (2012). Genome-wide identification of enhancers in skeletal muscle: the role of MyoD1. Genes & Development *26*, 2763–2779.

Boergesen, M., Pedersen, T.A., Gross, B., van Heeringen, S.J., Hagenbeek, D., Bindesboll, C., Caron, S., Lalloyer, F., Steffensen, K.R., Nebb, H.I., et al. (2012). Genome-Wide Profiling of Liver X Receptor, Retinoid X Receptor, and Peroxisome Proliferator-Activated Receptor in Mouse Liver Reveals Extensive Sharing of Binding Sites. Molecular and Cellular Biology *32*, 852–867.

Borneman, A.R., Gianoulis, T.A., Zhang, Z.D., Yu, H., Rozowsky, J., Seringhaus, M.R., Wang, L.Y., Gerstein, M., and Snyder, M. (2007). Divergence of Transcription Factor Binding Sites Across Related Yeast Species. Science *317*, 815–819.

Bourguet, W., Vivat, V., Wurtz, J.-M., Chambon, P., Gronemeyer, H., and Moras, D. (2000). Crystal Structure of a Heterodimeric Complex of RAR and RXR Ligand-Binding Domains. Molecular Cell *5*, 289–298.

Bourque, G., Leong, B., Vega, V.B., Chen, X., Lee, Y.L., Srinivasan, K.G., Chew, J.-L., Ruan, Y., Wei, C.-L., Ng, H.H., et al. (2008). Evolution of the mammalian transcription factor binding repertoire via transposable elements. Genome Res *18*, 1752–1762.

Boyer, L.A., Plath, K., Zeitlinger, J., Brambrink, T., Medeiros, L.A., Lee, T.I., Levine, S.S., Wernig, M., Tajonar, A., Ray, M.K., et al. (2006). Polycomb complexes repress developmental regulators in murine embryonic stem cells. Nature *441*, 349–353.

Braun, T., Buschhausen-Denker, G., Bober, E., Tannich, E., and Arnold, H.H. (1989). A novel human muscle factor related to but distinct from MyoD1 induces myogenic conversion in 10T1/2 fibroblasts. The EMBO Journal *8*, 701–709.

Braun, T., Rudnicki, M.A., Arnold, H.H., and Jaenisch, R. (1992). Targeted inactivation of the muscle regulatory gene Myf-5 results in abnormal rib development and perinatal death. Cell *71*, 369–382.

Bricambert, J., Miranda, J., Benhamed, F., Girard, J., Postic, C., and Dentin, R. (2010). Salt-inducible kinase 2 links transcriptional coactivator p300 phosphorylation to the prevention of ChREBP-dependent hepatic steatosis in mice. The Journal of Clinical Investigation *120*, 4316–4331.

Brinkman, A.B., Gu, H., Bartels, S.J.J., Zhang, Y., Matarese, F., Simmer, F., Marks, H., Bock, C., Gnirke, A., Meissner, A., et al. (2012). Sequential ChIP-bisulfite sequencing enables direct genome-scale investigation of chromatin and DNA methylation cross-talk. Genome Res. *22*, 1128–1138.

Brunk, B.P., Goldhamer, D.J., and Emerson, C.P. (1996). Regulated demethylation of the myoD distal enhancer during skeletal myogenesis. Dev Biol *177*, 490–503.

Bu, P., Evrard, Y.A., Lozano, G., and Dent, S.Y.R. (2007). Loss of Gcn5 acetyltransferase activity leads to neural tube closure defects and exencephaly in mouse embryos. Molecular and Cellular Biology *27*, 3405–3416.

Buckingham, M. (2001). Skeletal muscle formation in vertebrates. Current Opinion in Genetics & Development *11*, 440–448.

Buckingham, M. (2006). Myogenic progenitor cells and skeletal myogenesis in vertebrates. Current Opinion in Genetics & Development *16*, 525–532.

Buckingham, M., and Relaix, F. (2007). The role of Pax genes in the development of tissues and organs: Pax3 and Pax7 regulate muscle progenitor cell functions. Annu Rev Cell Dev Biol *23*, 645–673.

Bulynko, Y.A., and O'Malley, B.W. (2011). Nuclear Receptor Coactivators: Structural and Functional Biochemistry. Biochemistry *50*, 313–328.

Burattini, S., Ferri, P., Battistelli, M., Curci, R., Luchetti, F., and Falcieri, E. (2004). C2C12 murine myoblasts as a model of skeletal muscle development: morpho-functional characterization. Eur J Histochem *48*, 223–233.

Burris, T.P., Busby, S.A., and Griffin, P.R. (2012). Targeting Orphan Nuclear Receptors for Treatment of Metabolic Diseases and Autoimmunity. Chem Biol *19*, 51–59.

Bushue, N., and Wan, Y.-J.Y. (2010). Retinoid Pathway and Cancer Therapeutics. Adv Drug Deliv Rev *62*, 1285–1298.

Cao, Y., Kumar, R.M., Penn, B.H., Berkes, C.A., Kooperberg, C., Boyer, L.A., Young, R.A., and Tapscott, S.J. (2006). Global and gene-specific analyses show distinct roles for Myod and Myog at a common set of promoters. EMBO J. *25*, 502–511.

Cao, Y., Yao, Z., Sarkar, D., Lawrence, M., Sanchez, G.J., Parker, M.H., MacQuarrie, K.L., Davison, J., Morgan, M.T., Ruzzo, W.L., et al. (2010). Genome-wide MyoD Binding in Skeletal Muscle Cells: A Potential for Broad Cellular Reprogramming. Developmental Cell *18*, 662–674.

Caretti, G., Di Padova, M., Micales, B., Lyons, G.E., and Sartorelli, V. (2004). The Polycomb Ezh2 methyltransferase regulates muscle gene expression and skeletal muscle differentiation. Genes Dev *18*, 2627–2638.

Carpenter, S., and Karpati, G. (1979). Duchenne muscular dystrophy: plasma membrane loss initiates muscle cell necrosis unless it is repaired. Brain : A Journal of Neurology *102*, 147–161.

Casey, B.H., Kollipara, R.K., Pozo, K., and Johnson, J.E. (2018). Intrinsic DNA binding properties demonstrated for lineage-specifying basic helix-loop-helix transcription factors. Genome Res. *28*, 484–496.

Cha, B.S., Ciaraldi, T.P., Carter, L., Nikoulina, S.E., Mudaliar, S., Mukherjee, R., Paterniti, J.R., and Henry, R.R. (2001). Peroxisome proliferator-activated receptor (PPAR) gamma and retinoid X receptor (RXR) agonists have complementary effects on glucose and lipid metabolism in human skeletal muscle. Diabetologia *44*, 444–452.

Chakravarti, D., LaMorte, V.J., Nelson, M.C., Nakajima, T., Schulman, I.G., Juguilon, H., Montminy, M., and Evans, R.M. (1996). Role of CBP/P300 in nuclear receptor signalling. Nature *383*, 99–103.

Chakroun, I., Yang, D., Girgis, J., Gunasekharan, A., Phenix, H., Kærn, M., and Blais, A. (2015). Genome-wide association between Six4, MyoD, and the histone demethylase Utx during myogenesis. FASEB Journal *29*, 4738–4755.

Chambon, P. (2005). The Nuclear Receptor Superfamily: A Personal Retrospect on the First Two Decades. Molecular Endocrinology *19*, 1418–1428.

Chan, H.M., and La Thangue, N.B. (2001). p300/CBP proteins: HATs for transcriptional bridges and scaffolds. Journal of Cell Science *114*, 2363–2373.

Chandra, S., Terragni, J., Zhang, G., Pradhan, S., Haushka, S., Johnston, D., Baribault, C., Lacey, M., and Ehrlich, M. (2015). Tissue-specific epigenetics in gene neighborhoods: myogenic transcription factor genes. Human Molecular Genetics *24*, 4660.

Chandraratna, R.A., and Sanders, M.E. (2017a). Treatment of autoimmune diseases with combinations of rxr agonists and thyroid hormones.

Chandraratna, R.A., and Sanders, M.E. (2017b). Treatment of cancer with combinations of rxr agonists and thyroid hormones.

Chandraratna, R.A., and Sanders, M.E. (2017c). Treatment of muscular disorders with combinations of rxr agonists and thyroid hormones.

Chandraratna, R.A., and Sanders, M.E. (2018). Treatment of nervous system disorders using combinations of rxr agonists and thyroid hormones.

Chang, A.T., Liu, Y., Ayyanathan, K., Benner, C., Jiang, Y., Prokop, J.W., Paz, H., Wang, D., Li, H.-R., Fu, X.-D., et al. (2015). An evolutionarily conserved DNA architecture determines target specificity of the TWIST family bHLH transcription factors. Genes Dev *29*, 603–616.

Chatterjee, S., Mizar, P., Cassel, R., Neidl, R., Selvi, B.R., Mohankrishna, D.V., Vedamurthy, B.M., Schneider, A., Bousiges, O., Mathis, C., et al. (2013). A Novel Activator of CBP/p300 Acetyltransferases Promotes Neurogenesis and Extends Memory Duration in Adult Mice. Journal of Neuroscience *33*, 10698–10712.

Chen, J., and Li, Q. (2011). Life and death of transcriptional co-activator p300. Epigenetics *6*, 957–961.

Chen, J.D., and Evans, R.M. (1995). A transcriptional co-repressor that interacts with nuclear hormone receptors. Nature *377*, 454–457.

Chen, H., Lin, R.J., Schiltz, R.L., Chakravarti, D., Nash, A., Nagy, L., Privalsky, M.L., Nakatani, Y., and Evans, R.M. (1997). Nuclear receptor coactivator ACTR is a novel histone acetyltransferase and forms a multimeric activation complex with P/CAF and CBP/p300. Cell *90*, 569–580.

Chen, J., St-germain, J.R., and Li, Q. (2005). B56 Regulatory Subunit of Protein Phosphatase 2A Mediates Valproic Acid-Induced p300 Degradation B56 Regulatory Subunit of Protein Phosphatase 2A Mediates Valproic Acid-Induced p300 Degradation. Molecular and Cellular Biology *25*, 525–532.

Chen, J., Wang, Y., Hamed, M., Lacroix, N., and Li, Q. (2015). Molecular Basis for the Regulation of Transcriptional Coactivator p300 in Myogenic Differentiation. Scientific Reports *5*, 13727.

Chen, L., Fish, A.E., and Capra, J.A. (2018). Prediction of gene regulatory enhancers across species reveals evolutionarily conserved sequence properties. PLOS Computational Biology *14*, e1006484.

Cheng, W., Wang, L., Yang, B., Zhang, R., Yao, C., He, L., Liu, Z., Du, P., Hammache, K., Wen, J., et al. (2014). Self-renewal and Differentiation of Muscle Satellite Cells Are Regulated by the Fas-associated Death Domain. J. Biol. Chem. *289*, 5040–5050.

Chiba, H., Clifford, J., Metzger, D., and Chambon, P. (1997). Distinct retinoid X receptor-retinoic acid receptor heterodimers are differentially involved in the control of expression of retinoid target genes in F9 embryonal carcinoma cells. Mol Cell Biol *17*, 3013–3020.

Choi, S.H., Gearhart, M.D., Cui, Z., Bosnakovski, D., Kim, M., Schennum, N., and Kyba, M. (2016). DUX4 recruits p300/CBP through its C-terminus and induces global H3K27 acetylation changes. Nucleic Acids Res. *44*, 5161–5173.

Choudhary, C., Kumar, C., Gnad, F., Nielsen, M.L., Rehman, M., Walther, T.C., Olsen, J.V., and Mann, M. (2009). Lysine Acetylation Targets Protein Complexes and Co-Regulates Major Cellular Functions. Science *325*, 834–840.

Cianferotti, L., Cox, M., Skorija, K., and Demay, M.B. (2007). Vitamin D receptor is essential for normal keratinocyte stem cell function. PNAS *104*, 9428–9433.

Ciurciu, A., Komonyi, O., Pankotai, T., and Boros, I.M. (2006). The Drosophila Histone Acetyltransferase Gcn5 and Transcriptional Adaptor Ada2a Are Involved in Nucleosomal Histone H4 Acetylation. Mol Cell Biol *26*, 9413–9423.

Claessens, F., and Gewirth, D.T. (2004). DNA recognition by nuclear receptors. Essays Biochem. *40*, 59–72.

Clements, A., Rojas, J.R., Trievel, R.C., Wang, L., Berger, S.L., and Marmorstein, R. (1999). Crystal structure of the histone acetyltransferase domain of the human PCAF transcriptional regulator bound to coenzyme A. EMBO J *18*, 3521–3532.

Conboy, C.M., Spyrou, C., Thorne, N.P., Wade, E.J., Barbosa-Morais, N.L., Wilson, M.D., Bhattacharjee, A., Young, R.A., Tavaré, S., Lees, J.A., et al. (2007). Cell Cycle Genes Are the Evolutionarily Conserved Targets of the E2F4 Transcription Factor. PLOS ONE *2*, e1061.

Conerly, M.L., Yao, Z., Zhong, J.W., Groudine, M., and Tapscott, S.J. (2016). Distinct Activities of Myf5 and MyoD Indicate Separate Roles in Skeletal Muscle Lineage Specification and Differentiation. Developmental Cell *36*, 375–385.

Cossu, G., Angelis, L.D., Borello, U., Berarducci, B., Buffa, V., Sonnino, C., Coletta, M., Vivarelli, E., Bouche, M., Lattanzi, L., et al. (2004). Determination, diversification and multipotency of mammalian myogenic cells. Int. J. Dev. Biol. *44*, 699–706.

Cotnoir-White, D., Laperrière, D., and Mader, S. (2011). Evolution of the repertoire of nuclear receptor binding sites in genomes. Mol. Cell. Endocrinol. *334*, 76–82.

Cremona, M.A., Sangalli, L.M., Vantini, S., Dellino, G.I., Pelicci, P.G., Secchi, P., and Riva, L. (2015). Peak shape clustering reveals biological insights. BMC Bioinformatics *16*, 349.

Creyghton, M.P., Cheng, A.W., Welstead, G.G., Kooistra, T., Carey, B.W., Steine, E.J., Hanna, J., Lodato, M.A., Frampton, G.M., Sharp, P.A., et al. (2010). Histone H3K27ac separates active from poised enhancers and predicts developmental state. Proceedings of the National Academy of Sciences *107*, 21931–21936.

Cui, H., Bansal, V., Grunert, M., Malecova, B., Dall'Agnese, A., Latella, L., Gatto, S., Ryan, T., Schulz, K., Chen, W., et al. (2017). Muscle-relevant genes marked by stable H3K4me2/3 profiles and enriched MyoD binding during myogenic differentiation. PLOS ONE *12*, e0179464.

Cummings, J.L., Zhong, K., Kinney, J.W., Heaney, C., Moll-Tudla, J., Joshi, A., Pontecorvo, M., Devous, M., Tang, A., and Bena, J. (2016). Double-blind, placebo-controlled, proof-of-concept trial of bexarotene Xin moderate Alzheimer's disease. Alzheimers Res Ther *8*.

Dancy, B.M., and Cole, P.A. (2015). Protein Lysine Acetylation by p300/CBP. Chemical Reviews *115*, 2419–2452.

D'Angelo, M.A., Gomez-Cavazos, J.S., Mei, A., Lackner, D.H., and Hetzer, M.W. (2012). A change in nuclear pore complex composition regulates cell differentiation. Developmental Cell *22*, 446–458.

Daniel, B., Nagy, G., Hah, N., Horvath, A., Czimmerer, Z., Poliska, S., Gyuris, T., Keirsse, J., Gysemans, C., Van Ginderachter, J.A., et al. (2014). The active enhancer network operated by liganded RXR supports angiogenic activity in macrophages. Genes & Development *28*, 1562–1577.

Das, C., Lucia, M.S., Hansen, K.C., and Tyler, J.K. (2009). CBP/p300-mediated acetylation of histone H3 on lysine 56. Nature *459*, 113–117.

Davidson, E.H. (2010). Emerging properties of animal gene regulatory networks. Nature *468*, 911–920.

Davis, R.L., Weintraub, H., and Lassar, A.B. (1987). Expression of a single transfected cDNA converts fibroblasts to myoblasts. Cell *51*, 987–1000.

Davydov, E. V., Goode, D.L., Sirota, M., Cooper, G.M., Sidow, A., Batzoglou, S., Margulies, E., Cooper, G., Asimenos, G., Thomas, D., et al. (2010). Identifying a High Fraction of the Human Genome to be under Selective Constraint Using GERP++. PLoS Computational Biology *6*, e1001025.

Dawson, M.I., and Xia, Z. (2012). The Retinoid X Receptors and Their Ligands. Biochim Biophys Acta *1821*, 21–56.

Deblois, G., and Giguère, V. (2008). Nuclear Receptor Location Analyses in Mammalian Genomes: From Gene Regulation to Regulatory Networks. Mol Endocrinol *22*, 1999–2011.

Delgado, I., Huang, X., Jones, S., Zhang, L., Hatcher, R., Gao, B., and Zhang, P. (2003). Dynamic gene expression during the onset of myoblast differentiation in vitro. Genomics *82*, 109–121.

Delvecchio, M., Gaucher, J., Aguilar-Gurrieri, C., Ortega, E., and Panne, D. (2013). Structure of the p300 catalytic core and implications for chromatin targeting and HAT regulation. Nat Struct Mol Biol *20*, 1040–1046.

Desvergne, B. (2007). RXR: from partnership to leadership in metabolic regulations. Vitam. Horm. *75*, 1–32.

Dhawan, J., and Rando, T.A. (2005). Stem cells in postnatal myogenesis: molecular mechanisms of satellite cell quiescence, activation and replenishment. Trends Cell Biol. *15*, 666–673.

Di Gennaro, E., Bruzzese, F., Caraglia, M., Abruzzese, A., and Budillon, A. (2004). Acetylation of proteins as novel target for antitumor therapy: Review article. Amino Acids *26*, 435–441.

Di Padova, M., Caretti, G., Zhao, P., Hoffman, E.P., and Sartorelli, V. (2007). MyoD Acetylation Influences Temporal Patterns of Skeletal Muscle Gene Expression. Journal of Biological Chemistry *282*, 37650–37659.

Diehl, A.G., and Boyle, A.P. (2018). Conserved and species-specific transcription factor co-binding patterns drive divergent gene regulation in human and mouse. Nucleic Acids Res *46*, 1878–1894.

Dilworth, F.J., Fromental-Ramain, C., Yamamoto, K., and Chambon, P. (2000). ATP-Driven Chromatin Remodeling Activity and Histone Acetyltransferases Act Sequentially during Transactivation by RAR/RXR In Vitro. Molecular Cell *6*, 1049–1058.

Dilworth, F.J., Seaver, K.J., Fishburn, A.L., Htet, S.L., and Tapscott, S.J. (2004). In vitro transcription system delineates the distinct roles of the coactivators pCAF and p300 during MyoD/E47-dependent transactivation. PNAS *101*, 11593–11598.

Dodou, E., Xu, S.-M., and Black, B.L. (2003). mef2c is activated directly by myogenic basic helix-loop-helix proteins during skeletal muscle development in vivo. Mechanisms of Development *120*, 1021–1032.

Doynova, M.D., Markworth, J.F., Cameron-Smith, D., Vickers, M.H., and O'Sullivan, J.M. (2017). Linkages between changes in the 3D organization of the genome and transcription during myotube differentiation in vitro. Skeletal Muscle *7*, 5.

Dror, I., Golan, T., Levy, C., Rohs, R., and Mandel-Gutfreund, Y. (2015). A widespread role of the motif environment in transcription factor binding across diverse protein families. Genome Res *25*, 1268–1280.

Du, C., Jin, Y.-Q., Qi, J.-J., Ji, Z.-X., Li, S.-Y., An, G.-S., Jia, H.-T., and Ni, J.-H. (2012). Effects of Myogenin on Expression of Late Muscle Genes through MyoD-Dependent Chromatin Remodeling Ability of Myogenin. Mol Cells *34*, 133–142.

Dunham, I., Kundaje, A., Aldred, S.F., Collins, P.J., Davis, C.A., Doyle, F., Epstein, C.B., Frietze, S., Harrow, J., Kaul, R., et al. (2012). An integrated encyclopedia of DNA elements in the human genome. Nature *489*, 57–74.

Eberharter, A., and Becker, P.B. (2002). Histone acetylation: a switch between repressive and permissive chromatin. Second in review series on chromatin dynamics. EMBO Reports *3*, 224–229.

Echeverria, P.C., and Picard, D. (2010). Molecular chaperones, essential partners of steroid hormone receptors for activity and mobility. Biochimica et Biophysica Acta (BBA) - Molecular Cell Research *1803*, 641–649.

Edmondson, D.G., and Olson, E.N. (1989). A gene with homology to the myc similarity region of MyoD1 is expressed during myogenesis and is sufficient to activate the muscle differentiation program. Genes & Development *3*, 628–640.

Edmondson, D.G., and Olson, E.N. (1993). Helix-loop-helix proteins as regulators of muscle-specific transcription. The Journal of Biological Chemistry *268*, 755–758.

Edmondson, D.G., Brennan, T.J., and Olson, E.N. (1991). Mitogenic repression of myogenin autoregulation. J. Biol. Chem. *266*, 21343–21346.

Eeckhoute, J., Carroll, J.S., Geistlinger, T.R., Torres-Arzayus, M.I., and Brown, M. (2006). A cell-type-specific transcriptional network required for estrogen regulation of cyclin D1 and cell cycle progression in breast cancer. Genes & Development *20*, 2513–2526.

Eid, J.E., Kung, A.L., Scully, R., and Livingston, D.M. (2000). p300 interacts with the nuclear proto-oncoprotein SYT as part of the active control of cell adhesion. Cell *102*, 839–848.

Emili, A., Greenblatt, J., and Ingles, C.J. (1994). Species-specific interaction of the glutamine-rich activation domains of Sp1 with the TATA box-binding protein. Mol Cell Biol *14*, 1582–1593.

Endo, T. (2015). Molecular mechanisms of skeletal muscle development, regeneration, and osteogenic conversion. Bone *80*, 2–13.

Ernst, J., and Kellis, M. (2012). ChromHMM: automating chromatin-state discovery and characterization. Nature Methods *9*, 215–216.

Ernst, J., and Kellis, M. (2017). Chromatin state discovery and genome annotation with ChromHMM. Nat Protoc *12*, 2478–2492.

Ernst, J., Kheradpour, P., Mikkelsen, T.S., Shoresh, N., Ward, L.D., Epstein, C.B., Zhang, X., Wang, L., Issner, R., Coyne, M., et al. (2011). Mapping and analysis of chromatin state dynamics in nine human cell types. Nature *473*, 43–49.

Eto, I. (2000). Molecular cloning and sequence analysis of the promoter region of mouse cyclin D1 gene: implication in phorbol ester-induced tumour promotion. Cell Proliferation *33*, 167–187.

Fang, F., Xu, Y., Chew, K.-K., Chen, X., Ng, H.-H., and Matsudaira, P. (2014). Coactivators p300 and CBP maintain the identity of mouse embryonic stem cells by mediating long-range chromatin structure. Stem Cells *32*, 1805–1816.

Faralli, H., and Dilworth, F.J. (2012). Turning on Myogenin in Muscle: A Paradigm for Understanding Mechanisms of Tissue-Specific Gene Expression. Comparative and Functional Genomics *2012*, 1–10.

Faralli, H., Wang, C., Nakka, K., Benyoucef, A., Sebastian, S., Zhuang, L., Chu, A., Palii, C.G., Liu, C., Camellato, B., et al. (2016). UTX demethylase activity is required for satellite cell–mediated muscle regeneration. J Clin Invest *126*, 1555–1565.

Farol, L.T., and Hymes, K.B. (2004). Bexarotene: a clinical review. Expert Rev Anticancer Ther *4*, 180–188.

Filion, G.J., van Bemmel, J.G., Braunschweig, U., Talhout, W., Kind, J., Ward, L.D., Brugman, W., de Castro, I.J., Kerkhoven, R.M., Bussemaker, H.J., et al. (2010). Systematic Protein Location Mapping Reveals Five Principal Chromatin Types in Drosophila Cells. Cell *143*, 212–224.

Fong, A.P., Yao, Z., Zhong, J.W., Cao, Y., Ruzzo, W.L., Gentleman, R.C., and Tapscott, S.J. (2012). Genetic and Epigenetic Determinants of Neurogenesis and Myogenesis. Developmental Cell *22*, 721–735.

Fong, A.P., Yao, Z., Zhong, J.W., Johnson, N.M., Farr, G.H., Maves, L., and Tapscott, S.J. (2015). Conversion of MyoD to a neurogenic factor: binding site specificity determines lineage. Cell Rep *10*, 1937–1946.

Francetic, T., Le May, M., Hamed, M., Mach, H., Meyers, D., Cole, P.A., Chen, J., and Li, Q. (2012). Regulation of Myf5 Early Enhancer by Histone Acetyltransferase p300 during Stem Cell Differentiation. Molecular Biology *1*, 1–17.

Fueyo, R., Iacobucci, S., Pappa, S., Estarás, C., Lois, S., Vicioso-Mantis, M., Navarro, C., Cruz-Molina, S., Reyes, J.C., Rada-Iglesias, Á., et al. (2018). Lineage specific transcription factors and epigenetic regulators mediate TGFβ-dependent enhancer activation. Nucleic Acids Res *46*, 3351–3365.

Fulco, M., Schiltz, R.L., Iezzi, S., King, M.T., Zhao, P., Kashiwaya, Y., Hoffman, E., Veech, R.L., and Sartorelli, V. (2003). Sir2 regulates skeletal muscle differentiation as a potential sensor of the redox state. Mol. Cell *12*, 51–62.

Gampe, R.T., Montana, V.G., Lambert, M.H., Wisely, G.B., Milburn, M.V., and Xu, H.E. (2000). Structural basis for autorepression of retinoid X receptor by tetramer formation and the AF-2 helix. Genes & Development *14*, 2229–2241.

Gan, Q., Yoshida, T., McDonald, O.G., and Owens, G.K. (2007). Concise Review: Epigenetic Mechanisms Contribute to Pluripotency and Cell Lineage Determination of Embryonic Stem Cells. STEM CELLS *25*, 2–9.

Gaudel, C., Schwartz, C., Giordano, C., Abumrad, N.A., and Grimaldi, P.A. (2008). Pharmacological activation of PPARβ promotes rapid and calcineurin-dependent fiber

remodeling and angiogenesis in mouse skeletal muscle. American Journal of Physiology - Endocrinology and Metabolism *295*.

Gayraud-Morel, B., Chrétien, F., Flamant, P., Gomès, D., Zammit, P.S., and Tajbakhsh, S. (2007). A role for the myogenic determination gene Myf5 in adult regenerative myogenesis. Developmental Biology *312*, 13–28.

Gayraud-Morel, B., Chrétien, F., Jory, A., Sambasivan, R., Negroni, E., Flamant, P., Soubigou, G., Coppée, J.-Y., Santo, J.D., Cumano, A., et al. (2012). Myf5 haploinsufficiency reveals distinct cell fate potentials for adult skeletal muscle stem cells. J Cell Sci *125*, 1738–1749.

Geiman, T.M., and Robertson, K.D. (2002). Chromatin remodeling, histone modifications, and DNA methylation—how does it all fit together? Journal of Cellular Biochemistry *87*, 117–125.

Gerber, M., and Shilatifard, A. (2003). Transcriptional elongation by RNA polymerase II and histone methylation. J Biol Chem *278*, 26303–26306.

Gerber, A.N., Klesert, T.R., Bergstrom, D.A., and Tapscott, S.J. (1997). Two domains of MyoD mediate transcriptional activation of genes in repressive chromatin: a mechanism for lineage determination in myogenesis. Genes Dev. *11*, 436–450.

Germain, P., Staels, B., Dacquet, C., Spedding, M., and Laudet, V. (2006). Overview of nomenclature of nuclear receptors. Pharmacol. Rev. *58*, 685–704.

Gerstein, M.B., Kundaje, A., Hariharan, M., Landt, S.G., Yan, K.-K., Cheng, C., Mu, X.J., Khurana, E., Rozowsky, J., Alexander, R., et al. (2012). Architecture of the human regulatory network derived from ENCODE data. Nature *489*, 91–100.

Glass, C.K., and Rosenfeld, M.G. (2000). The coregulator exchange in transcriptional functions of nuclear receptors. Genes Dev. *14*, 121–141.

Goldhamer, D.J., Faerman, A., Shani, M., and Emerson, C.P. (1992). Regulatory elements that control the lineage-specific expression of myoD. Science (New York, N.Y.) *256*, 538–542.

Goldhamer, D.J., Brunk, B.P., Faerman, A., King, A., Shani, M., and Emerson, C.P. (1995). Embryonic activation of the myoD gene is regulated by a highly conserved distal control element. Development (Cambridge, England) *121*, 637–649.

Goodman, R.H., and Smolik, S. (2000). CBP/p300 in cell growth, transformation, and development. Genes & Development *14*, 1553–1577.

Gordân, R., Shen, N., Dror, I., Zhou, T., Horton, J., Rohs, R., and Bulyk, M.L. (2013). Genomic regions flanking E-box binding sites influence DNA binding specificity of bHLH transcription factors through DNA shape. Cell Rep *3*, 1093–1104.

Grégoire, S., Xiao, L., Nie, J., Zhang, X., Xu, M., Li, J., Wong, J., Seto, E., and Yang, X.-J. (2007). Histone Deacetylase 3 Interacts with and Deacetylates Myocyte Enhancer Factor 2. Molecular and Cellular Biology *27*, 1280–1295.

Gregoretti, I.V., Lee, Y.-M., and Goodson, H.V. (2004). Molecular evolution of the histone deacetylase family: functional implications of phylogenetic analysis. J Mol Biol *338*, 17–31.

Grifone, R., Demignon, J., Giordani, J., Niro, C., Souil, E., Bertin, F., Laclef, C., Xu, P.-X., and Maire, P. (2007). Eya1 and Eya2 proteins are required for hypaxial somitic myogenesis in the mouse embryo. Developmental Biology *302*, 602–616.

Gronemeyer, H., Gustafsson, J.-Å., and Laudet, V. (2004). Principles for modulation of the nuclear receptor superfamily. Nature Reviews Drug Discovery *3*, 950–964.

Gu, W., and Roeder, R.G. (1997). Activation of p53 Sequence-Specific DNA Binding by Acetylation of the p53 C-Terminal Domain. Cell *90*, 595–606.

Gustafsson, M.K., Pan, H., Pinney, D.F., Liu, Y., Lewandowski, A., Epstein, D.J., and Emerson, C.P. (2002). Myf5 is a direct target of long-range Shh signaling and Gli regulation for muscle specification. Genes Dev *16*, 114–126.

Halevy, O., Novitch, B.G., Spicer, D.B., Skapek, S.X., Rhee, J., Hannon, G.J., Beach, D., and Lassar, A.B. (1995). Correlation of terminal cell cycle arrest of skeletal muscle with induction of p21 by MyoD. Science (New York, N.Y.) *267*, 1018–1021.

Halsall, J., Gupta, V., O'Neill, L.P., Turner, B.M., and Nightingale, K.P. (2012). Genes Are Often Sheltered from the Global Histone Hyperacetylation Induced by HDAC Inhibitors. PLoS ONE *7*, e33453.

Hamed, M., Khilji, S., Chen, J., and Li, Q. (2013). Stepwise acetyltransferase association and histone acetylation at the Myod1 locus during myogenic differentiation. Scientific Reports *3*, 2390.

Hamed, M., Khilji, S., Dixon, K., Blais, A., Ioshikhes, I., Chen, J., and Li, Q. (2017). Insights into interplay between rexinoid signaling and myogenic regulatory factor-associated chromatin state in myogenic differentiation. Nucleic Acids Res *45*, 11236–11248.

Hasty, P., Bradley, A., Morris, J.H., Edmondson, D.G., Venuti, J.M., Olson, E.N., and Klein, W.H. (1993). Muscle deficiency and neonatal death in mice with a targeted mutation in the myogenin gene. Nature *364*, 501–506.

Heidt, A.B., Rojas, A., Harris, I.S., and Black, B.L. (2007). Determinants of Myogenic Specificity within MyoD Are Required for Noncanonical E Box Binding. Molecular and Cellular Biology *27*, 5910–5920.

Heintzman, N.D., Stuart, R.K., Hon, G., Fu, Y., Ching, C.W., Hawkins, R.D., Barrera, L.O., Van Calcar, S., Qu, C., Ching, K.A., et al. (2007). Distinct and predictive chromatin signatures of transcriptional promoters and enhancers in the human genome. Nature Genetics *39*, 311–318.

Heintzman, N.D., Hon, G.C., Hawkins, R.D., Kheradpour, P., Stark, A., Harp, L.F., Ye, Z., Lee, L.K., Stuart, R.K., Ching, C.W., et al. (2009). Histone modifications at human enhancers reflect global cell-type-specific gene expression. Nature *459*, 108–112.

Heinz, S., Benner, C., Spann, N., Bertolino, E., Lin, Y.C., Laslo, P., Cheng, J.X., Murre, C., Singh, H., and Glass, C.K. (2010). Simple combinations of lineage-determining transcription factors prime cis-regulatory elements required for macrophage and B cell identities. Molecular Cell *38*, 576–589.

Hemberg, M., and Kreiman, G. (2011). Conservation of transcription factor binding events predicts gene expression across species. Nucleic Acids Res *39*, 7092–7102.

Hess, J., Angel, P., and Schorpp-Kistner, M. (2004). AP-1 subunits: quarrel and harmony among siblings. J. Cell. Sci. *117*, 5965–5973.

Higazi, A., Abed, M., Chen, J., and Li, Q. (2011). Promoter context determines the role of proteasome in ligand-dependent occupancy of retinoic acid responsive elements. Epigenetics *6*, 202–211.

Hirsinger, E., Duprez, D., Jouve, C., Malapert, P., Cooke, J., and Pourquie, O. (1997). Noggin acts downstream of Wnt and Sonic Hedgehog to antagonize BMP4 in avian somite patterning. Development *124*, 4605–4614.

Hnisz, D., Abraham, B.J., Lee, T.I., Lau, A., Saint-André, V., Sigova, A.A., Hoke, H.A., and Young, R.A. (2013). Super-Enhancers in the Control of Cell Identity and Disease. Cell *155*, 934–947.

Ho, L., and Crabtree, G.R. (2010). Chromatin remodelling during development. Nature *463*, 474–484.

Hodawadekar, S.C., and Marmorstein, R. (2007). Chemistry of acetyl transfer by histone modifying enzymes: structure, mechanism and implications for effector design. Oncogene *26*, 5528–5540.

Hollenberg, S.M., Weinberger, C., Ong, E.S., Cerelli, G., Oro, A., Lebo, R., Thompson, E.B., Rosenfeld, M.G., and Evans, R.M. (1985). Primary structure and expression of a functional human glucocorticoid receptor cDNA. Nature *318*, 635–641.

Hon, G.C., Hawkins, R.D., and Ren, B. (2009). Predictive chromatin signatures in the mammalian genome. Human Molecular Genetics *18*, R195–R201.

Hong, L., Schroth, G.P., Matthews, H.R., Yau, P., and Bradbury, E.M. (1993). Studies of the DNA binding properties of histone H4 amino terminus. Thermal denaturation studies reveal that acetylation markedly reduces the binding constant of the H4 “tail” to DNA. J. Biol. Chem. *268*, 305–314.

Hörlein, A.J., Näär, A.M., Heinzel, T., Torchia, J., Gloss, B., Kurokawa, R., Ryan, A., Kamei, Y., Söderström, M., and Glass, C.K. (1995). Ligand-independent repression by the thyroid hormone receptor mediated by a nuclear receptor co-repressor. Nature *377*, 397–404.

Hsing, E.-W., Shiah, S.-G., Peng, H.-Y., Chen, Y.-W., Chuu, C.-P., Hsiao, J.-R., Lyu, P.-C., and Chang, J.-Y. (2019). TNF-α-induced miR-450a mediates TMEM182 expression to promote oral squamous cell carcinoma motility. PLoS ONE *14*, e0213463.

Hu, J.S., Olson, E.N., and Kingston, R.E. (1992). HEB, a helix-loop-helix protein related to E2A and ITF2 that can modulate the DNA-binding ability of myogenic regulatory factors. Molecular and Cellular Biology *12*, 1031–1042.

Huang, D.W., Sherman, B.T., and Lempicki, R.A. (2008). Systematic and integrative analysis of large gene lists using DAVID bioinformatics resources. Nature Protocols *4*, 44–57.

Hutcheson, D.A., Zhao, J., Merrell, A., Haldar, M., and Kardon, G. (2009). Embryonic and fetal limb myogenic cells are derived from developmentally distinct progenitors and have different requirements for β-catenin. Genes Dev. *23*, 997–1013.

Iezzi, S., Cossu, G., Nervi, C., Sartorelli, V., and Puri, P.L. (2002). Stage-specific modulation of skeletal myogenesis by inhibitors of nuclear deacetylases. PNAS *99*, 7757–7762.

Iezzi, S., Padova, M.D., Serra, C., Caretti, G., Simone, C., Maklan, E., Minetti, G., Zhao, P., Hoffman, E.P., Puri, P.L., et al. (2004). Deacetylase Inhibitors Increase Muscle Cell Size by Promoting Myoblast Recruitment and Fusion through Induction of Follistatin. Developmental Cell *6*, 673–684.

Inukai, S., Kock, K.H., and Bulyk, M.L. (2017). Transcription factor–DNA binding: beyond binding site motifs. Curr Opin Genet Dev *43*, 110–119.

Iyer, A., Fairlie, D.P., and Brown, L. (2012). Lysine acetylation in obesity, diabetes and metabolic disease. Immunology & Cell Biology *90*, 39–46.

Iyer, N.G., Özdag, H., and Caldas, C. (2004). p300/CBP and cancer. Oncogene *23*, 4225–4231.

Jang, H.S., Shin, W.J., Lee, J.E., and Do, J.T. (2017). CpG and Non-CpG Methylation in Epigenetic Gene Regulation and Brain Function. Genes (Basel) *8*.

Janssen, I., Heymsfield, S.B., Wang, Z., and Ross, R. (2000). Skeletal muscle mass and distribution in 468 men and women aged 18–88 yr. Journal of Applied Physiology *89*, 81–88.

Jenuwein, T., and Allis, C.D. (2001). Translating the Histone Code. Science *293*, 1074–1080.

Ji, X., Dadon, D.B., Abraham, B.J., Lee, T.I., Jaenisch, R., Bradner, J.E., and Young, R.A. (2015). Chromatin proteomic profiling reveals novel proteins associated with histone-marked genomic regions. Proc Natl Acad Sci U S A *112*, 3841–3846.

Jiang, Y., Sahoo, T., Michaelis, R.C., Bercovich, D., Bressler, J., Kashork, C.D., Liu, Q., Shaffer, L.G., Schroer, R.J., Stockton, D.W., et al. (2004). A mixed epigenetic/genetic model for oligogenic inheritance of autism with a limited role for UBE3A. American Journal of Medical Genetics Part A *131A*, 1–10.

Jin, Q., Yu, L.-R., Wang, L., Zhang, Z., Kasper, L.H., Lee, J.-E., Wang, C., Brindle, P.K., Dent, S.Y.R., and Ge, K. (2011). Distinct roles of GCN5/PCAF-mediated H3K9ac and CBP/p300-mediated H3K18/27ac in nuclear receptor transactivation. The EMBO Journal *30*, 249–262.

Jin, W., Shang, Y., Peng, J., and Jiang, S. (2016). Histone H3 Methyltransferase Suv39h1 Prevents Myogenic Terminal Differentiation by Repressing MEF2 Activity in Muscle Cells. Int J Mol Sci *17*.

Jin, Z., Zhou, S., Ye, H., Jiang, S., Yu, K., and Ma, Y. (2019). The mechanism of SP1/p300 complex promotes proliferation of multiple myeloma cells through regulating IQGAP1 transcription. Biomedicine & Pharmacotherapy *119*, 109434.

Jones, P.A., and Liang, G. (2009). Rethinking how DNA methylation patterns are maintained. Nature Reviews Genetics *10*, 805–811.

Jones, P.A., Wolkowicz, M.J., Rideout, W.M., Gonzales, F.A., Marziasz, C.M., Coetzee, G.A., and Tapscott, S.J. (1990). De novo methylation of the MyoD1 CpG island during the establishment of immortal cell lines. Proc Natl Acad Sci U S A *87*, 6117–6121.

Joshi, S., Davidson, G., Gras, S.L., Watanabe, S., Braun, T., Mengus, G., and Davidson, I. (2017). TEAD transcription factors are required for normal primary myoblast differentiation in vitro and muscle regeneration in vivo. PLOS Genetics *13*, e1006600.

Jost, J.-P., Oakeley, E.J., Zhu, B., Benjamin, D., Thiry, S., Siegmann, M., and Jost, Y.-C. (2001). 5-Methylcytosine DNA glycosylase participates in the genome-wide loss of DNA methylation occurring during mouse myoblast differentiation. Nucleic Acids Res *29*, 4452–4461.

Juan, A.H., Wang, S., Ko, K.D., Zare, H., Tsai, P.-F., Feng, X., Vivanco, K.O., Ascoli, A.M., Gutierrez-Cruz, G., Krebs, J., et al. (2016). Roles of H3K27me2 and H3K27me3 Examined During Fate Specification of Embryonic Stem Cells. Cell Rep *17*, 1369–1382.

Kahane, N., Cinnamon, Y., and Kalcheim, C. (2002). The roles of cell migration and myofiber intercalation in patterning formation of the postmitotic myotome. Development *129*, 2675–2687.

Kaimori, J.-Y., Maehara, K., Hayashi-Takanaka, Y., Harada, A., Fukuda, M., Yamamoto, S., Ichimaru, N., Umehara, T., Yokoyama, S., Matsuda, R., et al. (2016). Histone H4 lysine 20 acetylation is associated with gene repression in human cells. Scientific Reports *6*, 24318.

Kalkhoven, E. (2004). CBP and p300: HATs for different occasions. Biochem Pharmacol *68*, 1145–1155.

Kamei, Y., Xu, L., Heinzel, T., Torchia, J., Kurokawa, R., Gloss, B., Lin, S.-C., Heyman, R.A., Rose, D.W., Glass, C.K., et al. (1996). A CBP Integrator Complex Mediates Transcriptional Activation and AP-1 Inhibition by Nuclear Receptors. Cell *85*, 403–414.

Kaplan, R., Gan, X., Menke, J.G., Wright, S.D., and Cai, T.-Q. (2002). Bacterial lipopolysaccharide induces expression of ABCA1 but not ABCG1 via an LXR-independent pathway. Journal of Lipid Research *43*, 952–959.

Karmodiya, K., Krebs, A.R., Oulad-Abdelghani, M., Kimura, H., and Tora, L. (2012). H3K9 and H3K14 acetylation co-occur at many gene regulatory elements, while H3K14ac marks a subset of inactive inducible promoters in mouse embryonic stem cells. BMC Genomics *13*, 424.

Kassar-Duchossoy, L., Gayraud-Morel, B., Gomès, D., Rocancourt, D., Buckingham, M., Shinin, V., and Tajbakhsh, S. (2004). Mrf4 determines skeletal muscle identity in Myf5:Myod double-mutant mice. Nature *431*, 466–471.

Kastner, P., Grondona, J.M., Mark, M., Gansmuller, A., LeMeur, M., Decimo, D., Vonesch, J.L., Dollé, P., and Chambon, P. (1994). Genetic analysis of RXR alpha developmental function: convergence of RXR and RAR signaling pathways in heart and eye morphogenesis. Cell *78*, 987–1003.

Kersten, S., Lichtenstein, L., Steenbergen, E., Mudde, K., Hendriks, H.F.J., Hesselink, M.K., Schrauwen, P., and Muller, M. (2009). Caloric Restriction and Exercise Increase Plasma ANGPTL4 Levels in Humans via Elevated Free Fatty Acids. Arteriosclerosis, Thrombosis, and Vascular Biology *29*, 969–974.

Khilji, S., Hamed, M., Chen, J., and Li, Q. (2018). Loci-specific histone acetylation profiles associated with transcriptional coactivator p300 during early myoblast differentiation. Epigenetics *13*, 642–654.

Khilji, S., Hamed, M., Chen, J., and Li, Q. (2020). Dissecting myogenin-mediated retinoid X receptor signaling in myogenic differentiation. Communications Biology *3*, 1–12.

Kim, T.H., Barrera, L.O., Zheng, M., Qu, C., Singer, M.A., Richmond, T.A., Wu, Y., Green, R.D., and Ren, B. (2005). A high-resolution map of active promoters in the human genome. Nature *436*, 876–880.

Koishi, K., Zhang, M., McLennan, I.S., and Harris, A.J. (1995). MyoD protein accumulates in satellite cells and is neurally regulated in regenerating myotubes and skeletal muscle fibers. Developmental Dynamics *202*, 244–254.

Komashko, V.M., Acevedo, L.G., Squazzo, S.L., Iyengar, S.S., Rabinovich, A., O'Geen, H., Green, R., and Farnham, P.J. (2008). Using ChIP-chip technology to reveal common principles of transcriptional repression in normal and cancer cells. Genome Res. *18*, 521–532.

Kornberg, R.D. (1974). Chromatin Structure: A Repeating Unit of Histones and DNA. Science *184*, 868–871.

Koster, K.P., Smith, C., Valencia-Olvera, A.C., Thatcher, G.R.J., Tai, L.M., and LaDu, M.J. (2017). Rexinoids as Therapeutics for Alzheimer's Disease: Role of APOE. Curr Top Med Chem *17*, 708–720.

Kouzarides, T. (2007). Chromatin Modifications and Their Function. Cell *128*, 693–705.

Kraus, W.L., and Kadonaga, J.T. (1998). p300 and estrogen receptor cooperatively activate transcription via differential enhancement of initiation and reinitiation. Genes & Development *12*, 331–342.

Krebs, A.R., Karmodiya, K., Lindahl-Allen, M., Struhl, K., and Tora, L. (2011). SAGA and ATAC Histone Acetyl Transferase Complexes Regulate Distinct Sets of Genes and ATAC Defines a Class of p300-Independent Enhancers. Molecular Cell *44*, 410–423.

Krezel, W., Dupé, V., Mark, M., Dierich, A., Kastner, P., and Chambon, P. (1996). RXR gamma null mice are apparently normal and compound RXR alpha +/-/RXR beta -/-/RXR gamma -/- mutant mice are viable. Proceedings of the National Academy of Sciences of the United States of America *93*, 9010–9014.

Kuang, S., Kuroda, K., Le Grand, F., and Rudnicki, M.A. (2007). Asymmetric Self-Renewal and Commitment of Satellite Stem Cells in Muscle. Cell *129*, 999–1010.

Kunarso, G., Chia, N.-Y., Jeyakani, J., Hwang, C., Lu, X., Chan, Y.-S., Ng, H.-H., and Bourque, G. (2010). Transposable elements have rewired the core regulatory network of human embryonic stem cells. Nat Genet *42*, 631–634.

Kundaje, A., Meuleman, W., Ernst, J., Bilenky, M., Yen, A., Heravi-Moussavi, A., Kheradpour, P., Zhang, Z., Wang, J., Ziller, M.J., et al. (2015). Integrative analysis of 111 reference human epigenomes. Nature *518*, 317–330.

Kung, A.L., Rebel, V.I., Bronson, R.T., Ch'ng, L.-E., Sieff, C.A., Livingston, D.M., and Yao, T.-P. (2000). Gene dose-dependent control of hematopoiesis and hematologic tumor suppression by CBP. Genes Dev. *14*, 272–277.

Kuninger, D., Kuzmickas, R., Peng, B., Pintar, J.E., and Rotwein, P. (2004). Gene discovery by microarray: identification of novel genes induced during growth factor-mediated muscle cell survival and differentiation. Genomics *84*, 876–889.

Lachner, M., O'Carroll, D., Rea, S., Mechtler, K., and Jenuwein, T. (2001). Methylation of histone H3 lysine 9 creates a binding site for HP1 proteins. Nature *410*, 116–120.

Laclef, C., Hamard, G., Demignon, J., Souil, E., Houbron, C., and Maire, P. (2003). Altered myogenesis in Six1-deficient mice. Development (Cambridge, England) *130*, 2239–2252.

Langmead, B., Trapnell, C., Pop, M., and Salzberg, S.L. (2009). Ultrafast and memory-efficient alignment of short DNA sequences to the human genome. Genome Biology *10*, R25.

Lara-Astiaso, D., Weiner, A., Lorenzo-Vivas, E., Zaretsky, I., Jaitin, D.A., David, E., Keren-Shaul, H., Mildner, A., Winter, D., Jung, S., et al. (2014). Chromatin state dynamics during blood formation. Science *345*.

Lassar, A.B., Davis, R.L., Wright, W.E., Kadesch, T., Murre, C., Voronova, A., Baltimore, D., and Weintraub, H. (1991). Functional activity of myogenic HLH proteins requires hetero-oligomerization with E12/E47-like proteins in vivo. Cell *66*, 305–315.

Le May, M., Mach, H., Lacroix, N., Hou, C., Chen, J., and Li, Q. (2011). Contribution of retinoid X receptor signaling to the specification of skeletal muscle lineage. Journal of Biological Chemistry *286*, 26806–26812.

Leblanc, B.P., and Stunnenberg, H.G. (1995). 9-cis retinoic acid signaling: changing partners causes some excitement. Genes Dev. *9*, 1811–1816.

Lee, B.-K., Jang, Y. jin, Kim, M., LeBlanc, L., Rhee, C., Lee, J., Beck, S., Shen, W., and Kim, J. (2019). Super-enhancer-guided mapping of regulatory networks controlling mouse trophoblast stem cells. Nature Communications *10*, 4749.

Lee, D.Y., Hayes, J.J., Pruss, D., and Wolffe, A.P. (1993). A positive role for histone acetylation in transcription factor access to nucleosomal DNA. Cell *72*, 73–84.

Lee, J.-E., Wang, C., Xu, S., Cho, Y.-W., Wang, L., Feng, X., Baldridge, A., Sartorelli, V., Zhuang, L., Peng, W., et al. (2013). H3K4 mono- and di-methyltransferase MLL4 is required for enhancer activation during cell differentiation. ELife *2*, e01503.

Lee, M.-J., Kim, Y.S., Kummar, S., Giaccone, G., and Trepel, J.B. (2008). Histone deacetylase inhibitors in cancer therapy. Curr Opin Oncol *20*, 639–649.

Lee, T.-F., Zhai, J., and Meyers, B.C. (2010). Conservation and divergence in eukaryotic DNA methylation. Proceedings of the National Academy of Sciences of the United States of America *107*, 9027–9028.

Lepper, C., Partridge, T.A., and Fan, C.-M. (2011). An absolute requirement for Pax7-positive satellite cells in acute injury-induced skeletal muscle regeneration. Development *138*, 3639–3646.

Levo, M., Zalckvar, E., Sharon, E., Dantas Machado, A.C., Kalma, Y., Lotam-Pompan, M., Weinberger, A., Yakhini, Z., Rohs, R., and Segal, E. (2015). Unraveling determinants of transcription factor binding outside the core binding site. Genome Res *25*, 1018–1029.

Li, H., and Durbin, R. (2009). Fast and accurate short read alignment with Burrows–Wheeler transform. Bioinformatics *25*, 1754–1760.

Li, E., Bestor, T.H., and Jaenisch, R. (1992). Targeted mutation of the DNA methyltransferase gene results in embryonic lethality. Cell *69*, 915–926.

Li, S., Chen, K., Zhang, Y., Barnes, S.D., Jaichander, P., Zheng, Y., Hassan, M., Malladi, V.S., Skapek, S.X., Xu, L., et al. (2019). Twist2 amplification in rhabdomyosarcoma represses myogenesis and promotes oncogenesis by redirecting MyoD DNA binding. Genes Dev. *33*, 626–640.

Lionikas, A., Cheng, R., Lim, J.E., Palmer, A.A., Blizard, D.A., Vandenbergh, D.J., Blizard, D.A., Lionikas, A., Cheng, R., Lim, J., et al. (2010). Fine-mapping of muscle weight QTL in LG/J and SM/J intercrosses. Physiological Genomics *42A*, 33–38.

Liu, L., Cheung, T.H., Charville, G.W., Hurgo, B.M.C., Leavitt, T., Shih, J., Brunet, A., and Rando, T.A. (2013). Chromatin Modifications as Determinants of Muscle Stem Cell Quiescence and Chronological Aging. Cell Rep *4*, 189–204.

Liu, R., Kim, K.-Y., Jung, Y.-W., and Park, I.-H. (2016). Dnmt1 regulates the myogenic lineage specification of muscle stem cells. Sci Rep *6*.

Lucarelli, M., Fuso, A., Strom, R., and Scarpa, S. (2001). The Dynamics of *Myogenin* Site-specific Demethylation Is Strongly Correlated with Its Expression and with Muscle Differentiation. J. Biol. Chem. *276*, 7500–7506.

Luquet, S., Lopez-Soriano, J., Holst, D., Fredenrich, A., Melki, J., Rassoulzadegan, M., and Grimaldi, P.A. (2003). Peroxisome proliferator-activated receptor controls muscle development and oxydative capability. The FASEB Journal *17*, 2299–2301.

Mal, A., and Harter, M.L. (2003). MyoD is functionally linked to the silencing of a muscle-specific regulatory gene prior to skeletal myogenesis. Proc Natl Acad Sci U S A *100*, 1735–1739.

Mangelsdorf, D.J., Thummel, C., Beato, M., Herrlich, P., Schütz, G., Umesono, K., Blumberg, B., Kastner, P., Mark, M., Chambon, P., et al. (1995). The nuclear receptor superfamily: The second decade. Cell *83*, 835–839.

Marks, P.A. (2010). Histone deacetylase inhibitors: A chemical genetics approach to understanding cellular functions. Biochimica et Biophysica Acta (BBA) - Gene Regulatory Mechanisms *1799*, 717–725.

Martínez-Cerdeño, V., Lemen, J.M., Chan, V., Wey, A., Lin, W., Dent, S.R., and Knoepfler, P.S. (2012). N-Myc and GCN5 Regulate Significantly Overlapping Transcriptional Programs in Neural Stem Cells. PLoS One *7*.

Massari, M.E., and Murre, C. (2000). Helix-Loop-Helix Proteins: Regulators of Transcription in Eucaryotic Organisms. Mol Cell Biol *20*, 429–440.

Maurice, T., Duclot, F., Meunier, J., Naert, G., Givalois, L., Meffre, J., Célérier, A., Jacquet, C., Copois, V., Mechti, N., et al. (2008). Altered Memory Capacities and Response to Stress in p300/CBP-Associated Factor (PCAF) Histone Acetylase Knockout Mice. Neuropsychopharmacology *33*, 1584–1602.

May, D., Blow, M.J., Kaplan, T., McCulley, D.J., Jensen, B.C., Akiyama, J.A., Holt, A., Plajzer-Frick, I., Shoukry, M., Wright, C., et al. (2012). Large-scale discovery of enhancers from human heart tissue. Nature Genetics *44*, 89–93.

McGrew, M.J., and Pourquié, O. (1998). Somitogenesis: segmenting a vertebrate. Current Opinion in Genetics & Development *8*, 487–493.

McKinnell, I.W., Ishibashi, J., Le Grand, F., Punch, V.G.J., Addicks, G.C., Greenblatt, J.F., Dilworth, F.J., and Rudnicki, M.A. (2008). Pax7 activates myogenic genes by recruitment of a histone methyltransferase complex. Nature Cell Biology *10*, 77–84.

McKinsey, T.A., Zhang, C.-L., Lu, J., and Olson, E.N. (2000). Signal-dependent nuclear export of a histone deacetylase regulates muscle differentiation. Nature *408*, 106–111.

McLean, C.Y., Bristor, D., Hiller, M., Clarke, S.L., Schaar, B.T., Lowe, C.B., Wenger, A.M., and Bejerano, G. (2010). GREAT improves functional interpretation of cis-regulatory regions. Nature Biotechnology *28*, 495–501.

Mendelsohn, C., Lohnes, D., Décimo, D., Lufkin, T., LeMeur, M., Chambon, P., and Mark, M. (1994). Function of the retinoic acid receptors (RARs) during development (II). Multiple abnormalities at various stages of organogenesis in RAR double mutants. Development *120*, 2749–2771.

Meryon, E. (1852). On Granular and Fatty Degeneration of the Voluntary Muscles. Medico-Chirurgical Transactions *35*, 73-84.1.

Mikkelsen, T.S., Ku, M., Jaffe, D.B., Issac, B., Lieberman, E., Giannoukos, G., Alvarez, P., Brockman, W., Kim, T.-K., Koche, R.P., et al. (2007). Genome-wide maps of chromatin state in pluripotent and lineage-committed cells. Nature *448*, 553–560.

Mikkelsen, T.S., Xu, Z., Zhang, X., Wang, L., Gimble, J.M., Lander, E.S., and Rosen, E.D. (2010). Comparative Epigenomic Analysis of Murine and Human Adipogenesis. Cell *143*, 156–169.

Millay, D.P., O'Rourke, J.R., Sutherland, L.B., Bezprozvannaya, S., Shelton, J.M., Bassel-Duby, R., Olson, E.N., O'Rourke, J.R., Sutherland, L.B., Bezprozvannaya, S., et al. (2013). Myomaker is a membrane activator of myoblast fusion and muscle formation. (Supp). Nature *499*, 301–305.

Minetti, G.C., Colussi, C., Adami, R., Serra, C., Mozzetta, C., Parente, V., Fortuni, S., Straino, S., Sampaolesi, M., Di Padova, M., et al. (2006). Functional and morphological recovery of dystrophic muscles in mice treated with deacetylase inhibitors. Nat. Med. *12*, 1147–1150.

Miranda, T.B., Morris, S.A., and Hager, G.L. (2013). Complex Genomic Interactions in the Dynamic Regulation of Transcription by the Glucocorticoid Receptor. Mol Cell Endocrinol *380*, 16–24.

Moncaut, N., Rigby, P.W.J., and Carvajal, J.J. (2013). Dial M(RF) for myogenesis. FEBS Journal *280*, 3980–3990.

Moran, J.L., Li, Y., Hill, A.A., Mounts, W.M., and Miller, C.P. (2002). Gene expression changes during mouse skeletal myoblast differentiation revealed by transcriptional profiling. Physiological Genomics *10*.

Moran-Salvador, E., and Mann, J. (2017). Epigenetics and Liver Fibrosis. Cellular and Molecular Gastroenterology and Hepatology *4*, 125–134.

Morgan, J., and Partridge, T. (2020). Skeletal muscle in health and disease. Disease Models & Mechanisms *13*.

Motta, M.C., Divecha, N., Lemieux, M., Kamel, C., Chen, D., Gu, W., Bultsma, Y., McBurney, M., and Guarente, L. (2004). Mammalian SIRT1 represses forkhead transcription factors. Cell *116*, 551–563.

Mukherjee, R., Davies, P.J.A., Crombie, D.L., Bischoff, E.D., Cesario, R.M., Jow, L., Hamann, L.G., Boehm, M.F., Mondon, C.E., Nadzan, A.M., et al. (1997). Sensitization of diabetic and obese mice to insulin by retinoid X receptor agonists. Nature *386*, 407–410.

Murphy, M.M., Lawson, J.A., Mathew, S.J., Hutcheson, D.A., and Kardon, G. (2011). Satellite cells, connective tissue fibroblasts and their interactions are crucial for muscle regeneration. Development *138*, 3625–3637.

Nahoum, V., Perez, E., Germain, P., Rodriguez-Barrios, F., Manzo, F., Kammerer, S., Lemaire, G., Hirsch, O., Royer, C. a, Gronemeyer, H., et al. (2007). Modulators of the structural dynamics of the retinoid X receptor to reveal receptor function. Proc Natl Acad Sci U S A *104*, 17323–17328.

Naidu, P.S., Ludolph, D.C., To, R.Q., Hinterberger, T.J., and Konieczny, S.F. (1995). Myogenin and MEF2 function synergistically to activate the MRF4 promoter during myogenesis. Mol Cell Biol *15*, 2707–2718.

Nègre, N., Brown, C.D., Ma, L., Bristow, C.A., Miller, S.W., Wagner, U., Kheradpour, P., Eaton, M.L., Loriaux, P., Sealfon, R., et al. (2011). A cis-regulatory map of the Drosophila genome. Nature *471*, 527–531.

Ngo, V., Chen, Z., Zhang, K., Whitaker, J.W., Wang, M., and Wang, W. (2019). Epigenomic analysis reveals DNA motifs regulating histone modifications in human and mouse. PNAS *116*, 3668–3677.

Nguyen, M.L.T., Jones, S.A., Prier, J.E., and Russ, B.E. (2015). Transcriptional Enhancers in the Regulation of T Cell Differentiation. Front Immunol *6*.

Nielsen, R., Pedersen, T.Å., Hagenbeek, D., Moulos, P., Siersbæk, R., Megens, E., Denissov, S., Børgesen, M., Francoijs, K.-J., Mandrup, S., et al. (2008). Genome-wide profiling of PPARγ:RXR and RNA polymerase II occupancy reveals temporal activation of distinct metabolic pathways and changes in RXR dimer composition during adipogenesis. Genes Dev. *22*, 2953–2967.

Nolte, R.T., Wisely, G.B., Westin, S., Cobb, J.E., Lambert, M.H., Kurokawa, R., Rosenfeld, M.G., Willson, T.M., Glass, C.K., and Milburn, M.V. (1998). Ligand binding and co-activator assembly of the peroxisome proliferator-activated receptor-gamma. Nature *395*, 137–143.

Nord, A.S., Blow, M.J., Attanasio, C., Akiyama, J.A., Holt, A., Hosseini, R., Phouanenavong, S., Plajzer-Frick, I., Shoukry, M., Afzal, V., et al. (2013). Rapid and Pervasive Changes in Genome-wide Enhancer Usage during Mammalian Development. Cell *155*, 1521–1531.

Odom, D.T., Dowell, R.D., Jacobsen, E.S., Gordon, W., Danford, T.W., MacIsaac, K.D., Rolfe, P.A., Conboy, C.M., Gifford, D.K., and Fraenkel, E. (2007). Tissue-specific transcriptional regulation has diverged significantly between human and mouse. Nature Genetics *39*, 730–732.

O'Dwyer, N.J., Neilson, P.D., and Nash, J. (1989). Mechanisms of muscle growth related to muscle contracture in cerebral palsy. Developmental Medicine and Child Neurology *31*, 543–547.

Ogryzko, V.V., Schiltz, R.L., Russanova, V., Howard, B.H., and Nakatani, Y. (1996). The Transcriptional Coactivators p300 and CBP Are Histone Acetyltransferases. Cell *87*, 953–959.

Ohkawa, Y., Yoshimura, S., Higashi, C., Marfella, C.G.A., Dacwag, C.S., Tachibana, T., and Imbalzano, A.N. (2007). Myogenin and the SWI/SNF ATPase Brg1 maintain myogenic gene expression at different stages of skeletal myogenesis. J. Biol. Chem. *282*, 6564–6570.

Okano, M., Bell, D.W., Haber, D.A., and Li, E. (1999). DNA Methyltransferases Dnmt3a and Dnmt3b Are Essential for De Novo Methylation and Mammalian Development. Cell *99*, 247–257.

Olguin, H.C., Yang, Z., Tapscott, S.J., and Olwin, B.B. (2007). Reciprocal inhibition between Pax7 and muscle regulatory factors modulates myogenic cell fate determination. J Cell Biol *177*, 769–779.

Ouamrane, L., Larrieu, G., Gauthier, B., and Pineau, T. (2003). RXR activators molecular signalling: involvement of a PPARα-dependent pathway in the liver and kidney, evidence for an alternative pathway in the heart. British Journal of Pharmacology *138*, 845–854.

Palacios, D., and Puri, P.L. (2006). The epigenetic network regulating muscle development and regeneration. Journal of Cellular Physiology *207*, 1–11.

Parthun, M.R. (2007). Hat1: the emerging cellular roles of a type B histone acetyltransferase. Oncogene *26*, 5319–5328.

Pazin, M.J., and Kadonaga, J.T. (1997). What's up and down with histone deacetylation and transcription? Cell *89*, 325–328.

Penn, B.H., Bergstrom, D.A., Dilworth, F.J., Bengal, E., and Tapscott, S.J. (2004). A MyoD-generated feed-forward circuit temporally patterns gene expression during skeletal muscle differentiation. Genes Dev. *18*, 2348–2353.

Pennacchio, L.A., Loots, G.G., Nobrega, M.A., and Ovcharenko, I. (2007). Predicting tissue-specific enhancers in the human genome. Genome Res. *17*, 201–211.

Penvose, A., Keenan, J.L., Bray, D., Ramlall, V., and Siggers, T. (2019). Comprehensive study of nuclear receptor DNA binding provides a revised framework for understanding receptor specificity. Nature Communications *10*, 2514.

Perdiguero, E., Sousa-Victor, P., Ballestar, E., and Muñoz-Cánoves, P. (2009). Epigenetic regulation of myogenesis. Epigenetics *4*, 541–550.

Perenthaler, E., Yousefi, S., Niggl, E., and Barakat, T.S. (2019). Beyond the Exome: The Non-coding Genome and Enhancers in Neurodevelopmental Disorders and Malformations of Cortical Development. Front. Cell. Neurosci. *13*.

Perissi, V., and Rosenfeld, M.G. (2005). Controlling nuclear receptors: the circular logic of cofactor cycles. Nature Reviews Molecular Cell Biology *6*, 542–554.

Peterson, C.L., and Workman, J.L. (2000). Promoter targeting and chromatin remodeling by the SWI/SNF complex. Curr Opin Genet Dev *10*, 187–192.

Phan, H.M., Xu, A.W., Coco, C., Srajer, G., Wyszomierski, S., Evrard, Y.A., Eckner, R., and Dent, S.Y.R. (2005). GCN5 and p300 share essential functions during early embryogenesis. Developmental Dynamics *233*, 1337–1347.

Podobinska, M., Szablowska-Gadomska, I., Augustyniak, J., Sandvig, I., Sandvig, A., and Buzanska, L. (2017). Epigenetic Modulation of Stem Cells in Neurodevelopment: The Role of Methylation and Acetylation. Front. Cell. Neurosci. *11*.

Polesskaya, A., Naguibneva, I., Fritsch, L., Duquet, A., Ait-Si-Ali, S., Robin, P., Vervisch, A., Pritchard, L.L., Cole, P., and Harel-Bellan, A. (2001). CBP/p300 and muscle differentiation: no HAT, no muscle. The EMBO Journal *20*, 6816–6825.

Pu, Q., Patel, K., and Huang, R. (2015). The lateral plate mesoderm: a novel source of skeletal muscle. Results Probl Cell Differ *56*, 143–163.

Puri, P.L., and Sartorelli, V. (2000). Regulation of muscle regulatory factors by DNA-binding, interacting proteins, and post-transcriptional modifications. Journal of Cellular Physiology *185*, 155–173.

Puri, P.L., Avantaggiati, M.L., Balsano, C., Sang, N., Graessmann, A., Giordano, A., and Levrero, M. (1997a). p300 is required for MyoD-dependent cell cycle arrest and muscle-specific gene transcription. The EMBO Journal *16*, 369–383.

Puri, P.L., Sartorelli, V., Yang, X.J., Hamamori, Y., Ogryzko, V.V., Howard, B.H., Kedes, L., Wang, J.Y., Graessmann, A., Nakatani, Y., et al. (1997b). Differential roles of p300 and PCAF acetyltransferases in muscle differentiation. Molecular Cell *1*, 35–45.

Quinlan, A.R., and Hall, I.M. (2010). BEDTools: a flexible suite of utilities for comparing genomic features. Bioinformatics *26*, 841–842.

Quinn, M.E., Goh, Q., Kurosaka, M., Gamage, D.G., Petrany, M.J., Prasad, V., and Millay, D.P. (2017). Myomerger induces fusion of non-fusogenic cells and is required for skeletal muscle development. Nature Communications *8*, 15665.

Rada-Iglesias, A., Bajpai, R., Swigut, T., Brugmann, S.A., Flynn, R.A., and Wysocka, J. (2011). A unique chromatin signature uncovers early developmental enhancers in humans. Nature *470*, 279–283.

Radman-Livaja, M., and Rando, O.J. (2010). Nucleosome positioning: how is it established, and why does it matter? Dev Biol *339*, 258–266.

Raisner, R., Kharbanda, S., Jin, L., Jeng, E., Chan, E., Merchant, M., Haverty, P.M., Bainer, R., Cheung, T., Arnott, D., et al. (2018). Enhancer Activity Requires CBP/P300 Bromodomain-Dependent Histone H3K27 Acetylation. Cell Reports *24*, 1722–1729.

Ramachandran, B., Yu, G., Li, S., Zhu, B., and Gulick, T. (2008). Myocyte Enhancer Factor 2A Is Transcriptionally Autoregulated. J Biol Chem *283*, 10318–10329.

Ramírez, F., Ryan, D.P., Grüning, B., Bhardwaj, V., Kilpert, F., Richter, A.S., Heyne, S., Dündar, F., and Manke, T. (2016). deepTools2: a next generation web server for deep-sequencing data analysis. Nucleic Acids Res *44*, W160–W165.

Rawls, A., Morris, J.H., Rudnicki, M., Braun, T., Arnold, H.H., Klein, W.H., and Olson, E.N. (1995). Myogenin's functions do not overlap with those of MyoD or Myf-5 during mouse embryogenesis. Developmental Biology *172*, 37–50.

Relaix, F., and Zammit, P.S. (2012). Satellite cells are essential for skeletal muscle regeneration: the cell on the edge returns centre stage. Development *139*, 2845–2856.

Relaix, F., Montarras, D., Zaffran, S., Gayraud-Morel, B., Rocancourt, D., Tajbakhsh, S., Mansouri, A., Cumano, A., and Buckingham, M. (2006). Pax3 and Pax7 have distinct and overlapping functions in adult muscle progenitor cells. J Cell Biol *172*, 91–102.

Relaix, F., Demignon, J., Laclef, C., Pujol, J., Santolini, M., Niro, C., Lagha, M., Rocancourt, D., Buckingham, M., and Maire, P. (2013). Six Homeoproteins Directly Activate Myod Expression in the Gene Regulatory Networks That Control Early Myogenesis. PLOS Genetics *9*, e1003425.

Rhodes, S.J., and Konieczny, S.F. (1989). Identification of MRF4: a new member of the muscle regulatory factor gene family. Genes Dev. *3*, 2050–2061.

Robinson, J.T., Thorvaldsdóttir, H., Winckler, W., Guttman, M., Lander, E.S., Getz, G., and Mesirov, J.P. (2011). Integrative genomics viewer. Nature Biotechnology *29*, 24–26.

Roh, T.-Y., Cuddapah, S., and Zhao, K. (2005). Active chromatin domains are defined by acetylation islands revealed by genome-wide mapping. Genes & Development *19*, 542–552.

Rosenfeld, M.G., Lunyak, V.V., and Glass, C.K. (2006). Sensors and signals: a coactivator/corepressor/epigenetic code for integrating signal-dependent programs of transcriptional response. Genes & Development *20*, 1405–1428.

Roth, J.-F., Shikama, N., Henzen, C., Desbaillets, I., Lutz, W., Marino, S., Wittwer, J., Schorle, H., Gassmann, M., and Eckner, R. (2003). Differential role of p300 and CBP acetyltransferase during myogenesis: p300 acts upstream of MyoD and Myf5. The EMBO Journal *22*, 5186–5196.

Roudier, F., Ahmed, I., Bérard, C., Sarazin, A., Mary-Huard, T., Cortijo, S., Bouyer, D., Caillieux, E., Duvernois-Berthet, E., Al-Shikhley, L., et al. (2011). Integrative epigenomic mapping defines four main chromatin states in Arabidopsis. The EMBO Journal *30*, 1928–1938.

Rudnicki, M.A., and Jaenisch, R. (1995). The MyoD family of transcription factors and skeletal myogenesis. BioEssays *17*, 203–209.

Rudnicki, M.A., Braun, T., Hinuma, S., and Jaenisch, R. (1992). Inactivation of MyoD in mice leads to up-regulation of the myogenic HLH gene Myf-5 and results in apparently normal muscle development. Cell *71*, 383–390.

Rudnicki, M.A., Schnegelsberg, P.N., Stead, R.H., Braun, T., Arnold, H.H., and Jaenisch, R. (1993). MyoD or Myf-5 is required for the formation of skeletal muscle. Cell *75*, 1351–1359.

Ruijter, A.J.M. de, Gennip, A.H. van, Caron, H.N., Kemp, S., and Kuilenburg, A.B.P. van (2003). Histone deacetylases (HDACs): characterization of the classical HDAC family. Biochem J *370*, 737–749.

Ryall, J.G., Dell'Orso, S., Derfoul, A., Juan, A., Zare, H., Feng, X., Clermont, D., Koulnis, M., Gutierrez-Cruz, G., Fulco, M., et al. (2015). The NAD+-Dependent SIRT1 Deacetylase Translates a Metabolic Switch into Regulatory Epigenetics in Skeletal Muscle Stem Cells. Cell Stem Cell *16*, 171–183.

Said, R.S., Mustafa, A.G., Asfour, H.A., and Shaqoura, E. (2017). Myogenic Satellite Cells: Biological Milieu and Possible Clinical Applications. Pak J Biol Sci *20*, 1–11.

Santos-Rosa, H., Schneider, R., Bannister, A.J., Sherriff, J., Bernstein, B.E., Emre, N.C.T., Schreiber, S.L., Mellor, J., and Kouzarides, T. (2002). Active genes are tri-methylated at K4 of histone H3. Nature *419*, 407–411.

Santos-Rosa, H., Valls, E., Kouzarides, T., and Martínez-Balbás, M. (2003). Mechanisms of P/CAF auto-acetylation. Nucleic Acids Res *31*, 4285–4292.

Sapin, V., Dollé, P., Hindelang, C., Kastner, P., and Chambon, P. (1997). Defects of the chorioallantoic placenta in mouse RXRalpha null fetuses. Developmental Biology *191*, 29–41.

Sartorelli, V., and Caretti, G. (2005). Mechanisms underlying the transcriptional regulation of skeletal myogenesis. Curr Opin Genet Dev *15*, 528–535.

Sartorelli, V., Huang, J., Hamamori, Y., and Kedes, L. (1997). Molecular mechanisms of myogenic coactivation by p300: direct interaction with the activation domain of MyoD and with the MADS box of MEF2C. Molecular and Cellular Biology *17*, 1010–1026.

Schierle, S., and Merk, D. (2019). Therapeutic modulation of retinoid X receptors – SAR and therapeutic potential of RXR ligands and recent patents. Expert Opinion on Therapeutic Patents *29*, 605–621.

Schmidt, D., Wilson, M.D., Ballester, B., Schwalie, P.C., Brown, G.D., Marshall, A., Kutter, C., Watt, S., Martinez-Jimenez, C.P., Mackay, S., et al. (2010). Five-Vertebrate ChIP-seq Reveals the Evolutionary Dynamics of Transcription Factor Binding. Science *328*, 1036–1040.

Schoenfelder, S., and Fraser, P. (2019). Long-range enhancer-promoter contacts in gene expression control. Nat Rev Genet *20*, 437–455.

Schwaiger, M., Schönauer, A., Rendeiro, A.F., Pribitzer, C., Schauer, A., Gilles, A.F., Schinko, J.B., Renfer, E., Fredman, D., and Technau, U. (2014). Evolutionary conservation of the eumetazoan gene regulatory landscape. Genome Research *24*, 639–650.

Seligson, D.B., Horvath, S., Shi, T., Yu, H., Tze, S., Grunstein, M., and Kurdistani, S.K. (2005). Global histone modification patterns predict risk of prostate cancer recurrence. Nature *435*, 1262–1266.

Sen, P., Lan, Y., Li, C.Y., Sidoli, S., Donahue, G., Dou, Z., Frederick, B., Chen, Q., Luense, L.J., Garcia, B.A., et al. (2019). Histone Acetyltransferase p300 Induces De Novo Super-Enhancers to Drive Cellular Senescence. Mol Cell *73*, 684-698.e8.

de la Serna, I.L., Carlson, K.A., and Imbalzano, A.N. (2001). Mammalian SWI/SNF complexes promote MyoD-mediated muscle differentiation. Nature Genetics *27*, 187–190.

de la Serna, I.L., Ohkawa, Y., Berkes, C.A., Bergstrom, D.A., Dacwag, C.S., Tapscott, S.J., and Imbalzano, A.N. (2005). MyoD targets chromatin remodeling complexes to the myogenin locus prior to forming a stable DNA-bound complex. Mol. Cell. Biol. *25*, 3997–4009.

Shahbazian, M.D., and Grunstein, M. (2007). Functions of Site-Specific Histone Acetylation and Deacetylation. Annual Review of Biochemistry *76*, 75–100.

Shefer, G., Van de Mark, D.P., Richardson, J.B., and Yablonka-Reuveni, Z. (2006). Satellite-cell pool size does matter: Defining the myogenic potency of aging skeletal muscle. Developmental Biology *294*, 50–66.

Shen, D., Yu, X., Wu, Y., Chen, Y., Li, G., Cheng, F., and Xia, L. (2018). Emerging roles of bexarotene in the prevention, treatment and anti-drug resistance of cancers. Expert Rev Anticancer Ther *18*, 487–499.

Shen, L., Shao, N., Liu, X., Nestler, E., Metzker, M., Daniel, C.K., Karyn, M.S., David, E.L., Richard, K.W., Mardis, E., et al. (2014). ngs.plot: Quick mining and visualization of next-generation sequencing data by integrating genomic databases. BMC Genomics *15*, 284.

Shen, Q., Cline, G.W., Shulman, G.I., Leibowitz, M.D., and Davies, P.J.A. (2004). Effects of rexinoids on glucose transport and insulin-mediated signaling in skeletal muscles of diabetic (db/db) mice. J. Biol. Chem. *279*, 19721–19731.

Shen, Y., Yue, F., McCleary, D.F., Ye, Z., Edsall, L., Kuan, S., Wagner, U., Dixon, J., Lee, L., Lobanenkov, V. V., et al. (2012). A map of the cis-regulatory sequences in the mouse genome. Nature *488*, 116–120.

Sherman, S.I., Gopal, J., Haugen, B.R., Chiu, A.C., Whaley, K., Nowlakha, P., and Duvic, M. (1999). Central hypothyroidism associated with retinoid X receptor-selective ligands. N. Engl. J. Med. *340*, 1075–1079.

Shklover, J., Etzioni, S., Weisman-Shomer, P., Yafe, A., Bengal, E., and Fry, M. (2007). MyoD uses overlapping but distinct elements to bind E-box and tetraplex structures of regulatory sequences of muscle-specific genes. Nucleic Acids Res *35*, 7087–7095.

Shulman, A.I., and Mangelsdorf, D.J. (2005). Retinoid x receptor heterodimers in the metabolic syndrome. The New England Journal of Medicine *353*, 604–615.

Sif, S. (2004). ATP-dependent nucleosome remodeling complexes: enzymes tailored to deal with chromatin. J Cell Biochem *91*, 1087–1098.

Simone, C., Forcales, S.V., Hill, D.A., Imbalzano, A.N., Latella, L., and Puri, P.L. (2004). p38 pathway targets SWI-SNF chromatin-remodeling complex to muscle-specific loci. Nat. Genet. *36*, 738–743.

Singh, K., and Dilworth, F.J. (2013). Differential modulation of cell cycle progression distinguishes members of the myogenic regulatory factor family of transcription factors. FEBS J *280*, 3991–4003.

Sirri, V., Leibovitch, M.P., and Leibovitch, S.A. (2003). Muscle regulatory factor MRF4 activates differentiation in rhabdomyosarcoma RD cells through a positive-acting C-terminal protein domain. Oncogene *22*, 5658–5666.

Skorija, K., Cox, M., Sisk, J.M., Dowd, D.R., MacDonald, P.N., Thompson, C.C., and Demay, M.B. (2005). Ligand-Independent Actions of the Vitamin D Receptor Maintain Hair Follicle Homeostasis. Mol Endocrinol *19*, 855–862.

Spicuglia, S., and Vanhille, L. (2012). Chromatin signatures of active enhancers. Nucleus *3*, 126–131.

Spitz, F., and Furlong, E.E.M. (2012). Transcription factors: from enhancer binding to developmental control. Nature Reviews Genetics *13*, 613–626.

Spivakov, M., and Fisher, A.G. (2007). Epigenetic signatures of stem-cell identity. Nat. Rev. Genet. *8*, 263–271.

Stender, J.D., Kim, K., Charn, T.H., Komm, B., Chang, K.C.N., Kraus, W.L., Benner, C., Glass, C.K., and Katzenellenbogen, B.S. (2010). Genome-Wide Analysis of Estrogen Receptor α DNA Binding and Tethering Mechanisms Identifies Runx1 as a Novel Tethering Factor in Receptor-Mediated Transcriptional Activation. Mol Cell Biol *30*, 3943–3955.

Sucov, H.M., Dyson, E., Gumeringer, C.L., Price, J., Chien, K.R., and Evans, R.M. (1994). RXR alpha mutant mice establish a genetic basis for vitamin A signaling in heart morphogenesis. Genes & Development *8*, 1007–1018.

Suganuma, T., and Workman, J.L. (2011). Signals and Combinatorial Functions of Histone Modifications. Annual Review of Biochemistry *80*, 473–499.

Sun, H.-J., Xu, X., Wang, X.-L., Wei, L., Li, F., Lu, J., and Huang, B.-Q. (2006). Transcription factors Ets2 and Sp1 act synergistically with histone acetyltransferase p300 in activating human interleukin-12 p40 promoter. Acta Biochim. Biophys. Sin. (Shanghai) *38*, 194–200.

Sun, X.-J., Man, N., Tan, Y., Nimer, S.D., and Wang, L. (2015). The Role of Histone Acetyltransferases in Normal and Malignant Hematopoiesis. Front Oncol *5*.

Tajbakhsh, S., Borello, U., Vivarelli, E., Kelly, R., Papkoff, J., Duprez, D., Buckingham, M., and Cossu, G. (1998). Differential activation of Myf5 and MyoD by different Wnts in explants of mouse paraxial mesoderm and the later activation of myogenesis in the absence of Myf5. Development *125*, 4155–4162.

Tanaka, T., and De Luca, L.M. (2009). Therapeutic Potential of "Rexinoids" in Cancer Prevention and Treatment. Cancer Research *69*.

Tanaka, Y., Naruse, I., Maekawa, T., Masuya, H., Shiroishi, T., and Ishii, S. (1997). Abnormal skeletal patterning in embryos lacking a single Cbp allele: A partial similarity with Rubinstein–Taybi syndrome. PNAS *94*, 10215–10220.

Tanaka, Y., Naruse, I., Hongo, T., Xu, M.-J., Nakahata, T., Maekawa, T., and Ishii, S. (2000). Extensive brain hemorrhage and embryonic lethality in a mouse null mutant of CREB-binding protein. Mechanisms of Development *95*, 133–145.

Tapscott, S.J. (2005). The circuitry of a master switch: Myod and the regulation of skeletal muscle gene transcription. Development *132*, 2685–2695.

Taylor, S.M., and Jones, P.A. (1979). Multiple new phenotypes induced in 10T1/2 and 3T3 cells treated with 5-azacytidine. Cell *17*, 771–779.

Thompson, P.R., Wang, D., Wang, L., Fulco, M., Pediconi, N., Zhang, D., An, W., Ge, Q., Roeder, R.G., Wong, J., et al. (2004). Regulation of the p300 HAT domain via a novel activation loop. Nat. Struct. Mol. Biol. *11*, 308–315.

Thurman, R.E., Rynes, E., Humbert, R., Vierstra, J., Maurano, M.T., Haugen, E., Sheffield, N.C., Stergachis, A.B., Wang, H., Vernot, B., et al. (2012). The accessible chromatin landscape of the human genome. Nature *489*, 75–82.

Torchia, J., Glass, C., and Rosenfeld, M.G. (1998). Co-activators and co-repressors in the integration of transcriptional responses. Current Opinion in Cell Biology *10*, 373–383.

Trapnell, C., Pachter, L., and Salzberg, S.L. (2009). TopHat: discovering splice junctions with RNA-Seq. Bioinformatics (Oxford, England) *25*, 1105–1111.

Trapnell, C., Williams, B.A., Pertea, G., Mortazavi, A., Kwan, G., van Baren, M.J., Salzberg, S.L., Wold, B.J., and Pachter, L. (2010). Transcript assembly and quantification by RNA-Seq reveals unannotated transcripts and isoform switching during cell differentiation. Nature Biotechnology *28*, 511–515.

Trisciuoglio, D., Di Martile, M., and Del Bufalo, D. (2018). Emerging Role of Histone Acetyltransferase in Stem Cells and Cancer (Hindawi).

Umansky, K.B., Gruenbaum-Cohen, Y., Tsoory, M., Feldmesser, E., Goldenberg, D., Brenner, O., and Groner, Y. (2015a). Runx1 Transcription Factor Is Required for Myoblasts Proliferation during Muscle Regeneration. PLOS Genetics *11*, e1005457.

Umansky, K.B., Feldmesser, E., and Groner, Y. (2015b). Genomic-wide transcriptional profiling in primary myoblasts reveals Runx1-regulated genes in muscle regeneration. Genom Data *6*, 120–122.

Usardi, A., Iyer, K., Sigoillot, S.M., Dusonchet, A., and Selimi, F. (2017). The immunoglobulin-like superfamily member IGSF3 is a developmentally regulated protein that controls neuronal morphogenesis. Developmental Neurobiology *77*, 75–92.

Vahid, F., Zand, H., Nosrat-Mirshekarlou, E., Najafi, R., and Hekmatdoost, A. (2015). The role dietary of bioactive compounds on the regulation of histone acetylases and deacetylases: a review. Gene *562*, 8–15.

Vernimmen, D., and Bickmore, W.A. (2015). The Hierarchy of Transcriptional Activation: From Enhancer to Promoter. Trends Genet. *31*, 696–708.

Vierstra, J., Rynes, E., Sandstrom, R., Zhang, M., Canfield, T., Hansen, R.S., Stehling-Sun, S., Sabo, P.J., Byron, R., Humbert, R., et al. (2014). Mouse regulatory DNA landscapes reveal global principles of cis-regulatory evolution. Science *346*, 1007–1012.

Visel, A., Blow, M.J., Li, Z., Zhang, T., Akiyama, J.A., Holt, A., Plajzer-Frick, I., Shoukry, M., Wright, C., Chen, F., et al. (2009). ChIP-seq accurately predicts tissue-specific activity of enhancers. Nature *457*, 854–858.

Vo, N., and Goodman, R.H. (2001). CREB-binding Protein and p300 in Transcriptional Regulation. Journal of Biological Chemistry *276*, 13505–13508.

Voigt, P., Tee, W.-W., and Reinberg, D. (2013). A double take on bivalent promoters. Genes Dev *27*, 1318–1338.

Vojinovic, J., and Damjanov, N. (2011). HDAC Inhibition in Rheumatoid Arthritis and Juvenile Idiopathic Arthritis. Mol Med *17*, 397–403.

Wales, S., Hashemi, S., Blais, A., and McDermott, J.C. (2014). Global MEF2 target gene analysis in cardiac and skeletal muscle reveals novel regulation of DUSP6 by p38MAPK-MEF2 signaling. Nucleic Acids Research *42*, 11349–11362.

Wang, L., and Dent, S.Y. (2014). Functions of SAGA in development and disease. Epigenomics *6*, 329–339.

Wang, Y.X., and Rudnicki, M.A. (2011). Satellite cells, the engines of muscle repair. Nat. Rev. Mol. Cell Biol. *13*, 127–133.

Wang, A., Yue, F., Li, Y., Xie, R., Harper, T., Patel, N.A., Muth, K., Palmer, J., Qiu, Y., Wang, J., et al. (2015). Epigenetic Priming of Enhancers Predicts Developmental Competence of hESC-Derived Endodermal Lineage Intermediates. Cell Stem Cell *16*, 386–399.

Wang, Y.-L., Faiola, F., Xu, M., Pan, S., and Martinez, E. (2008a). Human ATAC Is a GCN5/PCAF-containing Acetylase Complex with a Novel NC2-like Histone Fold Module That Interacts with the TATA-binding Protein. J Biol Chem *283*, 33808–33815.

Wang, Y.-X.Y., Zhang, C.C.-L., Yu, R.R.T., Cho, H.K., Nelson, M.M.C., Bayuga-Ocampo, C.R., Ham, J., Kang, H., Evans, R.M., Abou, M., et al. (2004). Regulation of Muscle Fiber Type and Running Endurance by PPARδ. PLoS Biology *2*, e294.

Wang, Z., Zang, C., Rosenfeld, J.A., Schones, D.E., Barski, A., Cuddapah, S., Cui, K., Roh, T.-Y., Peng, W., Zhang, M.Q., et al. (2008b). Combinatorial patterns of histone acetylations and methylations in the human genome. Nat. Genet. *40*, 897–903.

Wang, Z., Zang, C., Cui, K., Schones, D.E., Barski, A., Peng, W., and Zhao, K. (2009). Genome-wide Mapping of HATs and HDACs Reveals Distinct Functions in Active and Inactive Genes. Cell *138*, 1019–1031.

Watson, P.J., Fairall, L., and Schwabe, J.W.R. (2012). Nuclear hormone receptor co-repressors: Structure and function. Mol Cell Endocrinol *348–135*, 440–449.

Webster, C., Silberstein, L., Hays, A.P., and Blau, H.M. (1988). Fast muscle fibers are preferentially affected in Duchenne muscular dystrophy. Cell *52*, 503–513.

Weintraub, H., Tapscott, S.J., Davis, R.L., Thayer, M.J., Adam, M.A., Lassar, A.B., and Miller, A.D. (1989). Activation of muscle-specific genes in pigment, nerve, fat, liver, and fibroblast cell lines by forced expression of MyoD. Proceedings of the National Academy of Sciences of the United States of America *86*, 5434–5438.

White, R.B., Biérinx, A.-S., Gnocchi, V.F., and Zammit, P.S. (2010). Dynamics of muscle fibre growth during postnatal mouse development. BMC Dev Biol *10*, 21.

Whyte, W.A., Bilodeau, S., Orlando, D.A., Hoke, H.A., Frampton, G.M., Foster, C.T., Cowley, S.M., and Young, R.A. (2012). Enhancer decommissioning by LSD1 during embryonic stem cell differentiation. Nature *482*, 221–225.

Whyte, W.A., Orlando, D.A., Hnisz, D., Abraham, B.J., Lin, C.Y., Kagey, M.H., Rahl, P.B., Lee, T.I., and Young, R.A. (2013). Master transcription factors and mediator establish super-enhancers at key cell identity genes. Cell *153*, 307–319.

Wightman, F., Ellenberg, P., Churchill, M., and Lewin, S.R. (2012). HDAC inhibitors in HIV. Immunology & Cell Biology *90*, 47–54.

Wilson, B.G., and Roberts, C.W.M. (2011). SWI/SNF nucleosome remodellers and cancer. Nat Rev Cancer *11*, 481–492.

Witt, O., Deubzer, H.E., Milde, T., and Oehme, I. (2009). HDAC family: What are the cancer relevant targets? Cancer Letters *277*, 8–21.

Witte, S., Bradley, A., Enright, A.J., and Muljo, S.A. (2015). High-density P300 enhancers control cell state transitions. BMC Genomics *16*, 903.

Woo, Y.H., and Li, W.-H. (2012). Evolutionary conservation of histone modifications in mammals. Molecular Biology and Evolution *29*, 1757–1767.

Wright, W.E., Sassoon, D.A., and Lin, V.K. (1989). Myogenin, a factor regulating myogenesis, has a domain homologous to MyoD. Cell *56*, 607–617.

Wu, Y., and Smas, C.M. (2008). Expression and regulation of transcript for the novel transmembrane protein Tmem182 in the adipocyte and muscle lineage. BMC Research Notes *1*, 85.

Wu Ct, null, and Morris, J.R. (2001). Genes, genetics, and epigenetics: a correspondence. Science *293*, 1103–1105.

Xiao, H., Hasegawa, T., and Isobe, K. (2000). p300 Collaborates with Sp1 and Sp3 in p21 waf1/cip1 Promoter Activation Induced by Histone Deacetylase Inhibitor. J. Biol. Chem. *275*, 1371–1376.

Xu, J., Watts, J.A., Pope, S.D., Gadue, P., Kamps, M., Plath, K., Zaret, K.S., and Smale, S.T. (2009). Transcriptional competence and the active marking of tissue-specific enhancers by defined transcription factors in embryonic and induced pluripotent stem cells. Genes & Development *23*, 2824–2838.

Xu, W., Edmondson, D.G., Evrard, Y.A., Wakamiya, M., Behringer, R.R., and Roth, S.Y. (2000). Loss of Gcn5l2 leads to increased apoptosis and mesodermal defects during mouse development. Nat Genet *26*, 229–232.

Yablonka-Reuveni, Z. (2011). The Skeletal Muscle Satellite Cell: Still Young and Fascinating at 50. J Histochem Cytochem. *59*, 1041–1059.

Yablonka-Reuveni, Z., Rudnicki, M.A., Rivera, A.J., Primig, M., Anderson, J.E., and Natanson, P. (1999). The Transition from Proliferation to Differentiation Is Delayed in Satellite Cells from Mice Lacking MyoD. Dev Biol *210*, 440–455.

Yaffe, D., and Saxel, O. (1977). Serial passaging and differentiation of myogenic cells isolated from dystrophic mouse muscle. Nature *270*, 725–727.

Yamauchi, T., Yamauchi, J., Kuwata, T., Tamura, T., Yamashita, T., Bae, N., Westphal, H., Ozato, K., and Nakatani, Y. (2000). Distinct but overlapping roles of histone acetylase PCAF and of the closely related PCAF-B/GCN5 in mouse embryogenesis. PNAS *97*, 11303–11306.

Yao, T.-P., Oh, S.P., Fuchs, M., Zhou, N.-D., Ch'ng, L.-E., Newsome, D., Bronson, R.T., Li, E., Livingston, D.M., and Eckner, R. (1998). Gene Dosage–Dependent Embryonic Development and Proliferation Defects in Mice Lacking the Transcriptional Integrator p300. Cell *93*, 361–372.

Yoon, J.C., Chickering, T.W., Rosen, E.D., Dussault, B., Qin, Y., Soukas, A., Friedman, J.M., Holmes, W.E., and Spiegelman, B.M. (2000). Peroxisome proliferator-activated receptor gamma target gene encoding a novel angiopoietin-related protein associated with adipose differentiation. Molecular and Cellular Biology *20*, 5343–5349.

Yue, F., Cheng, Y., Breschi, A., Vierstra, J., Wu, W., Ryba, T., Sandstrom, R., Ma, Z., Davis, C., Pope, B.D., et al. (2014). A comparative encyclopedia of DNA elements in the mouse genome. Nature *515*, 355–364.

Zammit, P.S. (2017). Function of the myogenic regulatory factors Myf5, MyoD, Myogenin and MRF4 in skeletal muscle, satellite cells and regenerative myogenesis. Seminars in Cell & Developmental Biology *72*, 19–32.

Zammit, P.S., Golding, J.P., Nagata, Y., Hudon, V., Partridge, T.A., and Beauchamp, J.R. (2004). Muscle satellite cells adopt divergent fates a mechanism for self-renewal? J Cell Biol *166*, 347–357.

Zeng, Z., Sun, Z., Huang, M., Zhang, W., Liu, J., Chen, L., Chen, F., Zhou, Y., Lin, J., Huang, F., et al. (2015). Nitrostyrene Derivatives Act as RXRα Ligands to Inhibit TNFα Activation of NF-κB. Cancer Res. *75*, 2049–2060.

Zentner, G.E., Tesar, P.J., and Scacheri, P.C. (2011). Epigenetic signatures distinguish multiple classes of enhancers with distinct cellular functions. Genome Research *21*, 1273–1283.

Zhang, G., and Pradhan, S. (2014). Mammalian epigenetic mechanisms. IUBMB Life *66*, 240–256.

Zhang, C., Zhong, J.F., Stucky, A., Chen, X.-L., Press, M.F., and Zhang, X. (2015). Histone acetylation: novel target for the treatment of acute lymphoblastic leukemia. Clin Epigenetics *7*.

Zhang, H., Postigo, A.A., and Dean, D. (1999). Active Transcriptional Repression by the Rb–E2F Complex Mediates G1 Arrest Triggered by p16INK4a, TGFβ, and Contact Inhibition. Cell.

Zhang, Q., Vashisht, A.A., O'Rourke, J., Corbel, S.Y., Moran, R., Romero, A., Miraglia, L., Zhang, J., Durrant, E., Schmedt, C., et al. (2017). The microprotein Minion controls cell fusion and muscle formation. Nat Commun *8*, 15664.

Zhang, Y., Babin, J., Feldhaus, A.L., Singh, H., Sharp, P.A., and Bina, M. (1991). HTF4: a new human helix-loop-helix protein. Nucleic Acids Research *19*, 4555.

Zhang, Y., Liu, T., Meyer, C.A., Eeckhoute, J., Johnson, D.S., Bernstein, B.E., Nusbaum, C., Myers, R.M., Brown, M., Li, W., et al. (2008). Model-based analysis of ChIP-Seq (MACS). Genome Biology *9*, R137.

Zhao, W.-X., Tian, M., Zhao, B.-X., Li, G., Liu, B., Zhan, Y.-Y., Chen, H.-Z., and Wu, Q. (2007). Orphan Receptor TR3 Attenuates the p300-Induced Acetylation of Retinoid X Receptor-α. Molecular Endocrinology *21*, 2877–2889.

Zheng, J., Wang, R., Zambraski, E., Wu, D., Jacobson, K.A., and Liang, B.T. (2007). Protective roles of adenosine A1, A2A, and A3 receptors in skeletal muscle ischemia and reperfusion injury. Am J Physiol Heart Circ Physiol *293*, H3685–H3691.

Zheng, Y., Trivedi, T., Lin, R.C., Fong-Yee, C., Nolte, R., Manibo, J., Chen, Y., Hossain, M., Horas, K., Dunstan, C., et al. (2017). Loss of the vitamin D receptor in human breast and prostate cancers strongly induces cell apoptosis through downregulation of Wnt/β-catenin signaling. Bone Research *5*, 1–12.

Zhou, V.W., Goren, A., and Bernstein, B.E. (2011). Charting histone modifications and the functional organization of mammalian genomes. Nature Reviews Genetics *12*, 7–18.

Zhu, G.-H., Huang, J., Bi, Y., Su, Y., Tang, Y., He, B.-C., He, Y., Luo, J., Wang, Y., Chen, L., et al. (2009). Activation of RXR and RAR signaling promotes myogenic differentiation of myoblastic C2C12 cells. Differentiation; Research in Biological Diversity *78*, 195–204.